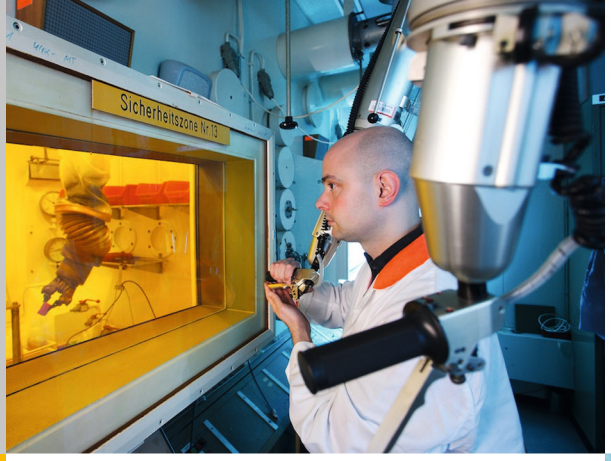

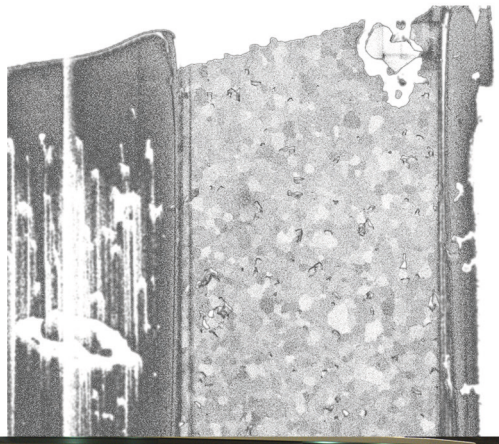

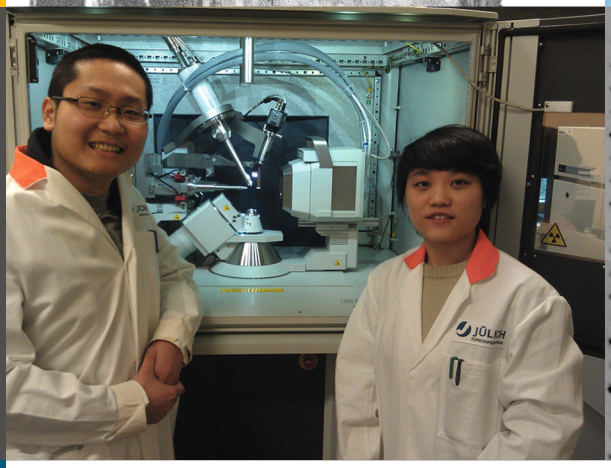

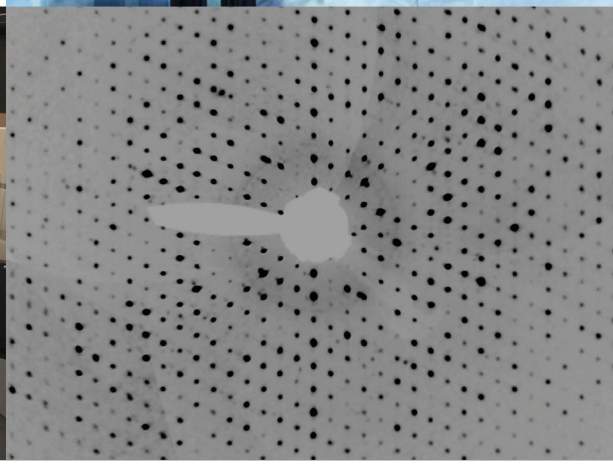

Institute of Energy and Climate Research
IEK-6: Nuclear Waste Management
Report 2011/2012

Material Science for Nuclear Waste Management

M. Klinkenberg, S. Neumeier, D. Bosbach (Editors)

JÜLICH
FORSCHUNGSZENTRUM

Mitglied der Helmholtz-Gemeinschaft

Schriften des Forschungszentrums Jülich
Reihe Energie & Umwelt / Energy & Environment Band / Volume 197

Forschungszentrum Jülich GmbH
Institut für Energie- und Klimaforschung (IEK)
Nukleare Entsorgung und Reaktorsicherheit (IEK-6)

Institute of Energy and Climate Research IEK-6: Nuclear Waste Management Report 2011 / 2012

Material Science for Nuclear Waste Management

M. Klinkenberg, S. Neumeier, D. Bosbach (Editors)

Schriften des Forschungszentrums Jülich
Reihe Energie & Umwelt / Energy & Environment Band / Volume 197

ISSN 1866-1793 ISBN 978-3-89336-920-1

Bibliographic information published by the Deutsche Nationalbibliothek.
The Deutsche Nationalbibliothek lists this publication in the Deutsche Nationalbibliografie; detailed bibliographic data are available in the Internet at http://dnb.d-nb.de.

Middle Cover picture, right
by courtesy of NRG, Petten, NL

Publisher and Distributor: Forschungszentrum Jülich GmbH
Zentralbibliothek
52425 Jülich
Tel: +49 2461 61-5368
Fax: +49 2461 61-6103
Email: zb-publikation@fz-juelich.de
www.fz-juelich.de/zb

Cover Design: Grafische Medien, Forschungszentrum Jülich GmbH

Printer: Grafische Medien, Forschungszentrum Jülich GmbH

Schriften des Forschungszentrums Jülich
Reihe Energie & Umwelt / Energy & Environment, Band / Volume 197

ISSN 1866-1793
ISBN 978-3-89336-920-1

TABLE OF CONTENTS

1 Institute's Profile

The Nuclear Waste Management section of the Institute of Energy and Climate Research (IEK-6) performs fundamental as well as applied research and development for the safe management of nuclear waste covering issues from the atomic scale to the macroscopic scale of actual waste packages and waste compounds / materials.

After the reactor accident in Fukushima (Japan) in 2011, the German Government decided to shut down immediately eight of 17 nuclear power plants. In the following, the German parliament decided with support of a broad societal consensus to terminate nuclear energy production in Germany, with the last nuclear power plant to be shutdown in 2022. Projections indicate that about a total of 17,200 tons of spent nuclear fuel will be generated by 2022. About 300,000 m^3 of low and intermediate level mostly cementitious waste are forecasted to accumulate after shutdown and decommissioning of all German nuclear power plants. The safe management and ultimately the safe disposal of radioactive waste remain grand scientific, political and societal challenges to be met in the next decades. IEK-6 research addresses a number of challenges arising from these new constraints.

IEK-6 research with respect to the **long-term safety of nuclear disposal** includes work on spent nuclear fuel corrosion and the formation of secondary phases – the radio(geo)chemistry of the deep geological repository nearfield, thus contributing to the scientific basis of the safety case. In order to study **innovative waste management strategies** IEK-6 research groups are also focusing on partitioning of actinides and the development of ceramic waste forms. The research programme is supported by a strong **"structure research"** group covering the field of solid state chemistry, crystallography and computational science to model actinide bearing compounds. Application oriented waste management concepts for special categories of radioactive waste are developed by integrating (1) the development of **non-destructive essay techniques**, for which IEK-6 is well known for decades and (2) **waste treatment procedures**. Furthermore, (3) some of this research is guided by the **product quality control group for radioactive waste (PKS)** which is operated by IEK-6 on behalf of the Federal Office of Radiation Protection (BfS) since 1987, to qualify radioactive waste packages in Germany. The IEK-6 **nuclear safeguards group** coordinates on behalf of Federal Ministry of Economics and Technology (BMWi) the German contribution to the **IAEA safeguards support programme**. JÜLICH will become a member of the **IAEA network of analytical laboratories** (qualification process started in 2013) by combining the analytical capabilities of three units (IEK-6, ZEA-3 & S) in JÜLICH. A **scientific collaboration with the IAEA safeguards laboratories** has been established to develop actinide bearing reference materials for particle analysis within the framework of nuclear forensics.

The research programme in JÜLICH is focused on radio- and nuclear chemistry aspects with a special focus on solid state / material science issues relevant for the management of nuclear waste. IEK-6 operates radiochemistry laboratories equipped with state-of-the-art analytical facilities to study atomic scale ordering phenomena and the microstructure on

different scales – sub-nanometre to micrometre. Recent instrumental upgrades / installations (last 5 years) include 2 Raman spectrometer, powder & single crystal XRD and FIB for TEM studies. A central hot cell facility (GHZ) is operated in JÜLICH in which IEK-6 uses two hot cells for spent nuclear fuel corrosion studies. One of the hot cells is equipped for in-situ Raman measurements. The computational science group relies on the JÜLICH and RWTH Aachen university infrastructure in high performance computing within the JARA (Jülich Aachen Research Alliance) High Performance Computing framework incl. the latest installation at the JÜLICH computing centre JUQUEEN.

“Material science for the safe management of nuclear waste”

1.1. Staff

80 staff members (Mai 2013)

37 scientists	15 PhD students	4 graduands
12 engineers & technicians	7 laboratory assistants	5 administration

1.2. Organization chart

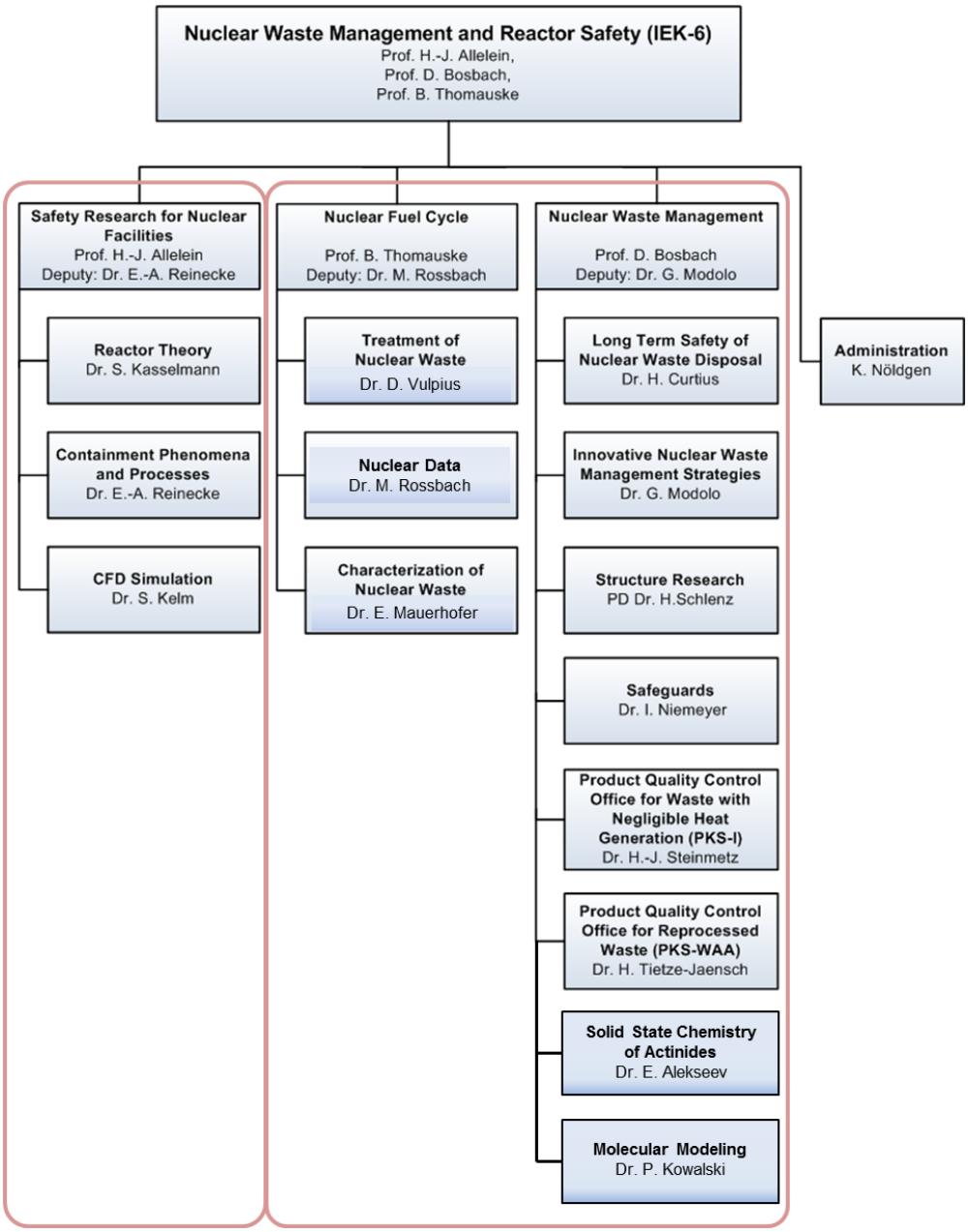

Fig. 1: Organization chart of the Institute of Energy and Climate Research (IEK-6), Nuclear Waste Management and Reactor Safety devision.

1.3. Budget

2011

Budget 2011: 9,42 M€

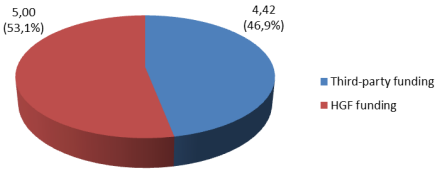

Third-party funding 2011

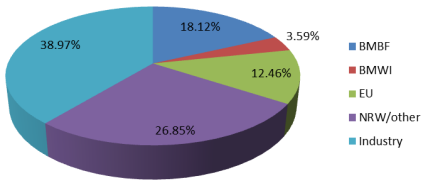

2012

Budget 2012: 9,15 M€

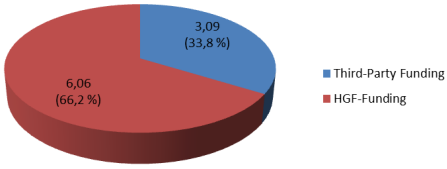

Third-party funding 2012

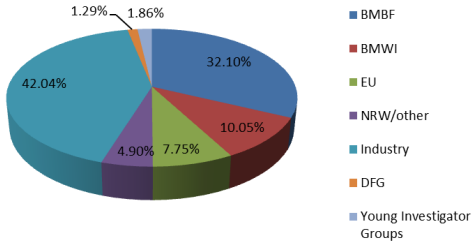

2 Key Research Topics

2.1. Long Term Safety of Nuclear Waste Disposal

The disposal of high-level nuclear waste in deep geological formations poses major scientific and social challenges to be met in the next decades. One of the key issues is related to the long term safety of a waste repository system over extended periods of time - typically time frames of up to a million years are taken into account when designing waste repositories, due to the long half-live of some of the radionuclides. There is a consensus in the scientific community that deep geological disposal offers the largest long term isolation potential - it relies on the passive safety of the geological formation. There seems also to be a consensus in the scientific community that long-term predictions regarding the (radio)geochemical evolution of a waste repository system should be guided by equilibrium thermodynamics and geochemical insights.

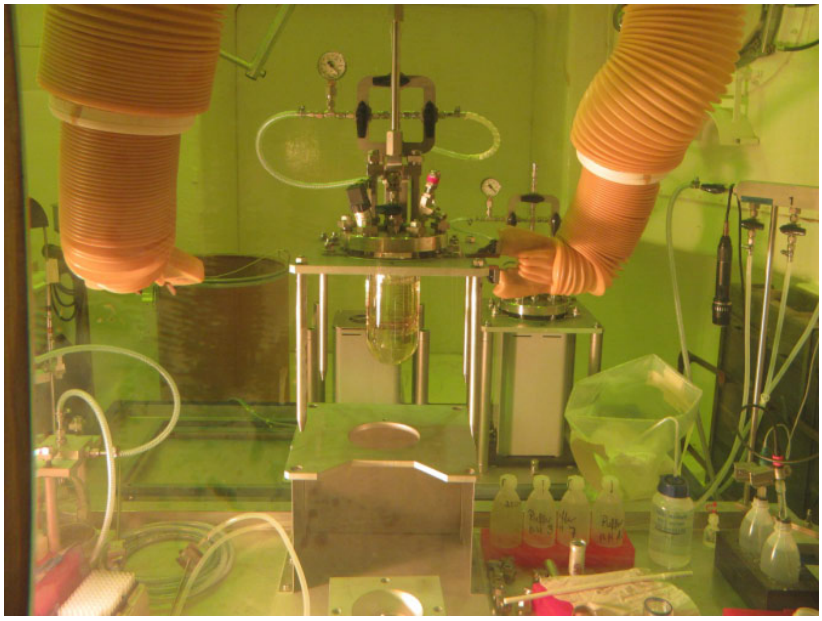

Fig. 2: Static leaching experiment with spent fuel samples in order to determine the radionuclide release fraction and to characterize the secondary phase formation by in-situ Raman measurements.

Furthermore, a molecular-level process understanding can help improving the confidence in available data on radionuclide behaviour in the geosphere beyond a simple phenomenological description.
rames of up to a million years are taken into account when designing waste repositories, due to the long half-live of some of the radionuclides. There is a consensus in the scientific

community that deep geological disposal offers the largest long term isolation potential - it relies on the passive safety of the geological formation. There seems also to be a consensus in the scientific community that long-term predictions regarding the (radio)geochemical evolution of a waste repository system should be guided by equilibrium thermodynamics and geochemical insights.

The principal way that radionuclides can be transported away from a deep geological disposal facility and towards the biosphere is in the form of dissolved species in ground water (Fig. 2).
Therefore, research at IEK-6 is focusing on the interaction of ground water with nuclear waste forms, particularly with spent nuclear fuels and the (geo)technical barriers (the so called near field of a repository system). Radionuclides may be released from the waste matrix upon interaction with ground water. At IEK-6 investigations are focused on the determination of the volatile fast/instant radionuclide release fraction. This work is embedded within the European project FIRST NUCLIDES. At the same time, corrosion products form and dissolved radionuclides may bind to these secondary phases by one or more distinct sorption reactions. The immobilisation of radionuclides by isostructural incorporation (irreversible process) in secondary phases, hence the formation of solid solutions is investigated at IEK-6 in detail. The research with respect to these solid solutions is related to: a.) derive structural models, b.) investigate physical-chemical properties under repository relevant-conditions and c.) obtain thermodynamic data. The work is embedded in three projects (SKIN, ImmoRAD, VESPA).

Contact: Dr. Hildegard Curtius
h.curtius@fz-juelich.de

2.2. Innovative Nuclear Waste Management Strategies

The R&D programme dedicated to “Innovative nuclear waste management strategies” focuses on the separation of long-lived radionuclides (minor actinides, ^{129}I, ^{99}Tc etc.) from high active waste solution (Partitioning) and subsequent conversion into ceramic materials (Conditioning).

Fig. 3: Partitioning of Minor Actinides using mixer-settler units.

Partitioning

Research on the separation of radionuclides from nuclear waste solutions is based on highly selective hydrometallurgical separation processes. For a successful separation of specific waste components, a fundamental understanding of the principles of the complexation of radionuclides in aqueous and organic extractant solution is a crucial issue. Research covers the fields of thermodynamics, hydrodynamics and kinetics of liquid-liquid extraction as well as the long-term operation of the solvent (hydrolysis and radiolysis). This includes also recycling and cleaning of the solvent and the management of secondary waste.

Highly sophisticated analytical techniques (e.g. X-ray diffraction, laser spectrometry, NMR) are used to understand the complexation and extraction mechanisms. This is now being undertaken in close cooperation with European partners under the on-going European Union project SACSESS (duration 2013-2016) and in a current project F-KOM (duration 2012-2015) funded by the German Federal Ministry of Education and Research (BMBF). This knowledge is important to develop multi-scale models to be used in a simulation code, which is an indispensable tool to operate such processes in a safe manner. The flow-sheets are tested and evaluated by comparing them with model predictions.

Conditioning

Ceramic waste forms for the immobilisation of actinides have been investigated extensively in the last few decades since they seem to exhibit certain advantages over other waste forms (incl. borosilicate glasses and spent fuel). Most on-going nuclear waste management strategies do not include ceramic waste forms. However, it still seems important to study this option, e.g. with respect to specific waste streams and certain constraints regarding deep geological disposal. Research focuses on single-phase ceramics such as Monazite and zirconium-oxide-based materials and includes:

- synthesis (sol-gel route, hydrothermal synthesis and co-precipitation),
- structural and microstructural characterisation using state-of-the-art spectroscopic/diffraction (Raman, XRD, TRLFS) and microscopic techniques (SEM, FIB/TEM),
- thermodynamic stability and reactivity under conditions relevant for nuclear disposal, in particular with respect to leaching/corrosion in aqueous environments as well as
- studies on radiation damage.

Finally, a fundamental understanding of these aspects will help to improve long-term safety assessments of deep geological disposal concepts using these materials.
This work is part of a German joint research project “Conditioning” funded by BMBF (2012-2015).

Contact: Dr. Giuseppe Modolo
g.modolo@fz-juelich.de

2.3. Structure Research

The chemical and physical properties of a material are determined by its chemical composition, chemical bonds and particularly by its structure, no matter if crystalline or amorphous materials (glasses) are investigated. According to nuclear waste management mainly ceramics and glasses are considered for the immobilization of actinides. For the purpose of understanding material properties and for the development of such new materials, knowing the structure is an indispensable prerequisite. As an example the crystal structure of the mineral monazite is determined as a function of varying amounts of Uranium (U) and Thorium (Th) using x-ray powder diffraction, in order to detect structural changes due to varying chemical composition and possible radiation damage caused by the radioactive decay of U and Th. Further candidate phases for the immobilization of actinides are e.g. pyrochlore, Ce-, U- and Th-oxides, as well as U- and Th-silicates.

At the IEK-6 structure research is performed using diffraction, spectroscopic analysis and computer simulations. X-ray synchrotron diffraction and spectroscopy experiments are performed at large research facilities like ANKA (Karlsruhe), HASYLAB (Hamburg) or ESRF (Grenoble). Neutron diffraction experiments are performed in cooperation with the RWTH Aachen, e.g. at the nuclear research reactor FRM II (Garching). To be able to examine further structural details complementary analytical methods like Raman spectroscopy (Fig. 4) and IR spectroscopy are applied. Irradiation experiments are performed using e.g. heavy ions like Kr^{+} in a Transmission Electron Microscope (TEM) at dedicated facilities in Saclay and Orsay (France). Finally, structure models are generated by computer simulations (Reverse Monte Carlo) and the radiation damage of a solid can be simulated using advanced Monte Carlo algorithms.

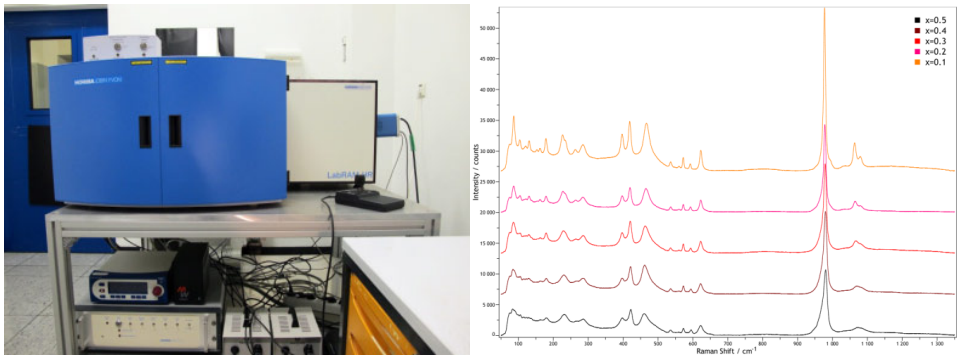

Fig. 4: Raman spectrometer (Horiba LabRAM HR) and Raman spectra of synthetic monazite-type phases with composition $Nd_{1-x}Ca_{0.5x}Th_{0.5x}PO_4$.

Contact: PD Dr. Hartmut Schlenz
h.schlenz@fz-juelich.de

2.4. Solid State Chemistry of Actinides (Helmholtz Young Investigator Group)

The actinide elements are of particular concern due to their long half-life and their high radiotoxicity. Knowledge of the stability and the reactivity of actinide compounds under conditions relevant for a waste repository system require a sound understanding of their solid state chemistry. From a solid state chemistry perspective, the actinides with their characteristic 5f electrons, exhibit an extremely complex redox and binding behaviour in particular in the solid state. The relationship between structure of actinide based materials and their properties is one of the most important questions of fundamental actinide science. The research of the proposed “Solid State Chemistry of Actinides” groups is oriented on understanding fundamental properties of actinide based solid compounds. The research includes an understanding of the formation of complex phases and their structure, thermodynamic and material properties. The priority in research is given to mineral-like and naturally occurring materials. Mostly, those phases are based on oxo-anions. State-of-the art techniques are used for structure characterization and thermodynamic characterization of synthetized phases. The work is mostly focused on U and Th but some experiments are carried out with transuranic elements (Np, Pu). The formation of materials is studied under normal and extreme conditions (high-temperature/high-pressure). The first results (2011-2012) shows significant difference between phases formation in similar systems under normal and extreme conditions. The potential behaviour of Am^{3+} and Cm^{3+} under extreme conditions is studied with using Ln^{3+} as surrogates.

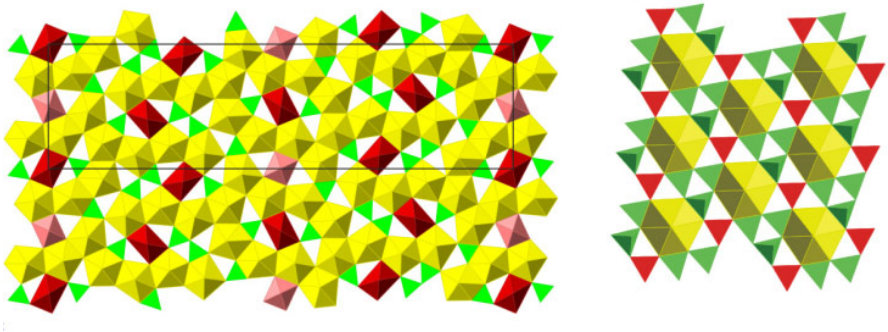

Fig. 5: Left: The complexity of layer in the structure of $K_{12}(UO_2)_{19}(UO_4)(B_2O_5)_2(BO_3)_6(BO_2OH)O_{10}\cdot nH_2O$ obtained from high-temperature/high-pressure conditions. UO_2O_4 square bipyramids are shown in red, UO_2O_5 pentagonal bipyramids are shown in yellow, UO_4O_2 (U(VI)) tetraoxide cores are shown in pink, BO_3 is green. Right: The standard layer in actinide borates obtained from low temperature reaction. UO_8 polyhedra are shown in yellow, BO_3 and BO_4 in red and green, respectively.

Contact: Dr. Evgeny Alekseev
e.alekseev@fz-juelich.de

2.5. Jülich Young Investigator Group: Atomistic Modeling

Understanding the behavior and safe management of radionuclide-bearing materials such as nuclear waste is a challenge for the nuclear technology. One of the main reasons for that is the limited understanding of the atomic-scale processes associated with the interaction of radionuclides with different materials, which also limits the availability of materials for safe storage of nuclear waste. On the other hand the continuous improvement in the performance of computers resulting in huge and progressive increase in computing power, by a factor of ~1000 per decade, opens the possibility to simulate the behavior of even complex radionuclide-bearing materials using first principle (*ab initio*) methods and such studies can provide valuable information on the chemical and physical properties of radionuclide-bearing materials. The aim of our studies is to use the world-class computing resources located at Forschungszentum Jülich and allied institutions and state-of-the-art quantum chemistry software for performing virtual experiments that could reveal crucial information on the underlying mechanisms governing the interaction of radionuclides with various materials, including these constituting the storage environment. Such computer simulations can be used for predicting the formation of new radionuclide-bearing crystalline-solids (secondary phases), investigation of their physical and chemical properties and in general for studying of the change in the materials properties upon incorporation of radionuclides. Radionuclide-bearing materials often exhibit interesting properties by forming topologically different structures that contain metals in different oxidation states or exhibiting different coordination environments, such as 7-folded coordinated Uranium in $Ba_2(UO_2)_3(PO_4)_2$ borophosphate (Fig. 6).

Fig. 6: Left: one of the electronic orbitals responsible for bonding between U atom (grey) and neighbouring O atoms (red) in $Ba_2(UO_2)_3(PO_4)_2$ borophosphate. Interaction between Uranium f orbital and Oxygen p orbitals is clearly visible. An atomic scale analysis of charge distribution provides information on the bonding environment. Right: Computer cluster at RWTH Aachen used in the investigation within Jülich-Aachen Research Alliance (JARA).

Formation of such structures and their stability can be understood through investigation of the atomic scale properties of the investigated systems such as their electronic structure. The challenge is to understand the structure-property relationship of these materials. In that aspect *ab initio* computer simulations can provide a unique insight into the atomic-scale processes responsible for structure formation. Our goal is to complement the ongoing experimental work on radionuclide-bearing materials by providing information on their electronic structure and thermodynamic stability as well as by modeling their spectra (such as Raman or IR spectra) in order to better understand behavior of these materials and interpret their measured spectral signatures. The long-term goal of such a joined theoretical and experimental studies aims at the development and characterization of new, advanced materials for safe management of nuclear waste, which could immobilize dangerous actinides elements under various different storage conditions and prevent potential leaks of dangerous elements into environment.

Contact: Dr. Piotr Kowalski
p.kowalski@fz-juelich.de

2.6. Characterisation of Nuclear Waste

Radioactive waste has to meet the specifications and acceptance criteria defined by national regulatory and management authorities. For this reason, appropriate quality control procedures have to be carried out to quantify relevant radioactive isotopes and non-radioactive toxic elements present in the waste. Within these procedures non-destructive assay techniques are preferred to minimize inspection time and to reduce the radiation exposure of personal. Furthermore, secondary waste by invasive sampling and subsequent radiochemical analysis of the obtained material will be avoided. The Waste Characterization group at IEK-6 is developing innovative passive and active non-destructive analytical techniques (Fig. 7) assisted by modern computational simulation tools for the accurate and reliable characterization of radioactive waste packages at industrial scale.
In support of method development nuclear data measurements are carried out at the FRM II reactor in Garching or the Budapest Neutron Centre (BNC) with cold and thermal neutrons and at the Nuclotron facility in Dubna, Russia, with spallation neutrons. Neutron capture cross sections of actinides, such as ^{237}Np, ^{242}Pu, or ^{243}Am will be determined to develop analytical methods based on active neutron interrogation.

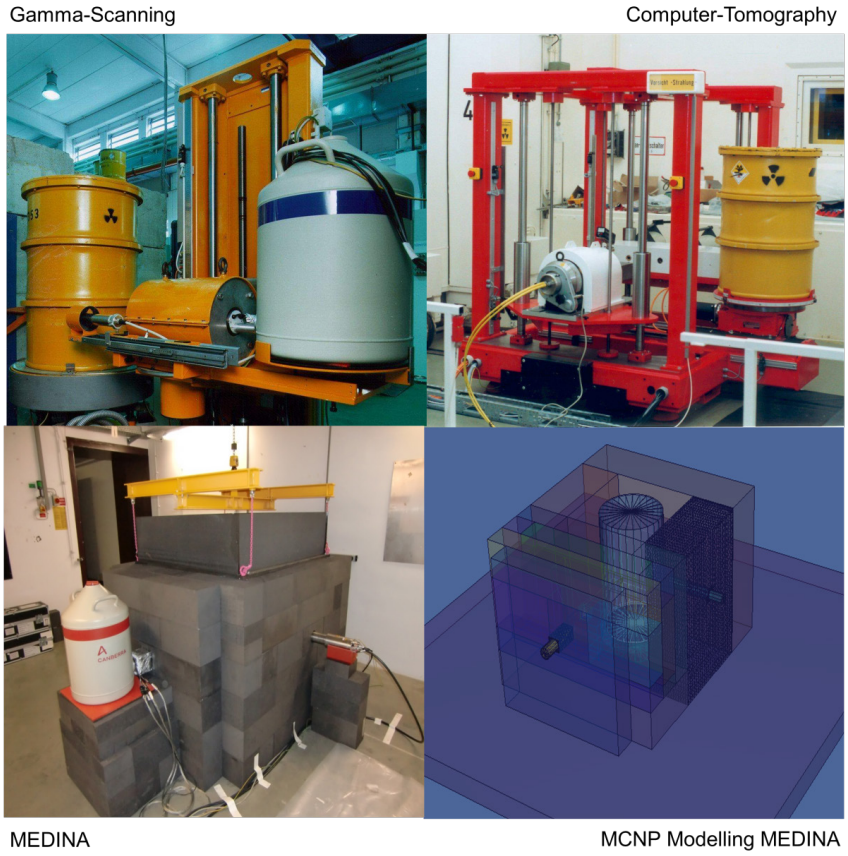

Fig. 7: Non-destructive analytical techniques: Gamma-Scanning, Computer-Tomography, and Prompt-Gamma-Neutron-Activation-Analysis (PGNAA).

Contact: Dr. Eric Mauerhofer
e.mauerhofer@fz-juelich.de

2.7. Nuclear Data for Waste Characterisation

Nuclear data of actinides, such as cross sections, energies and intensities of gamma transitions are scarce or only known with high uncertainties. Being the basic input data for any calculation of nuclear reactions, e.g. reactivity, or production rate of actinides, nuclear data should be as accurately known as possible under current experimental conditions.

Sample preparation for reactor irradiations of actinides has been optimized to yield accurately characterized targets. Small amounts of $^{237}NpO_2$ and $^{242}PuO_2$ powder and also of ^{241}Am solution (Fig. 8) were encapsulated in high purity quartz blades and irradiated at the Budapest Research Reactor and at the FRM II Reactor in Garching. By addition of small amounts of gold foil the neutron flux of the guided cold neutron beam from the prompt gamma neutron activation analysis instrument (PGAA) was determined to extract the neutron capture cross section from the activity of the (n, γ) product. In addition, partial gamma ray production cross sections of individual prompt gamma rays can be deduced. This information will help to refine nuclear data tables but also will have impact on current decay scheme evaluations. In that respect a co-operation with the Nuclear Data Group of Lawrence Berkeley National Laboratory (LBNL) was initiated. A Memorandum of Understanding for joint research in nuclear data of actinides was signed by Budapest, FRM II and Forschungszentrum Jülich to enhance the capabilities of experimental investigations using PGAA for actinide nuclear data.

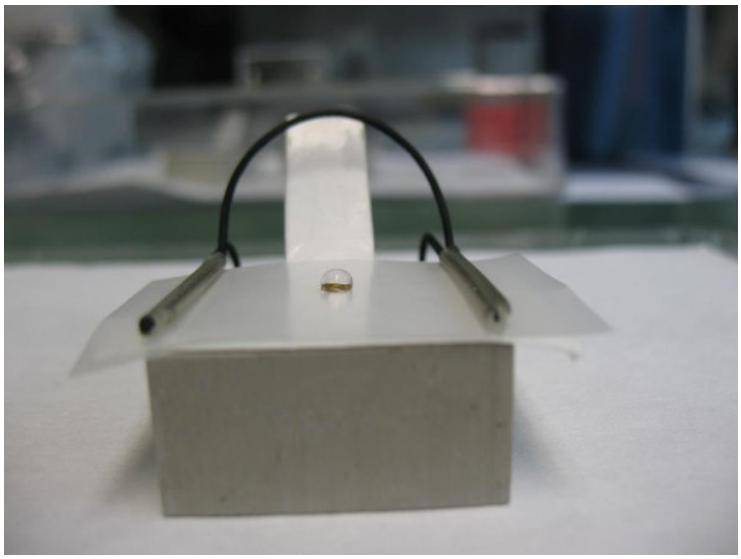

Fig. 8: A drop of ca. 5 MBq ^{241}Am on a 3 mm diam. gold foil (0.45 mg) on a 0.2 mm thick Suprasil© quartz blade (40x40 mm). (Picture: PTB Braunschweig).

Contact: Dr. Matthias Rossbach
m.rossbach@fz-juelich.de

2.8. Nuclear Waste Treatment

The application of radionuclides in science, health care and industry generates radioactive wastes which have to be collected, treated and finally disposed. Radioactive wastes are materials which consist of a non-radioactive base material which is contaminated with one or more radionuclides.

The main aim of the research activities in the Nuclear Waste Treatment Group of IEK-6 is the investigation of the chemical structures which radionuclides form in non-radioactive waste matrices. With this knowledge, methods for the nuclear decontamination of these waste matrices can be developed. Waste matrices decontaminated in such a way can be reused for new technical applications or disposed in a more favourable strategy. The removed radionuclides are also interesting if they can be separated from the nuclear waste in a highly enriched form. Such radionuclides like tritium (^{3}H) and radiocarbon (^{14}C) are commercially requested materials which are more and more difficult to provide on the international markets.

At present, the main intention of our research activities is the development of treatment methods for neutron-irradiated nuclear graphite. Nuclear graphite is high-purity graphite which was used in nuclear reactors as neutron moderator and neutron reflector. Radionuclides like ^{3}H and ^{14}C were formed in this graphite by interaction of neutrons with impurities which are present in high-purity graphite, too. These radionuclides can be removed from the graphite matrix, e.g. by thermal treatment. Afterwards, the removed radionuclides as well as the decontaminated graphite can be used for further applications.

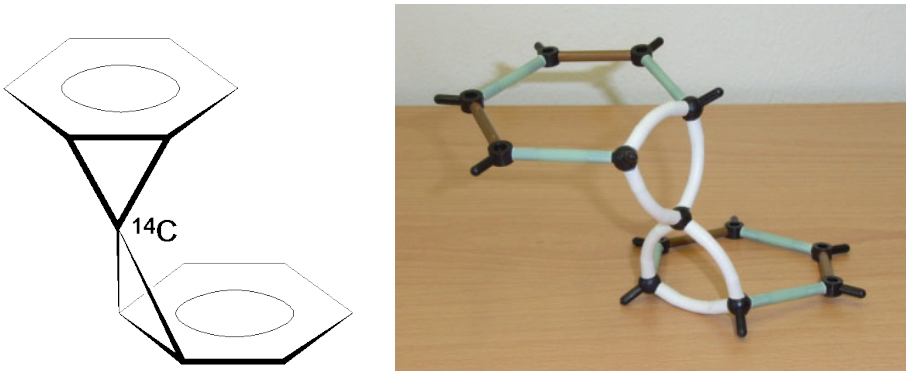

Fig. 9: Simplified model of a ^{14}C interstitial atom in graphite (spiropentane structure).

Contact: Dr. Dirk Vulpius
d.vulpius@fz-juelich.de

2.9. International Safeguards

Safeguards are activities by which the International Atomic Energy Agency (IAEA), in accordance with the Nuclear Non-Proliferation Treaty (NPT), can verify that a State is in compliance with its international commitments not to use nuclear programmes for nuclear-weapons purposes. The NPT requires the Member States to cooperate with the IAEA in order to facilitate the application of safeguards in these States. On this basis, the IAEA and the German Government agreed upon the “Joint Programme on the Technical Development and Further Improvement of IAEA Safeguards” in 1978. Since summer 1985, the Forschungszentrum Jülich has coordinated the programme implementation in close cooperation with the German Government, represented by the Federal Ministry of Economics and Technology (BMWi). Since May 2009, IEK-6 has been in charge of coordinating the German Support Programme (GER SP) to the IAEA within Forschungszentrum Jülich.

Recent tasks of the GER SP (about 30 in 2012) focus on the implementation of containment and surveillance systems (NGSS, EOSS), development and implementation of measurement methods and techniques for the non-destructive (DMCA, HM-5) and destructive analysis of nuclear materials and environmental samples (LIBS). Other tasks enhance geoscientific methods and techniques for safeguards purposes, such as seismic and acoustic measurements for detecting undeclared activities at geological repositories, satellite imagery processing and geoinformation tools. Using mathematical models, procedures for estimating optimal inspection strategies as well as for supporting IAEA’s State level concept (acquisition path analysis) were developed.

Besides scientific management of the GER SP, the group also carries out R&D in three areas: Satellite imagery processing, acquisition path analysis and safeguards analytics.

Firstly, the use of remote sensing in support of nuclear non-proliferation and arms control regimes is being investigated. Particular attention is given to the development of object-based and non-coherent approaches for detecting and classifying changes in very high resolution optical and high resolution SAR satellite imagery respectively. IEK-6 is partner within the European Copernicus initiative, aimed at establishing a European capacity for Earth Observation.

Secondly, tools for better implementing State-level safeguards are being developed. One important tool is the acquisition path analysis (APA) which is to be improved with regard to methodology, automation and visualization. By analyzing all plausible paths that a State could consider in order to acquire weapons usable material, APA is expected to help allocating safeguards measures and inspectorate’s resources for the particular State.

Thirdly, IEK-6 cooperates with the IAEA Safeguards Analytical Service on the development and advancement of analytical techniques. A joint research project is dedicated to the production and characterisation of particles for quality assurance and quality control. As the availability of monodisperse uranium- and plutonium-containing particles with well-defined properties such as size, density, elemental and/or isotopic composition is limited so far, the project intends to assist the IAEA in acquiring particle reference materials.

In February 2013, the German Federal Ministry of Economics and Technology nominated Forschungszentrum Jülich as a candidate laboratory for the IAEA’s Network of Analytical Laboratories (NWAL) for destructive analysis of nuclear materials. The scope of the analysis to be performed by IEK-6 together with Central Division of Analytical Chemistry (ZCH) and Safety and Radiation Protection (S) will cover the analysis of uranium based materials and matrices and special analyses. The qualification process involves several steps and has a projected time-frame of 2 years.

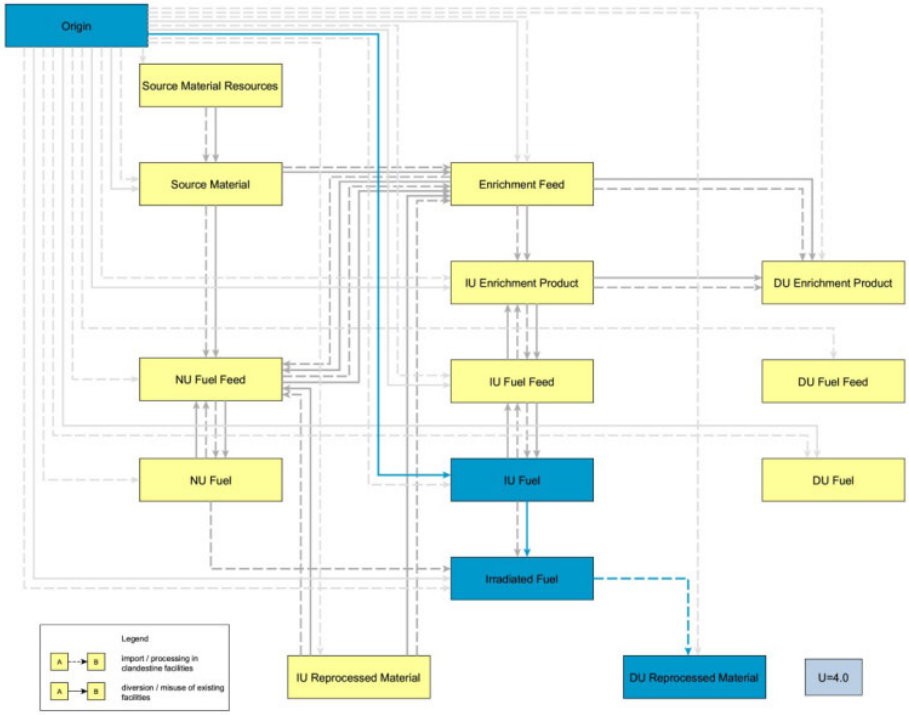

Fig. 10: One typical Acquisition Path for a particular State with high technical capabilities but without declared reprocessing facilities. The path consists of three steps: diversion of indirect use fuel from declared stock, misuse of an existing declared reactor to irradiate the fuel and reprocessing in an undeclared facility of the irradiated fuel to obtain weapons usable plutonium. The path has an unattractiveness score of 4.0 leading to rank 49 out of 1043 paths in the list of the most attractive paths for the given State.

Contact: Dr. Irmgard Niemeyer
i.niemeyer@fz-juelich.de

2.10. Product Quality Control of Radioactive Waste & Packages

Introduction

Product Quality Control is the examination of radioactive waste to “verify the compliance of waste properties with the acceptance criteria of a repository” (DIN 25401-9).

Already in the year 1985 the Product Quality Control Office for Radioactive Waste (PKS) has been installed at the Institute for Energy Research (IEK-6) on request of the German Federal Office for Radiation Protection (BfS). PKS advices and supports the BfS on the basis of §20 ATG (German atomic act) as an independent consulting expert group to verify the compliance of radioactive waste properties with repository relevant acceptance criteria. PKS renders expertise on technical methods for the conditioning and packaging of radiological waste and checks product quality control plans to be appropriate for the conditioning and disposal purposes. Moreover, PKS inspects reprocessing and conditioning plants, audits radwaste manufacturers and checks waste package inventory declarations and accompanying documentation prior to final disposal for the compliance with the required specifications and applicable relevant inventory limits. PKS also examines and assesses the methodological and analytical methods applied by the waste manufacturer. A large amount of PKS activities comprises the product quality control of radiological waste from the decommissioning of nuclear facilities, like phased-out nuclear power plants. The effect of product quality control contributes significantly to the safety of a nuclear waste repository.

Hosting the Product Quality Control Office for radioactive waste in Germany at the institute IEK-6 underlines its position in the field of waste characterization and in the evaluation of the long-term safety properties of radioactive waste to be acceptable for a repository in Germany.

PKS is organized two-fold:

1.) **PKS-WAA** is the sole group of experts authorized by BfS for the quality control of high- and medium-active nuclear waste from reprocessing facilities abroad (La Hague, France, and Sellafield, UK) and from the domestic high-level vitrification plant VEK of WAK Karlsruhe.

2.) **PKS-I** provides expertize for the BfS in the field of low- and medium-active German domestic waste from nuclear power plants, research institutions and Federal State Collecting Facilities to be characterized and prepared for final disposal. Basis for the quality control of waste & waste packages are the LAW/MAW waste repository KONRAD waste acceptance criteria. This geological repository should be in in the near future.

2.10.1 Product Quality Control of Radioactive Waste – High Level Waste from Reprocessing

High-level radioactive waste requires specific care and attention for its very long-term and high radiotoxic potential. No decision on a conceivable “direct disposal” path for merely untreated high-level waste has yet been made in Germany. However, spent fuel dissolution for reprocessing has been employed until 2005, and still today residual vitrification methods are being used for the appropriate conditioning of high level waste from spent fuel of German nuclear power plants.

The expected result of nuclear waste product quality control is that all radioactive waste residues can be disposed of safely over a very long period of time. This is achieved by threefold tasks of the PKS-WAA team:

1.) **Waste conditioning process qualification:** to assess and evaluate the production processes applied to produce waste residues compliant with the officially approved waste properties and repository acceptance criteria.
2.) **Production process inspection and manufacturer’s auditing:** to make sure that all production is performed orderly within the production process guidelines and that only conform waste packages compliant with the well-defined product properties and repository acceptance criteria are being produced and prepared for their final disposal in Germany.
3.) **Documentation checking:** to assess all the documentation to accompany the waste residue packages and to check if all nuclear inventory declarations are correct, comprehensive and complete.

The PKS-WAA team, which are currently three scientists, two engineers, two Ph.D students and a project assistant, reports directly and solely to the authority in charge, the Federal Office for Radiation Protection (BfS). All reprocessing and vitrification of high-level waste residues and proportionate conditioning of the by-products are conformed in fully quality assured production processes at the reprocessing sites in La Hague in France, Sellafield in the UK and a domestic site at the WAK in Karlsruhe.

Fig. 11: Left: Documentation to verify the repository relevant properties. Right: Containers filled with vitrified and compacted waste.

Contact: Dr. Holger Tietze-Jaensch
h.tietze@fz-juelich.de

2.10.2 Product Quality Control of Low and Intermediate Level Radioactive Waste (LAW/MAW)

Radioactive waste products and waste packages have to be in compliance with the technical acceptance requirements for the German waste repository KONRAD. Repository-relevant features, radionuclide inventories and related activities as well as container parameters have to be documented and are checked by the independent experts of PKS-I.

LAW/MAW arises from nuclear power production, nuclear industry, research, medicine and technology as well as from the dismantling of nuclear installations. Accordingly, conducting a thorough and competent control and evaluation demands integrated competence in various scientific and engineering special fields. Often various technical details, complex issues and inter-relations as well as vast quantities of data have to be understood, analyzed, checked and evaluated by PKS-I. The results are summarized in written expert reviews and evaluation reports.

In executing its tasks as a federal expert group the PKS-I in many ways is corresponding with waste producers, waste conditioning or interim storage facilities and nuclear companies, as well as nuclear licensing and supervisory authorities or government ministries of the individual German Federal States. Concerning the incineration of German LAW the control activities of PKS-I are not only limited to domestic plants but also include audits or inspections in foreign facilities, at present in France and Belgium and forthcoming in USA. Moreover, many radioactive isotopes or sealed sources used in Germany have been produced in the former Soviet Union. To be able to evaluate the completeness or reliability of corresponding waste declarations PKS-I maintains close links also to Russian organizations, in particular to Rosatom, JSC Isotop, and SIA 'RADON' (Moscow).

As a multidisciplinary group PKS-I in 2012 consisted of nine scientists and engineers assisted by one office administrator. The lean management organization of PKS-I is divided into two areas of activity focusing either on "conditioning process qualification and documentation" or on "nuclear technology, nuclear reactors and computation".

Fig. 12: Left: KONRAD repository. Right: Container for KONRAD.

Contact: Dr. Hans-Jürgen Steinmetz
h.j.steinmetz@fz-juelich.de

3 Facilities

The institute operates several radiochemical laboratories (750 m^2) for experimental work with radioactive material including alpha emitters (actinides). About 500 m^2 are licensed according to the German Atomic Energy Act which permits the handling of nuclear fuels. One part of the controlled area is used for the development of non-destructive characterisation methods for radioactive waste applying neutron sources. In addition to the radiochemical laboratory equipment, the controlled area provides glove boxes which enable the handling of radioactive materials. Furthermore, analytical instruments, such as α-, β-, and γ-spectrometry, as well as x-ray diffraction, Raman spectroscopy and electron microscopy are available.

3.1. Single Pass Flow Through Experiments (SPFT)

New single-pass flow through experiments (SPFT) were established in 2012 at the IEK-6 as part of the corrosion laboratory. SPFT are the most commonly applied dynamic type of experiments to determine dissolution rates of nuclear waste. The SPFT set up prevents the progressive accumulation of reaction products which may affect the element release rate. During the experiment, a continuous flow of fresh influent solution keeps up constant, well defined chemical conditions within the flow-through reactor.
Two different types of SPFT experiments were set up, (1) SPFT for the temperature range between room temperature and 90 °C and (2) a pressurized SPFT setup for temperatures above 100 °C (Fig. 13, right). Around 20 SPFT experiments which mainly consist of PFA and Teflon parts are now simultaneously run in order to systematically explore the dissolution kinetics of phosphate and zirconia based ceramic waste forms.

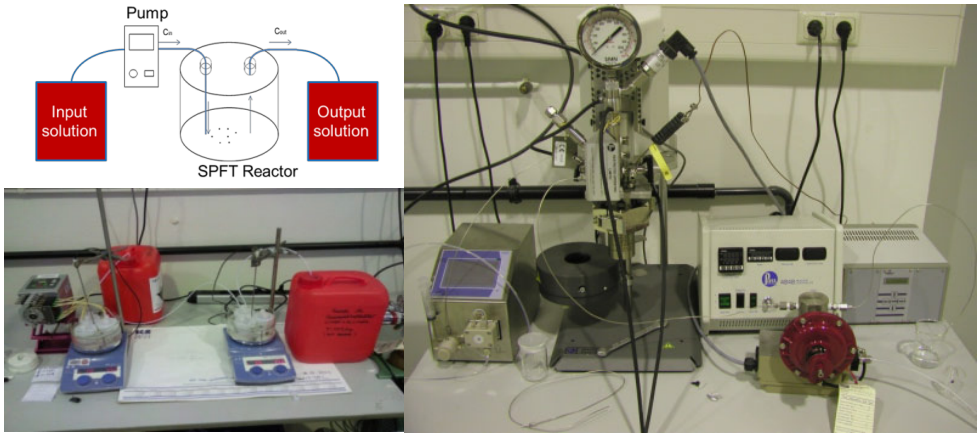

Fig. 13: Left: Working principle of SPFT-experiments and PFA-based set-up. Right: pressurized SPFT experiment for high-temperature experiments.

In addition, a titanium and PEEK based setup is used to carry out experiments above 100 °C (Fig. 13, right). The setup consists of a pressurized titanium mixed-flow reactor, a high-performance pressure HPLC pump (p_{max} = 60 bar) and a computer controlled high precision outlet valve which is automatically opened and closed according to a set pressure within the titanium reactor. Thus, a constant fluid flow can be guaranteed although the solution flowing into the reactor is at room temperature and the solution flowing out of the reactor may well be above 200 °C. During the experiments, the pressure can be adjusted to keep the water below the boiling point, ensuring a well-defined contact between the aqueous solution and the nuclear waste form.

3.2. X-ray Diffraction Analysis

The IEK-6 runs the Single-crystal X-ray diffractometer which is equipped with the state-of-the-art SuperNova system (Fig. 14, left). It has a multi-layer X-ray optics (CuKα and MoKα). The SuperNova combines high intensity Nova X-ray micro-source with the 165 mm fast, high performance Eos™ CCD detector. Mounted on a 4-circle goniometer (Fig. 14, right), the copper radiation Nova X-ray source provides up to 3x the intensity of a 5 kW rotating anode generator with optics and the data quality of a micro-focus rotating anode. Additionally, the SuperNova goniometer has been designed to accept all major open flow cryogenic sample cooling device, including CryojetJet (Oxford Instruments) liquid nitrogen device (90 – 500 K). With this equipment we are able to provide a full structural characterization of radioactive single crystals including very small objects (up to 10-15 microns) in wide temperature range.

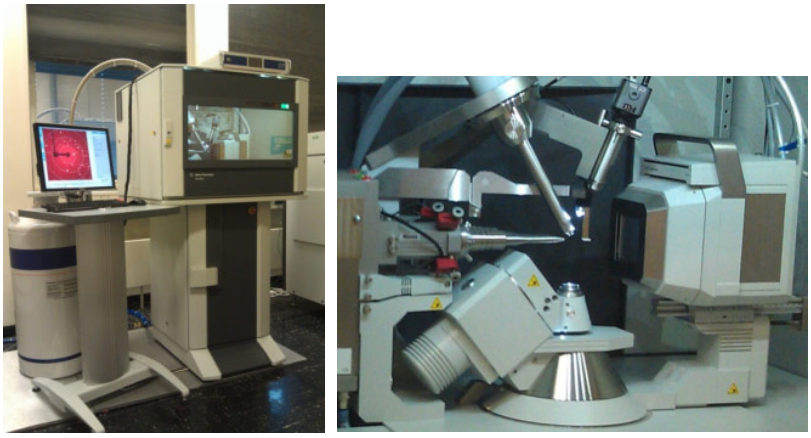

Fig. 14:Left: The complete SuperNova system. Right: The View of the SuperNova goniometer.

The IEK-6 also runs two Bruker x-ray powder diffractometer. The first one (D8) is equipped with a copper tube (Cu K_α), a molybdenum tube (Mo K_α) and two suitable detector systems (scintillation counter and Si semiconductor detector), in order to perform X-ray diffraction analysis on crystalline, semi-crystalline and amorphous samples. Radioactive and non-radioactive powder samples can be measured. Additionally, a climate chamber is available on request that enables *in situ* measurements at different atmospheres and humidities and at temperatures up to 250°C.

The second diffractometer (D4) is equipped with a copper tube (Cu Kα) and a multi-sample stage (66 samples) as well as with a fast LynXEye detector, appropriate for high throughput measurements. The D4 can also be used for any kind of analysis, with the exception of radial distribution function determination and *in situ* measurements using the climate chamber.
In principle all kinds of analysis can be performed by the structure research group according to x-ray diffraction: qualitative and quantitative phase analysis, cell constant determination, structure analysis, structure refinement (Rietveld) and the determination of radial distribution functions are possible.

3.3. Hot Cell Facility, GHZ

On 17th September 2012 the IEK-6 started a leaching experiment with spent fuel samples in the working hot cell (number 601) located at the hot cell building (GHZ).
In Fig. 15 the closed autoclave system with the fuel sample immersed in groundwater is shown. Raman spectroscopy is used to identify the secondary phases formed due to corrosion processes of the fuel sample. For that reason the Raman instrument is attached to a fibre-optic connected to a Raman sensor which is located in the hot-cell. In-situ measurements of the fuel sample can be directly performed. Through a special inlet at the autoclave lid the Raman sensor can be inserted while the distance to the fuel surface can be varied manually. In Fig. 15 the Raman equipment in front of the hot cell is visible.

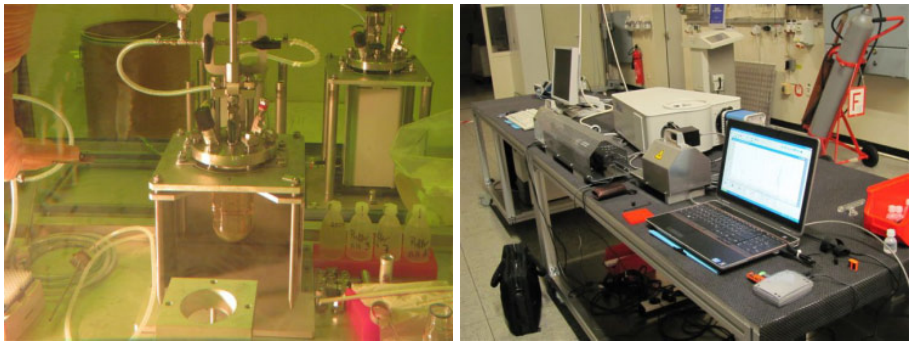

Fig. 15: Left: Autoclave with fuel sample. Right: Raman equipment located in front of the hot cell.

3.4. Raman Spectroscopy

Horiba raman spectrometer LabRAM HR Vis (400 – 1100 nm), currently equipped with a He-Ne laser (wavelength λ = 633 nm, visible red light), a Diode laser (wave length λ = 785 nm, NIR), an edge filter, two gratings (600 and 1800), focus length 800 mm, a peltier cooled solid state detector, five objectives (x10, x50, x100, x50 NIR, x100 NIR), a safety energy supply system, a safety box for the microscope and a video camera for sample observation using reflected or transmitted visible light.

3.5. Gas Chromatography

The new gas chromatograph system consists of two PerkinElmer Clarus 580 devices (Fig. 16). One device is equipped with a packed column for measuring larger quantities of gases and the other device is equipped with a capillary column for measuring smaller quantities of gases. In addition, the system is equipped with a radiation detector for measuring radioactive gases. Our system is particularly designed for measuring gaseous samples. Gaseous samples, for example, arise from radioactive waste. An objective of our institute is to determine the chemical and radiological composition of such gaseous samples.

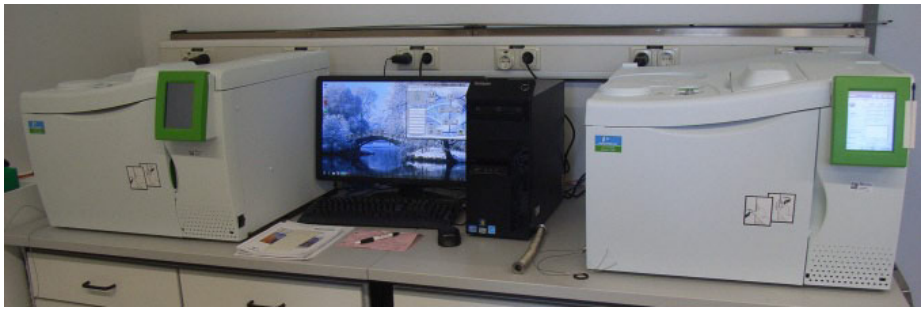

Fig. 16: Gas chromatograph PerkinElmer Clarus 580.

3.6. Electron Microscopy

- **ESEM (Environmental Scanning Electron Microscope)**
  - Quanta 200 F from FEI: high resolution field emission SEM
  - High/low vacuum, and ESEM: up to 2700 Pa: Investigation of wet samples at ESEM-mode
  - Detectors: Everhart Thornley SE-detector (high vac.), Gaseous large field SE-detector (low vac.), BSE-detector (high/low vac.), Gaseous analytical detector (GAD) BSE-detector (low vac.), Gaseous secondary electron detector (GSED) (ESEM)
  - EDX: Apollo X Silicon Drift Detector (SDD) from EDAX
  - WDX: TEXS LambdaSpec from EDAX

- **FIB (Focused Ion Beam)**
  - NVision 40 Cross Beam Workstation from Zeiss
  - High resolution field emission GEMINI SEM
  - High performance SIINT zeta FIB column
  - Gas injection system
  - Detectors: In-column: EsB detector with filtering grid for BSE detection; In-lense: SE detector; chamber: Everhardt Thornley SE detector, 4Q BSE detector, GEMINI® multimode BF/DF STEM (Scanning Transmission Electron Microscopy) detector.
  - EDX: INCA energy dispersive x-ray spectroscopy from Oxford Instruments
  - EBSD: Nordlys II Electron Backscattered Diffraction detector from Oxford Instruments.

3.7. Non-destructive Assay Testing

Segmented Gamma-Scanner GERNOD II.

The Segmented Gamma-Scanner GERNOD II is used for the characterization of 200-L or 400-L drums radioactive waste with wide range of matrices and isotopic compositions. The Gamma-Scanner consists of a mechanical part, a control unit, a detection system and a system unit and operator interface. The mechanical system consists basically of a turntable to accommodate different waste drums (max. weight 6000 kg) and a platform for the vertical movement of the gamma detection and collimation unit. The driving units comprise stepping motors with superior positioning capabilities. The positioning of the drum and detector is handled by a SPS control unit. This offers superior positioning capabilities together with highly reliable performance and control of the system status. Scanning programs are performed either continuously (fast measurements) or in a step by step mode (long time measurements). The detection of gamma emitting nuclides is performed by an HPGe detector connected to a digital spectrometer for signal processing and data acquisition. The detector can be used together with different collimators depending on the type of application. A dose rate meter is attached to the detector to record the dose rate at the surface of the drum over the whole assay period. All routine operator interactions are carried out via a PC-based control system using the software SCANNER32 developed in cooperation with a professional software engineering company for ease operations and reliable data handling.

Transmission and Emission Tomography System

The Transmission and Emission Tomography System developed at IEK-6 is an advanced tool for the characterization of 200-L radioactive waste drums. The radiation emitted from a ^{60}Co transmission source (200 GBq in DU shielding) is collimated in the direction of 4 fast scintillation detectors located in the detector collimation shielding bank to perform 4 transmission measurements at the same time. Meanwhile, the 3 HPGe-detectors are used for the emission measurements of the waste drum. An irradiation of these detectors by the transmission source is avoided by the source and detector collimation. Two stepping motors move the drum horizontally and rotate it between two measurement steps respectively. On the data collected for each measurement a pulse height analysis is performed. This leads to the basic data sets for the algorithms used for Transmission Computer Tomography, Emission Computer Tomography and Digital Radiography.

MEDINA

MEDINA (Multi-Element Detection based on Instrumental Neutron Activation) is an innovative analytical technique based on prompt and delayed gamma neutron activation analysis for non destructive assay of 200-L waste packages.

3.8. Radiochemical Analytics

- **LSC (Liquid Scintillation Counter):**
  - Analysis of aqueous and organic samples
  - Quantulus (PerkinElmer), Autosampler, Ultra low activity determination, determination of environmental activity (^{14}C), α,β discrimination
  - TRI-CARB 2020 (PerkinElmer) Autosampler > 100 samples

- **α-spectrometry:**
  - Qualitative and quantitative analysis of α-emitter, Si-detector, low level detection

- **γ-spectrometry:**
  - HP Ge-detector (N_2-cooled), NaI-detector, LaBr-detecor, Radionuclide detection with low γ-energy (^{55}Fe: E_γ < 5.9 kEV), low level detection, borehole detector

3.9. Miscellaneous

- ICP-MS ELAN 6100 DRC (PerkinElmer SCIEX)
- STA 449C Netzsch
- FTIR-spectrometer: Equinox 55 (Bruker), KBr-pellets, ATR (attenuated total reflection), TGA
- Dilatometer DIL 402C (Netzsch)
- Induction furnace (Linn High Therm GmbH), max. temperature 2500 °C, mass spectrometer for analysis of combustion gases
- High temperature furnace HTK 8 (GERO GmbH), max. temperature 2200 °C
- BET AUTOSORB-1 (Quantachrome Instruments)
- Spectral photometer CADAS 100
- Granulometer CILAS 920
- Autoclaves
- Gas chromatography (Siemens AG)
- Vacuum hot press HP W 5 (FCT Systeme), max. temperature 2200 °C, press capacity max. 50 kN, 5 x 10^{-2} mbar

4 Scientific and Technical Reports 2011/2012

4.1. UO_2 spent fuel – microstructure and radionuclide inventory

H. Curtius, E. Müller , H. W. Müskes, M. Klinkenberg, D. Bosbach

Corresponding author: h.curtius@fz-juelich.de

Abstract

Spent UO_2 fuel samples produced for High Temperature Reactors (HTR) are used by the IEK-6. The investigations focus on the determination of the fast/instant radionuclide release fraction with respect to the high burn-up of these fuel samples. In order to gain information of the microstructure, which has an enormous impact on the release rates, a triple-coated isotropic fuel particle (TRISO coated particle) was grinded and polished. Subsequently the obtained polished specimen was investigated with ESEM (Environmental Scanning Electron Microscope). Big pores and metallic islands were visible. An elemental mapping was performed and the elements Cs, Xe, Mo, Zr, U, O, Si and C were identified clearly. As expected the volatile elements Cs and Xe were mainly detected in the surrounding buffer.
Another ESEM investigation was performed with the fuel kernel itself. Big grains but small pores were visible at the periphery. The metallic islands were visible as hexagonal platelets and contained the elements Zr, Tc, Mo.
In order to gain information of the radionuclide inventory first a gamma spectrometric measurement of an intact TRISO coated particle was performed. The activities of the elements Cs, Eu, Cer, Ru, Sb, Rh, Pr and Am present in the coated particle were determined and the measured values were comparable to the calculated values. To distinguish clearly between the elemental distribution within the fuel kernel and the coatings a selective cracking process and a separation step was developed. The fuel kernel and the coatings were dissolved respectively leached and the solutions obtained were analysed by different analytic tools. From the results obtained the elements Am, Pu, U, Eu, Cer, Cm, Pr, Sr and Tc were located quantitatively within the kernel. The behaviour of the element Cs was extremely different. Due to the low oxygen potential during irradiation a significant Cs release (95%) from the fuel-kernel to the buffer/iPyC layer took place.

Introduction

In the 1980s a program started with a modern, low enriched UO_2 TRISO-coated particle system coupled with high-quality manufacturing specifications designed to meet new HTGR plant design needs. The manufacturing of high-quality spherical fuel elements containing low enriched UO_2 TRISO coated fuel particles was performed during the time period 1980 to 1988. Five production lines (GLE-3, Phase 1, GLE-4/1, GLE-4/2 and Proof Test) were performed by NUKEM Technologies GmbH, Germany. In total 59400 spherical fuel elements were produced. The low enriched UO_2 fuel kernels produced for the high-quality fuel particles in the German Fuel Development Program were based on a modified sol-gel, external gelation microsphere fabrication process development by NUKEM Technologies and known as the gel-precipitation process [1].

At the High Flux Reactor in Petten an experiment was performed which was called HFR-EU1bis [2]. Five fuel pebbles from the German production AVR GLE-4/2 were used. These fuel pebbles had a diameter of 60 mm and mainly consist of graphite. Each fuel pebble contained about 9560 so called TRISO coated particles with 502-micron diameter UO_2 kernels, having 16.76 ^{235}U wt% enrichment; coating thickness were approximately 92, 40, 35 and 40 micron for porous carbon buffer, inner dense pyrocarbon layer (iPyC), silicon carbide (SiC) and outer dense pyrocarbon layer (oPyC) (Fig. 17). A coated particle represents a miniature fuel element of about 1 mm in diameter.

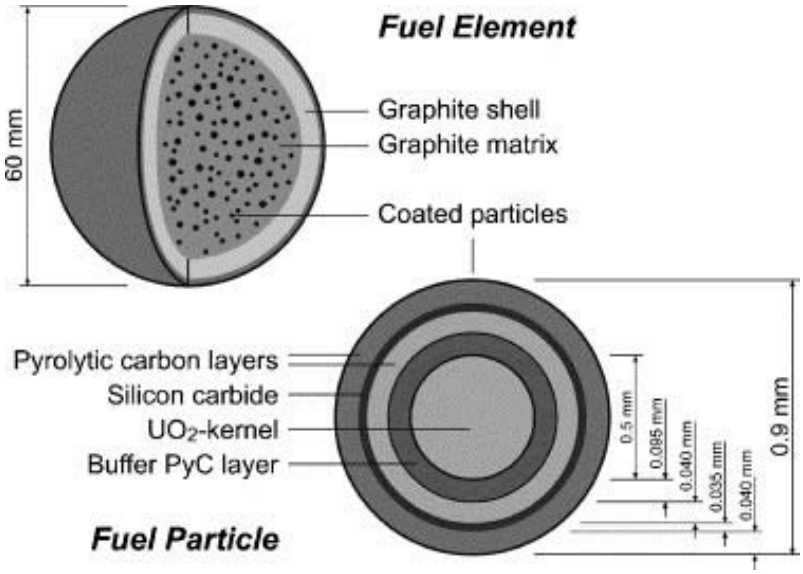

Fig. 17: Design of a fuel element and a TRISO coated fuel particle.

The irradiation of the fuel pebbles at the High Flux Reactor in Petten started on 9 September 2004. After 249 full effective power days the experiment was terminated on 18 October 2005. For the pebble HFREU1bis/2 a burn-up of 10.2 % FIMA was determined. More experimental details are given in [3].
From the pebble HFR-EU1bis/2 TRISO coated particles were isolated and send to the Forschungszentrum Jülich in December 2011.

1. Microstructure investigations of the spent fuel sample before leaching

A TRISO coated particle was embedded in a resin (Araldit DBF CH and Aradur HY 951) under vacuum. After 48 h a grinding and polishing process was performed. The wet grinding process was performed using sandpaper (SiC type, 35 µm and 22 µm). As last step a wet polishing of the sample was performed with sandpaper (SiC-type, 5 µm). In Fig. 18 (right) a polished specimen embedded in the resin is shown.

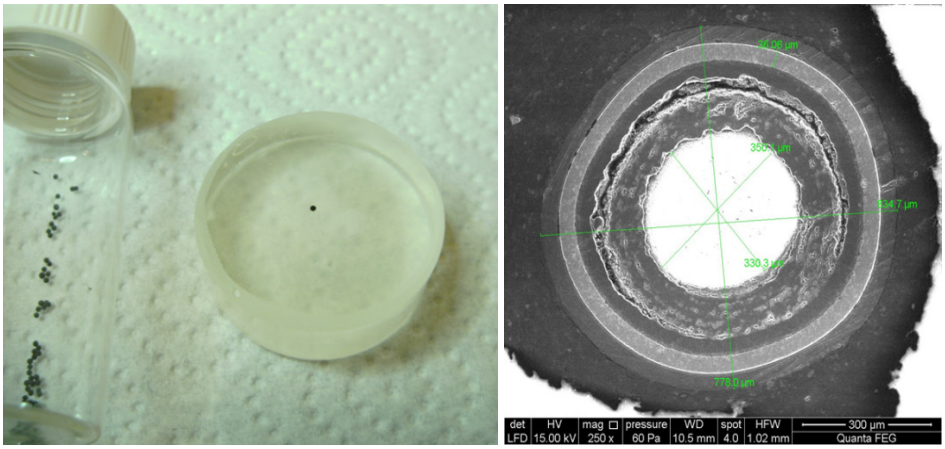

Fig. 18: TRISO coated fuel particle embedded in resin (left) and polished TRISO coated fuel particle (SEM).

The so prepared sample was then investigated with an environmental scanning electron microscope (ESEM).
In Fig. 18 (left) the SEM photo of the polished irradiated TRISO coated particle is shown. The polishing step was performed till the UO_2 kernel was 350 µm in diameter. Clearly the three tight coatings are visible. Due to the pressure build up during the irradiation period the porous buffer of the CP was pressed and a gap did form.
The UO_2 surface of the polished specimen itself is covered with big pores (up to 20 µm in size) and many metallic inclusions are visible (results from an elemental mapping did indicate the presence of Mo up to 8.4 wt%).
In the region between kernel and buffer a high accumulation of the fission gas Xe and the element Cs was determined indicating their high volatility. For the whole UO_2 kernel-surface the elements C, O, Si, U, Zr, Mo and Cs were identified clearly.
Besides the polished specimen investigations were focused on the microstructure of the periphery of the fuel kernel itself. A crack process was started using a modified micrometer screw and a self-constructed sample device. It was possible to separate the coatings from the fuel kernel selectively. For the fuel-kernel large grains (up to 112 µm) are visible clearly (Fig. 19 (right)). The elemental mapping revealed the presence of the following main elements: C 34.30 wt%, O 6.79 wt%, Zr 0.79 wt%, Mo 4.82 wt%, Tc 2.02 wt%, U 48.29 wt%, Cs 1.24 wt%. Nice metallic islands as hexagonal platelets (average size approximately 3 µm) are visible (Fig. 19 (left)) at the periphery and an elemental mapping reveal the presence of Mo 20.35 wt% , Zr 3.12 wt% and Tc 5.13 wt%.

2. Radionuclide inventory

The radionuclide inventory was calculated with the OCTOPUS code [3] after a cool-down period of 1749 days after end of irradiation on 18th October 2005. In Tab. 1 the main radioisotopes and their activities for a coated particle (CP) are summarized. In order to compare these calculated values to measured values a gamma spectrometric measurement was performed. The irradiated TRISO coated particle was placed in a polyethylene tube, closed and the measurement was started.

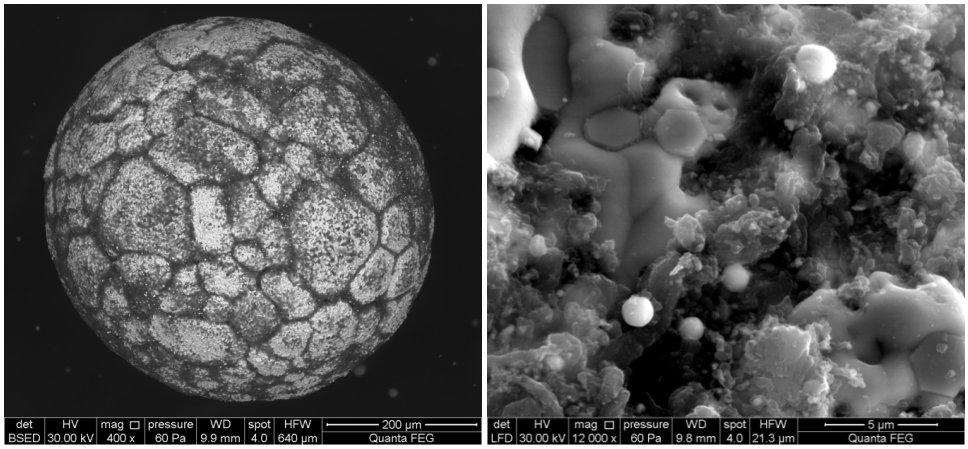

Fig. 19: View of the UO_2 fuel kernel (left) and metallic precipitates as hexagonal platelets (right).

The uncertainties of the values obtained are in the range between 10 to 13 %.The measured activities fit the calculated values quite well. After the gamma spectrometric measurement of the CP (coated particle) a crack process was started using a modified micrometer screw and a self-constructed sample device. It was possible to separate the coatings from the fuel kernel selectively. The coatings were placed in a 20 mL polyethylene vial. Then 10 mL Thorex reagenz (mixture of 13 M HNO_3, 0.05 M HF and 0.1 M $Al(NO_3)_3$ x 9 H_2O) was added and leaching was performed for 7 days. The isolated fuel kernel was placed in a 20 mL polyethylene vial and dissolved completely in 10 mL Thorex reagenz. Both sample solutions were used for further separation steps and different analytical tools (alpha-, beta- and gamma-spectrometric measurements) were performed in order to compare the calculated values to the measured activities and to gain informations about the elemental distribution between coatings and fuel kernel. With respect to the radionuclide distribution between fuel-kernel and coatings the radionuclides under investigations were quantitatively found within the fuel-kernel. Cs is the only element which behaved quite different. Only appoximately 5 % was still present in the fuel-kernel. During the irradiation a low oxygen potential developped. Taken carbon oxidation into account the oxygen potential reached a low value of about –600 kJ/mol [4]. Under these conditions Cs did not form ternary compounds and was stable in atomic form as gas. In this form Cs was released from the fuel-kernel and accumulated in the buffer/iPyC region.

For a coated particle the activities of the elements Cs, Eu, Cer, Ru, Sb, Rh, Pr and Am were determined by γ-spectroscopy and the results were comparable to the calculated values.

To distinguish clearly between the elemental distribution within the fuel kernel and the coatings a selective cracking, separation and dissolution/leaching step was performed. Then the radioisotopes were identified by different analytical tools and their activities were determined.

Tab. 1: Radionuclide activities for a coated particle (CP) (uranium mass of 0.60476 mg) calculated with the OCTOPUS code (date: august 2010).

Nuclide	Bq/CP
H-3	2.37E+04
Sr-90	4.11E+06
Y-90	4.11E+06
Tc-99	9.86E+02
Ru-106	2.34E+06
Sb-125	3.95E+05
Cs-134	1.51E+06
Cs-137	6.47E+06
Pr-144	2.06E+06
Cer-144	2.05E+06
Eu-154	2.23E+05
Eu-155	1.22E+05
U-234	1.42E+02
U-235	2.95E+00
U-236	2.59E+01
Np-237	1.48E+01
Pu-238	5.75E+04
Pu-239	1.37E+04
Pu-240	1.69E+04
Pu-241	4.39E+06
Am-241	3.91E+04
Cm-244	1.20E+04

With the exception of Cs all radionuclides were found nearly quantitatively in the kernel. Due to the low oxygen potential during irradiation Cs behaved like a fission gas. Up to 95 % of Cs released from the kernel and this amount was detected in the coatings (buffer and iPyC).
In future work the fission gas released during the crack process will be analysed and isolated fuel kernels will be leached under oxic and anoxic/reducing conditions in order to determine the highly soluble radionuclide release fraction.

Acknowledgement

The research leading to these results has received funding from the European Union's European Atomic Energy Community's (Euratom) Seventh Framework Programme FP7/2007-2011 under grant agreement n° 295722 (FIRST-Nuclides project).

References

[1] Kadner M., Baier J., Production of Fuel Kernels for High-Temperature Reactor Fuel Elements. Kerntechnik 18, 413-420, 1977.

[2] Fütterer M.A., Berg G., Toscano E., Bakker K. (2006). Irradiation results of AVR fuel pebbles at increased temperature and burn-up in the HFR Petten. 3rd International Topical Meeting on High Temperature Reactor Technology, Johannesburg, South Africa, B00000035

[3] Fütterer M.A., Berg G., Marmier A., Toscano E., Freis D., Bakker, Groot de S., (2008). Results of AVR fuel pebble irradiation at increased temperature and burn-up in the HFR Petten. Nuclear Engineering and Design 238, 2877-2885

[4] Barrachin, M., Dubourg, R., Groot. de S., Kissane, M. P., Bakker, K. (2011) Fission-product behaviour in irradiated TRISO-coated particles: Results of the HFR-EU-1bis experiment and their interpretation. Journal of Nuclear Materials 415, 104-116.

4.2. Preparation, structure and stability of Zr(IV)-containing layered double hydroxides (LDHs)

K. Rozov, H. Curtius, D. Bosbach

Corresponding author: k.rozov@fz-juelich.de

Abstract

LDHs or "hydrotalcite-like" solids are of interest in environmental geochemistry because they have wide chemical compositions due to the substitution of various cations and especially due to the anion-exchange properties. Therefore, LDHs are potential buffers for retention of hazardous anionic radionuclides. In our study LDHs with variable Zr-content were synthesized at 25 ^{o}C and characterized in order to investigate the influence of substitution of four-valent cations on their stability and anion-exchange properties.

PXRD demonstrated that pure Mg-Al-Zr(IV) LDHs precipitated within the Zr mole fraction range $x\mathrm{Zr}_{solid}$ = Zr/(Zr+Al) = 0.0 - 0.5. The variation of the lattice parameters as function of $x\mathrm{Zr}_{solid}$ was in agreement with Vegard's law confirming the presence of solid solution series throughout this compositional range. The presence of additional X-ray reflexes typical for brucite was observed for precipitates with $x\mathrm{Zr}_{solid} \geq 0.5$.

Results of the chemical analyses revealed that the increase of the Zr-content in the co-precipitating solutions led to the formation of solids with significantly reduced Mg/(Al+Zr) ratios indicating that the trace amounts of Zr decreases the stability of the LDH structure and that during the syntheses the formation of several phases can occurred. Moreover, variations in the stoichiometries of pure LDHs might indicate that the incorporation of 1 Zr-containing specie into the LDH occurred with a simultaneous replacement of 1 Al- and 2 Mg-containing species. Future EXAFS analyses can provide more data in order to investigate the mechanisms of Zr incorporation in detail.

The Gibbs free energy minimization software GEM-Selektor was applied in order to provide the first estimates of the molar Gibbs free energies for Zr-containing LDHs. We observed that the value of Gibbs free energy of the pure Mg-Al-LDH composition (-3619.04 ± 15.27 kJ/mol) was significantly lower than those values for Zr-containing LDHs. The addition only of 0.1 molar units of Zr(IV) into the pure hydrotalcite increased the Gibbs free energy of formation by more than 150 kJ/mol. This reflected again the significant impact of Zr-incorporation on the stability of LDHs. Further syntheses and dissolution tests will be performed in order to obtain more data about the thermodynamic properties of LDHs and to predict their behavior under repository-relevant conditions.

Introduction

The disposal of radioactive waste in geological environments calls for the development of new radionuclide-binding materials. These materials have to: (1) be stable at repository-relevant conditions and (2) prevent the migration of radionuclides to biosphere. Layered double hydroxide phases are of interest to these studies due to their ability to retain a very wide range of different cations (like, Li^{+}, Ba^{2+}, Mg^{2+}, Fe^{2+}, Ni^{2+}, Al^{3+}, Fe^{3+}, Cr^{3+}, Ga^{3+}, Sc^{3+}, Zr^{4+}, *etc.*) [1-7] and especially due to their anion-exchange properties. The anion-exchange properties of LDHs with the general formula $[M^{II}_{(1-x)}M^{III}_{(x)}(OH)_2]^{x+}[A^{y-}_{x/y}\cdot nH_2O]^{x-}$ result directly from their structure which is composed by positive charged brucite-like layers (the first set

brackets) and intercalated anions which are accompanied by molecules of water (the second set of brackets). This means that LDHs can be considered as potential buffer materials for the retention of mobile, soluble and long-lived radioactive anions (like, ^{14}Cl, ^{129}I, ^{36}Cl, ^{79}Se *etc.*) [8]. However, at present time, the understanding of the retention properties, behavior of LDHs in aqueous environment and applying these substances for geochemical modeling at conditions of nuclear repositories are hampered by scarce data on their thermodynamic and solubility properties. The problem of retrieving thermodynamic data and predicting stability of LDHs has been recently touched only in a few studies [9-13]. The present work focused on the synthesis, characterization of chloride-bearing Mg-Al LDHs with incorporated Zr(IV) cations in the structure. This Mg-Al-LDH type was identified as a characteristic secondary phase in the corrosion products of research nuclear fuel samples [4,14]. Using various experimental techniques (X-ray powder diffraction, infrared spectroscopic measurements, thermogravimetric analysis, scanning electron microscopy, energy dispersive X-ray spectroscopy), the primary objective was to ascertain to the presence of a continuous solid solution series for Zr-containing LDHs (*i.e.*, isostructural incorporation of Zr(IV)). The next objectives were: 1) to quantify the standard Gibbs free energies of formation with the help of thermodynamic modeling based on the chemical analysis of solid and liquid phases at equilibrium and; 2) to provide the substitution scheme of Zr-incorporation into the LDH structure.

Materials and Methods

LDH solids with variable contents of Zr were synthesized by co-precipitation at 25 ^{o}C and at constant *pH* = 10.00 ± 0.05. The Mg-Al-Zr-chloride containing solutions with Zr/(Al+Zr) = 0-1 and Mg/(Al+Zr) ≈ 3:1 ratios were dropped into a reactor with water under stirring. To maintain the *pH* value constant a NaOH solution was added simultaneously.

The contents of Mg, Zr, Al and Na in the precipitates and solutions after syntheses were determined by ICP-OES method. Cl^--anions were analyzed photometrically.

The PXRD measurements were applied for structural characterization. No internal standards for possible specimen displacement were used. Infrared spectra of precipitates were acquired in order to identify the interlayer composition (anions and water-molecules). TGA-DSC was carried out in order to determine the contents of H_2O, OH^--groups and Cl^--anions in the solids. The weight loss of the solids was analyzed from 25 ^{o}C to 1000 ^{o}C with a heating rate of 10 ^{o}C/min. The morphology of the synthesized crystallites was studied by the low-pressure scanning electron microscopy (SEM). Gibbs free energies of formation of the solids were estimated with the assumption of a thermodynamic equilibrium between solutions after syntheses (Tab. 2) and precipitates (Tab. 3). On the first step, using the results of chemical analyses the speciation of aqueous phases has been modeled. The activities and chemical potentials of all relevant components (*i.e.*, Mg^{2+}, Al^{3+}, Zr^{4+}, OH^-, Cl^-) were calculated with support of GEM-Selektor code [15], NAGRA-PSI and SUPCRT/Slop98 chemical thermodynamic database [16,17]; Then, the Gibbs free energies were estimated from the chemical potentials of solutes and from the stoichiometric coefficients for the solids.

Tab. 2: Compositions of aqueous solutions (pH = 10.00±0.05) after syntheses at 25 °C.

Mole fraction of Zr in solid	Mg, [mmol/kg H_2O]	Al, [µmol/kg H_2O]	Zr, [µmol/kg·H_2O]	Na, [mmol/kg H_2O]	Cl, [mmol/kg H_2O]
0.086	4.762	1.141	0.506	184.760	300
0.138	51.263	1.143	0.507	190.486	300
0.186	7.013	1.095	0.540	169.189	310
0.267	8.603	1.140	0.506	174.326	300
0.291	8.273	1.143	0.507	177.072	300
0.365	14.947	1.098	0.541	169.480	300
0.488	19.395	1.097	0.541	157.688	310

Tab. 3: Stoichiometric formulae of synthesized Zr-containing solids

Stoichiometric formulae "water-free" composition	Zr mole fraction, xZr_{solid} = $nZr/(nZr+nAl)$	nMg/(nAl+nZr) solid	G_f(298K), [kJ/mol]
$Mg_{2.768}Al_{0.914}Zr_{0.086}Cl_{0.577}(OH)_{8.045}$	0.086	2.768	-3459.41
$Mg_{2.681}Al_{0.862}Zr_{0.138}Cl_{0.638}(OH)_{7.862}$	0.138	2.681	-3387.37
$Mg_{2.662}Al_{0.814}Zr_{0.186}Cl_{1.026}(OH)_{7.484}$	0.186	2.662	-3384.78
$Mg_{2.410}Al_{0.733}Zr_{0.267}Cl_{0.575}(OH)_{7.512}$	0.267	2.410	-3222.86
$Mg_{2.527}Al_{0.709}Zr_{0.291}Cl_{0.751}(OH)_{7.594}$	0.291	2.527	-3320.76
$Mg_{2.326}Al_{0.635}Zr_{0.365}Cl_{0.381}(OH)_{7.636}$	0.365	2.326	-3193.11
$Mg_{2.005}Al_{0.512}Zr_{0.488}Cl_{0.346}(OH)_{7.152}$	0.488	2.005	-2971.14

Results and Discussion

PXRD technique was used to demonstrate that precipitates (Tab. 3) are indeed pure LDHs and to proof that the Zr-containing precipitates form continuous solid solution series. We observed that the precipitates with 0 < xZr_{solid} < 0.488 display diffraction patterns (Fig. 20) typical for pure LDH phases [18]. However, precipitates with xZr_{solid} > 0.488 shown additional reflexes attributed to the $Mg(OH)_2$ phase. Moreover, from chemical analyses of the synthesized solids (Tab. 3) it was clearly seen that the increase of xZr led to the formation of precipitates with significantly reduced Mg/(Al+Zr) ratios and the desired 3:1 ratio was not observed. Consequently, the variation of the stoichiometries in the brucite-like layers was expressed as $Mg_{3-2x}Al_{1-x}Zr_x$-formulae and thus, the substitution mechanism might include the incorporation of 1 Zr-specie with simultaneous replacement of 1 Al and 2 Mg- species.

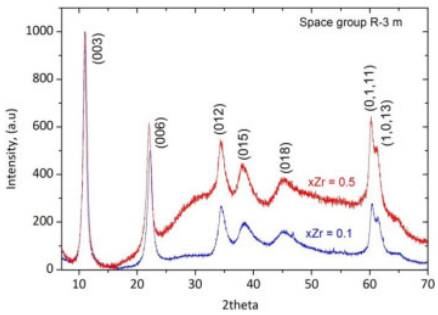

Fig. 20: X-ray diffractograms of synthetic hydrotalcite-like solids with xZr_{solid} = 0.10 and 0.50.

As seen in Fig. 21a and Fig. 21b, the unit-cell parameter a_o = b_o correlates with the measured mole fractions of Zr as well as with the Mg/(Al+Zr) ratios. These dependences are in good agreement with the theoretical calculated curves. These curves were constructed based on the regular octahedral brucite-like layers having the stoichiometry $Mg_{3-2x}Al_{1-x}Zr_x$ and using the known ionic radii of Mg, Al, and Zr in octahedral coordination (0.72Å, 0.54Å, 0.72Å, respectively). It demonstrated that variations of the unit-cell parameter a_o=b_o follow the Vegard's law and confirm the presence of a solid solution series in the range of 0 < xZr < 0.488.

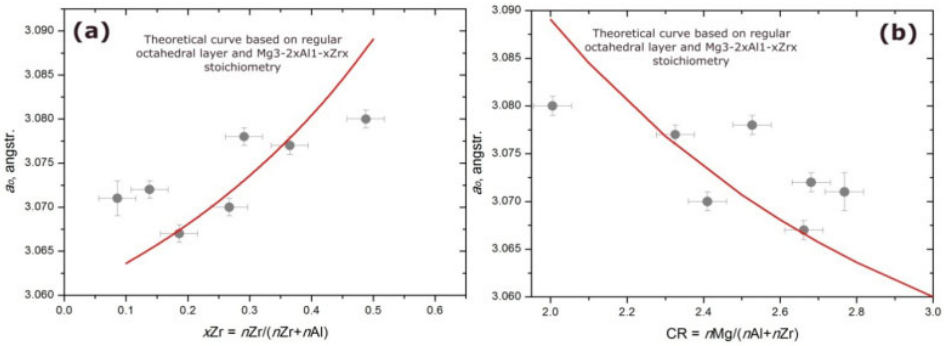

Fig. 21: The lattice parameter a_o=b_o as functions of solid solution compositions.

Infrared spectroscopic measurements had been performed to identify the nature of interlayer and to investigate its interaction with the brucite-like layers. The IR-spectra showed very strong OH^-- and H_2O-stretching bands at 3450 cm^{-1} and 1640 cm^{-1}, respectively. Strong bands at 850 cm^{-1} were attributed to the translational movements of the oxygen in the brucite-like layers. A quite weak band due to adsorbed CO_3^{2-} was detected at 1370 cm^{-1}. The presence of CO_3^{2-} was explained by very strong affinity of LDHs for this anion.
For the calculation of the molar Gibbs free energies the possible effect of oversaturation was neglected and the equilibrium state between the precipitated solids and their corresponding "synthesis solutions" was assumed. This allowed to calculate the molar Gibbs free energies [$G^o_f(298)$] of the precipitates by modelling the aqueous compositions and calculating the chemical potentials of relevant dissolved compounds as described before. The estimated $G^o_f(298)$ values of LDHs were regressed against xZr_{solid}. We observed that the Zr-incorporation into the LDH structure had a significant effect. The addition of only 0.1 Zr mole increased the solubility by more than 150 kJ/mol. Nevertheless, the uncertainties of the estimated $G^o_f(298)$ values were significant. Our analysis demonstrated that this scatter of calculated values origins mainly from errors measured for the solid compositions and at the present stage it is not possible to obtain predictive $G^o_f(298)$ values for the solids which may include higher Zr amounts.

Conclusions

The aim of the present work was to investigate the aqueous solubilities of Zr-containing LDH solids by using the analytical data of the syntheses (by co-precipitation) experiments carried out at ambient conditions (25 ^oC, P = 1 bar). LDHs with different zirconium mole fractions xZr_{solid} = Zr/(Zr+Al) varying from 0 to 0.488 have been successfully synthesized. The

observed Mg /(Zr+Al) ratios of these precipitates were significantly reduce in comparison with this ratio (3:1) in the starting syntheses solutions. This fact and the estimated values of the unit-cell parameters suggested a provisional substitution scheme. The incorporation of 1 Zr-specie led to a simultaneous replacement of 1 Al and 2 Mg- species from the LDH. Results of thermodynamic modelling did show that trace amounts of Zr incorporated into the LDH had a significant effect on their stability.

Acknowledgements

We wish to thank the BMWF for the financial support within the project ImmoRAD (Förderkennzeichen: 02NUK019C).

References

[1] Aramendia, M.A. et al.: Comparative study of Mg/M(III) (M = Al, Ga, In) layered double hydroxides obtained by coprecipitation and the sol-gel method. Journal of Solid State Chemistry 168(1), 156-161 (2002).

[2] Boclair, J.W. et al.: Layered double hydroxide stability. Formation of Cr(III)-containing layered double hydroxides directly from solution. Chemistry of Materials 11(2), 303-307 (1999).

[3] Carteret, C. et al.: Tunable composition of Ni(II)-Al(III) and Ni(II)-Fe(III) layered hydroxides within a wide range of layer charge. Solid State Sciences 13(1), 146-150 (2011).

[4] Curtius, H. et al.: Preparation and characterization of Zr-IV-containing Mg-Al-Cl layered double hydroxide. Radiochimica Acta 97(8), 423-428 (2009).

[5] Rousselot, I. et al.: Insights on the structural chemistry of hydrocalumite and hydrotalcite-like materials: Investigation of the series $Ca_2M^{3+}(OH)_6Cl\cdot 2H_2O$ (M^{3+}: Al^{3+}, Ga^{3+}, Fe^{3+}, and Sc^{3+}) by X-ray powder diffraction. Journal of Solid State Chemistry 167(1), 137-144 (2002).

[6] Ulibarri, M.A. et al.: Effects of Hydrothermal Treatment on Textural Properties of $[Al_2Li(OH)_6]_2CO_3\cdot nH_2O$. Journal of Materials Science 22(4), 1168-1172 (1987).

[7] Wang, J.D. et al.: Synthetic and Catalytic Studies of Inorganically Pillared and Organically Pillared Layered Double Hydroxides. Applied Clay Science 10(1-2), 103-115 (1995).

[8] NAGRA TECHNICAL REPORT 02-05: Project Opalinus Clay. Demonstration of disposal feasibility for spent fuel, vitrified high-level waste and long-lived intermediate-level waste (Entsorgungsnachweis), NAGRA: Wettingen 2002.

[9] Allada, R.K. et al.: Thermochemistry of hydrotalcite-like phases intercalated with CO_3^{2-}, NO_3^-, Cl^-, I^-, and ReO_4^-. Chemistry of Materials 17(9), 2455-2459 (2005).

[10] Allada, R.K. et al.: Thermochemistry and aqueous solubilities of hydrotalcite-like solids. Science 296(5568), 721-723 (2002).

[11] Johnson, C.A., Glasser, F.P.: Hydrotalcite-like minerals ($M_2Al(OH)_6(CO_3)_{0.5}\cdot xH2O$, where M = Mg, Zn, Co, Ni) in the environment: synthesis, characterization and thermodynamic stability. Clays and Clay Minerals 51(1), 1-8 (2003).

[12] Rozov, K. et al.: Solubility and thermodynamic properties of carbonate-bearing hydrotalcite-pyroaurite solid solutions with 3:1 Mg/(Al+Fe) mole ratio. Clays and Clay Minerals 59(3), 215-232 (2011).

[13] Rozov, K. et al.: Synthesis and characterization of the LDH hydrotalcite-pyroaurite solid-solution series. Cement and Concrete Research 40(8), 1248-1254 (2010).

[14] Mazeina, L. et al.: Characterisation of secondary products of uranium-aluminium material test reactor fuel element corrosion in repository-relevant brine. Journal of Nuclear Materials 323(1), 1-7 (2003).

[15] Kulik, D., GEM-Selektor. Research package for thermodynamic modelling of aquatic (geo)chemical systems by Gibbs Energy Minimization (GEM). http://gems.web.psi.ch.

[16] Hummel, W. et al.: Nagra/PSI chemical thermodynamic data base 01/01. Radiochimica Acta 90(9-11), 805-813 (2002).

[17] Shock, E.L. et al.: Inorganic species in geologic fluids: Correlations among standard molal thermodynamic properties of aqueous ions and hydroxide complexes. Geochimica et Cosmochimica Acta 61(5), 907-950 (1997).

[18] Malherbe, F., Besse, J.P.: Investigating the effects of guest-host interactions on the properties of anion-exchanged Mg-Al hydrotalcites. Journal of Solid State Chemistry 155(2), 332-341 (2000).

4.3. Properties of $USiO_4$, coffinite – a high pressure Raman study

S. Labs[1], J.D. Bauer[2], S. Weiß[3], L. Bayarjargal[2], H. Curtius[1], B. Winkler[2].

1) Forschungszentrum Jülich GmbH, Institut für Energie- und Klimaforschung – Nukleare Entsorgung (IEK-6), 52425 Jülich, Germany.
2) Goethe-Universität Frankfurt am Main, Institut für Geowissenschaften, Abteilung Kristallografie, Altenhöferallee 1b, 60438 Frankfurt am Main, Germany.
3) Helmholtz-Zentrum Dresden-Rossendorf, Institut für Ressourcenökologie, Bautzener Landstraße 400, 01314 Dresden, Germany.

Corresponding author: s.labs@fz-juelich.de

Abstract

In this study we have investigated the high pressure behavior of $USiO_4$ by confocal micro-Raman spectroscopy. Raman spectra were collected in the range of 0 to 19 GPa and the pressure shifts were derived from the peak positions. With exception of the first lattice mode, all pressure shifts are positive. The splitting of the SiO_4 antisymmetric stretch mode into two separate signals is observed above 7 GPa. However, no discontinuities or sudden changes in the spectra could be observed that could account for a phase transition of the structure up to 19 GPa at 300 K. This contradicts the results of Zhang et al. [1], who reported a phase-transformation at 14 – 17 GPa. Furthermore, the behavior of $USiO_4$ under high pressure is for the first time investigated with Raman spectroscopy.

Introduction

Today, UO_2 is considered to be the thermodynamically most stable uranium phase under anoxic conditions and hence the delimiting factor in the safety assessment of final repository in deep geological formation for direct disposal of spent nuclear fuel (SNF). However, it is supposed that under reducing conditions UO_2 in contact with silica-rich waters, such as groundwater or pore water, (silica concentration > 10^{-4} mol/L) can react to coffinite, $USiO_4$ (Langmuir's criterion).[2] As SNF consists to > 90 % of UO_2, the safety assessment can benefit greatly from taking coffinite into account as secondary phase. Coffinite has been studied extensively before, however, most investigations rely on the use of natural samples. These samples are often metamict and associated with uraninite (UO_2), thorianite (ThO_2), rare earth elements, arsenic, selenide, and organic matter. [3] While high pressures are not of specific importance for a possible final repository, the structural behavior of $USiO_4$ at elevated pressures yields important information on the general phase stability. The gathered data also presents a solid basis for comparison with calculated data and can be useful for the verification and interpretation of models.
Studies about the behavior of $USiO_4$ at high pressure first were performed by Liu in 1982 [4]. However, only natural coffinite samples were investigated and the decomposition from the tetragonal zircon-type $USiO_4$ to UO_2 and SiO_2 (coesit) structure was already detected below 10 GPa. Above 10 GPa and up to 30 GPa UO_2 and SiO_2 (stishovit) were present. Samples in that study were heated to about 800 – 1000 °C. Contrary to these results, Zhang et al. [1] detected the transition from zircon to scheelite-type between 15 - 17 GPa by in situ X-ray diffraction. These experiments were performed at room temperature with pressures up to 45 GPa.

Materials and Methods

Sample Preparation

The $USiO_4$ samples used in this study were prepared via a hydrothermal route and characterized with X-ray diffraction (XRD) concerning phase purity and crystallinity. High resolution transmission electron microscopy (HRTEM) measurements were performed to further exclude the presence of impurities and especially minor amounts of UO_2 as far as possible. Lattice parameters of the starting material were determined by XRD and refined through Rietveld refinement as a = 6.9862(2) Å and c= 6.2610(4) Å.

A promising specimen was loaded into a Boehler-Allmax type diamond-anvil-cell (DAC) [5], equipped with a tungsten gasket. The 140 µm in diameter gasket hole was laser drilled into pre-indented (to 40–50 µm thickness) tungsten gaskets and served as sample chamber. Several small ruby grains were included in the sample chamber and the pressure was measured using standard ruby fluorescence technique. [6] Ne was used as hydrostatic pressure medium.

Raman Spectroscopy

Confocal micro-Raman measurements were carried out with a Renishaw Raman System (RM-1000) equipped with a Leica DMLM optical microscope, a grating with 1800 grooves per mm, and a Peltier-cooled charge-coupled device (CCD) detector. For excitement the 532 nm emission line of a Nd:YAG laser was used. We employed a 20 objective lens with a long working distance. The spectra were recorded in the range from 100 to 1200 cm^{-1} with exposure times of 150 s and a laser power of 66 mW to 100 mW at different pressures up to 18.7 GPa. The system was calibrated using the band at 519 cm^{-1} of a Si wafer [7]. All obtained spectra were background corrected and fitted using Pseudovoigt functions employing the “Fityk” software package [8].

Results and Discussion

Under ambient pressure, five distinct peaks can be observed in the Raman spectra of $USiO_4$ - the peak at 478 cm^{-1} is to be regarded as an artifact (Fig. 22). An additional very weak peak can be observed at 585 cm^{-1}.

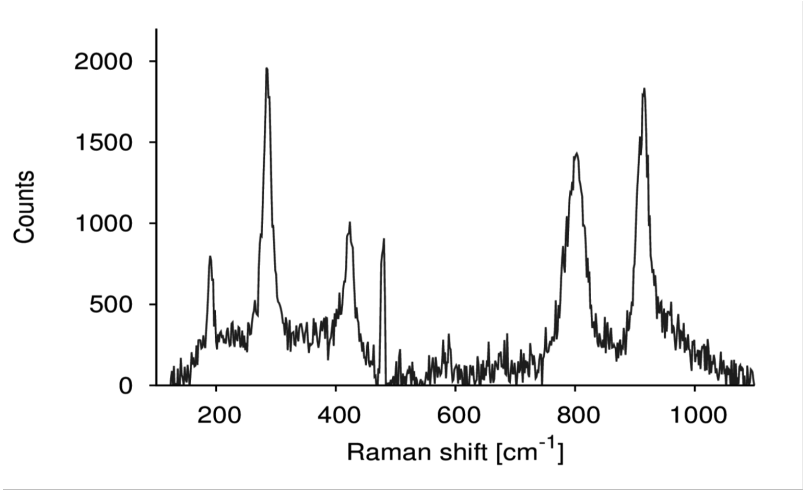

Fig. 22: Raman spectra of coffinite, $USiO_4$, at ambient pressure and 300 K.

As seen in Tab. 4 we assigned the corresponding modes to the wavenumbers according to the measurements performed on $ThSiO_4$ by Syme et al. [9] and the high-pressure Raman study of the zircon-scheelit-phase transition by Knittle and Williams [10].

Tab. 4: List of the ambient pressure frequencies and the calculated pressure shifts from linear fit of the peak positions (Fig. 24).

ν_0 [cm^{-1}]	$d\nu/dp$ [cm^{-1}/GPa]	assignment
192	- 0.67 ± 0.12	lattice mode
290	3.78 ± 0.13	lattice mode
423	1.41 ± 0.07	SiO_4 bend (ν_2)
585	2.32 ± 0.27	SiO_4 antisymmetric stretch (ν_4)
800	0.78 ± 0.23	SiO_4 symmetric stretch (ν_1)
914	4.42 ± 0.14	SiO_4 antisymmetric stretch (ν_3)

In the ambient pressure Raman spectra of $ZrSiO_4$ only the corresponding five strong modes of our spectrum can be observed. According to Knittle and Williams the zircon-scheelit-phase transitions in $ZrSiO_4$ takes place around 23 GPa. The mode at 585 cm^{-1}, which we assigned as SiO_4 antisymmetric stretch mode, appears only above 23.2 GPa in $ZrSiO_4$, where Knittle and Williams assign it as a SiO_4 bend mode in the high-pressure scheelit phase. The SiO_4 antisymmetric stretch mode at 914 cm^{-1} is lower than in $ZrSiO_4$, but in a normal range for the most silicates. This mode splits up with increasing pressure. At 3 GPa a slight shoulder in the peak's form can be detected. Above 7 GPa there are undoubtedly two rather sharp peaks present (Fig. 23).

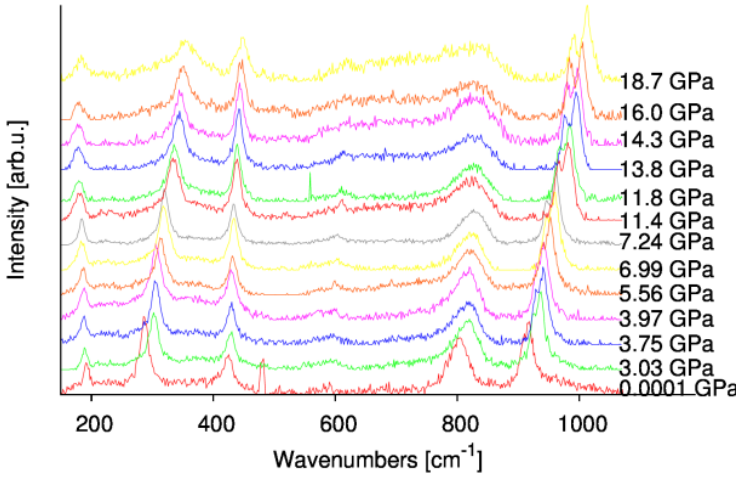

Fig. 23: Raman spectra of coffinite, $USiO_4$, in the pressure range from 0 to 18.7 GPa.

There are several possible explanations for this behavior. One is that the evolving shoulder above 3 GPa is a completely new lattice mode and a sign that indeed a pressure induced phase-transformation has taken place. However, this is rather unlikely, as the other modes and pressure shifts remain unchanged, and the value for a solely pressure induced phase transition would be extremely low for an orthosilicate. Another possibility is, that the SiO_4 antisymmetric stretch (ν_3) is of E_g type and looses it's degeneracy with pressure increase. According to Syme et al. [9] an E_g type (ν_3) mode exists in $ThSiO_4$, but at considerably lower wavenumbers and in any case below the B_{1g} (ν_3) and the SiO_4 symmetric stretch (ν_1) mode.
The SiO_4 symmetric stretch mode broadens upon pressure increase and is hardly resolvable above 16 GPa. Knittel and Williams assigned observed the same effect in their sample at 15 GPa, but argued that in their case the freezing of the pressure medium significantly contributed to this.
While all other modes drift to higher wavenumbers with increasing pressure, the first lattice mode experiences a negative pressure shift. This is conclusive with a general compression of the lattice and hence stronger intermolecular bonds. However, to the best of our knowledge this has not been detected in zircon-type orthosilicates before. We do not detect any sudden changes or discontinuities in wavenumbers or pressure shifts up to 18.7 GPa (Fig. 24). The pressure shifts for the SiO_4 bend (ν_2) and the SiO_4 antisymmetric stretch (ν_3) modes are well in the range for orthosilicates. But the pressure shift of the SiO_4 symmetric stretch (ν_1) mode is considerably low with 0.78 ± 0.23 cm^{-1}/GPa as compared to that of 4.1 ± 0.2 cm^{-1}/GPa in $ZrSiO_4$ [10].

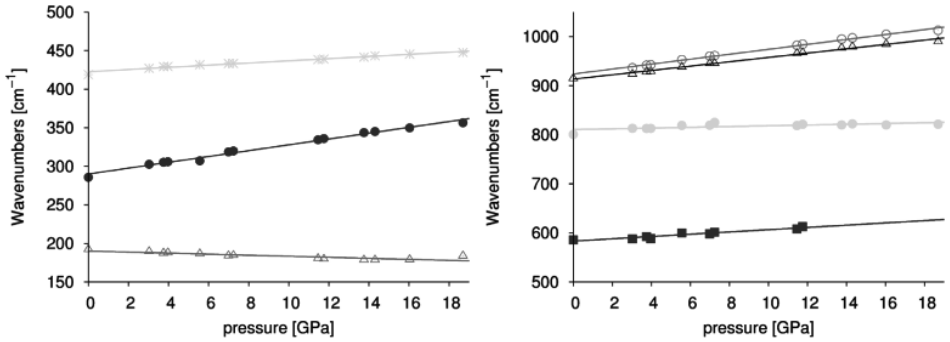

Fig. 24: Raman frequencies as a function of pressure. Left: Peak positions and fit-functions of the lattice modes and the silicate ν_2 mode; right: Peak positions and fit-functions of the Raman modes between 500 and 1100 cm^{-1}.

Conclusions

While the zircon-scheelit-phase transition is common in many ABO_4 compounds (A = Sc, Y, REE; B = V, As), especially the vanadates [11], this kind of first order crystal to crystal phase transition is rare in silicates because of kinetic hindering. The conversion at ambient temperature therefore could be regarded as a rare and anomalous behavior. [10] From the present Raman spectra it is not plausible to conclude a zircon-scheelit-phase transition has taken place within the measured range up to 18.7 GPa. It has to be noted though, that Zhang et al. used a methanol/ethanol/water mixture as pressure medium, which is known to not act ideally hydrostatic in higher pressure ranges. The pressure at which the phase transition can be observed, therefore, has shifted to higher values due to the use of neon as pressure

medium. However, in this study we collected Raman and high-pressure Raman spectra of $USiO_4$ for the first time. We derived the pressure shifts and are able to show that they are in the range of those common for silicates. The negative value of the pressure shift for the first observed lattice mode, does agree with a strengthening of the lattice. This might be attributed to a pressure induced $U^{4+} \rightarrow U^{5+}$ transition as proposed by Zhang et al. [4] but has to remain speculative at the moment.

Acknowledgements

Financial support from Federal Ministry of Education and Research (BMBF) under grants 02NUK019C (FZJ) and 02NUK019E (Uni Frankfurt) is gratefully acknowledged.

References

[1] F.X. Zhang et al. (2009): *Structural transition and electron transfer in coffinite, $USiO_4$, at high pressure,* Am. Min. **94,** 916 – 920.

[2] D. Langmuir (1978): *Uranium solution-mineral equilibria at low temperatures with applications to sedimentary ore deposits*, Geochim. Cosmochim. Acta **42**, 547-569.

[3] H.-J. Förster (2006): *Composition and origin of intermediate solid solutions in the system thorite–xenotime–zircon–coffinite*, Lithos **88** 35– 55

[4] L. Liu (1982): *Phase transformations in MSiO4 compounds at high pressures and their geophysical implications* , Earth Plan.Life Sci.Lett.**57**,110-116.

[5] R. Boehler (2006): *New diamond cell for single-crystal x-ray diffraction*, Rev. Sci. Instrum. **77** 115103.

[6] H.K. Mao and P.M. Bell (1986): *Calibration of the ruby pressure gauge to 800 kbar under quasi-hydrostatic conditions* J. Geophys. Res. **91** 4673.

[7] P.A. Temple and C.E. Hathaway (1973): *Multiphonon Raman Spectrum of Silicon* Phys. Rev. B **7** 3685.

[8] M. Wojdyr (2010): *Fityk: a general-purpose peak fitting program* J. Appl. Cryst. **43**, 1126.

[9] R.W.G. Syme et al. (1977): *Raman spectrum of synthetic zircon ($ZrSiO_4$) and thorite ($ThSiO_4$)*, J. Phys. C: Sol.State Phys. **10**, 1335-1348.

[10] E. Knittle and Q. Williams (1993): *High-pressure Raman spectroscopy of $ZrSiO_4$: Observation of the zircon to scheelite transition at 300 K*, Am. Min. **78,** 245 – 252.

[11] V.S. Stubican and R. Roy, (1963): *Relation of equilibrium phase-transition pressure to ionic radii* Joumal of Applied Physics, **34**, 1888-I890. (1963): *High-pressure scheelites tructure polymorphs of rare-earth vanadates and arsenates* Zeitschrift für Kristallographie, **I** 19

4.4. Recrystallization of Barite in the presence of Radium

F. Brandt, M. Klinkenberg, U. Breuer[1], K. Rozov, D. Bosbach

[1]ZCH Central Division of Analytical Chemistry, Research Centre Jülich GmbH, Jülich, Germany,

Corresponding author: f.brandt@fz-juelich.de

Introduction

The possible solubility control of Ra by coprecipitation of a $Ra_xBa_{1-x}SO_4$ solid solution has been demonstrated in many cases e.g. Doerner & Hoskins, 1925 [1]. However, an open question is whether a Ra containing solution will equilibrate with solid $BaSO_4$ under repository relevant conditions due to barite recrystallization. Here, Ra enters a system in which barite is in equilibrium with the aqueous solution. Previous studies have indicated that uptake of Ra is not limited by pure adsorption at close to equilibrium conditions but involves a significant fraction of the bulk solid [2,3].
Here we present barite recrystallization experiments in the presence of Ra at ambient conditions. In addition, thermodynamic calculations were carried out to gain a deeper understanding of the Ra - $BaSO_4$ exchange process.

Recrystallization experiments

Sample preparation and characterization - Two different types of barite powders with varying grain size distribution and morphology were used during the Ra uptake experiments. The first barite was a synthetic, high purity barite (XR-HR10) from Sachtleben Chemie® GmbH, which was provided by Enzo Curti (Paul Scherrer Institute PSI, Villingen, Switzerland). The same barite was used in the experiments of [2] and [3]. The second barite was a commercially available barium sulfate from Aldrich with a purity of 99.998 %. XRD confirmed that both powders are pure barite within the precision of this method.
A coarse fraction of the Sachtleben barite and a fine fraction of the Aldrich barite were separated. The specific surface area of the separated Sachtleben barite as determined via Kr-BET is S_{BET} = 0.17 m²/g. The specific surface area of the fine Aldrich barite fraction was determined as S_{BET} = 1.7 m²/g. SEM observations indicated that the Aldrich barite consisted of rounded particles forming agglomerates. The particles showed smooth crystal surfaces with small pores. The mean particle size was < 2 µm (Fig. 25 a, b). The Sachtleben barite consisted of blocky crystals with a particle size of > 10 µm (Fig. 25 c, d). The morphology was dominated by barite cleavage planes.

Experimental setup - Batch recrystallization experiments were performed at ambient conditons (23 ± 2 °C). The barites were pre-treated for 4 weeks in 10 mL of 0.2 n NaCl solutions in 25 mL glass bottles. Afterwards, 10 mL of a Ra^{2+} containing solution were added, resulting in a total volume of 20 mL, an ionic strength of 0.1 n NaCl, and a concentration of $5.0 \cdot 10^{-6}$ mol/L $^{226}Ra^{2+}$. The ionic strength was chosen to be comparable to granitic ground waters e.g. at the Äspö site in Sweden. Experiments were carried out with a solid/liquid ratio of 5 g/L and 0.5 g/L. In regular time intervals 500 µL of the aqueous solution were taken and then filtered. The liquid was filtered through Advantec ultrafilters (MWCO = 10,000 Da) and then analyzed for the Ra and Ba concentration.

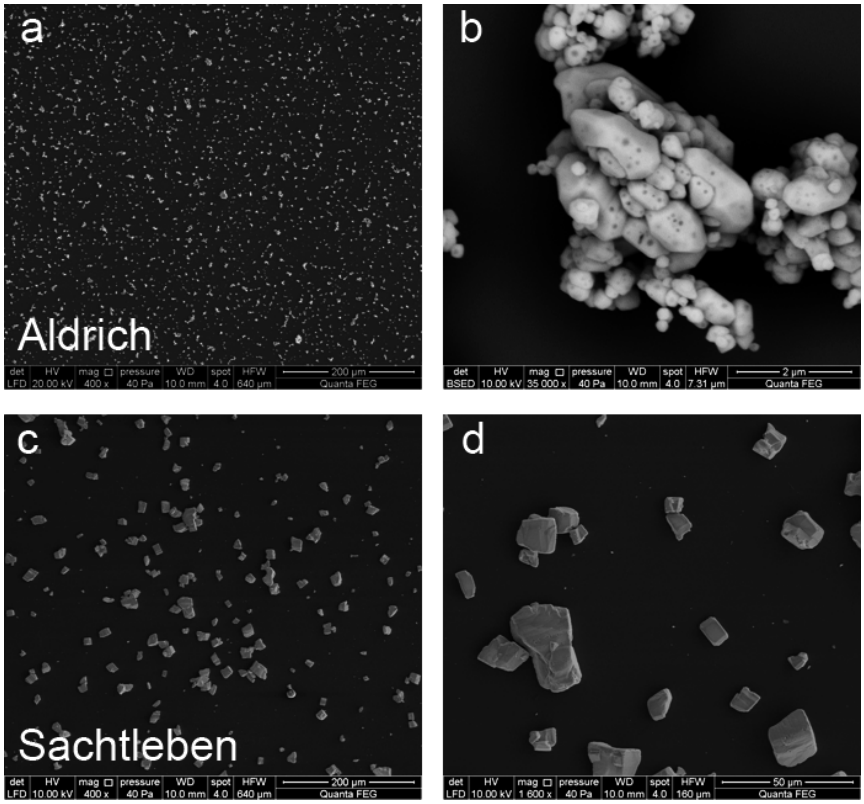

Fig. 25: SEM images of equilibrated Aldrich (a, b) and Sachtleben (c, d) barite. The magnification of the detail images b and d was adjusted to the actual grain size whereas the overview in a and c has identical magnifications.

Analysis of the aqueous solutions - The Ra concentration in solution was examined via Gamma spectrometry using a N_2 cooled high purity (HP) Ge-detector. The Ba concentration in solution was quantified via ICP-MS using an ICP-MS ELAN 6100 DRC (PerkinElmer SCISX) instrument.

Analysis of the solids – The morphology of the barite crystals was studied using the environmental scanning electron microscope FEI Quanta 200 F. In order to avoid artifacts due to precipitation of NaCl, $BaSO_4$ or $RaSO_4$, the samples were separated from their solution by two washing steps in iso-propanol. The samples were then prepared as a suspension on a Si wafer and subsequently dried.
The spatial distribution of Ra and Ba within the recrystallized barite powders was analyzed using an ION-TOF instrument equipped with a Cs source. The raw data were reconstructed and analyzed using the ION-TOF software package.

Modeling of the thermodynamic solid solution – aqueous solution equilibrium

A comprehensive discussion in which the expressions for the relationship between solid solution compositions and aqueous solution composition are derived can be found e.g in [4]. The solubility product approach and especially the graphical representation of the solid-solution aqueous-solution (SS-AS) equilibrium has been proposed by Lippmann [5] and allows formulating the solid solution solubilities by using simple expressions in terms of activities of dissolved components which are related to the compositions of solid and aqueous phases.

Based on the Lippmann theory, the complete equilibration of a SS – AS system can be calculated, provided that the solubilities of the endmembers and the interaction parameters are known. Here, SS - AS equilibrium calculations were carried out for the $BaSO_4$ – $RaSO_4$ – H_2O system with the GEMS – PSI code [6, 7] in combination with the NAGRA – PSI thermodynamic database [8].

Results & Discussion

Recrystallization at room temperature – The temporal evolution of the Ra and Ba concentrations in solution is shown in Fig. 26. In total, seven experiments with 5 g/L of Sachtleben barite were carried out. Mean values and the standard deviation were calculated from replicate experiments and were used for error bars in Fig. 26. Ba concentrations indicate near to equilibrium conditions after ~ 1 day. Typical Ba concentrations are close to equilibrium concentrations of pure barite at 0.5 g/L and slightly higher than the expected Ba concentration at 5 g.

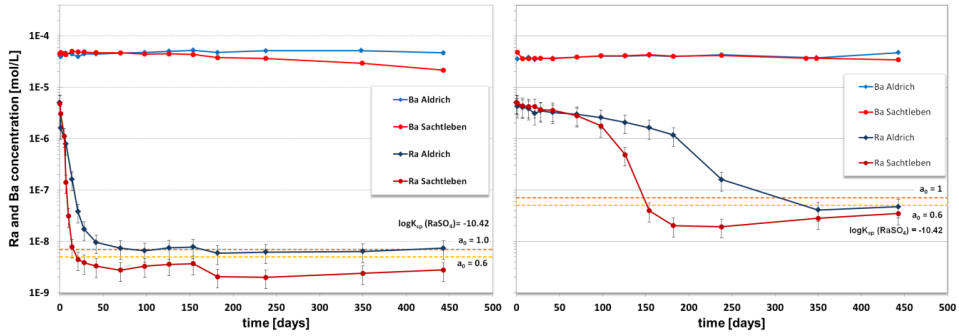

Fig. 26: Left: temporal evolution of the Ra and Ba concentrations with 5 g/L of barite; Right: results for 0.5 g/L

The general shape of the c(Ra) vs. time curves is similar in the experiments with 0.5 and 5 g/L, although the Ra decrease is much faster using 5 g/L of barite.

In the experiments with 5 g/L, a first stage of the Ra concentration decrease is observed within the first week for both barites, followed by a decrease of more than two orders of magnitude after 2 weeks for Sachtleben and 5 weeks for the Aldrich barite. The final Ra concentration of Sachtleben (~ $3 \cdot 10^{-9}$ mol/L) is slightly lower than the final Ra concentration observed for Aldrich (~ $6 \cdot 10^{-9}$ mol/L), although Aldrich has a significantly higher specific surface area. Similarly, the final concentration of Ra is slightly lower for the Sachtleben experiment with 0.5 g/L.

The recrystallization was modeled using the GEMS-PSI code combined with the NAPSI-PSI data base. However, if the recommended value of log Ksp($RaSO_4$) of -10.26 is used, only negative interaction parameters a_0 would be possible to fit the observed final Radium concentrations. This would be in contradiction with a_0 values proposed by Zhu [9] and Curti et al. [3] and with general trends of the sulfate salts [10 – 12]. All these publications suggest positive a_0.

The available solubility products of $RaSO_4$ as published in literature are based on very few experimental studies e.g. Nikitin & Tolmatscheff (1933) [13] or Lind et al. (1918) [14]. In contrast to $BaSO_4$, for $RaSO_4$ the available data do not provide sufficiently tight constrains on the value of $\log K_{RaSO4}$. The results of Paige et al. (1998) [15] showed that slight variation in the fitting procedure applied to the same data produced the variation within the range of 10.21 – 10.41 in $\log K_{RaSO4}$ values. A combination of $\log K_{RaSO4}$ = -10.41 with a positive a_0 could be used to model the new experimental data.

TOF-SIMS was carried out on a Sachtleben barite sample from the 0.5 g/L experiment taken after 443 days in order to examine the spatial Ra distribution within the recrystallized barite. Fig. 27 shows an overlay of the integrated elemental signal of Ba (top) and Ra (bottom) with the complementary electron microscopy image. The integrated Ra concentration corresponds with the size of the barite particles, i.e. all particles contain Ra in similar amounts. A depth profile of the respective Ba and Ra concentrations was reconstructed from the TOF-SIMS data (Fig. 27 b). A homogenous Ra concentration distribution was observed for the large barite crystal in the middle of the SEM image (Fig. 27 a).

The Ba/Ra ratio was calculated from several TOF-SIMS measurements, using the integrated elemental signals (Fig. 27 c). Mass balance calculations for the Sachtleben barite suggest a mole fraction of $X_{RaSO4(s)} = 2.3 \cdot 10^{-3}$, assuming full recrystallization at the end of the experiment. The Ra/Ba intensity distribution of Fig. 27 c has its maximum between 2 and $4 \cdot 10^{-3}$, corresponding well with the macroscopic results.

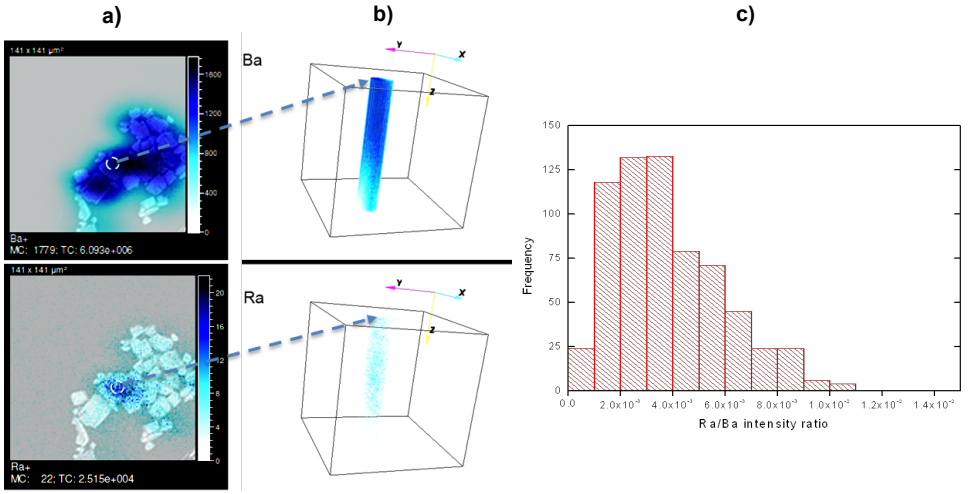

Fig. 27: a) Combined SEM and TOF-SIMS image of barite 1.5 after 350 days of recrystallization. The blue colour indicates the integrated TOF-SIMS signal of the respective element; b) Depth profiles reconstructed for the indicated X-Y areas of the left images (a). c) Evaluation of Ra/Ba intensities as calculated from the TOF-SIMS measurements. The calculated Ra/Ba based on mass balance is $2.3 \cdot 10^{-3}$.

Conclusions

The recrystallization experiments starting with a Ra concentration of $5 \cdot 10^{-6}$ mol/L show a very efficient uptake of Ra by barite. The experimental data can be fitted best with a solubility product of the $RaSO_4$ endmember of log Ksp = -10.41 and a Guggenheim parameter a_0 = 0.6. TOF-SIMS analyses of the final radiobarite powders indicate a full recrystallization leading to a homogenous distribution of Ra within the particles. The Ra/Ba ratios calculated from the experiments via mass balance correspond well with the typical Ra/Ba intensity ratio obtained via TOF-SIMS.

References

[1] Doerner, H. A. & Hoskins, W. M. Co-precipitation of radium and barium sulfates Journal of the American Chemical Society, 1925, 47, 662-675

[2] Bosbach, D.; Böttle, M. & Metz, V. Experimental study on Ra^{2+} uptake by barite ($BaSO_4$), SKB Technical Report TR-10-43 Waste Management, Svensk Kärnbränslehantering AB, 2010

[3] Curti, E.; Fujiwara, K.; Iijima, K.; Tits, J.; Cuesta, C.; Kitamura, A.; Glaus, M. & Müller, W. Radium uptake during barite recrystallization at 23±2°C as a function of solution composition: An experimental ^{133}Ba and ^{226}Ra tracer study Geochimica et Cosmochimica Acta, 2010, 74, 3553-3570

[4] Prieto, M. Thermodynamics of Solid Solution-Aqueous Solution Systems Thermodynamics and Kinetics of Water-rock Interaction, 2009, 70, Mineralog Soc Amer; Geochem Soc

[5] Lippmann, F., Phase diagrams depicting aqueous solubility of binary mineral systems. N. Jb. Miner. Abh 1980, 139, 1-25.

[6] Kulik, D.; Wagner, T.; Dmytrieva, S.; Kosakowski, G.; Hingerl, F.; Chudnenko, K. & Berner, U. GEM-Selektor geochemical modeling package: Numerical kernel GEMS3K for coupled simulation codes. Computational Geosciences, 2012 (in press)

[7] Wagner, T.; Kulik, D.; Hingerl, F. & Dmytrieva, S. GEM-Selektor geochemical modeling package: TSolMod library and data interface for multicomponent phase models Canadian Mineralogist, 2012, 50, 701 - 723

[8] Hummel, W.; Berner, U.; Curti, E.; Pearson, F. J. & Thoenen, T. Nagra / PSI Chemical Thermodynamic Data Base 01/01; Nagra technical report 02-16 2002

[9] Zhu, C. Coprecipitation in the barite isostructural family: 1. binary mixing properties 1 Geochimica et Cosmochimica Acta, 2004, 68, 3327-3337

[10] Glynn, P., 2000. Solid-solution solubilities and thermodynamics: Sulfates, carbonates and halides. Sulfate Minerals - Crystallography, Geochemistry and Environmental Significance 40, 481-511.

[11] Kiseleva, I. A., Kotelnikov, A. R., Martynov, K. V., Ogorodova, L. P., and Kabalov, J. K., 1994. Thermodynamic Properties of Strontianite-Witherite Solid-Solution (Sr,Ba)Co_3. Phys Chem Miner 21, 392-400.

[12] Plummer, L. N. & Busenberg, E., 1987. Thermodynamics of Aragonite-Strontianite Solid-Solutions - Results from Stoichiometric Solubility at 25-Degrees-C and 76-Degrees-C. Geochim Cosmochim Ac 51, 1393-1411.

[13] Nikitin, B., Tolmatscheff, P., 1933. Article on the validity of mass effect law. II. Quantitative determination of solubility of radium-sulfate in sodium-sulfate solutions and in water. Zeitschrift für physikalische Chemie – Abteilung A – Chemische Thermodynamik Kinetik Elektrochemie Eigenschaftslehre 167, 260-272.

[14] Lind, S.C., Underwood, J.E., Whittemore, C.F., 1918. The solubility of pure radium sulfate. The Journal of the American Chemical Society XL, 465-472.

[15] Paige, C.R., Kornicker, W.A., Hileman, O.E.J., Snodgrass, W.J., 1998. Solution equilibria for uranium ore processing: The $BaSO_4$-H_2SO_4-H_2O system and the $RaSO_4$-H_2SO_4-H_2O system. Geochimica et Cosmochimica Acta 62, 15-23.

4.5. The recovery of minor actinides from high active waste solutions using innovative hydrometallurgical partitioning processes

G. Modolo, A. Wilden, P. Kaufholz, C. Schreinemachers, F. Sadowski, S. Lange, J. Assenmacher
Corresponding author: g.modolo@fz-juelich.de

Abstract

European research over the last decade has resulted in the development of multi-cycle processes for minor actinide partitioning. The Jülich laboratory (IEK-6) as partner within previous and current European contracts (NEWPART, PARTNEW, EUROPART, ACSEPT, SACSESS), belongs to one of the leading laboratories in the process development of innovative hydrometallurgical partitioning processes. The research covers also the design, synthesis and assessment of new organic extracting molecules and new diluents. A fundamental understanding of the principles of complexation, including thermodynamics and kinetics, is crucial.
Hence, the present paper summarizes the recent achievements within the development of new partitioning processes and on fundamental solvent extraction studies.

Introduction

The implementation of an actinide recycling strategy is a widely studied option for the management of used nuclear fuel. Currently, the twice-through fuel cycle (e.g. France, UK) is used industrially in order to recover uranium and plutonium from used nuclear fuel whilst the fission products and minor actinides (MA) Np, Am, and Cm are vitrified in nuclear glass. A further stage involving the recycling of the MA using the Partitioning and Transmutation strategy (P&T)[1-4] could contribute significantly to reducing the volume of high level waste in a geological repository and to decreasing the waste's long-term hazards originating from the long half-life of the actinides. Besides plutonium, the MA are the main contributors to the long-term heat production and radiotoxicity of the nuclear waste. Their separation and subsequent transmutation to short-lived or stable elements could reduce the environmental burden of a prospective deep geological repository, possibly contributing to an increased social acceptance of nuclear energy and improved security against misappropriation of the waste material. Consequently, research into new partitioning processes for the selective separation of MA is being carried out in many countries (e.g. USA[5-7], India[8-9], and Japan[10-12]).
In Europe, a multi-cycle separation strategy has been developed within the NEWPART, PARTNEW, and EUROPART contracts, with participation of IEK-6. This collaborative research resulted in the development and demonstration of several processes in Jülich and ITU Karlsruhe: e.g. DIAMEX[13], TODGA[14], ALINA[15], SANEX-BTBP[16], LUCA[17]. A review of these processes was recently published by Modolo et al.[18]
Within the recent European research project ACSEPT (Actinide reCycling by SEParation and Transmutation)[19-20] the development of new extractants and innovative separation processes with a reduced number of cycles was achieved. A schematic representation of the studied processes is given in Fig. 28.

The GANEX (Grouped ActiNide EXtraction) process (Fig. 28, left) aims at the co-separation of all trans-uranium (TRU) elements in a single process as an alternative to the PUREX process. It consists of two steps: selective extraction of uranium, and then partitioning of actinides from fission products and lanthanides.

Single-cycle processes (Fig. 28, right) are advantageous in comparison to multi-cycle processes as they would make the advanced reprocessing of nuclear waste easier and more economical. Two concepts based on the PUREX (or COEX) process have been studied: the "innovative-SANEX" concept and the "1-cycle SANEX" concept. In the "1-cycle SANEX" concept, the direct and selective extraction of the trivalent actinides from PUREX raffinate by a highly selective solvent system is desired. This is a complicated task since the PUREX raffinate includes a wide range of elements with varied concentrations. Especially the separation of trivalent actinides (An(III)) from trivalent lanthanides (Ln(III)) is a difficult task, due to the similar chemical properties of the two groups of elements.
In the "innovative-SANEX" process, An(III) and Ln(III) are co-extracted from a PUREX raffinate and the MA are separated from the Ln(III) by a selective stripping step.[21-23] In France, an americium-selective extraction process (ExAm) was recently presented by the CEA.[24].

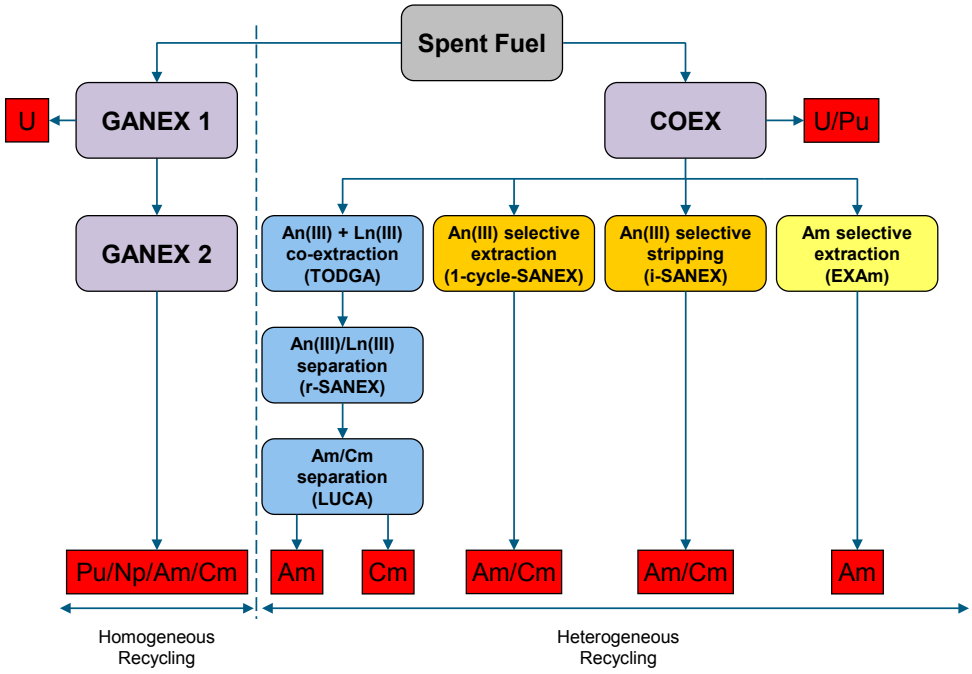

Fig. 28: European partitioning process strategy.

In the new FP-7 project SACSESS (Safety of Actinide Separation Processes, Start March 2013) an alternative process to those already developed will be studied, allowing the partitioning of americium alone, reducing the hazards related to the handling of curium in fuel for enhanced safety.

The present paper gives a summary of our latest achievements regarding the development of innovative partitioning processes and towards the fundamental understanding of the exceptional behavior of most effective extractants.

Development of innovative processes

GANEX

A new approach which was studied within the ACSEPT project is the GANEX concept[25-26] addressing the simultaneous partitioning of all TRU elements for homogeneous recycling of actinides in Generation IV systems. Bulk uranium is removed in the GANEX 1st cycle, most probably using a monoamide extractant; the GANEX 2nd cycle then separates the TRU. Different approaches have been proposed.[25-27]

Finally, a solvent composed of TODGA + DMDOHEMA in kerosene has been shown to effectively co-extract TRU (including Pu) and lanthanide ions.[26, 28-30] The TRU can then be stripped from the loaded solvent using selective hydrophilic complexing agents.[31] One of the challenges in the development of a credible GANEX process was to find a substituent for oxalic acid (as masking agent for Zr, Mo) because of the formation of Pu oxalate precipitates, due to the high Pu concentration in the GANEX feed.

The problem of co-extraction of some fission and corrosion products such as Zr, Mo, Sr, Ru, Fe or Pd is well-known and occurs in several innovative partitioning processes (DIAMEX, innovative SANEX, 1-cycle SANEX). Within the PhD study of Sypula[32] (2008-2011) it was found, that the hydrophilic complexing agent cyclohexanediaminetetraacetic acid (CDTA) can be used to efficiently mask Zr and Pd in the feed under GANEX solvent extraction conditions, preventing them from being extracted from HAR simulant solutions. CDTA can furthermore be used to mask Zr and Pd in TODGA and DIAMEX based solvents.[33]

A relatively small concentration of CDTA was sufficient to complex those two problematic elements and keep them in the aqueous phase while the lanthanides and TRU were efficiently extracted. The complexing agent was able to handle high concentrations of Zr, one of the most abundant elements in HAR solutions, still preventing its extraction into the organic solvent. The efficiency of CDTA to complex Zr and Pd in a HAR solution was also demonstrated at a high Pu concentration of 17 g/L. The substitution of oxalic acid by CDTA can be an optimal solution for processes like the GANEX process were major quantities of Pu have to be handled. Taking all these advantages into account CDTA is a promising substituent for the commonly used masking agents oxalic acid and HEDTA. However, very slow extraction kinetics of zirconium were observed in the presence of CDTA which calls for further investigations of the thermodynamic and kinetic properties of CDTA-metal complexes at moderate and high nitric acid concentration.

Innovative-SANEX

The hydrophilic complexing agent CDTA was also studied for the application in an innovative-SANEX process. In this process, An(III) are co-extracted with Ln(III). The selective separation step in this kind of process is the An(III) stripping step. Several requirements for an innovative SANEX process had to be met:

- Highly efficient extraction of An(III) and Ln(III)
- Management of undesired metal ion and nitric acid co-extraction
- Loading of the solvent
- High separation of An(III) from Ln(III) in the An(III) stripping section
- Solvent recycling

In his PhD study, Sypula[32] was able to develop an extraction system successfully dealing with the first three points. A solvent comprising TODGA in TPH/5% 1-octanol was chosen. TODGA extracts An(III) and Ln(III) with the desired high efficiency and with good kinetics. The limited loading capacity and tendency of 3rd phase formation of the solvent was overcome using 5% 1-octanol as phase modifier.
CDTA was again proven to mask Zr and Pd in the feed. The co-extraction of Mo can be managed using oxalic acid in the scrubbing steps and the co-extraction of Sr can be managed using a low nitric acid scrubbing. The nitric acid scrubbing is furthermore required for the An(III) selective stripping step.
Geist et al. at KIT recently introduced the new hydrophilic complexing agent SO_3-Ph-BTP (Fig. 29) for the An(III) selective stripping step. This molecule combines the high selectivity of the well-known BTP family of extractants with a high solubility in aqueous phases. Now, the selective stripping of An(III) becomes possible, even at relatively high nitric acid concentrations up to 1 mol/L HNO_3.[31]

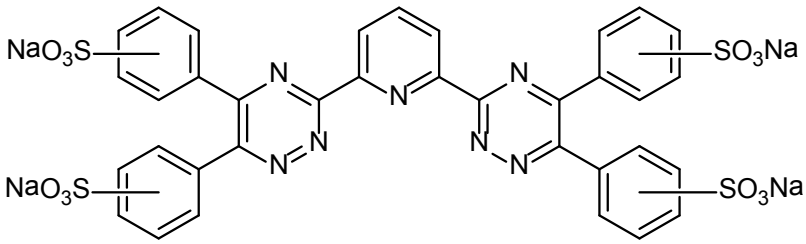

Fig. 29: The An(III) selective complexing agent SO_3-Ph-BTP (2,6-bis(5,6-di(sulfophenyl)-1,2,4-triazin-3-yl)pyridine).

A 32-stage flow-sheet was designed using computer-code calculations with the software "SX process"[21] and successfully tested in the annular centrifugal contactor battery installed in the IEK-6 laboratories.

1-cycle SANEX

A solvent comprising 0.015 mol/L $CyMe_4$BTBP and 0.005 mol/L TODGA in an aliphatic diluent (40% TPH + 60% 1-octanol) was proposed recently at IEK-6 to achieve the desired direct and selective extraction of the trivalent actinides, after gathering data from batch experiments.[34] The results from single stage centrifugal contactor tests were used to develop a 32-stage flow-sheet, which was designed at KIT-INE.[35] The flow-sheet is shown in Fig. 30.

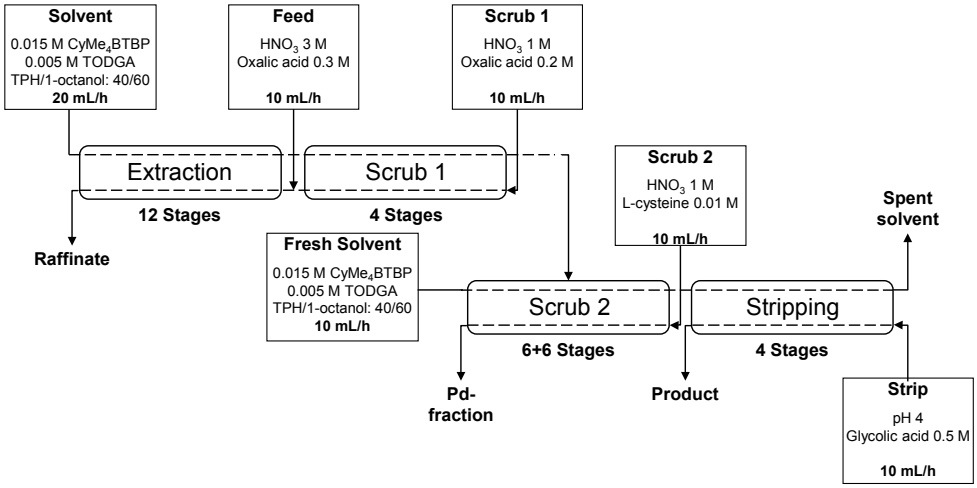

Fig. 30: 32-stage flow-sheet of the 1-cycle SANEX spiked demonstration test.

In 2011, a full continuous counter-current centrifugal contactor test using a simulated PUREX raffinate solution containing trace amounts of Am(III) and Cm(III) was demonstrated at IEK-6.[36] The lab-scale applicability of the developed 1-cycle SANEX process was shown. The MA were recovered to ≥99.4% and separated from the bulk of the fission and activation products in just a single process. This process represents a significant improvement in advanced nuclear fuel partitioning processes with respect to the direct selective recovery of Am(III) and Cm(III) from PUREX raffinate becoming possible. However, some drawbacks of the proposed process are slow kinetics and low solubility of the selective extractant in the solvent. Both aspects and a hot demonstration need to be further studied.

Fundamental studies

In close collaboration with Twente University, Reading University, and KIT many new ligands have been screened for their complexation and extraction properties. Those ligands involved organic extracting molecules as well as aqueous complexants for either the selective masking of metal ions or the selective stripping of An(III) from loaded solvents. Among the most promising molecules were $CyMe_4BTPhen$,[37] SO_3-Ph-BTP[31] and methylated TODGA derivatives.[38-39]

SO_3-Ph-BTP is an aqueous complexant which can be used for the selective complexation of An(III) and thereby for selective stripping of those metal ions from loaded solvents (*cf.* chapter on innovative-SANEX). The molecule was already tested in the European GANEX process and in IEK-6 in the innovative-SANEX process.

The complexation of TODGA and methylated derivatives was studied in solvent extraction (IEK-6) and Time Resolved Laser Fluorescence Spectroscopy (TRLFS) at KIT. A distinct influence of the degree of substitution on the complex formation of metal ions was shown and conditional complex formation constants were determined. This systematical study clearly showed the influence of structural changes of the extractants on the extraction

behavior. The new ligands are discussed for usage in An(III)+Ln(III) co-extraction processes and might provide several improved properties compared to TODGA. $CyMe_4BTPhen$ (developed at University Reading) is currently studied as an improvement of the $CyMe_4BTBP$ molecule, the current European reference molecule for the selective separation of An(III) from Ln(III), and may be used in regular SANEX and 1-cycle SANEX processes. Furthermore, the molecule is tested in innovative diluents (e.g. ionic liquids) to improve the understanding of the fundamental reasons for its high selectivity.

Modified Diglycolamides

The diglycolamide class of ligands, with the TODGA extractant as most prominent member, has proven to be very successful in many processes (e.g. TODGA process, innovative-SANEX). After the discovery of the high extraction efficiency towards An(III) and Ln(III), many structural modifications have been studied, mainly focusing on the side-chains of the amide moiety. A recent review of Ansari et al. gives a comprehensive overview.[40]

However, a structural modification of the back-bone of the ligand has not been studied extensively. Iqbal et al. from Twente University studied several modifications, including the addition of methyl-groups to the central methylene-carbons, as shown in Fig. 31.[38]

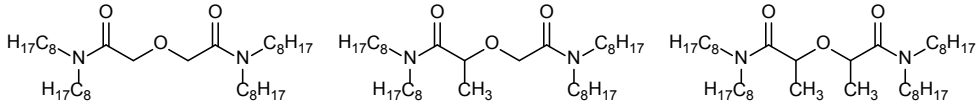

Fig. 31: Structures of TODGA, Me-TODGA, and Me_2-TODGA.

The addition of the methyl-groups lead to a decrease of the extraction efficiency of the ligands towards An(III), Ln(III), and Sr(II). Fig. 32 shows the Am(III) and Eu(III) distribution ratios as a function of the nitric acid concentration for extraction with 0.1 mol/L ligand in TPH, respectively. For all three ligands, the distribution ratios increase with increasing nitric acid concentration, while the distribution ratios decrease with increasing sterical bulk of the ligand. Especially the reduction of Sr(II) distribution ratios is a great benefit in view of process development, as a special Sr(II) management can be omitted. This simplifies the flow-sheets and the process development of new partitioning processes.

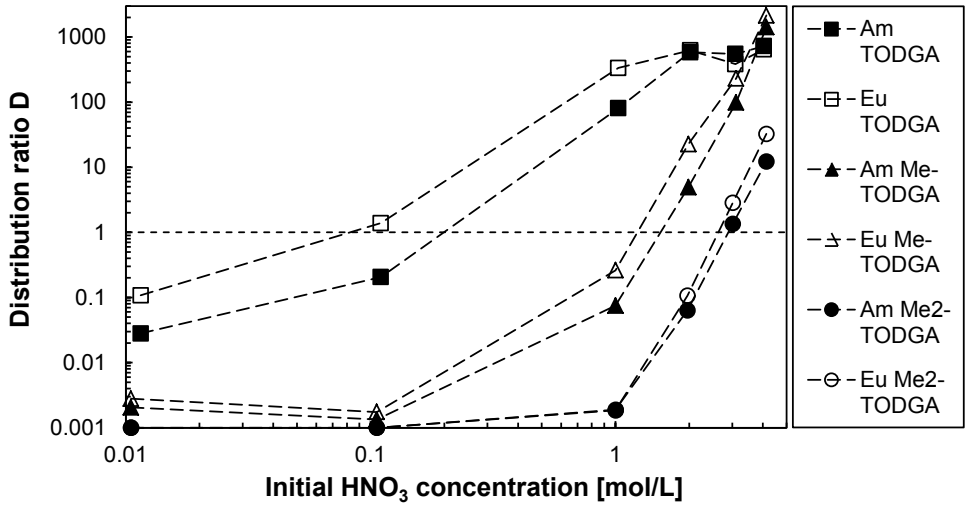

Fig. 32: Extraction of Am(III) (filled symbols) and Eu(III) (open symbols) by TODGA (squares), Me-TODGA (triangles) and Me_2-TODGA (circles).

The complexation of An(III) and Ln(III) was furthermore studied using solvent extraction and time-resolved laser induced fluorescence spectroscopy (TRLFS) in close collaboration with KIT. It was found that the conditional stability constants decrease in the order TODGA > Me-TODGA > Me_2-TODGA, in the same way as the distribution ratios decrease. The formation of 1:3 complexes was found in solvent extraction and TRLFS studies. In the TRLFS experiments, also the formation of intermediate 1:1 complex species was observed.[39]

This study gave a thorough insight into the impact of systematic changes in the back-bone structure of the diglycolamide ligands on their extraction and complexation behaviour. On the basis of the gained information, further optimization of the TODGA-type oxygen donor ligands is foreseeable.

$CyMe_4$BTPhen extraction studies in ionic liquids

$CyMe_4$BTBP (Fig. 33) is the current European reference molecule for SANEX-type processes. The extractant shows good extraction of An(III) with a high separation from the Ln(III) and good hydrolytic and radiolytic stability. The good performance of the extractant has been demonstrated in several laboratory-scale process tests.[16, 36] However, the solubility in common organic diluents is very limited and the kinetics of extraction are rather low. Therefore, research focused on improvements of the molecule, leading to the phenantroline-derived $CyMe_4$BTPhen.

For metal ion complexation with $CyMe_4$BTBP, a conformational change of the *trans*-conformation to the less favored *cis*-conformation is required, as shown in Fig. 33. The rigidification of the bipyridyl back-bone of the BTBP lead to the *cis*-locked $CyMe_4$BTPhen ligand. Hence, the molecule is pre-organized for metal complexation, leading to an increased extraction efficiency towards An(III), while keeping the high selectivity towards Ln(III), a higher solubility in hydrocarbon diluents, and faster kinetics.[37]

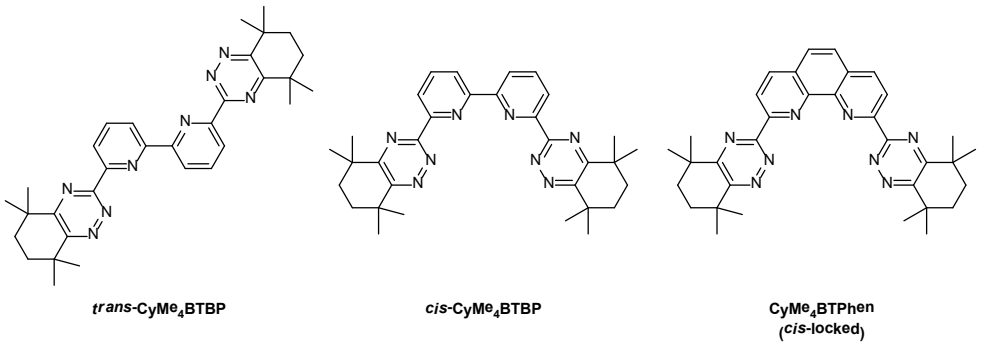

Fig. 33: Structures of $CyMe_4BTBP$ (left and middle) and $CyMe_4BTPhen$ (right).

Ionic liquids are a relatively new class of diluents. Usually they are defined as salts with a melting point below 100°C. Some properties of ionic liquids make them interesting diluents for application in nuclear partitioning processes, as they are not flammable, have very low vapor pressures and often show good radiolytic stability. Furthermore, as combinations of (organic) cations and anions are used, the miscibility and polarity of the ionic liquid can be adjusted. Potential drawbacks are the high viscosity and the high price of the ionic liquids.
Imidazolium based ionic liquids are commonly used. One prominent example is [bumim][Tf_2N], shown in Fig. 34.

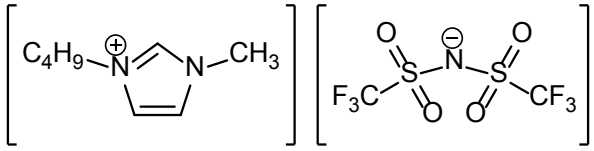

Fig. 34: Structure of [bumim][Tf_2N] ([3-butyl-1-methyl-1*H*-imidazolium] [bis((trifluoromethyl) sulfonyl)amide]).

Solvent extraction studies using $CyMe_4BTPhen$ in [bumim][Tf_2N] showed an interesting nitric acid dependency. The involvement of two different extraction mechanisms was postulated and will be further studied together with I. Billard (CNRS Strasbourg) and M. Meyer (CNRS Dijon).

Conclusions

Used fuel from nuclear power plants has to be managed in a safe manner, respectful of the environment and socially acceptable to the public. Amongst the different strategies studied to manage safely the long-lived radioactive waste, partitioning and transmutation allows a reduction of the amount, the radiotoxicity and the thermal power of these wastes, leading to an optimal use of the geological repository sites.

All the separation processes described in this paper are based on liquid-liquid extraction which benefit from the experience gained over 60 years R&D in actinide separation science. Among the various parameters to take into account when developing a new separation system for An(III) separation, the most important ones are the following.

- High affinity regarding the trivalent actinides
- High selectivity over nitric acid and other metal ions in the feed (e.g. corrosion products, lanthanides and other fission products)
- Kinetics of the extraction and back-extraction
- Stability towards high acid environment and strong radiation field
- Decrease of secondary waste (CHON principle) and down-stream compatibility towards following processes (e.g. conversion)

In fundamental studies, theoretical extraction approaches are to be developed by complementary investigations (e.g. molecular modeling, NMR studies, XRD analysis of solid Ln/An complexes, TRLFS and EXAFS studies), which describe the exceptional behavior of the new extractants in detail, aiming at developing even more efficient new ligands.

It is important to improve the mechanistic understanding of the chemical and physical reactions involved in the solvent extraction processes (thermodynamics and kinetics).This is done in close cooperation with European partners under the current FP7 EU-project SACSESS (duration 2013-2015) and in the current BMBF-funded project f-Kom.

This knowledge is important to develop multi-scale models to be used in a simulation code, which is an indispensable tool to operate such processes in a safe manner. In addition, these processes require a comprehensive study of the multiform safety issues that any chemical process requires under operation or mal-operation conditions. Last but not least, the long term performance of the solvent (hydrolysis and radiolysis), its recycling, cleaning and the management of secondary waste, need to be further studied.

Acknowledgements

The authors thank the Universities Twente and Reading for providing organic extractants in high quality and substantial amounts. KIT, ITU, Heidelberg University, CNRS Strasbourg, and CNRS Dijon are acknowledged for the collaboration in this research, especially for the calculation of process flow-sheets and the speciation of metal complexes using time-resolved laser fluorescence spectroscopy. Furthermore, the authors acknowledge the financial support of the European Commission in the projects: NEWPART (FI4I-CT96-0010), PARTNEW (FIKW-CT2000-00087), EUROPART (F16W-CT-2003-508854), ACSEPT (FP7-CP-2007-211267), and SACSESS (Project No. 323282), as well as the financial support of the German Federal Ministry of Education and Research (BMBF, Contract No. 02NUK012E, 02NUK020E).

References

[1] OECD-NEA (1999): Paris, France.
[2] Magill, J. et al. (2003): Nuclear Energy Vol. 42 (5), 263-277.
[3] González-Romero, E.M. (2011): Nucl. Eng. Des. Vol. 241 (9), 3436-3444.
[4] Greneche, D. et al. (2008): Forschungszentrum Jülich GmbH: Jülich, Vol. 15.
[5] Todd, T.A. et al. (2012): ATALANTE2012, Montpellier, France, 02-07 September.
[6] Nilsson, M. et al. (2007): Solvent Extr. Ion Exch. Vol. 25 (6), 665-701.
[7] Horwitz, E.P. et al. (1985): Solvent Extr. Ion Exch. Vol. 3 (1-2), 75-109.

[8] Gujar, R.B. et al. (2010): Solvent Extr. Ion Exch. Vol. 28 (3), 350-366.
[9] Gujar, R.B. et al. (2010): Solvent Extr. Ion Exch. Vol. 28 (6), 764-777.
[10] Morita, Y. et al. (1996): Solvent Extr. Ion Exch. Vol. 14 (3), 385-400.
[11] Tachimori, S. et al. (2001): Nihon Genshiryoku Gakkaishi Vol. 43 (12), 1235-1241.
[12] Tachimori, S. et al. (2009): Chap. 1 in Ion Exchange and Solvent Extraction, A Series of Advances, Vol. 19, Moyer, B.A., CRC Taylor and Francis: pp 1-63.
[13] Modolo, G. et al. (2007): Separ. Sci. Technol. Vol. 42 (3), 439-452.
[14] Magnusson, D. et al. (2009): Solvent Extr. Ion Exch. Vol. 27 (1), 26-35.
[15] Modolo, G. et al. (2002): Solvent Extr. Ion Exch. Vol. 20 (2), 195-210.
[16] Magnusson, D. et al. (2009): Solvent Extr. Ion Exch. Vol. 27 (2), 97-106.
[17] Modolo, G. et al. (2010): Radiochim. Acta Vol. 98 (4), 193-201.
[18] Modolo, G. et al. (2012): Radiochim. Acta Vol. 100 (8-9, Plutonium Futures), 715-725.
[19] Bourg, S. ACSEPT Homepage. http://www.acsept.org/.
[20] Bourg, S. et al. (2011): Nucl. Eng. Des. Vol. 241 (9), 3427-3435.
[21] Magnusson, D. et al. (2012): Proc. Chem. Vol. 7, 245-250.
[22] Wilden, A. et al. (2012): Proc. Chem. Vol. 7, 418-424.
[23] Geist, A. et al. (2010): 11th Information Exchange Meeting on Actinide and Fission Product Partitioning & Transmutation (IEMPT11), San Francisco, USA, 01.-05.11.2010.
[24] Rostaing, C. et al. (2012): ATALANTE2012, Montpellier, France, 02-07 September.
[25] Aneheim, E. et al. (2010): in Nuclear Energy and the Environment, Vol. 1046, Wai, C.M., et al., American Chemical Society: Washington, pp 119-130.
[26] Bell, K. et al. (2012): Proc. Chem. Vol. 7, 392-397.
[27] Miguirditchian, M. et al. (2009): Proceedings of GLOBAL 2009, Paris, France, pp 1036-1040.
[28] Brown, J. et al. (2012): Solvent Extr. Ion Exch. Vol. 30 (2), 127-141.
[29] Carrot, M.J. et al. (2013): Solvent Extr. Ion Exch., Vol. 31 (5), 463-482.
[30] Taylor, R. et al. (2012): ATALANTE2012, Montpellier, France, 02-07 September.
[31] Geist, A. et al. (2012): Solvent Extr. Ion Exch. Vol. 30 (5), 433-444.
[32] Sypula, M. (2013): Dissertation, RWTH Aachen.
[33] Sypula, M. et al. (2012): Solvent Extr. Ion Exch. Vol. 30 (7), 748-764.
[34] Wilden, A. et al. (2011): Solvent Extr. Ion Exch. Vol. 29 (2), 190-212.
[35] Magnusson, D. et al. (2013): Solvent Extr. Ion Exch. Vol. 31 (1), 1-11.
[36] Wilden, A. et al. (2013): Solvent Extr. Ion Exch. Vol. 31 (5), 519-537.
[37] Lewis, F.W. et al. (2011): J. Am. Chem. Soc. Vol. 133 (33), 13093-13102.
[38] Iqbal, M. et al. (2010): Supramol. Chem. Vol. 22 (11), 827-837.
[39] Wilden, A. et al. (2013): Solvent Extr. Ion Exch., Vol. 31(7) accepted, DOI: 10.1080/07366299.2013.833791
[40] Ansari, S.A. et al. (2012): Chem. Rev. Vol. 112 (3), 1751-1772.

4.6. Synthesis and dissolution kinetics of ZrO_2-Nd_2O_3 pyrochlore and defect fluorite ceramics

S. Finkeldei, F. Brandt, A. Bukaemskiy, S. Neumeier, G. Modolo, D. Bosbach

Corresponding author: s.finkeldei@fz-juelich.de

Introduction

The conditioning of separated waste streams after partitioning is considered as an alternative to advanced reprocessing or the direct disposal of spent fuel (Fig. 35). Even though the total activity of the spent fuel remains the same within the partitioning and conditioning (P & C) strategy, embedding the nuclides in tailor-made host phases leads to an improved retention of the nuclides. A separate disposal of the minor actinides (MA = Cm, Am, Np) within ceramic waste forms is of major interest as they are the main contributors to the long-term radiotoxicity.

Due to their inherent stability oxidic crystalline materials seem to be very promising candidates for the conditioning of these MA. Especially pyrochlore type ceramics are known to be very stable against corrosion and radiation damage [1-3]. The pyrochlore structure $A_2B_2X_6Y$ is very flexible. The A position is typically occupied by trivalent cations e.g. Sc, Y, Tl or the rare earth elements. At the B position tetravalent cations are located which typically belong to the 3d, 4d and 5d transition metals. However, the pyrochlore structure is very flexible and also formed with cations in the oxidation state +II and +V which allows the presence of dopants e.g. pentavalent radionuclides Np(V) in the crystal structure. As a consequence of radiation damage, zirconia based pyrochlores undergo a phase transition to the defect fluorite crystal structure [4]. In contrast titanate pyrochlores are getting amorphous due to radiation damages. The preservation of a crystalline structure is a main asset of ZrO_2-based pyrochlores as potential host phases. No consistent experimental data regarding the dissolution kinetics of zirconia based pyrochlores and defect fluorite are available so far.

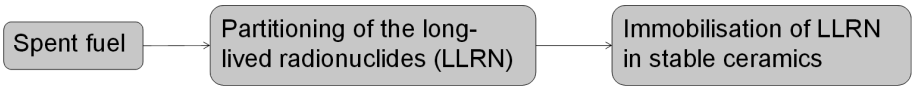

Fig. 35: Main steps of the P & C strategy for the disposal of high level nuclear waste.

Materials and Methods

Powder preparation for dissolution experiments

The powders for dissolution experiments were synthesised via simultaneous coprecipitation of Nd-Zr hydroxides [5]. After a calcination step and pressing of pellets, the crystallisation of pyrochlore or defect fluorite took place during sintering at 1600 °C. Afterwards, well defined powders for the dissolution experiments were prepared from the pellets. After crushing the pellets, the powder was obtained via wet sieving with a mesh size of 180 µm, 100 µm and 50 µm. The fraction from 100 – 180 µm was washed to remove the fines and was used for the dissolution experiments. The powder, which was later on used for dissolution experiments, was characterised via electron microscopy and X-ray diffraction. The specific surface area was determined by N_2-BET-measurements.The specific surface area varied

between 0.71 - 1.63 m^2/g for the powders with the different chemical compositions. Hydrochloric acid with a concentration of c(HCl) = 0.1 mol/l was used as leachant in all experiments to allow a comparison of the results to the existing literature data of zirconia based pyrochlores [6].

Experimental setup of batch experiments

For the batch experiments 200 mg of pyrochlore (33.3 mol% Nd_2O_3) powder were transferred to a 30 mL Nalgene vial. Afterwards 25 mL of a 0.1 mol/L HCl solution were added. The solid/liquid concentration was 7 g/L. The closed vials were placed in a shaking oil bath of 90 °C (Fig. 36, left). The samples were pre-leached for 28d to remove fines and avoid dissolution at high-reactive surface sites from the crushing of the pellets within the dissolution experiments.
The pretreated powder was then used for batch dissolution experiments at the same solid/liquid ratio. At regular time intervals (1, 3, 10, 14, 21, 28, 50, 127 d) a sample of 500 µL was taken and filtered with a USY-1 filter (10000 Dalton). As a quarter of the whole leachant was needed to measure the Zr concentration, the determination for Zr was only possible when the experiment was ended. Therefore, batch experiments could only give little information about the Zr release rate, whereas Nd release could be well monitored with this setup. The Nd-concentration was measured by ICP-MS.

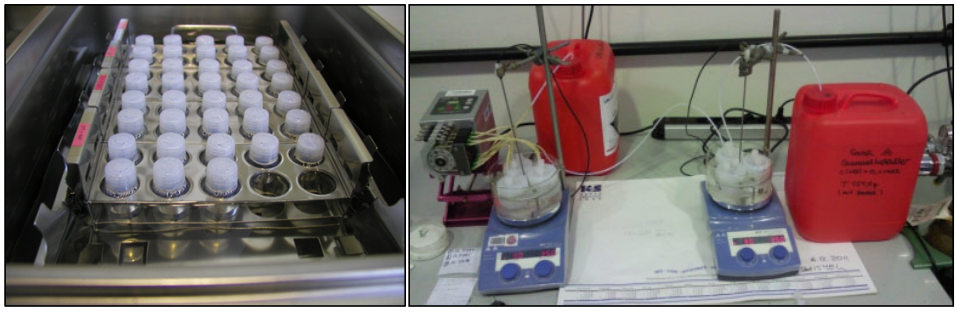

Fig. 36 Experimental set up of batch experiments (left) and dynamic dissolution experiments (right).

Experimental setup of dynamic experiments

The setup of the dynamic experiments consisted of a feed solution, a peristaltic pump, a flow-through reactor and a collection bottle (Fig. 36, right). The peristaltic pump was adjusted to a flow rate of 0.16 ml/min. For the dynamic dissolution experiments the following compositions were used:

- defect fluorite with 15.61 mol% Nd_2O_3
- pyrochlore with 33.3 mol% Nd_2O_3

The reactors were heated in an oil bath to 90 °C. The samples were filtered with a USY-1 filter (10000 Dalton) and diluted to determine the concentration via ICP-MS measurements.

Results and Discussion

Electron microscopy

Scanning electron microscopy (SEM) indicated that the sieved particles were relatively similar in size and only minor amounts of particles in small size were present. In Fig. 37 it can be seen, that the microstructure is dependent on the chemical composition. For the defect fluorite with 15.61 mol% Nd_2O_3 (cf. Fig. 37, left) the surface of the particles is much rougher than for the ideal pyrochlore (33.3 mol% Nd_2O_3). This is in agreement with the specific surface area (N_2-BET), which was higher for the defect fluorite sample. However, for the sample with a higher Nd content and the pyrochlore structure a higher porosity was observed (cf. Fig. 37, right).

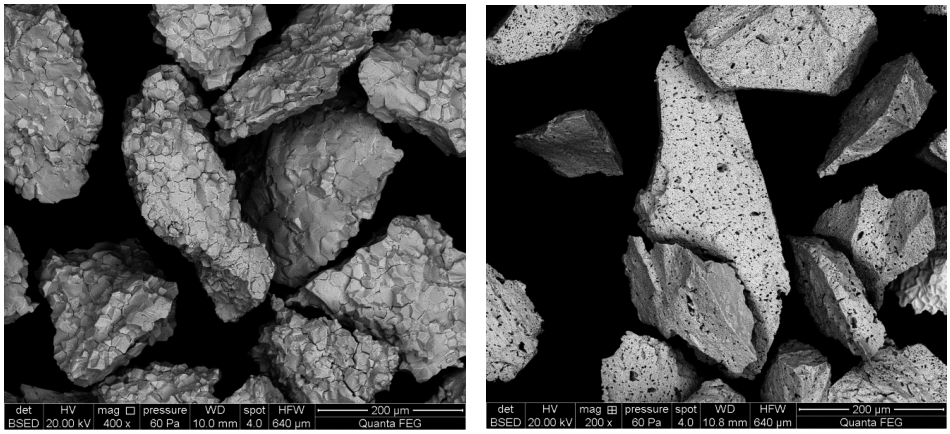

Fig. 37: Back scattered electron (BSE) image of the 180 – 100 µm fraction for the defect fluorite sample with 15.61 mol% Nd_2O_3 (left) and the pyrochlore sample with 33.3 mol% Nd_2O_3 (right).

Dissolution kinetics of pyrochlore ceramics

The temporal evolution of the measured concentrations in solution during pyrochlore dissolution experiments is shown in Fig. 38. Due to analytical restrictions for Zr (adsorption on filters and the limited amount of available solution) only the Nd dissolution rates could be determined in the batch experiment. Fig. 38 (right) shows the normalised concentration of Nd and Zr released from pyrochlore within a dynamic dissolution experiment. The initital dissolution is incongruent as the Nd release is about two orders of magnitude higher than the release of Zr. After 21 days a nearly congruent dissolution of both elements is observed for the steady state.

The normalised dissolution rate for the batch experiments was in the range between $3 \cdot 10^{-5}$ $gm^{-2}d^{-1}$ during the initial phase and $2 \cdot 10^{-5}$ $gm^{-2}d^{-1}$ at later stages of the experiments, based on the Nd-release. This is in good agreement with the dynamic experiment with pyrochlore which resulted in a Nd-based steady state dissolution rate of $1 \cdot 10^{-5}$ $gm^{-2}d^{-1}$. In addition, the dynamic dissolution experiments allow the determination of a Zr-based dissolution rate which is about $0.5 \cdot 10^{-5}$ $gm^{-2}d^{-1}$.

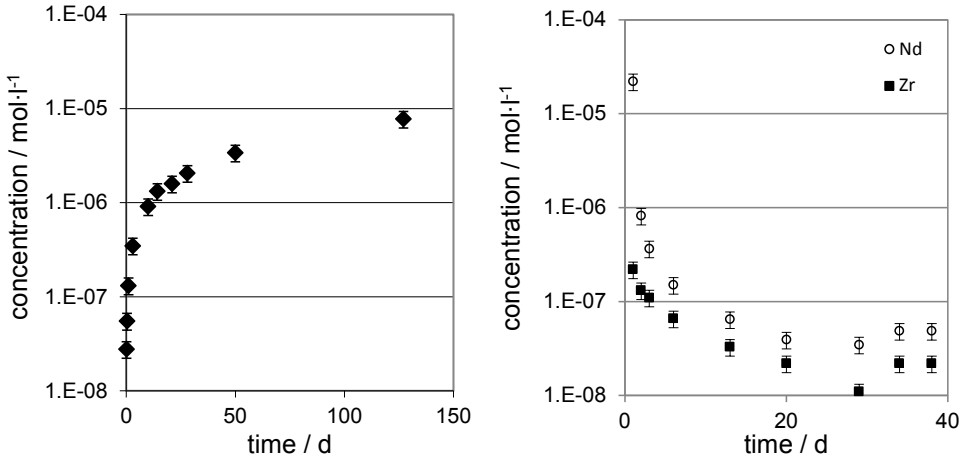

Fig. 38: Release concentration of Nd from the pyrochlore normalised to the chemical composition of the pyrochlore in the batch experiment (left) and of Nd and Zr a dynamic experiment leading to disintegration of the agglomerates (right).

The initial incongruent dissolution could be explained by two possible mechanisms. The first would be the leached layer formation (cf. Fig. 39, left) while the second would be a preferential release at the pores and grain boundaries (cf. Fig. 39, right). For the leached layer formation the steady state release of Nd would be determined by the dissolution kinetics of Zr after a higher initial release of Nd.

If Nd would be enriched at the grain boundaries and the pores, an initial release of Nd would be expected for a preferential release at the pores and grain boundaries. Later on, this would cause the disintegration of the agglomerates leading to an increase in the surface. As the specific surface area is a parameter which influences the normalised dissolution rate the disintegration would be accompanied by an increase of N_L, which is not observed. After finishing the dissolution experiments the powders will be examined by electron microscopy. A closer look to the cross section by means of a focused ion beam (FIB) and SEM/transmission electron microscopy (TEM) might gain further insight into the dissolution mechanism.

Fig. 39: Scheme of possible mechanisms for the initial incongruent dissolution: leached layer formation (left), preferential dissolution at pores and grain boundaries (right).

Comparison of defect fluorite and pyrochlore

In general the dissolution rates of the defect fluorite and the pyrochlore crystal structure are similar. In early stages of the dynamic dissolution experiment, the dissolution of the defect fluorite is highly incongruent, whereas at steady state congruent dissolution rates in the order of $0.3 \cdot 10^{-5}$ $gm^{-2}d^{-1}$ were determined from the release of Nd and Zr.

Conclusions

Within this study batch and dynamic dissolution experiments were carried out for Nd_2O_3-ZrO_2 ceramics with the defect fluorite and the pyrochlore crystal structure. The normalised dissolution rates from batch and dynamic experiments yielded comparable results. Nevertheless dynamic experiments are better suited for the observation of congruent and incongruent dissolution behaviour as they allow a comparison of the Nd- and Zr-release rates. The dissolution rate of the defect fluorite composition is slightly lower than for the pyrochlore. Therefore, a structural transition from pyrochlore to the defect fluorite has very little influence on the dissolution behaviour. As a consequence, radiation can only increase the dissolution rate of zirconia based pyrochlore ceramics due to the induction of structural defects, whereas the phase transition has no significant impact.

References

[1] Ewing, R.C., *Safe management of actinides in the nuclear fuel cycle: Role of mineralogy.* Comptes Rendus Geoscience, 2011. **343**(2-3): p. 219-229.
[2] Lian, J., et al., *Ion-irradiation-induced amorphization of $La_2Zr_2O_7$ pyrochlore.* Physical Review B, 2002. **66**(5).
[3] Lumpkin, G.R., *Ceramic waste forms for actinides.* Elements, 2006. **2**(6): p. 365-372.
[4] Sickafus, K.E., et al., *Radiation-induced amorphization resistance and radiation tolerance in structurally related oxides.* Nature Materials, 2007. **6**(3): p. 217-223.
[5] Chen, H.F., et al., *Coprecipitation synthesis and thermal conductivity of $La_2Zr_2O_7$.* Journal of Alloys and Compounds, 2009. **480**(2): p. 843-848.
[6] Kamizono, I.H., S. Muraoka, *Durability of Zirconium-Containing Ceramic Waste Forms in Water.* J. Am. Ceram. Soc., 1991. **74**(4): p. 863-864.

4.7. Monazite as a suitable actinide waste form

H. Schlenz, J. Heuser, A. Neumann, S. Schmitz, D. Bosbach

Corresponding author: h.schlenz@fz-juelich.de

Abstract

The conditioning of radioactive waste from nuclear power plants and in some countries even of weapons plutonium is an important issue for science and society. Therefore the research on appropriate matrices for the immobilization of fission products and actinides is of great interest. Beyond the widely used borosilicate glasses, ceramics are promising materials for the conditioning of actinides like U, Np, Pu, Am and Cm. Monazite-type ceramics with general composition $LnPO_4$ (*Ln* = La to Gd) and solid solutions of monazite with cheralite or huttonite represent important materials in this field. Monazite appears to be a promising candidate material, especially because of its outstanding properties regarding radiation resistance and chemical durability. This article summarizes the most recent results concerning the characterization of monazite and respective solid solutions. The aim is to demonstrate the suitability of monazite as a secure and reliable waste form for actinides.

Introduction

Nuclear waste management strategies comprise, besides the direct disposal of spent nuclear fuel, the integration of fission products and actinides that result from reprocessed high-level waste in the structures of inorganic solids, such as glasses, glass-ceramics or ceramics. These solid materials are expected to show at least a high chemical durability and radiation resistance, in order to constitute a first barrier for biosphere isolation. Within this context mineralogy can play an important role [1]. We can learn from nature how such materials can be created and the respective long-term durability can be derived from the natural analogues. One prominent example is the mineral monazite, an orthophosphate with a rather simple and low-symmetric crystal structure. Nevertheless, despite the natural incorporation of significant amounts of radioactive thorium and uranium, this mineral can hardly be found in a metamict state [2,3]. The responsible structure-property relations are not yet fully understood, even though scientists all around the world have been working on this issue for decades [4,5]. This article summarizes the research regarding monazite as a suitable actinide waste form. At the end of this article the reader might get the impression, that there are still a lot of interesting scientific tasks left for the future and that it is worth dealing with them.

In the following this article will mainly be restricted to the structural properties and the radiation resistance of monazite-type phases. Due to space limitations other topics like the crystal chemistry of monazite-type phases, crystal growth and sintering, the high temperature and the high pressure behaviour as well as the chemical durability are described in detail elsewhere [6].

Structural properties of monazite

The crystal structure of monazite is characterized by alternating $[PO_4]$-tetrahedra and $[AO_9]$-polyhedra that share common edges, thereby forming chains parallel to the c-axes. A is a di-, tri- or tetravalent cation. Fig. 40 shows the crystal structure of synthetic $CePO_4$ as an example (SG P 2_1/n, Z = 4). More detailed descriptions of the monazite crystal structure with varying composition were e.g. given by [7] and also lattice energies and bonding

characteristics were determined for the pure phases [8]. In Tab. 5 we calculated the weighted mean values of the relevant unit cell parameters and the respective volume of the unit cell $\langle V_{uc} \rangle_w$ [Å^3] for the pure monoclinic lanthanide orthophosphates ranging from $LaPO_4$ to $DyPO_4$, with the exception of $PmPO_4$. To this purpose selected reference data were applied [7,9-12,14]. Only such reference data were considered that appeared to be of reasonable quality including standard errors of the published cell constants. Especially for radioactive $PmPO_4$ only less precise and inaccurate data are available [13] that did not satisfy the quality demands for the regression analysis and even for $DyPO_4$ only data without standard errors are available [14]. Fig. 41 shows the result of the linear regression analysis, where $\langle V_{uc} \rangle_w$ [Å^3] is plotted as a function of the cubic value of the respective cationic radius $\langle r_K^3 \rangle$ [Å^3] for La^{3+} to Tb^{3+}. In addition, the respective values for three different solid solution series $La_{1-x}Ce_xPO_4$ [15], $La_{1-x}Gd_xPO_4$ [16] and $Sm_{1-x}Ce_xPO_4$ [17] have been included for the fit. One can easily recognize the clear linear correlation for the whole compositional range and that the determined data for the pure phases and the solid solutions fit perfectly well. This result supports the assumption that the latter are ideal. The following equation can now be used for the calculation of $\langle V_{uc} \rangle_w$ ($R^2 = 0.99641$):

$$\langle V_{uc} \rangle_w \text{ [Å}^3\text{]} = (198.31819 \pm 0.97985) + (59.82710 \pm 0.61589) \cdot r_K^3 \text{ [Å]}$$

This equation is strictly speaking only valid for thermodynamically stable monazite-type phases $Ln^{III}PO_4$ and $(Ln_1^{III},Ln_2^{III})PO_4$. However, using this equation a more probable value $\langle V_{uc} \rangle_w$ = 287.89 ± 1.90 Å^3 for $PmPO_4$ can be calculated. $GdPO_4$ marks the limit for stable monoclinic orthophosphates. When a phase transition to the tetragonal zircon-type structure occurs, irregular $[AO_9]$-polyhedra transform to almost regular $[AO_8]$-polyhedra and even irregular $[PO_4]$-tetrahedra with four different P-O bond lengths ranging from about 1.52 Å to 1.56 Å become regular with only a single P-O bond length.

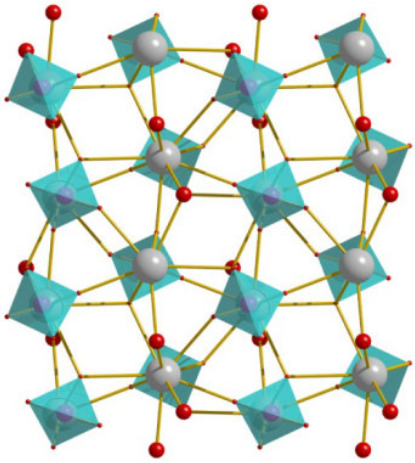

Fig. 40: Crystal structure of $CePO_4$. Viewing direction parallel [001] (Ce - grey, P - purple, O - red, $[PO_4]$ - teal).

$GdPO_4$, $TbPO_4$, $DyPO_4$ and $HoPO_4$ can be synthesized with both monazite- and zircon-type crystal structure, where tetragonal $TbPO_4$, $DyPO_4$ and $HoPO_4$ with zircon-type structure denote the stable phases, respectively. It is assumed that mainly temperature and the pH-value of the solution from which the phosphates precipitate control the structure creation.

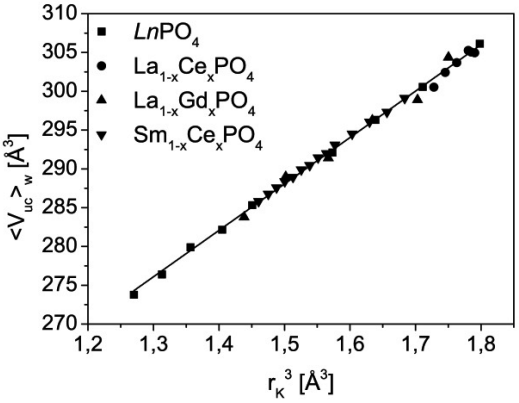

Fig. 41: Linear fit of the weighted mean values of the corresponding unit cell volumes $\langle V_{uc}\rangle_w$ [Å^3], respectively, as a function of the cubic radii $\langle r_K^3\rangle$ [Å^3] of the nine-fold coordinated lanthanide cations in the pure monoclinic orthophosphates (Table 5) and the solid solutions $La_{1-x}Ce_xPO_4$ [15], $La_{1-x}Gd_xPO_4$ [16] and $Sm_{1-x}Ce_xPO_4$ [17]. Error bars are within symbol size.

Tab. 5: Weighted mean values of the relevant unit cell parameters and the volume of the unit cell $\langle V_{uc}\rangle_w$ [Å^3] for the monoclinic lanthanide orthophosphates ranging from $LaPO_4$ to $DyPO_4$ (with the exception of $PmPO_4$; see text). Numbers in paranthesis denote the standard deviations of the mean values, respectively. No standard errors are available for $DyPO_4$.

Composition	$\langle a_0\rangle_w$ [Å]	$\langle b_0\rangle_w$ [Å]	$\langle c_0\rangle_w$ [Å]	$\langle\beta\rangle_w$ [°]	$\langle V_{uc}\rangle_w$ [Å^3]	References
$LaPO_4$	6.8351(3)	7.0784(3)	6.5012(4)	103.28(1)	306.13(6)	[7,9-11]
$CePO_4$	6.7970(2)	7.0247(2)	6.4724(2)	103.45(1)	300.56(4)	[7,9-11]
$PrPO_4$	6.7695(4)	6.9890(3)	6.4427(3)	103.56(1)	296.32(6)	[7,9-11]
$NdPO_4$	6.7416(4)	6.9585(3)	6.4081(3)	103.67(1)	292.10(6)	[7,9-11]
$SmPO_4$	6.6888(3)	6.8948(2)	6.3725(3)	103.87(1)	285.32(5)	[7,9-11]
$EuPO_4$	6.6663(4)	6.8660(3)	6.3518(4)	103.95(1)	282.15(6)	[7,9-11]
$GdPO_4$	6.6511(1)	6.8471(1)	6.3342(1)	104.00(1)	279.90(3)	[7,9-11]
$TbPO_4$	6.6212(0.4)	6.8127(0.4)	6.3179(0.1)	104.11(0.1)	276.39(1)	[11,12]
$DyPO_4$	6.593	6.792	6.305	104.15	273.77	[14]

Radiation damage

Even though monazite minerals contain up to 52 wt% ThO_2 and up to 16 wt% UO_2 [3,18], there are no known natural samples that show a metamictization that could be characterized as a significant radiation damage. Most natural monazites were irradiated over long periods, due to the integrated α-emitters, such as Th and U. Thereby the accumulated doses are comparable to those obtained by a high loading of synthetic monazite with Th, U and Pu. Unlike other mineral phases the crystal structure of monazite is always intact in spite of such

high radiation levels, due to the ability to heal radiation damage at relatively low temperatures. However, it must be considered that natural monazite is exposed for very long periods, at a comparably low radiation intensity. The radiation doses of ceramic waste matrices, however, are substantially higher than those in natural samples. As a result, high doses of radiation in comparably short periods are accumulated (a few thousand years), and in extreme cases, prevent the self-healing of structural damage. Amorphization is accompanied by an expansion and a breaking up of crystal grains in the ceramic. Therefore the possible contact or boundary surfaces for penetrating solutions are increased and also the solubility of monazite. The studies conducted so far, however, document a very high radiation resistance of highly loaded synthetic monazites [19-24]. Nevertheless, the crystal structures of monazite-type orthophosphates basically can be destroyed by four different kinds of irradiation experiments. The first choice is the incorporation of short-lived actinides like ^{238}Pu (half-life of 87.7 years) and ^{244}Cm (half-life of 18.1 years) in order to study self-irradiation due to α-recoil effects. Such experiments are very demanding and time consuming, simply because an experiment can last a couple of years. The structure of monazite $LuPO_4$, doped with 1 wt% ^{244}Cm was not damaged during a long-term experiment of 18 years [22]. During this time the number of events was $5 \cdot 10^{16}$ α/mg, corresponding to a radiation dose of synthetic monazite, loaded with 10 wt% of ^{238}Pu, over a period of 2300 years. Burakov et al. [23] used $PuPO_4$ and $(La,Pu)PO_4$, doped with ^{238}Pu in order to demonstrate the dependence of the radiation resistance as a function of the composition. The crystal structure of $(La,Pu)PO_4$ is stable up to a dose of $1.19 \cdot 10^{25}$ α/m^3, whereas $PuPO_4$ became amorphous at a dose of $4.2 \cdot 10^{24}$ α/m^3. The authors concluded that the radiation damage behaviour of monazite strictly depends on the chemical composition and therefore further investigations are required. The second option is gamma irradiation, utilizing ^{60}Co or ^{137}Cs sources in order to simulate the effects of β-particles and γ-radiation. Only very little work has been done on ceramics so far, because permanent damage can hardly be achieved this way [19]. The next option is neutron irradiation, but again the damage from α-particles and α-recoils can only be simulated roughly this way [19]. Therefore it is not really surprising that to date most of the radiation damage studies on monazite used charged particles for irradiation, like electrons, protons, α-particles or heavy ions. Radiation damage of a ceramic is mainly caused by α-recoil effects, by most of the total number of displacements of atoms in the crystal structure produced by ballistic processes. That is why irradiation experiments using e.g. heavy ions of the elements Ar, Kr, Xe, Au or Pb are a very suitable way for simulating α-recoil effects, especially for the investigation of homogeneous single-phase waste forms like monazite. Systematic irradiation studies of natural and synthetic monazite-type phosphates conducted by Meldrum et al. (e.g. [2,25]) with $Ln PO_4$ (*Ln* = La, Ce, Pr, Nd, Sm, Eu, Gd) showed that the critical amorphization temperature increases systematically with increasing atomic number of the lanthanide cation. According to their results the crystal structure of $LaPO_4$ cannot be destroyed by irradiation above 60°C and that of $GdPO_4$ not above 210°C. The information about the determined irradiation-enhanced activation energies for annealing varies as a function of the energy of the irradiating ions. Reasonable values e.g. for 800 keV Kr^{2+} were determined by Meldrum et al. [25], where E_a ranges from 0.032 eV ($LaPO_4$) to 0.093 eV ($EuPO_4$). Using e.g. 1.5 MeV Kr^+ ions for irradiation, a rather low value E_a = 0.02 eV is obtained for $LaPO_4$. The critical amorphization dose, expressed as displacements per atom (dpa), is a function of temperature. The determined values for $LaPO_4$ vary between 0.15 dpa (T = -273.15 °C) and about 1.66 dpa (T = 29.85°C). Similar variations as a function of temperature were also observed for other compositions [26], but up to higher critical amorphization temperatures, respectively.

Conclusions

The basic question of this article is whether monazite is a suitable actinide waste form that is ready for application within the context of actual nuclear waste management strategies. From the reviewed facts that where summarized so far [6], an affirmative answer can clearly be given to this question. Monazite and synthetic monazite-type orthophosphates own all imperative properties for the save and long-term disposal of actinides: a sufficient chemical flexibility and a high structural flexibility, a high waste loading, a low volume swelling, a high mechanical strength, existing practical chemical synthesis routes and established ceramic processes and finally a high chemical durability and radiation stability. However, there are still a couple of open questions that need to be answered in order to improve and refine the material properties. Ewing and Wang [26] already stated that monazite is an important candidate material for the immobilization of actinides, as well as certain high-level waste stream compositions. Based on the aforementioned we strongly support this statement. They also mentioned some of the open questions that still need to be answered, because only minor progress could be made during the last decade. A major concern is the effect of composition on chemical durability and radiation resistance. Chemical impurities like U, Th and Ca on the *A*-site as well as higher amounts of Si, as seen in natural samples, lead to a higher barrier of recrystallization. Consistently the critical amorphization dose is decreased and the critical temperature increased. Further research in this field will cause the need for a more detailed understanding of the structural processes that occur during irradiation, in order to enable the development of improved materials. One major disadvantage of monazite-type phases is the high melting temperatures of approx. 2000 °C, that poses a real challenge to processing technology. This latter fact represents one important topic in motivating continued research especially on solid solutions like $Ln_{1-2x}^{III}M_x^{II}An_x^{IV}PO_4$ and $Ln_{1-x}^{III}An_x^{IV}(PO_4)_{1-x}(SiO_4)_x$. Such compositions might show decreased melting temperatures. Within this context the improvement of precursors for synthesis and the influence of their morphology on the obtained crystal quality is an important issue. One might think about the decrease of melting and sintering temperatures by the use of reactive nano-particles or by the forced application of wet synthesis routes. And what are the optimum values for pressure, temperature and time during sintering, as a function of composition? In the past most of these questions were answered partially for rather simple compositions but little work has been done so far on the more advanced solid solutions mentioned above (see e.g. [27] for a list of recently investigated compositions). In summary there are still a lot of open questions that are of strong scientific and practical interest and in our opinion it is truly worth dealing with them.

Acknowledgements

This work was supported by the German Research Foundation DFG (Project-Numbers: SCHL 495/3-1 and RO 2055/7-1). The financial support is gratefully acknowledged.

References

[1] R.C. Ewing, Comptes Rendus Geoscience **343** (2011) 219.
[2] A. Meldrum et al., Geochimica et Cosmochimica Acta **62** (1998) 2509.
[3] G.R. Lumpkin, Elements **2** (2006) 365.
[4] F.G. Karioris et al., Radiation Effects Letters **58** (1981) 1.
[5] L.A. Boatner, In: Phosphates, 48, p. 87, Mineral Soc Amer (2002).
[6] H. Schlenz et al., Z. Kristallogr. **228** (2013) 113.
[7] Y.X. Ni et al., American Mineralogist **80** (1995) 21.
[8] H. Li et al., Inorganic Chemistry **48** (2009) 4542.
[9] J.G. Pepin and E.R. Vance, Journal of Inorganic & Nuclear Chemistry **43** (1981) 2807.
[10] A.T. Aldred, Acta Crystallographica **B40** (1984) 569.

[11] S.V. Ushakov et al., Journal of Materials Research **16** (2001) 2623.
[12] H. Schlenz and J. Heuser, Journal of Solid State Chemistry (2012) submitted.
[13] F. Weigel et al., Journal of the American Ceramic Society **48** (1965) 383.
[14] Y. Hikichi et al., Journal of the American Ceramic Society **71** (1988) C354.
[15] R.S. de Biasi et al., Journal of Applied Crystallography **20** (1987) 319.
[16] O. Terra et al., New Journal of Chemistry **27** (2003) 957.
[17] J. Heuser, Master's thesis, Rheinische Friedrich-Wilhelms-Universitaet Bonn, Germany (2011).
[18] G.R. Lumpkin and T. Geisler-Wierwille, In: Comprehensive Nuclear Materials, 5, p. 563, Elsevier B.V. (2012).
[19] W.J. Weber et al., Journal of Materials Research **13** (1998) 1434.
[20] A. Meldrum et al., Mineralogical Magazine **64** (2000) 185.
[21] R.C. Ewing et al., Transformation Processes in Minerals **39** (2000) 319.
[22] J.S. Luo and G.K. Liu, Journal of Materials Research **16** (2001) 366.
[23] B.E. Burakov et al., Materials Research Society, MRS Proceedings (2004) 824.
[24] V.Picot et al., Journal of Nuclear Materials **381** (2008) 290.
[25] A. Meldrum et al., Physical Review **B56** (1997) 13805.
[26] R.C. Ewing and L.M. Wang, In: Phosphates, 48, p. 673, Mineral Soc Amer (2002).
[27] N. Clavier et al., Journal of the European Ceramic Society **31** (2011) 941.

4.8. Differentiating between actinide borates obtained from normal and extreme conditions.

Shijun Wu,[1,2,3] Shuao Wang,[4,5] Wulf Depmeier,[2] Thomas E. Albrecht-Schmitt,[6] Evgeny V. Alekseev[1,7*]

[1] Institute for Energy and Climate Research (IEK-6), Forschungszentrum Jülich GmbH, 52428 Jülich, Germany
[2] Institute of Geosciences, Kiel University, 24118 Kiel, Germany
[3] Guangzhou Institute of Geochemistry, Chinese Academy of Sciences, 511 Kehua Street, 510640 Guangzhou, P. R. China
[4] Actinide Chemistry Group, Chemical Sciences Division, Lawrence Berkeley National Laboratory, Berkeley, CA 94720, USA
[5] Department of Chemistry, University of California, Berkeley, Berkeley, California 94720, USA
[6] Department of Chemistry and Biochemistry, Florida State University, 102 Varsity Way, Tallahassee, Florida 32306-4390, USA
[7] Institut für Kristallographie, RWTH Aachen University, 52066 Aachen, Germany

Corresponding author: e.alekseev@fz-juelich.de

Abstract

In recent years, a series of actinide borates were obtained from traditional and extreme conditions. In this scientific report we describe the main methods of their synthesis and differences of their structures.

Introduction

One nuclear waste management strategy is the vitrification of high level radioactive wastes using borosilicate glasses [1]. Although most of the uranium is recovered from wastes during reprocessing, the produced borosilicate glasses still contain some uranium and plutonium as well as minor transuranics such as neptunium and americium [2] as well as up to 16.9 % B_2O_3 [3]. Some nuclear waste repositories possess strongly reducing conditions, with U(IV), Pu(III/IV) and Np(IV) as the dominant oxidation states, it could be beneficial to obtain information about actinide borate species in certain scenarios.
Furthermore, the management of the high level waste associated with the reactor accident in Fukushima Daiichi (Japan) in 2011 could benefit from a profound understanding of the actinyl borate compounds. During the accident, boric acid containing sea water was pumped into the reactor core for cooling purposes [4]. Our results reported here may provide supporting information that can help to improve specific nuclear waste management strategies.

Materials and Methods

The actinide borates were obtained using several different methods. The first one is the H_3BO_3 flux method. The standard (normal) conditions for this methods included 180-280 °C treatment of actinide source (for example uranyl nitrate for U) in an excess of boric acids using sealed vessels. Using such methods with some variations, we obtained a series of An^{3+}, An^{4+}, An^{5+} and An^{6+} borates [5].
To perform the work in extreme conditions we used two different methods. First one is the synthesis in piston press with the ½" piston cylinder module of a Voggenreiter LP 1000-540/50. The detailed description of the method was given in Ref. [6]. Using this method we

were able to reach the pressure up to 4 GPa and temperature up to 1400 °C. The second extreme conditions method is the synthesis in supercritical water. The syntheses were performed at T = 650 °C and P = 200 MPa in a cold seal pressure vessel (CSPV) working with H_2O as the pressure medium. The details of such synthesis were given in Ref. [7].
Structural determinations were performed using standard lab facility (single crystal and powder diffractometers) from single crystals and powder samples obtained in syntheses described above.

Results and Discussion

We have extended the knowledge of actinide borate chemistry significantly using boric acid as a reactive flux over the course of the past three years [5]. Except for β-$UO_2B_2O_4$ (only BO_3 groups), boron exhibits both, BO_3 and BO_4 coordination in all the uranyl borates obtained by room temperature or boric acid flux methods. In contrast, the high temperature phases reported by Gasperin et al. [8] are solely based on BO_3 units, with only one exception, $Ni_7B_4UO_{16}$, which contains both, BO_3 and BO_4 [8e]. This lends itself to the statement that, as a rule, the coordination number of boron tends to be lower in high temperature uranyl borates than in the low temperature phases.
The An^{n+} cations coordination generated by oxo-borates polyhedra in the phases obtained from boric acid flux (normal conditions experiments) is quite similar. All phases (with only one exception, β-$UO_2B_2O_4$ [5s]) possess six oxygen atoms donated by BO_3 flat triangles and/or BO_4 tetrahedra to an equatorial plane of An^{n+} coordination environment [5]. The most common examples of such coordination are shown in the Fig. 42 .

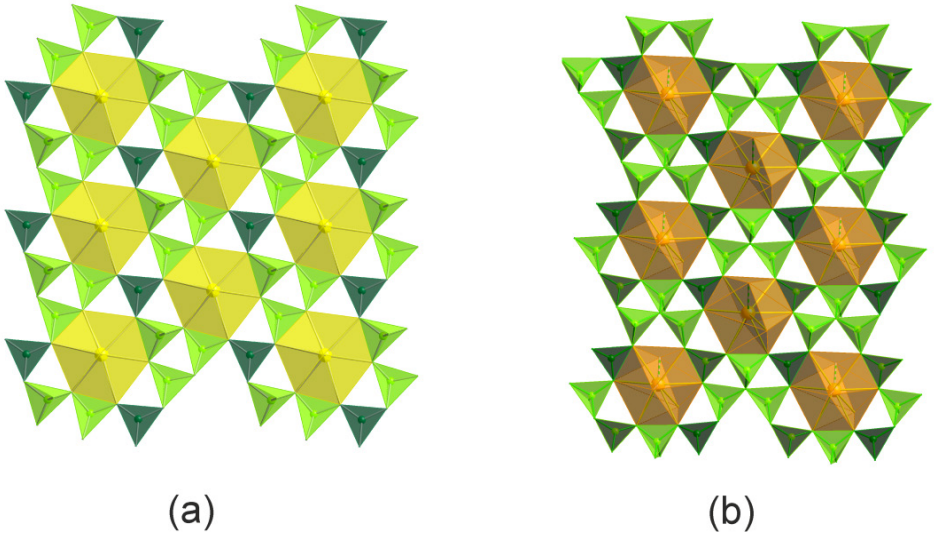

Fig. 42: Examples of An^{n+} cations oxo-borate environment in actinide borates obtained in normal conditions: (a) U^{6+} coordination in α-$(UO_2)_2[B_9O_{14}(OH)_4]$ [5s]; (b) Pu^{3+} coordination in $Pu_2[B_{12}O_{18}(OH)_4Br_2(H_2O)_3]\cdot 0.5H_2O$ [5i]. U polyhedra are shown in yellow, Pu in dark orange, BO_4 in light green and BO_3 in dark green.

The An^{n+} cations are staked in triangular holes of polyborate 2D or 3D frameworks. This coordination keeps in different actinide borates obtained from low/mild temperature conditions, even with different valence of An centers (from +3 to +6). It is noteworthy that in all these phases boron to actinides atomic ratios are equal or larger than 1.

In the last two years we started investigation of actinide borates formation under extreme conditions of pressure and temperatures using the methods mentioned above. The results of such investigations (mostly performed with U) demonstrate significant difference in chemistry and structures of actinide borates from normal and extreme conditions. First of all, the chemical composition is different. We have synthesized several phases under extreme conditions and in all pure uranium borates the B/U ratio was less than 1. This observation shows a significant difference in thermodynamic stability of actinide borates with excess of the boron atoms at HT/HP conditions. The second point is the dramatic increasing of the structures complexity of uranium borates from HT/HP reactions. The fragment of the crystal structure of $K_{12}[(UO_2)_{19}(UO_4)(B_2O_5)_2(BO_3)_6(BO_2OH)O_{10}]\cdot nH_2O$ (obtained from HT/HP conditions) is shown in the Fig. 43 [9].

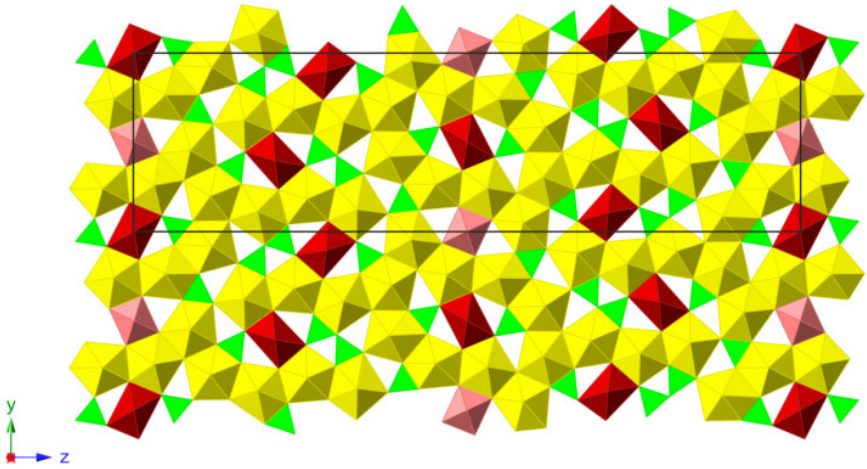

Fig. 43: View of the structure of $K_{12}[(UO_2)_{19}(UO_4)(B_2O_5)_2(BO_3)_6(BO_2OH)O_{10}]\cdot nH_2O$. UO_2O_4 square bipyramids are shown in red, UO_2O_5 pentagonal bipyramids are shown in yellow, UO_4O_2 (U(VI)) tetraoxide cores are shown in pink, BO_3 units are shown in green [9].

One can see that the structure of the layers in this phase is totally different from those in normal and mild conditions phases. U polyhedra are edge- or corner-sharing to form an infinite 2D sheet. All boron oxo-polyhedra are BO_3 triangles and that is quite different from phases obtained at normal conditions where BO_4 groups are the major content of the polyborate nets (Fig. 42). The number of possible UO_2^{2+} to BO_3 coordination is quite high in HT/HP phases. For example, as shown in Fig. 44 ten different coordination were observed in only three new HT/HP uranyl borates: $K_{12}[(UO_2)_{19}(UO_4)(B_2O_5)_2(BO_3)_6(BO_2OH)O_{10}]\cdot nH_2O$, $K_4[(UO_2)_5(BO_3)_2O_4]\cdot H_2O$, and $K_{15}[(UO_2)_{18}(BO_3)_7O_{15}]$ [9]. Two phases have three different oxygen environments of the uranium centers. It has to be mentioned that such diversity in the U – O coordination within one phase was rarely observed [10]. The structural and chemical complexity of uranyl borates obtained from HT/HP conditions is quite unusual for actinide borates and generally for actinide oxo-salts chemistry.

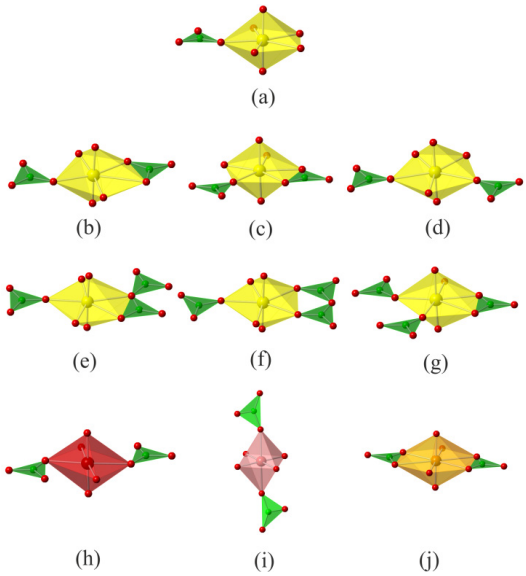

Fig. 44: Different coordination geometries of $(UO_2)^{2+}$ (UO_7 is yellow, UO_6 is red and UO_8 is orange) and $(UO_4)^{2-}$ centers with BO_3 groups (shown in green) in $K_{12}[(UO_2)_{19}(UO_4)(B_2O_5)_2(BO_3)_6(BO_2OH)O_{10}] \cdot nH_2O$, $K_4[(UO_2)_5(BO_3)_2O_4]\cdot H_2O$, and $K_{15}[(UO_2)_{18}(BO_3)_7O_{15}]$.[9]

Conclusions

In our work, we demonstrated a significant difference of actinides behaviors under normal and extreme conditions in complex $A^+ – An^{n+} – B_2O_3$ system (A^+ – alkali elements), including the chemical composition of the reaction products and their structural features. The complexity of actinide borates increases dramatically with increasing reactions temperatures and pressures. The work under extreme conditions will be extended with studies of other early actinides.

Acknowledgements

The authors are very grateful for the support provided by Helmholtz Association (VH-NG-815), by Deutsche Forschungsgemeinschaft (DE 412/43-1), by the Chemical Sciences, Geosciences, and Biosciences Division, Office of Basic Energy Sciences, Office of Science, Heavy Elements Chemistry Program, U.S. Department of Energy (DE-FG02-09ER16026), and National Natural Sciences Foundation of China (41103055).

References

[1] (a) Commission on Geosciences, Evironment and Resources, *Glass as a waste form and vitrification technology: Summary of an international workshop*. National Academy of Science: Washington D. C., 1996; (b) International Atomic Energy Agency, Spent fuel and high level waste: Chemical durability and performance under simulated repository conditions. International Atomic Energy Agency: Vienna, 2007.

[2] Grambow, B., *Elements*, **2006**, 2, 357-364.

[3] Ojovan, M. I.; Batyukhnova, O.G., Glasses for nuclear waste immobilization. Proc WM'07, WM-7061, **2007**.

[4] International Atomic Energy Agency. IAEA Fukushima Daiichi Status Report. 2nd Nov 2011.

[5] (a) Wang, S.; Alekseev, E. V.; Stritzinger, J. T.; Depmeier, W.; Albrecht-Schmitt, T. E., *Inorg. Chem.* **2010,** *49* (14), 6690-6696; (b) Wang, S.; Alekseev, E. V.; Ling, J.; Liu, G. K.; Depmeier, W.; Albrecht-Schmitt, T. E., *Chem. Mater.* **2010,** *22* (6), 2155-2163; (c) Wang, S.; Alekseev, E. V.; Stritzinger, J. T.; Liu, G. K.; Depmeier, W.; Albrecht-Schmitt, T. E., *Chem. Mater.* **2010,** *22* (21), 5983-5991; (d) Wang, S.; Alekseev, E. V.; Juan, D. W.; Miller, H. M.; Oliver, A. G.; Liu, G. K.; Depmeier, W.; Albrecht-Schmitt, T. E., *Chem. Mater.* **2011,** *23* (11), 2931-2939; (e) Wang, S.; Villa, E. M.; Diwu, J. A.; Alekseev, E. V.; Depmeier, W.; Albrecht-Schmitt, T. E., *Inorg. Chem.* **2011,** *50* (6), 2527-2533. (f) Wang, S.; Alekseev, E. V.; Depmeier, W.; Albrecht-Schmitt, T. E., *Chem. Commun.* **2011,** *47* (39), 10874-10885. (g) Wang, S.; Alekseev, E. V.; Miller, H. M.; Depmeier, W.; Albrecht-Schmitt, T. E., *Inorg. Chem.* **2010,** *49* (21), 9755-9757. (h) Wang, S.; Alekseev, E. V.; Depmeier, W.; Albrecht-Schmitt, T. E., *Chem. Commun.* **2010,** *46* (22), 3955-3957; (i) Wang, S.; Alekseev, E. V.; Juan, D. W.; Casey, W. H.; Phillips, B. L.; Depmeier, W.; Albrecht-Schmitt, T. E., *Angew. Chem. Int. Ed.* **2010,** *49* (6), 1057-1060; (j) Wang, S.; Alekseev, E. V.; Ling, J.; Skanthakumar, S.; Soderholm, L.; Depmeier, W.; Albrecht-Schmitt, T. E., *Angew. Chem. Int. Ed.* **2010,** *49* (7), 1263-1266; (k) Wang, S.; Alekseev, E. V.; Depmeier, W.; Albrecht-Schmitt, T. E., *Inorg. Chem.* **2011,** *50* (11), 4692-4694; (l) Wang, S.; Alekseev, E. V.; Depmeier, W.; Albrecht-Schmitt, T. E., *Inorg. Chem.* **2011,** *50* (6), 2079-2081; (m) Polinski, M. J.; Wang, S.; Alekseev, E. V.; Depmeier, W.; Albrecht-Schmitt, T. E., *Angew. Chem. Int. Ed.* **2011,** *50* (38), 8891-8894; (n) Wang, S.; Diwu, J.; Alekseev, E. V.; Jouffret, L. J.; Depmeier, W.; Albrecht-Schmitt, T. E., *Inorg. Chem.* **2012,** *51* (13), 7013-7016; (o) Wang, S.; Alekseev, E. V.; Depmeier, W.; Albrecht-Schmitt, T. E., *Inorg. Chem.* **2012,** *51* (1), 7-9; (p Polinski, M. J.; Wang, S.; Alekseev, E. V.; Depmeier, W.; Liu, G.; Haire, R. G.; Albrecht-Schmitt, T. E., *Angew. Chem. Int. Ed.* **2012,** *51* (8), 1869-1872; (q) Polinski, M. J.; Grant, D. J.; Wang, S.; Alekseev, E. V.; Cross, J. N.; Villa, E. M.; Depmeier, W.; Gagliardi, L.; Albrecht-Schmitt, T. E., *J. Am. Chem. Soc.* **2012,** *134* (25), 10682-10692; (r) Polinski, M. J.; Wang, S.; Cross, J. N.; Alekseev, E. V.; Depmeier, W.; Albrecht-Schmitt, T. E., *Inorg. Chem.* **2012,** *51* (14), 7859–7866.(s) Wang, S.; Alekseev, E. V.; Stritzinger, J. T.; Depmeier, W.; Albrecht-Schmitt, T. E., *Inorg. Chem.* **2010,** *49* (6), 2948-2953.

[6] Wu, S.; Kegler, P.; Wang, S.; Holzheid, A.; Depmeier, W.; Malcherek, T.; Alekseev, E. V.; Albrecht-Schmitt, T. E., *Inorg. Chem.* **2012,** *51* (7), 3941-3943.

[7] Wu, S.; Beermann, O.; Wang, S.; Holzheid, A.; Depmeier, W.; Malcherek, T.; Modolo, G.; Alekseev, E. V.; Albrecht-Schmitt, T. E., *Chem.-Eur. J.* **2012,** *18* (14), 4166-4169.

[8] (a) Gasperin, M., *Acta Crystallogr.* **1987,** C*43*, 2031-2033. (b) Gasperin, M., *Acta Crystallogr.* **1987,** C*43*, 1247-1250. (c) Gasperin, M., *Acta Crystallogr.* **1987,** C*43*, 2264-2266. (d) Gasperin, M., *Acta Crystallogr.* **1988,** C*44*, 415-416. (e) Gasperin, M., *Acta Crystallogr.* **1989,** C*45*, 981-983. (f) Gasperin, M., *Acta Crystallogr.* **1990,** C*46*, 372-374. (g) Behm, H., *Acta Crystallogr.* **1985,** C*41,* 642-645.

[9] Wu, S.; Wang, S.; Polinski, M.; Beermann, O.; Kegler, P.; Malcherek, T.; Holzheid, A.; Depmeier, W.; Bosbach, D.; Albrecht-Schmitt, T-E.; Alekseev, E.V., *Inorg. Chem.* **2013,** *52*, 5110-5118.

[10] (a) Piret, P.; Deliens, M., *Bull. Mineral.* **1982,** *105* (1), 125-128; (b) Demartin, F.; Diella, V.; Donzelli, S.; Gramaccioli, C. M.; Pilati, T., *Acta Crystallogr.* **1991,** B*47*, 439-446; (c) Alekseev, E. V.; Krivovichev, S. V.; Depmeier, W.; Siidra, O. I.; Knorr, K.; Suleimanov, E. V.; Chuprunov, E. V., *Angew. Chem. Int. Ed.* **2006,** *45* (43), 7233-7235.

4.9. Efficient methods for computation of actinides: uranium compounds and monazite orthophosphates from first principles

Piotr M. Kowalski, George Beridze, Ariadna Blanca Romero

Corresponding author: p.kowalski@fz-juelich.de

Abstract

Applied computational quantum chemistry is a rapidly growing research field that in the last decade spread into many new areas including the investigation of actinide-bearing systems for nuclear waste management. Density Functional Theory (DFT), which nowadays is the most widely used quantum chemical method, often dramatically fails to describe materials containing strongly correlated *f*-electrons. Here we show that simple modifications of the DFT allow to significantly improve the performance of the method in predicting structural and thermodynamic properties of uranium compounds and lanthanide-bearing monazite-type ceramics. Specifically, good results have been obtained with the DFT+U method and with the standard PBE functional with a modified enhancement function. Our studies suggest that with an appropriate choice of the already available computational methods it is possible to correctly compute structural and thermodynamic properties of actinide- and lanthanide-bearing materials with high computational efficiency.

Introduction

Over the last decade computational methods of quantum chemistry have been successfully applied to study minerals and fluids of chemically complex composition. Here we give a short overview of the current state of research in the field of computational chemistry of actinides, focusing on the application of DFT-based methods, and discuss potential areas for future development. We show that with an appropriate choice of the computational technique we are able to predict experimentally known enthalpies of reactions involving different Uranium-bearing gas species with an accuracy comparable to more computationally demanding post Hartree-Fock methods. We also perform a systematic investigation of lanthanide-bearing monazites in order to test the performance of different DFT-based methods in predicting structural and thermodynamic properties of these materials. We show that the thermodynamic mixing properties of solid solutions in these systems can be described with relatively inexpensive methods such as DFT+U [1], while the structural parameters of the lanthanide-bearing monazite ceramics can be accurately predicted using DFT exchange-correlation functionals specially designed for solids.

Materials and Methods

DFT is the most commonly used *ab initio* method in computational materials science [2]. Due to its computational efficiency, it can be applied to chemically complex systems containing up to several hundred atoms. On the other hand the more expensive, but more accurate post Hartree-Fock methods such as MP2, CCDT or CI [3] still cannot be applied to systems larger than first tens of atoms. However, the application of standard DFT to actinide-bearing

materials is often prohibitive. For instance, the AnO_2 solids (An=U, Np, Pu) are predicted to be metals, while these materials are insulators [4]. The enthalpies of reactions involving simple actinide-bearing complexes are significantly overestimated [5]. Here the performance of various DFT generalized gradient approximations for actinide and lanthanide materials is systematically investigated. The calculations were performed with quantum-espresso DFT plane wave code (www.quantum-espresso.org), using ultrasoft pseudopotentials to represent core electrons [6]. The energy cutoff was set at 50 Ry. In these studies, along with the standard generalized gradient approximation (GGA) functionals, such as the PBE [7] and PBEsol [8], we used the DFT+U method, which utilizes a Hubbard model to account for strong on-site coulomb repulsion between *f*-electrons [1]. In the case of Ln-bearing monazite, two variants of DFT+U calculations were tested. In the first variant the fixed value of the Hubbard *U* parameter of 6 eV was set for all lanthanides, while in the second variant the *U* parameter was determined for each specific compound using the linear response method [1].

Results and Discussion

Thermochemistry of simple Uranium complexes

Shamov et al. [5] compared the performance of various computational quantum chemical methods in the prediction of the enthalpies of various reactions involving simple gas-phase uranium-bearing compounds. They noted that standard DFT approaches significantly overestimate the reaction enthalpies by more than 100 kJ/mole and that reasonably accurate values could be obtained only using more advanced and more computationally intensive methods such as on hybrid DFT functionals or post-Hartree-Fock methods. Here we performed a similar study using different DFT functionals including the DFT+U method with U = 4.5 eV. In Fig. 45 we plot the mean absolute error of the enthalpies of 8 reactions relative to known experimental values. Consistently with [5], we observe that the average error of various standard DFT approaches is greater than 80 kJ/mole. The use of the DFT+U method allows decreasing the error to less than 60 kJ/mol. The especially significant improvement is observed for the dissociation reaction of uranium fluorides (Fig. 45). Interestingly, our calculations using the hybrid functional PBE0 [2] show only slight improvement relative to the standard PBE method. This shows that all-electron calculations have to be performed in order to reach chemical accuracy with this method. On the other hand, we note that different DFT functionals result in systematic, but slightly different offsets relative to the experimental values. This is clearly seen in Fig. 45, where we plot the results for the dissociation reaction of the uranium fluorides. The BPBE DFT functional gives a systematically better value compared to PBE functional. When one mixes the results of the two methods and derives the final enthalpy as E=E(PBE)-5(E(PBE)-E(BPBE)) the resulted values match the measurements fairly well. When applied to all the considered reactions such a simple correction scheme results in the error of about 25 kJ/mole, which is comparable to the error associated with MP2 or CCSD(T) methods or with the use of hybrid functionals (Fig. 45, PBE-BPBE corr.). We also find that the results of similar accuracy can be achieved by setting the value of the κ parameter in the PBE exchange functional enhancement function, F(s), to 6 (Fig. 45, modified PBE). Our studies thus show that simple modifications to the DFT methods can result in a substantial increase of their predictive power in relation to the thermodynamic properties of actinide-bearing materials.

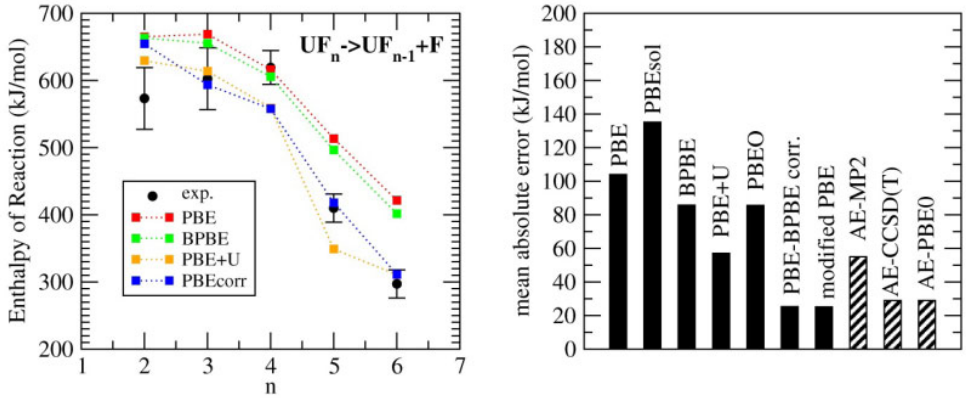

Fig. 45: Left: Enthalpies of dissociation reactions of uranium fluorides computed with different methods (see text). n gives the number of ligands; Right: A mean average error for the reaction enthalpies for 8 reactions reported in [5], for which experimental values are known. The considered reactions are: $UF_6+2UO_3->3UO_2F_2$, $UF_6+UO_2F_2->2UOF_4$, $UOF_4+UO_3->2UO_2F_2$, $UF_6->UF_5+F$, $UF_5->UF_4+F$, $UOF_4->UF_4+O$, $UO_2F_2->UO_2+2F$ and $UO_3->UO_2+O$. Solid bars represent our results while dashed bars are the results of [5] obtained by all-electrons (AE) calculations.

Monazite-type ceramics from first principles

Monazite has received great attention from nuclear waste management community due to its ability to incorporate large amounts of minor actinides and due to its high resistivity to self-irradiation [9]. Therefore it is actively investigated in our institute as a potential host phase for actinides. Our contribution to these studies aims at the comprehensive *ab initio* based characterization of different lanthanide- and actinide-bearing orthophosphates and in the prediction of the thermodynamic stability of various solid solutions with monazite structure. Our first aim was to test whether the structural parameters of different lathanide-bearing monazites can be reproduced with simple DFT methods. The computed structural parameters of different monazites are compared in Fig. 46. In our calculations we used both the PBE and PBEsol functionals. The PBEsol functional is a modification of the widely used PBE GGA approximation, in a sense that it improves the behavior of the exchange functional for slowly varying densities [8]. It has been shown, however, that this improvement in the description of solids occurs at the cost of a slightly worse prediction of their energies (Fig. 45). Our results show that PBEsol significantly outperforms the PBE functional in predicting the structural parameters of Ln-bearing monazites. The deviation of the predicted values from the experimental ones does not exceed 1 %. A similar trend is observed for the volumes. The PBE functional systematically overestimates the volume by about 3 % (Fig. 47). This shows that with an appropriate choice of the functional it is possible to reliably predict the structure parameters and volumes of different lanthanide-bearing monazites. Popa et al. [10] measured the excess enthalpy of solid solutions of $LaPO_4$ with $NdPO_4$, $EuPO_4$ and $GdPO_4$. They observed a systematic increase in the excess enthalpy with the atomic number of the substituting cation and interpreted this as a result of the increase in the size mismatch with La caused by the lanthanide contraction.

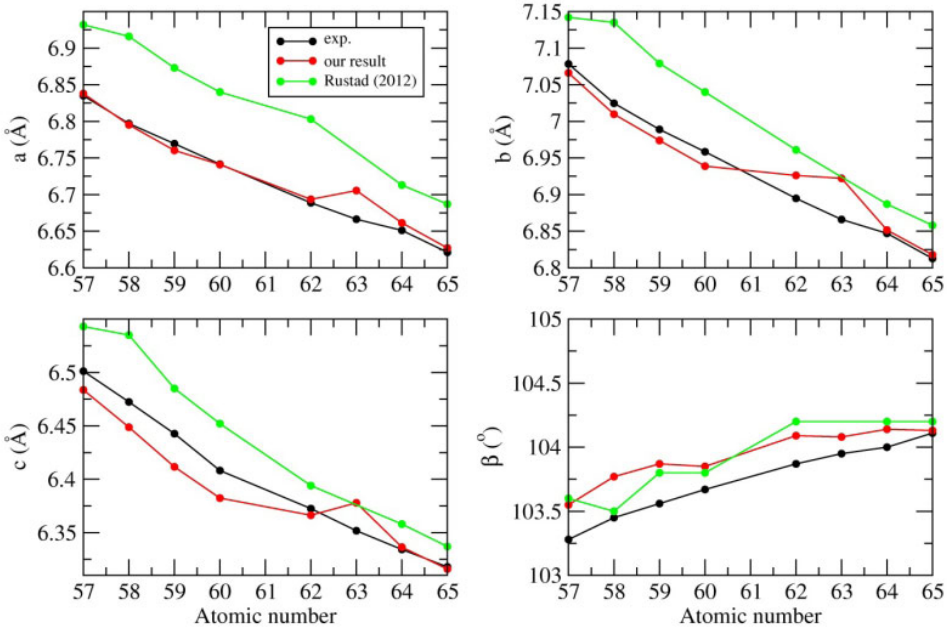

Fig. 46: Structural parameters of the $LnPO_4$ monazites derived from DFT calculations and measured experimentally [9]. Green points represent results of recent PBE calculation performed by Rustad [11].

In order to test the predictive power of DFT methods for monazite-type solid solutions we investigated systems containing 75 % of $LaPO_4$ and 25 % of $LnPO_4$ (Ln=Nd, Eu and Gd). The computed excess enthalpy was fitted with a simple empirical equation $\Delta H = x(1-x)W$, where W is the interaction parameter and x is the mole fraction of $LnPO_4$. The calculations were performed with PBE and PBEsol functionals and with the DFT+U method. DFT+U calculations were performed using PBEsol functional with fixed Hubbard U parameter value of 6 eV for all lanthanides and with the U value derived for each $LnPO_4$ compound using the linear response method [1]. The following values of U were obtained: 3.4 eV for La, 4.9 eV for Nd, 8.1 eV for Eu and 3.5 eV for Gd. The results of our calculations are summarized in Fig. 47. The DFT+U method correctly reproduces the decrease in volume with the size of the lanthanide atom and correctly predicts the increase in value of the interaction parameter W with decrease in the size of Ln. The W values predicted with different methods vary within 5 kJ/mol. However, in the case of La-Nd system the predicted value is significantly smaller than the experimental one. We note that the W values predicted here should be taken with caution. In our investigation we used the smallest possible super-cell of monazite containing four formula units. It is known, that the excess properties computed with the aid of small super-cells might be affected by effects of chemical ordering, and thus could significantly differ from values expected in the disordered limit. In our further studies the calculations will be repeated using larger super-cells.

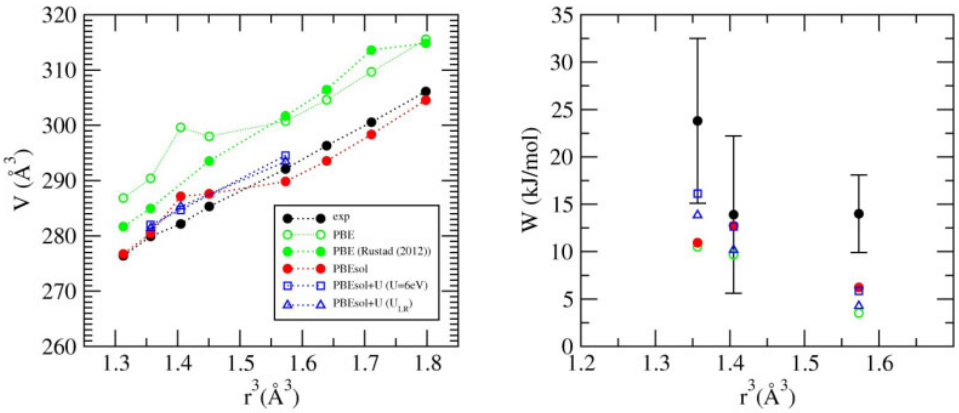

Fig. 47: Left: Predicted vs. measured volume of monazite systems as a function of the Ln size (r is the ionic radius of 9-fold coordinated Ln). Right: Interaction parameter W for solid solution of (Ln,X)PO_4. Filled black circles represent the measurements of [10].

Conclusions

Here we present our first results of *ab initio* investigation of the actinide- and lanthanide-bearing materials such as simple molecules and monazite-type compounds. We show that with an appropriate choice of the computational method the structural and thermodynamic properties of these materials can be computed with standard DFT methods or with computationally inexpensive extensions of these methods, such as DFT+U. We find that by mixing results obtained with different DFT functionals or by simple modification of the existing functionals a significant improvement in the reaction enthalpies can be easily achieved. We observe that the structural parameters of different monazite-type ceramics can be accurately predicted with the PBEsol functional. The energetics of excess mixing in monazite-type solid solutions is also fairly well reproduced, although additional effort is needed to investigate the effect of the system size on the predicted enthalpies of mixing. In general, our studies show that accurate predictions of the properties of actinide- and lanthanide-bearing materials can be obtained with relatively inexpensive computational approaches. An additional systematic effort is needed to test the performance of the discussed approaches on a larger set of Ln- and An-materials.

Acknowledgements

We acknowledge the computing time on RWTH Aachen cluster awarded through Jülich-Aachen research alliance (JARA-HPC).

References

[1] M. Cococcioni, S. de Gironcoli „Linear response approach to the calculation of the effective interaction parameters in the LDA+U method“, Physical Review B 71 (2005), 035105.
[2] W. Koch, M.C. Holthausen, 2000. „A chemist's guide to density functional theory“. Wiley-VCH, Weinheim.
[3] Ch. Hattig, „Beyond Hartree-Fock: MP2 and Coupled-Cluster Methods for Large SystemsComputational Nanoscience: Do It Yourself!“, J. Grotendorst, S. Bl ¨ugel, D. Marx (Eds.), John von Neumann Institute for Computing, Julich,NIC Series, Vol. 31, (2006), 245-278.
[4] X. D. Wen, R. L. Martin, T. M. Henderson, G. E. Scuseria, „Density functional theory studies of the electronic structure of solid state actinide oxides.“, Chem. Rev. 113 (2013), 1063.

[5] G. A. Shamov, G. Schreckenbach, and T. N. Vo „A Comparative Relativistic DFT and ab Initio Study on the Structure and Thermodynamics of the Oxofluorides of Uranium(IV), (V) and (VI)“, Chem. Eur. J. 13 (2007), 4932-4947.
[6] D. Vanderbilt, „Soft self-consistent pseudopotentials in a generalized eigenvalue formalism.“, Phys. Rev. B 41 (1990), 7892.
[7] J. P. Perdew, K. Burke, M. Ernzerhof, „Generalized Gradient Approximation Made Simple“, PRL 77, (1996), 3865.
[8] J. P. Perdew, A. Ruzsinszky, G. I. Csonka, O. A. Vydrov, G. E. Scuseria, L. A. Constantin, X. Zhou, K. Burke, „Restoring the Density-Gradient Expansion for Exchange in Solids and Surfaces“, PRL 100 (2008), 136406.
[9] H. Schlenz, J. Heuser, A. Neumann, S. Schmitz, D. Bosbach, „Monazite as a suitable actinide waste form”, Z. Kristallogr. 228 (2013), 113-123.
[10] K. Popa, R.J.M. Konings, T. Geisler, „High-temperature calorimetry of $(La_{1-x}Ln_x)PO_4$ solid solutions“, J. Chem. Thermodynamics 39 (2007), 236–239.
[11] J. R. Rustad, „Density functional calculations of the enthalpies of formation of rare-earth orthophosphates“, American Mineralogist 97 (2012), 791–799.

4.10. MEDINA – Multi Element Detection based on Instrumental Neutron Activation Analysis – a Nondestructive Analytical Technique fort the Assay of Toxic Elements and Substances in Radioactive Waste Packages

E. Mauerhofer[1], A. Havenith[2]

1) Institute of Energy and Climate Research – Nuclear Waste Management and Reactor Safety, Forschungszentrum Jülich GmbH, 52425 Jülich;

2) Institute of Nuclear Fuel Cycle, RWTH-Aachen, 52062 Aachen

Corresponding author: e.mauerhofer@fz-juelich.de

Abstract

A short description of the test facility MEDINA for the nondestructive identification and quantification of toxic elements in 200-L waste drums is given. The first results for the determination of cadmium in a concrete matrix are presented.

Introduction

In addition to the radioactive components, radioactive waste packages may contain non-radioactive hazardous and toxic substances such as heavy metals that can adversely affect human health and the environment [1]. After a sufficient decay time the radioactivity of the waste will become harmless but the chemically toxic substances will persist. The disposal of such radioactive waste packages must comply with relevant regulations in order to avoid groundwater pollution. To cope with the European regulation [2], the long term disposal of radioactive waste in dedicated European repositories must prevent any pollution of ground water from toxic chemicals, even long after the radioactivity of the waste has reached the level of the natural radioactivity [3]. Additionally, the waste must contain low amounts of reactive chemicals, in order to avoid gas production that would impact the integrity of the waste matrix [4]. Accordingly, the German agency responsible for radioactive waste management, BfS (Bundesamt für Strahlenschutz), has indeed defined acceptability limits concerning toxic and reactive elements/substances for the disposal of radioactive waste packages in KONRAD (Germany).

In principle, traceability and quality controls in the waste production and conditioning processes allow the quantification of these chemicals. However, poor or no information is available for the so-called historical waste that needs to be characterized. As a consequence, a nondestructive analytical technique based on Prompt and Delayed Gamma Neutron Activation Analysis (P&DGNAA) was developed at IEK-6. In a first study that started in 2006, it was experimentally demonstrated that the prompt and delayed gamma neutron activation analysis using a 14 MeV neutron generator is suitable to determine the chemical composition of large samples [5-7]. Based on the results of this study the test facility MEDINA (Multi Element Detection based on Instrumental Neutron Activation Analysis) was developed in 2009 in cooperation with the Institute of Nuclear Fuel Cycle of the RWTH-Aachen for the assay of 200-l waste packages and its performance and response were investigated experimentally and numerically for optimization. The modeling of the test facility MEDINA using the MCNP simulation code and the validation of the measurements simulations were performed in collaboration with the Nuclear Measurement Laboratory of CEA Cadarache [8-9]. An international patent has been filled for the MEDINA technology [10].

The test facility MEDINA

The test facility MEDINA designed for the assay of 200-l drums filled with radioactive waste is shown in Fig. 48. The drum is positioned on a turntable inside an irradiation chamber made exclusively of graphite acting as neutron moderator and reflector. For radioprotection purpose the wall thickness of the graphite chamber is about 40 cm. The inner dimension of the irradiation chamber is 80 × 80 × 120 cm and the outer dimension 160 × 200 × 155 cm. The amount of graphite was about 6500 kg. Hydrogenous material like polyethylene or paraffin were prohibited in the irradiation chamber so as to further the determination of the hydrogen content of the sample by analyzing the prompt gamma-ray at 2.22 MeV. The drum is irradiated with 14 MeV neutrons produced by a deuterium-tritium (D-T) neutron generator (GENIE 16GT, EADS SODERN). The neutron generator is positioned horizontally in a wall of the irradiation chamber with its tritium-target located at mid-height of the waste drum and at a distance of 55 cm from the center of the waste drum. It is operated at a neutron emission of 8·107 n/s in pulse mode with a repetition rate of 1 KHz. The length of the neutron pulse corresponding to the 14 MeV neutron irradiation time is set to 50 µs. The detection of the prompt and delayed gamma rays emitted from the waste drum is performed with a 104 % n-type HPGe (CANBERRA) detector placed in a wall of the irradiation chamber perpendicular to the neutron generator. The distance between the detector window and the center of the waste drum is 105 cm so that the volume of a 200-L drum is fully assayed. The detector housing is entirely surrounded by ^{6}LiF plates [5] made of a mixture of ^{6}LiF powder and water glass to avoid thermal neutron capture in the germanium crystal. The detector signals are processed through a fast spectroscopy amplifier with Gated Integrator (CANBERA Model 2022) by a 16k Multi-Channel-Analyzer (ORTEC Model Aspec-927) interfaced to a PC via USB 2.0. By triggering the Multi-Channel-Analyzer on the start of the neutron pulse via a Digital Delay Generator (Signal Recovery Model 9650A) a delay of 20 µs after the end of the neutron pulse and a counting time of 930 µs between neutron pulses are set. The gamma spectra are recorded in Zero Dead Time mode with the software GammaVision-32 (ORTEC). The analysis of the gamma spectra is carried out with the spectroscopy software Gamma-W (Westmeier GmbH).

Fig. 48: Test facility MEDINA (Multi Element Detection based on Instrumental Neutron Activation) developed at IEK-6 FZJ for the assay of 200-L waste drums (left). Modular mockup drums with concrete blocks and concrete block lined with a cadmium plate (right).

In order to investigate the performance of the facility MEDINA 200-l mockup drums filled with blocks of concrete Maxit 2015 GNS (height 20 cm, diameter 10 cm, density 1.35 g/cm^3) of well-known elemental composition were fabricated. The modular configuration of the mockup drums allows simulating inhomogeneous waste matrices by substituting the concrete blocks by other substances such as lead or mercury or by lining partially the concrete blocks with a material plate e.g. cadmium plate (Fig. 48).

Results and Discussion

Numerous measurements with different samples were done in order to investigate the performance and the response of the facility MEDINA. The results obtained from the measurement of a cadmium plate placed at various radial and axial positions in a 200-l concrete drum are presented. The cadmium plate had a surface of 12.5 × 12.5 cm^2, a thickness of 1 mm and a mass of 134.4 g. The weight of concrete was 200 kg and the weight of the drum 53 kg. The measurements were done according to the irradiation and counting parameters described above. Eight angular dependent gamma-ray spectra were each recorded over 1860 s for a discrete drum rotation step of 45°. For example the angular dependent count rate distributions of the 558.32 keV prompt gamma ray of cadmium obtained for a plate placed at a height of 71 cm and various radial positions (6,17 and 28 cm) in the concrete drum are shown in
Fig. 49a. Their Gaussian shapes reflect well the inhomogeneous distribution of cadmium in the concrete matrix. The scattering of the Gaussian distribution is related to the radial position of the plate. The count rates of the prompt gamma rays induced by the thermal neutron activation of the concrete were found independent on the drum rotation as the elements are homogenous distributed
Fig. 49b).

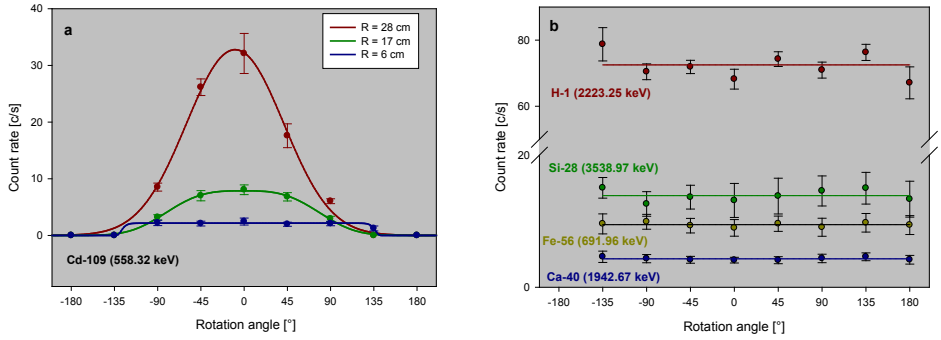

Fig. 49: Dependence of the count rate of the prompt gamma rays induced by the thermal neutron activation of elements in the concrete drum. a) Cadmium plate placed at a height of 71 cm and various radial positions R in the concrete matrix. The count rate distribution is fitted with a modified Gaussian. b) Hydrogen, silicon and calcium in concrete and iron in the steel drum.

The quantification of cadmium was achieved through the analysis of the angular count rate distributions. For this a model was applied taking into account the thickness and radial position of the cadmium plate, the local value of the thermal/epithermal neutron flux, the self-absorption of neutrons in the cadmium plate, the absorption of the gamma rays by the concrete matrix and the wall of the steel drum and the detector efficiency. The results are presented in Tab. 6. The calculated values for radial position and mass agree fairly well with the true values taken into account their uncertainties. For positions close to the drum center (R = 6 cm) the radial positions are determined with large uncertainties due to the poor angular resolution. At the height H = 9 cm and the radial position R = 6 cm the mass of cadmium is strongly underestimated. This is mainly due to the presence of the Sm_2O_3 magnet of the turntable stepper motor acting as a strong thermal neutron absorber and leading to a depression of the thermal neutron flux.

Tab. 6: Calculated radial position (R_{cal}) and mass (m_{cal}) for a cadmium plate placed at various positions in the concrete drum. The mass of the plate is 134.4 g.

H (cm)	R (cm)	$R_{cal.}$ (cm)	m_{cal} (g)
9	6	7.5± 6.0	70 ± 14
9	17	17.9 ± 2.9	108 ± 61
9	28	26.3 ± 1.6	119 ± 39
46	6	6.0 ± 5.3	135 ± 36
46	17	17.0 ± 4.7	127 ± 27
46	28	28.0 ± 2.8	113 ± 15
71	6	1.5 ± 2.3	100 ± 14
71	17	13.5 ± 1.0	148 ± 16
71	28	28.6 ± 2.7	125 ± 28

For the experimental conditions given above and a counting time of 1860 s the limit of detection (3σ) for cadmium is 6 g (0.0024 wt%) at a radial position of 28 cm i.e. close to the inner wall of the drum and 150 g (0.059 wt%) at the center of the drum.

Conclusions

In this work it was shown that the nondestructive determination of toxic elements in 200-L waste drums is possible with the facility MEDINA. Further developments will focus on the improvement of the sensitivity by reducing background radiation.

References

[1] Management of low and intermediate level radioactive wastes with regards to their chemical toxicity; IAEA-TECDOC-1325; International Atomic Energy Agency IAEA; December 2002.

[2] Council Directive 80/68/EEC of 17 December 1979 on the Protection of Groundwater Against Pollution Caused by Certain Dangerous Substances. The Council of the European Communities, 1979.

[3] Descamps, F.; Dujacquier, L.; Overview of European practices and facilities for waste management and disposal. Nucl. Eng. Des. 1-7, 176, 1997.

[4] Freedman, S., Corrosion of nonferrous metals in contact with concrete, Mod. Concr., 36, 1970.
[5] Kettler, J., Prompt-Gamma-Neutronen-Aktivierung-Analyse zur zerstörungsfreien Charakterisierung radioaktiver Abfälle, Energie & Umwelt, Band 82, ISBN 978-3-89336-665-1, Forschungszentrum Jülich 2010.
[6] Kettler, J.; Mauerhofer, E.; Rossbach, M.; Bosbach, D.; PGNAA for toxic Element Determination in Nuclear Waste Drums, Transactions of the American nuclear Society and Embedded Topical Meetings Risk Management and 2009 Young Professionals Congress, Nuclear Analytical Methods for the 21st Century, Volume 101, Page 100-101, ISSN 0003-018X.
[7] Bai, Y.; Wang, D.Z.; Mauerhofer, E.; Kettler, J.; MC simulation of thermal neutron flux of large samples irradiated by 14 MeV neutrons, Nuclear Science and Technology, Volume 21, 2010, Pages 11-15.
[8] Ma, J.L.; Carasco, C.; Perot, B.; Mauerhofer, E. et al., Prompt Gamma Neutron Activation Analysis of toxic elements in radioactive waste packages, Applied Radiation and Isotopes, Volume 70, Issue 7, July 2012, Pages 1261-1263, IRRMA 8 conference records, Kansas city (2011).
[9] Mauerhofer, E. ; Havenith, A.; Carasco, C. et al., Quantitative comparison between PGNAA measurements and MCNP calculations in view of the characterization of radioactive wastes in Germany and France, (2012) submitted to American Institute of Physics, under reviewing.
[10] Mauerhofer, E.; Kettler, J.; Neutron activation analysis using a standardized sample container for determining the neutron flux, WO/2012/10162, 26 January 2012.

4.11. SGSreco: An improved method for the reconstruction of activities in radioactive waste by segmented γ-scanning

Thomas Krings and Eric Mauerhofer

Corresponding author: tho.krings@fz-juelich.de

Introduction

Radioactive waste drums containing low and intermediate level waste have to fullfill national regulations prior to its transport, intermediate storage or final disposal [1]. To check the conformance of radioactive waste drums with national regulations, experimental methods are developed to quantify the isotope specific activity content. The most widely applied non-destructive assay to determine its isotope specific activity content in radioactive waste drums is Segmented Gamma-Scanning (SGS) [2]. In SGS a radioactive waste drum is rotated discretely in front of a collimated detection system. At each fixed sector a collimated detection unit records a gamma-ray-spectrum. After a revolution of the drum, the detection unit is lifted to the next segment and the drum is revolved. This procedure is repeated until the top of the drum is reached. The acquired gamma-ray-spectra are analyzed for the presence of isotope characteristic peaks. Based on these peaks count rate distributions as a function of the drum height and rotation angle are generated. Up to today the isotope specific activity content is calculated assuming a homogeneous matrix and activity distribution. These assumptions lead to analytical activity calculations based on the averaged count rate with an accuracy of around 30% [3,4]. As pointed out by an report of the European Commission, 25% of all radioactive waste drums analyzed at the Forschungszentrum Jülich exhibit a fairly homogeneous matrix and activity distribution [2]. About 75% of all radioactive waste drums exhibit a significant heterogeneous matrix and activity distributions heavily affecting the reliability and accuracy of the activity reconstruction in SGS.

In this work an improved method to reconstruct the activity of homogenously distributed gamma-emitting isotopes and a new method to reconstruct the activity of spatially concentrated gamma-emitting isotopes (point sources or hot spots) in standardized waste drums with internal shielding structures is presented. The software framework based on this method is called SGSreco. SGSreco is validated with simulations of waste matrices spatially concentrated activity distributions of long-lived radioactive isotopes ^{60}Co and ^{137}Cs. The activation product ^{60}Co and the fission product ^{137}Cs constitute the major isotope content in low and intermediate level radioactive waste from nuclear power plants. Furthermore, SGSreco is tested on SGS measurements a reference segment containing point sources of the above-mentioned isotopes. It is shown that SGSreco improves the accuracy and the reliability of the activity reconstruction in SGS and that the presented algorithm is suitable with respect to the framework requirement of industrial application.

Scanner-Design

The detection unit of the segmented gamma-scanner Gernod II at the Forschungs-zentrum Jülich is a high-purity germanium (HPGe) detector with a relative efficiency of 30%. The diameter of the HPGe crystal is 4.96 cm and its length is 5.31 cm. The detector is collimated by means of lead, which has a cylindrical collimation window with a diameter of 4 cm and a length of 20.6 cm. The distance d0 from the active detector surface to the center of the drum is 63 cm. Standardized 200-L waste drums have a height of 80 cm and an inner diameter of

56 cm. The wall of a waste drum consists of stainless steel with a density of 7.87 g/cm^3 and a thickness of 1.5 mm. A waste drum is scanned routinely in 20 segments with a height of 4 cm. Each segment is divided into 12 sectors leading to rotation steps of 30°. The counting time at each sector is 15 s. In total, 240 spectra are recorded at predefined points during the measurement of a radioactive waste drum. The overall counting time is 1 h. The alternative scan mode uses rotation steps of 15° resulting to 480 sectors and a total scan time of 2 h. This mode offers a more reliable data basis for the analysis of point spatially concentrated activity distributions.

A Priori Information

The conditioning of radioactive waste underlies the priority of volume reduction resulting in considerable savings of costs for the intermediate and final storage. Therefore, loose or solid, by material sorted, radioactive waste is filled in metal cartridges which are processed into compacts with a high-pressure compactor and fit into standard 200-L drums. During this process, each compact is documented with its weight, height and the waste material. Based on this information it is possible to calculate the average density of a compact. The compacted metal cartridge serves as a absorber around the waste matrix. The absorber thickness depends on the compact's height and can thus be calculated. The high-pressure compaction validates the deduction that the waste matrix is nearly homogeneous within the compact. This standard conditioned waste is the main input stream for SGS. Conclusively the density of the waste matrix and the density, material and thickness of the absorber structure are a priori known for each segment.

Methodology

The basic principle of SGSreco is the compact-wise analysis of count rate distributions associated with a certain isotope. A homogeneous count rate distribution will generate a constant count rate independent from the position of the detection unit. Activity point sources are expected to generate peaks in the count rate distribution. The peak shape is thereby relying on the position of the point source within in the compact and its activity.

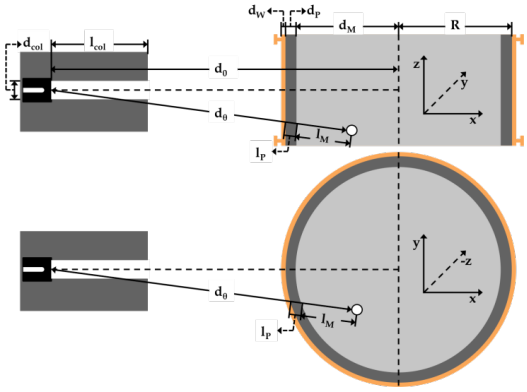

Fig. 50 Sketch of the geometric setup of a segmented gamma-scanner. The drum consists of an active matrix (light grey) a passive matrix (dark grey) and the drum wall (orange). The detection unit with the detector (black and the lead collimator (dark grey) is on the left hand side of the waste drum. The upper part shows a side view and the lower part a top view.

Within SGSreco the count rates generated by point sources are analytically calculated based on a geometric model as shown in Fig. 50. The count rate generated by a point source at an energy E_γ measured by the detection unit at a height z and at a rotation angle θ can be calculated by

$$T_\theta^z(E_\gamma, \vec{r}_S, A_S) = \varepsilon_0(E_\gamma) \cdot K(\vec{r}_S) \cdot I(E_\gamma) \cdot A_S \cdot e^{-\mu_W \cdot d_W} \cdot e^{-\mu_P \cdot l_P(\vec{r}_S)} \cdot e^{-\mu_M \cdot l_M(\vec{r}_S)} \quad (1)$$

Here, $\vec{r}_S$ is the position of the point source in cylindrical coordinates and A_S is its activity. Furthermore, $\varepsilon_0(E_\gamma)$ is the detection efficiency to a point source located axially to the detection unit, $K(\vec{r}_S)$ is the collimator response function [5] and $I(E_\gamma)$ is the emission probability. The exponential terms account for the absorption in the drum wall (index W) in the passive matrix (index P) and in the active matrix (index M). For a set of ns activity point sources and a homogeneous activity distribution in a given compact the total generated count rate can be calculated by

$$T_\theta^z(E_\gamma) = \overline{T}(E_\gamma) + \sum_{i=0}^{n_S} T_{i,\theta}^z(E_\gamma, \vec{r}_{S,i}, A_{S,i}), \quad (2)$$

with $\overline{T}(E_\gamma)$ beeing the averaged count rate generated by a homogeneous activity distribution. To determine optimal source and matrix parameter the log-likelihood function

$$\log(\mathcal{L}) = \sum_{j=1}^{n_\gamma} \sum_{i=1}^{n_{sec}} \log(p(R_\theta^z(E_\gamma) | T_\theta^z(E_\gamma))) \quad (3)$$

is minimized. Here, $p(R_\theta^z|T_\theta^z)$ is the Poisson-probability to measure a count rate of R_θ^z when expecting a count rate T_θ^z. The minimization process is initialized with the number of point sources and their first guess coordinates as given by a search for local maxima in the count rate distributions. SGSreco offers several fit modes as summarized in Tab. 7 with the corresponding set of fit parameter. The minimization itself and the determination of statistical errors are performed using the MINUIT program library for function minimizing and error analysis.

Tab. 7: Summary of the optional fit parameter and the available fit modi in SGSreco.

	Optional	**Minimum**	**Standard**	**Absorber**
Point source (per source)	r_S, φ_S, z_S A_S	r_S, φ_S A_S	r_S, φ_S, z_S A_S	r_S, φ_S, z_S A_S
Homogeneous activity distribution (per isotope)	$\overline{T}(E_\gamma)$		$\overline{T}(E_\gamma)$	$\overline{T}(E_\gamma)$
Waste matrix (per compact)	Absorber thickness Matrix density			Absorber thickness

The activity of a homogeneous isotope content is not a direct result of the fit. This isotope specific activity can be calculated based on the averaged count rate $\overline{T}(E_\gamma)$ according to the conventional method with a precision of around 30% [4]. In an alternative approach the homogeneous activity content is approximated by a set of closely distributed hypothetical point sources. This approximation allows the activity reconstruction by a numerical integration of equation (1) over the compact volume [6]. This integration is carried out in acceptable computation times of around 1.5 min on average desktop machines with a precision of between 2% and 4% and is thus the standard in SGSreco.

Results of the Simulation Study

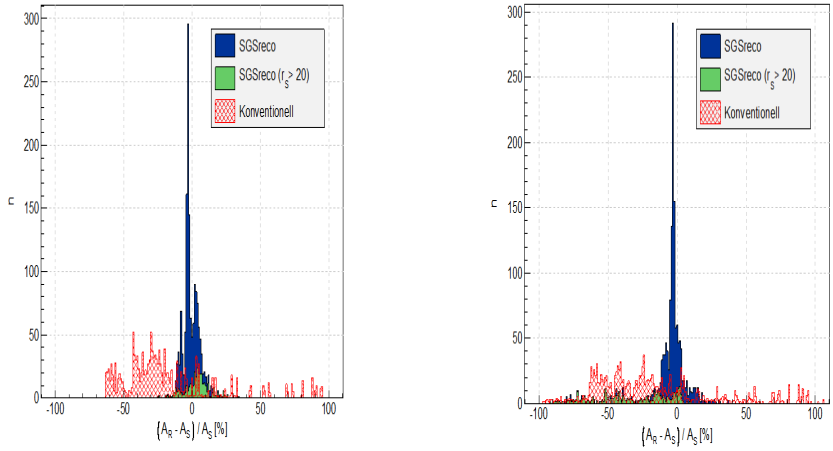

Fig. 51: Deviations of the reconstructed activity to the true activity for simulated ^{60}Co point sources in four different matrix types. The matrix densities are between 0.5 g/cm^3 and 2.3 g/cm^3. The left part shows the results for 15° rotation steps (alternative mode) and the right part for 30° (standard mode). The dashed red area shows the results using the conventional method and the blue and green area with SGSreco.

SGSreco is tested with simulated SGS measurements of various point source and matrix configurations. The simulations are performed using the Geant4 framework. In total four different matrix configurations with matrix densities ranging from 0.5 g/cm^3 to 2.3 g/cm^3 and matrix materials consisting of polyethylene and concrete are simulated. Point sources are embedded at about 400 different positions ranging from 0 cm to 25 cm radial offset in steps of 1cm and from 0° to 15° angular offset in 1° steps. The results of the activity reconstruction are summarized in Fig. 51. The reconstruction based on the conventional method results to activity values ranging from -70% to 100% apart from the true activity. The results based on SGSreco show mean deviations of about -1.56% and -3.13% for 15° and 30° rotation steps, respectively. The standard deviations of the distributions are 4.9% and 11.29%. Uncertainties on the reconstructed activities are determined to be between 3% and 5%. Furthermore, the results show, that the activity of point sources at positions with a radial offset >20 cm can be much more accurately reconstructed if a rotation step of 15° is applied. Conclusively, SGSreco is capable to reconstruct the activity of point sources in a waste matrix accurately and reliably.

Experimental Results

Due to the experimental validation a reference segment built of polyethylene with a density of 1.34 g/cm^3 and a height of 20 cm is constructed. This reference segment offers several slots to position point sources in the matrix. Experimental measurements are performed in standard scan mode with angular rotation steps of 30°. As a timesaving alternative to 15° rotational steps, the drum rotation is performed continuously. An integral-spectrum is taken during 30° of drum rotation. Since four segments are scanned the total scan time is 12 min in a single run. Measurements are done with an 11.43 MBq ± 10% ^{60}Co point source. The results of the activity reconstruction at 13 different positions are summarized in Table 8. The activity reconstruction meets the expectations given by the results of the simulations study well. For point source positions less than 20 cm from the symmetry axis of the drum the deviations from the true activity are less than 10%. Only for point sources at the very outer positions the deviations exceed 10%.

Tab. 8: Summary of the reconstruction of the point source parameter of a ^{60}Co point source embedded in the reference segment with SGSreco.

r_{true} [cm]	r_S [cm]	φ_{true} [deg]	φ_S [deg]	h_{true} [cm]	h_S [cm]	A_{hom} [kBq]	A_S [MBq]	$\Delta A/A$ [%]
5	5.11	0	2.20	6.2	6.42	1560	10.1	2.01
10	9.37	0	1.54	6.2	6.51	2110	11.1	-1.32
15	14.28	0	0.56	6.2	6.34	42.1	11.6	2.20
20	19.05	0	-0.08	6.2	6.12	-	12.3	8.04
25	22.92	0	0.29	6.2	6.15	-	13.6	19.06
10	9.47	7.5	8.90	6.2	6.45	286	11.0	-1.20
15	14.32	7.5	8.03	6.2	6.28	55.1	11.4	0.44
20	18.84	7.5	6.75	6.2	6.19	-	11.7	2.00
25	22.77	7.5	5.51	6.2	6.08	-	12.7	11.43
10	9.57	15	16.52	6.2	6.42	333	10.8	-2.29
15	14.39	15	15.82	6.2	6.19	-	11.4	-0.45
20	18.70	15	15.09	6.2	6.14	40.8	11.5	0.80
25	23.64	15	14.72	6.2	6.09	-	11.8	2.92

Conclusions

SGSreco is designed to reconstructed spatially concentrated as well as homogenously distributed isotope specific activity contents in radioactive waste drums. The reconstruction is based on fits of a physically motivated analytical model to the measured count rate distributions associated with a certain isotope. Within a simulation study it has been shown, that SGSreco is able to reconstruct the activities of point sources within a homogenous waste matrix with an accuracy of between 2% and 5%. Furthermore, the simulation study reveals that SGS measurements should be performed with drum rotation steps of 15° to

access the most reliable data basis for the reconstruction of point sources. These results have been confirmed by measurements of a ^{60}Co source in a reference drum segment with a polyethylene matrix, although the discrete drum rotation is replaced by a continuous rotation and spectra are taken integrally after each 30° of drum rotation. Overall, SGSreco offers a very accurate and reliable alternative to the conventional method for the reconstruction of activity contents in radioactive waste drums.

References

[19] P. Brennecke, (2011): Requirements on Radioactive Waste for Disposal (Waste Acceptance Requirements as of October 2010) - Konrad Repository -, Tech. rep., Bundesamt für Strahlenschutz.

[20] H.-J. Sanden et al., (1999): Optimisation of Gamma Assay Techniques for the Standard Quality Checking of Nuclear Waste Packages and Samples, Tech. rep., European Commission.

[21] P. Filß, (1989): Specific activity of large-volume sources determined by a collimated external gamma detector, Kerntechnik 54.

[22] P. Filß, (1995): Relation between the activity of a high-density waste drum and its gamma count rate measured with an unshielded Ge-detector, Applied Radiation and Isotopes 46.

[23] T. Krings, E. Mauerhofer, (2011): Reconstruction of the activity of point sources for the accurate characterization of nuclear waste drums by segmented gamma scanning., Applied Radiation and Isotopes 69.

[24] T. Krings et al. (2013): A numerical method to improve the reconstruction of the activity content in homogeneous radioactive waste drums, Nuclear Instruments and Methods A 701.

4.12. Actinide nuclear cross section data for characterization of nuclear waste

M. Rossbach, Ch. Genreith, T. Randriamalala
Corresponding author: m.rossbach@fz-juelich.de

Abstract
Accurate cross section data of actinides are crucial for criticality calculations of GEN IV reactors but also for analytical purposes such as nuclear waste characterization, decommissioning of nuclear installations and safeguard applications. Tabulated data are inconsistent and sometimes associated with large uncertainties. In beam techniques, like prompt gamma activation analysis (PGAA) using external neutron beams from high flux reactors offer a chance for determination of integral and partial neutron capture γ-ray production cross sections with a minimum uncertainty of around 2 to 3 %. Preliminary experiments have been conducted at FRM II, Garching, Germany to investigate the potential of PGAA for accurate cross section determination of actinides using well prepared ^{241}Am sources.
Preparation of samples for irradiation at the Budapest Reactor and FRM II in Garching of the ^{241}Am sources has been optimized together with PTB in Braunschweig. Two samples were irradiated together with gold flux monitors to extract the thermal neutron capture cross section.
Total thermal neutron capture cross section for ^{241}Am was calculated to 711.1 ± 33.9 b and 725.4 ± 34.4 b for the second sample.

Introduction
Accurate and reliable nuclear data are essential for basic nuclear physics and many applied fields in research and technology. From Astro- and Cosmo-Physics and –Chemistry, Geochronology, Hydrology, to energy production, research and technology and various applied fields in industry - everywhere are nuclear data in use and the predictions and results are just as good as the underlying input of nuclear data are accurate. Particularly in nuclear reactor design, transmutation and nuclear waste treatment and characterization neutron capture cross sections of fission products and long lived actinides are crucial in predicting correct criticality and radioactivity evolutions in simulation studies [1]. Some obvious discrepancies in international tabulations of actinide and fission product nuclear data, such as ENDF, JENDL or JEF have provoked intensive research to improve existing data or complement gaps where cross sections have not been determined so far [2].

Neutron capture cross sections are energy dependent following a 1/v behavior in the low energy region (meV) followed by a region with strong fluctuation, so called resonances (eV to keV) and a strong decline at higher energies of the incident neutron (MeV-range). In the higher energy range, however, other reaction channels such as (n,n'), (n,2n), (n,α) or (n,p) become accessible with an increasing significance. All these reaction channels feed excited states of product nuclides that de-excite by emission of prompt gamma rays (within 10^{-12} s), characteristic of these nuclides (prompt gamma NAA). De-excitation from metastable states occurs with a certain half-life by emission of delayed gamma rays which can also be used for characterization (NAA, neutron activation analysis). Both processes are used to extract

reaction rates (or 'cross sections') when accurate knowledge of the energy and amount of neutrons causing the reaction in question is available.
Qualitative and quantitative analysis of actinides is required in many different kind of materials, such as safeguards swipe samples, environmental samples, in samples from the nuclear fuel cycle as well in nuclear waste and in residues from waste processing due to their extraordinary radiotoxicity and detrimental effects on human health. In case of low concentrations of actinides mainly alpha spectrometry or mass spectrometry are currently applied. When high concentrations are involved gamma spectroscopy can help but this technique often suffers from high background from other accompanying radionuclides. Sensitive analysis in most cases is possible only after tedious chemical separation implying radiation exposure of personal and radioactive secondary waste. A direct, non-destructive analytical method could avoid these unfavorable effects without jeopardizing sensitivity and selectivity. Using the prompt gamma signature from active neutron interrogation of actinides could lead to the development of a versatile, non-destructive and sensitive analytical method for quantification of actinides when other methods are obsolete ore just not sensitive enough. The prerequisite for this development is the availability of accurate and precise nuclear data of the actinides under study.

Materials and Methods
Prompt Gamma Activation Analysis (PGAA) using thermal or cold neutron beams at high flux Research Reactors like Forschungsneutronenquelle Heinz Maier-Leibnitz, FRM II in Garching, Germany is an ideal tool for basic nuclear prompt and decay investigations as it provides well defined neutron energy, sample irradiation conditions in a low background environment, and sensitive and versatile detector and counting conditions [3]. The major constraint as experienced at FRM II is limited availability of beam time as PGAA facilities offering high enough neutron fluxes are just few worldwide. For our experiments we could also use the Budapest reactor PGAA system offering a lower neutron flux intensity of 7×10^7 n cm^{-2} s^{-1} compared to FRM II with 2×10^{10} n cm^{-2} s^{-1}. Both experimental facilities are described in more detail in [4, 5].

Sample preparation techniques for actinides have been developed at the Institute IEK-6 of the Research Centre in Jülich [6, 7]. 4 x 4 cm Suprasil© quartz sheets (0.2 ± 0.02 mm thick) have been purchased from Heraeus Quarzschmelze Hanau, Germany. ^{241}Am activity (185 MBq) was obtained from Eckert & Ziegler, Nuclitec, Braunschweig and delivered to PTB in Braunschweig, the German National Metrology Institute, for accurate preparation and calibration of the sources. A drop of the ^{241}Am solution was dried on the center of one of the quartz sheets and afterwards covered with another sheet. Two samples have been prepared by drying the droplet on top of small circular gold foils (3 mm diam., 0.003 mm thick), serving as neutron flux monitors. These were also sealed between Quartz sheets (Fig. 52, left) using epoxy. Specifications can be seen in Tab. 9. The activity of the ^{241}Am in the samples was determined with an uncertainty of 0.75 %, hence, the mass of ^{241}Am can be calculated with similar accuracy.

Tab. 9: Specification of the ^{241}Am targets.

No.	Activity [MBq]	Mass of ^{241}Am [µg]	Au mass [mg]
1	3.87 ± 0.03	30.50 ± 0.24	0.432 ± 0.005
2	4.66 ± 0.04	36.72 ± 0.28	0.434 ± 0.005
3	4.67 ± 0.04	36.8 ± 0.28	
4	4.33 ± 0.04	31.6 ± 0.25	
5	4.63 ± 0.04	36.5 ± 0.27	

Fig. 52: Left: A drop of ^{241}Am activity on top of a 3 mm diam. gold foil (courtesy by PTB Braunschweig). Right: An epoxy sealed quartz sandwich with a 3 mm pellet centered by a third slab with a 3 mm hole. The sandwich is sealed in Teflon© foil for safety purposes.

Our samples were irradiated for 5 to 12 h at a thermal equivalent flux of 2.5 · 10^{10} $cm^{-2}s^{-1}$. During the irradiation the gold foil was placed in front of the ^{241}Am. Then the samples were flipped, so that no photon absorption correction in the gold foil was necessary. The decay radiation was counted for 1 h.

Pellets of 3 mm diam. were pressed from $^{237}NpO_2$ and $^{242}PuO_2$ using a Specac mini pill press with modified dyes. The pellets were kept in the center of the Suprasil quartz plate sandwich by a third plate with a 3 mm diam. hole to house the pill (Fig. 52 right). The pellets were < 0.2 mm thick and weight varied between 3 and 6 mg each. Gold foil was again used as neutron flux monitor.

Quartz vials containing $^{237}NpO_2$ and $^{242}PuO_2$ powder as described in the last Jahresbericht, were irradiated at the FRM II PGAA facility for 9 to 18 h, too. The cross section of ^{242}Pu was calculated to 19.9 ± 4.0 b and that of ^{237}Np was calculated to 178.3 ± 8.0 b being in good agreement with the respective values calculated from the irradiation in Budapest as reported in the Jahresbericht 2011.

Results and Discussion

The neutron flux was determined using the area of the 412 keV peak of Au and the counting efficiency of the HPGe detector. The peaks were evaluated using Hypermet-PC [8]. During the irradiation, ^{242g}Am and ^{242m}Am is produced. Since the intensities of decay γ-rays from both, ^{242g}Am and ^{242m}Am, are weak, the Kα x-rays of ^{242}Pu are used which originate from the electron capture after β^+-decay of the ^{242g}Am (16.02(2) h) [9]. These x-rays at energy 99.5 keV and 103.4 keV are very close to the 98.97 keV and 102.98 keV γ–rays of ^{241}Am. Also

they are very close to each other with regard to the resolution of the detector. The corresponding part of the spectrum derived from the decay measurement of the first sample can be seen in Fig. 53, along with another measurement of the same sample a day later.
Corrections for photon absorption in the quartz glass, for the neutron absorption in the gold foil (0.3 %) and decay corrections were applied to obtain the activity. Using the neutron flux evaluated from Au, the ^{241}Am(n,γ)^{242g}Am ground state neutron capture cross section was determined. The branching ratio of 0.914(7) [10] of $^{242g+m}$Am allowed to calculate the total ^{241}Am(n,γ)^{242}Am thermal neutron capture cross section. The results are presented in Tab. 10.

Tab. 10: The ^{241}Am total and ground state thermal neutron capture (n,γ) cross sections deduced from the irradiation of two samples.

No.	σ_c(^{241}Am(n,γ)^{242g}Am) [b]	σ_c(^{241}Am(n,γ)^{242}Am) [b]
1	663.0 ± 28.8	725.4 ± 34.4
2	649.9 ± 28.2	711.1 ± 33.9

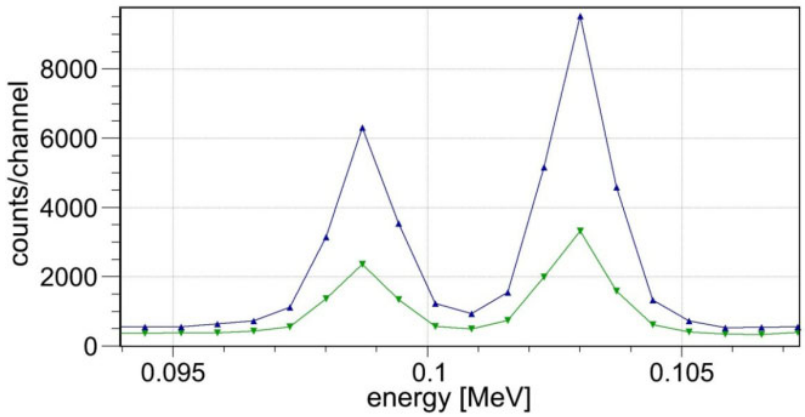

Fig. 53: Part of the spectrum obtained from a 1-h decay measurement directly after the irradiation (blue triangles) and after a day of decay (green triangles).

In Fig. 54 some of the ^{241}Am(n,γ)^{242}Am capture cross sections taken from the literature are illustrated in comparison with our own data [11]. The preliminary values obtained in this work are higher than most of the literature values, but close to the more recent ones, for instance to that of 749 ± 35 b by Lampoudis et al. presented at the ND 2013 conference [12]. The major contribution to the uncertainty in this work came from the intensity of the ^{242}Pu x-rays, all other uncertainties are at or below the 1% level.

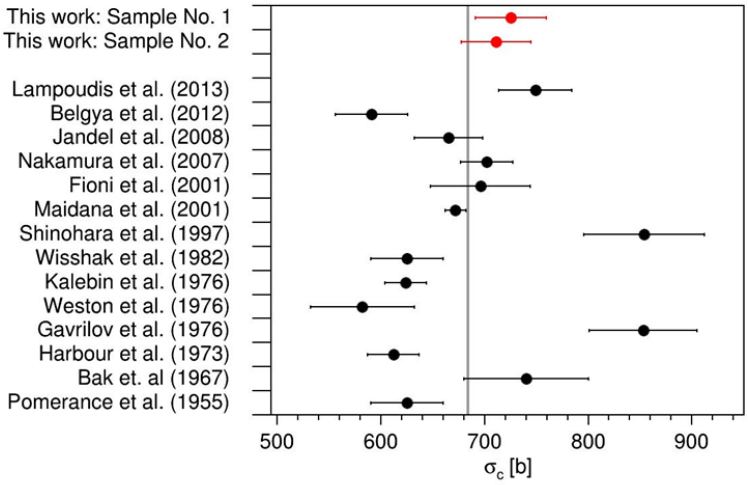

Fig. 54: The thermal neutron capture cross sections as calculated from the measurements described in this work (red) for both samples along values taken from literature (black). The ENDF/B-VII.1 value is given for comparison (grey).

Conclusions

As could be shown PGAA is a powerful tool not only to generate concentration data but also to extract nuclear baseline data from actinides, necessary to develop the analytical capabilities for their reliable and sensitive characterization in complex matrices. The successful elaboration of this ability will remain a challenging task for the next future.

Acknowledgements

This work has been carried out under BMBF contract 02 S 9052A. We greatly appreciate the financial support of the Bundesministerium für Bildung und Forschung. The beam time at the Budapest Research Reactor was supported by the European Commission within the Seventh Framework Prgramme through Fission-2012-ERINDA (project no. 269499). We are thankful for help in the preparation of our ^{241}Am samples by the PTB Braunschweig (Frau Ehlers). C.G. would like to express his gratitude for financial help through a contract by Dr. G. Caspary (N-D, Forschungszentrum Jülich GmbH).

References

[1] J. Kettler, E. Mauerhofer, M. Rossbach, D. Bosbach: Trans. Am. Nucl. Soc., (2009) Vol. 101, 100-101
[2] R.B. Firestone et al.: Proc. Int. Conf. Nucl. Data Sci & Technol., ND2013, March 4-8, 2013 New York, USA
[3] X. Lin, H. Gerstenberg, Ch. Lierse von Gostomski, R. Henkelmann, A. Türler, M. Rossbach: Applied Radiation Isotopes 67 (2009) 2092–2096
[4] P. Kudejova et al., J. Radioanal. and Nucl. Chem. 278, 691-695 (2008).
[5] Z. Rvay, T. Belgya, G. Molnr J. of Radioanal. Nucl. Chem. 265,261-265 (2005).
[6] C. Genreith, M. Rossbach, E. Mauerhofer, T. Belgya, G. Caspary , Nukleonika 57, 443-446 (2012).
[7] C. Genreith, M. Rossbach, E. Mauerhofer, T. Belgya, G. Caspary, J. Radioanal. Nucl. Chem. in press (2012).
[8] Z. Rvay, T. Belgya, G. Molnr J. of Radioanal. Nucl. Chem. 265,261-265 (2005).
[9] M. Bé et al., Table of Radionuclides Vol. V.: Bureau International des Poids et Mesures (2010).
[10] Fioni et al., Nucl. Phys. A 693,546-564 (2001)
[11] C. Genreith, M. Rossbach, Zs. Révay, P. Kudejova, Proc. Int. Conf. Nucl. Data Sci & Technol., ND2013, March 4-8, 2013 New York, USA
[12] C. Lampoudis, S. Kopecky, O. Bouland, F. Gunsing, G. Noguerre, A.J.M. Plompen, C. Saga, P. Schillebeeckx, and R. Wyants (2013) Eur. Phys. J. Plus **128** 86

4.13. Location and chemical bond of tritium and radiocarbon in neutron-irradiated nuclear graphite

D. Vulpius, W. von Lensa, B. Thomauske

Corresponding author: d.vulpius@fz-juelich.de

Abstract

The locations and the chemical forms (chemical bonds) of tritium and radiocarbon in neutron-irradiated nuclear graphite have been determined in order to develop principal strategies for the management of graphitic nuclear waste. Tritium can be bound in neutron-irradiated nuclear graphite as strongly adsorbed tritiated water (HTO), in oxygen-containing functional groups (e.g. C─OT) and as hydrocarbons (C─T). Radiocarbon is covalently bound with the graphite structure. The activity can be described by a homogeneously distributed part and a heterogeneously distributed part (enriched on surfaces or in hotspots).

Introduction

Worldwide over 250,000 tons of neutron-irradiated graphite from nuclear reactors are temporarily retained in interim storage facilities and reactor stores. There is a lack of comprehensive concepts for the management or final disposal of contaminated nuclear graphite.

For the conditioning of neutron-irradiated nuclear graphite it is necessary to know the location and the chemical bond of contaminating radionuclides. Only with this knowledge, we can predict the release or retention characteristics of radionuclides in neutron-irradiated nuclear graphite. Starting from this knowledge, we are able to develop methods for treatment of used nuclear graphite with respect to safer final disposal or reuse of graphite for new nuclear and non-nuclear applications. Also the recovery of radionuclides like tritium and radiocarbon for commercial uses could be a favourable option on account of the worldwide increasing request of these rare isotopes. If we know the location and the chemical bond of these isotopes in neutron-irradiated nuclear graphite, we can easily develop chemical or physical methods for their recovery and enrichment.

Results and Discussion

Nuclear graphite is an artificially produced product manufactured from filler and binder materials [1]. For the graphite moderator mainly petroleum or pitch coke is used for the filler and, as a binder, mainly coal-tar-pitch. However, in the case of the fuel compact or pebble matrix a mixture of crushed artefacts and natural graphite bound in formaldehyde resin is used. These components retain their principal structures in the fabricated graphite despite been subject to high temperature baking and graphitising processes. The microstructure of carbon brick, which can be considered as an incompletely graphitised nuclear graphite, shows this very well. In Fig. 55 (left), a large filler particle surrounded by semi-graphitised binder material can be seen.

This binder material is where many of the impurities are located, as can be seen in Fig. 55 (right). The white dots are impurities which can be detected by back-scattering electrons. These impurities mainly consist of oxides of aluminium, silicon and iron, but the easily neutron-activated elements such as cobalt and nickel are always affiliated to these main impurities.

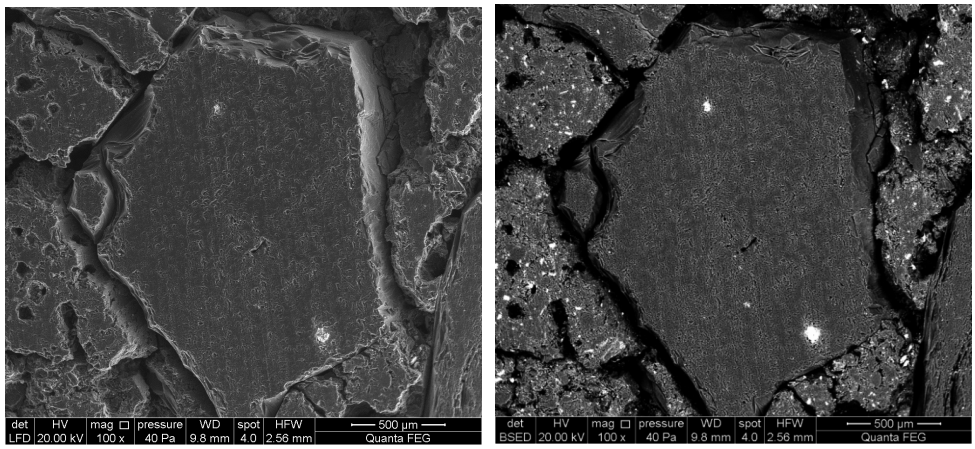

Fig. 55: Left: Scanning electron micrograph of carbon brick; right: Scanning electron micrograph of carbon brick in back-scattering electron mode.

Another element for neutron activation in nuclear graphite is nitrogen. The isotope ^{14}N reacts with thermal neutrons to form ^{14}C with a cross section of 1.93 barn. Graphite has a high affinity to adsorb nitrogen on its surfaces. These surfaces are not only the outer surfaces, but also the inner surfaces of the pore system. The adsorption profile of nitrogen can be detected by secondary ion mass spectroscopy (SIMS). Fig. 56 shows the depth profiles of ^{14}N (detected as CN^-) in irradiated and virgin reflector graphite from the Jülich experimental high-temperature pebble-bed reactor (AVR). These profiles were recorded after conditioning of the samples in vacuum for 3 days to avoid erroneous signals due to atmospheric nitrogen. Despite of these conditions, the profiles show an increased amount of nitrogen towards the surface of the graphite samples. Quantum mechanical calculations demonstrate that nitrogen should be adsorbed on graphite surfaces not by physisorption but by chemisorption to form covalent bonds [2, 3]. These covalent bonds between nitrogen and graphite are the reason for the relatively high amount of nitrogen in nuclear graphite (approx. 300 ppm). Under neutron irradiation, the nitrogen will be activated to form radiocarbon.

An important question is: Which is the location and the chemical bond of radiocarbon in neutron-irradiated nuclear graphite? The recoil energy of the ^{14}C atoms resulting from the n,p nuclear reaction is 41.4 keV. This energy is high enough to break any chemical bond. However, where are free binding sites for ^{14}C in graphite? Free binding sites are in vacancy structures on the surface of the graphite crystallites and micro-crystallites [4], between the graphite lattice planes [4] and, finally, on any carbon atom with free binding valences in disordered graphite structures or in amorphous carbon parts. Therefore, it can be postulated that ^{14}C is concentrated in neutron-irradiated nuclear graphite on surfaces, in near-surface structures and in disordered or amorphous parts of incompletely graphitised binder or filler materials.

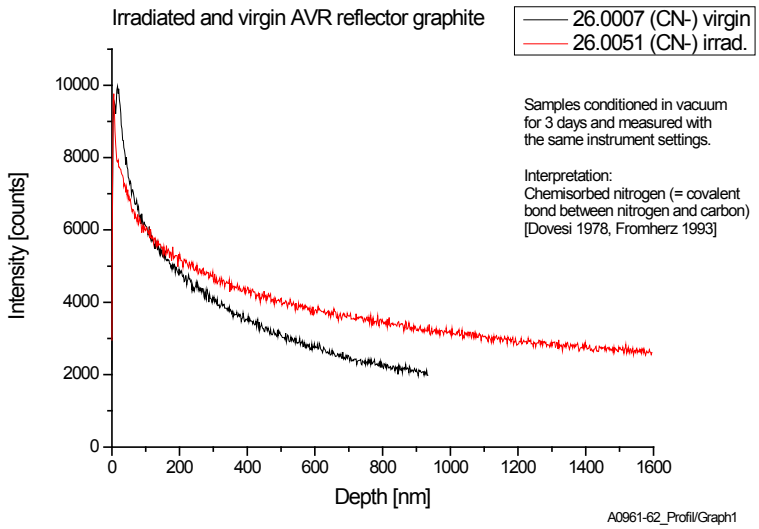

Fig. 56: Depth profiles of ^{14}N (detected as CN^-) in irradiated and virgin AVR reflector graphite.

An important experimental finding is that the distribution of radionuclides in neutron-irradiated nuclear graphite is inhomogeneous. The starting point of the evolution to this knowledge is the observation that there are not two graphite samples of the same reactor and from the same position of this reactor which have exactly the same amount of a given radionuclide.

The inhomogeneous distribution of radionuclides in neutron-irradiated nuclear graphite is also proved by secondary ion mass spectrometry (SIMS): We measured a graphite sample from the reflector of the AVR high-temperature reactor with an averaged ^{14}C inventory of 3.3E+05 Bq/g and we found a ^{14}C signal at 14.0039 u (Fig. 57). Then we re-measured this graphite sample and we did not find this signal anymore. To validate our measurements, we measured a ^{14}C reference material (chemical form: graphite) with an activity of 3.7E+08 Bq/g and we found a considerable signal at 14.0036 u (exact mass number of ^{14}C = 14.00324 u). With this signal, we calculated the related ^{14}C inventory of the AVR signal and obtained a value of 2.0E+07 Bq/g which is 60 times higher than the averaged ^{14}C inventory! From this result we concluded that ^{14}C must be present in irradiated graphite (at least partly) as “hotspots”.

Another assumption may be drawn from the SIMS measurements. SIMS was the only method by which ^{14}C was “chemically” detected. In the mass spectra, ^{14}C appeared only as single carbon ion. Other ^{14}C fragments were not found. A direct conclusion from the SIMS measurements to the speciation of ^{14}C is not possible because SIMS shows only molecular fragments; but it could be postulated by analogy that ^{14}C could be bound in irradiated graphite in the same way like the $^{12/13}C$ atoms in any graphite because the main $^{12/13}C$-containing fragment of any graphite obtained using SIMS is the single $^{12/13}C$ ion.

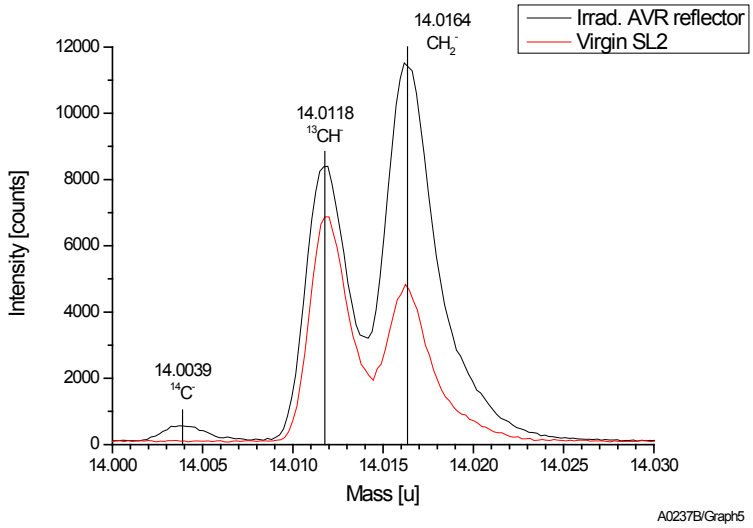

Fig. 57: Secondary ion mass spectra of irradiated AVR reflector graphite in comparison to virgin Saint-Laurent A2 graphite in the region of ^{14}C

The mass spectrometric detection of other radionuclides than ^{14}C is difficult because their concentrations are much less than that of ^{14}C. By evaluation of the spectra of Fig. 57, it was found a weak peak at the exact mass number of ^{3}H, 3.01605 u (Fig. 58). Other ^{3}H peaks were not found.

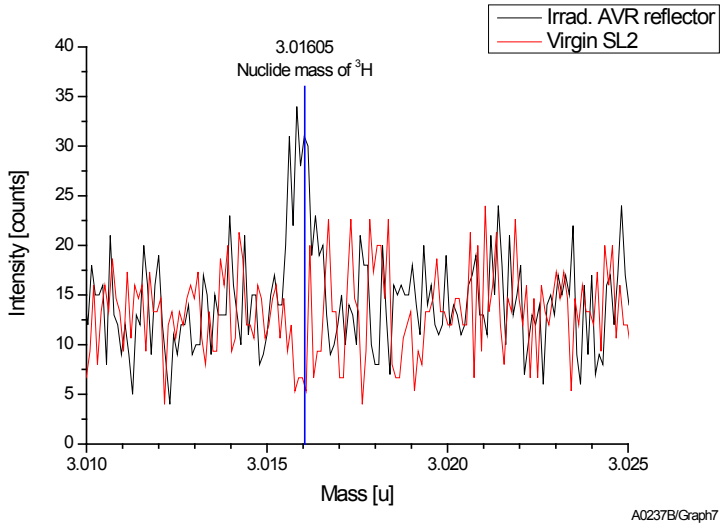

Fig. 58: Secondary ion mass spectra of irradiated AVR reflector graphite in comparison to virgin Saint-Laurent A2 graphite in the region of ^{3}H (same spectra as in Fig. 57)

An assignment of this peak to defined structural elements is also difficult because this peak may come from several structural elements such as adsorbed HTO or C–T and C–OT groups. Nevertheless, the following assumption may be made: If ^{3}H is detectable at all, then it must come from a hotspot similar to ^{14}C. An important indication is the inhomogeneous distribution of inactive hydrogen fragments in the mass spectrum of all types of graphite (virgin and irradiated), as shown in Fig. 59. Also ^{6}Li, one of the precursors of ^{3}H, is inhomogeneously distributed. Therefore, it can be assumed that at least one part of ^{3}H in neutron-irradiated graphite is located in the vicinity of ^{6}Li. It is probable that this ^{3}H has formed compounds with the surrounding carbon atoms so that it is now present as C–T compound.

As already indicated, SIMS offers the possibility to determine the spatial distribution of ions. Interesting ions in the negatively charged ion spectrum are H^-, CH^-, O^-, OH^-, CN^- and Cl^-. All these ions are distributed in a very inhomogeneous way and in part very clearly as hotspots, as can be seen in Fig. 59.

This finding is mainly important for the CN^- fragment because ^{14}N (natural amount: 99.64%) is activated to ^{14}C by neutron irradiation in a nuclear reactor. In spite of the relatively high recoil energy of 41.4 keV, ^{14}C will remain in the vicinity of its precursor. This is shown by molecular dynamic simulations of the transport behaviour of ^{14}C in irradiated nuclear graphite [5]. As can be seen in Fig. 60, the ^{14}C atom loses its kinetic energy in a perfect graphite lattice structure after a displacement distance of nearly 600 Å (60 nm). Therefore, ^{14}C will be concentrated in this region. After the detection of ^{14}N on graphite surfaces (Fig. 56) and the corresponding conclusion for the presence of ^{14}C, the present detection of ^{14}N as hotspot is the second mode of existence of ^{14}C in neutron-irradiated graphite.

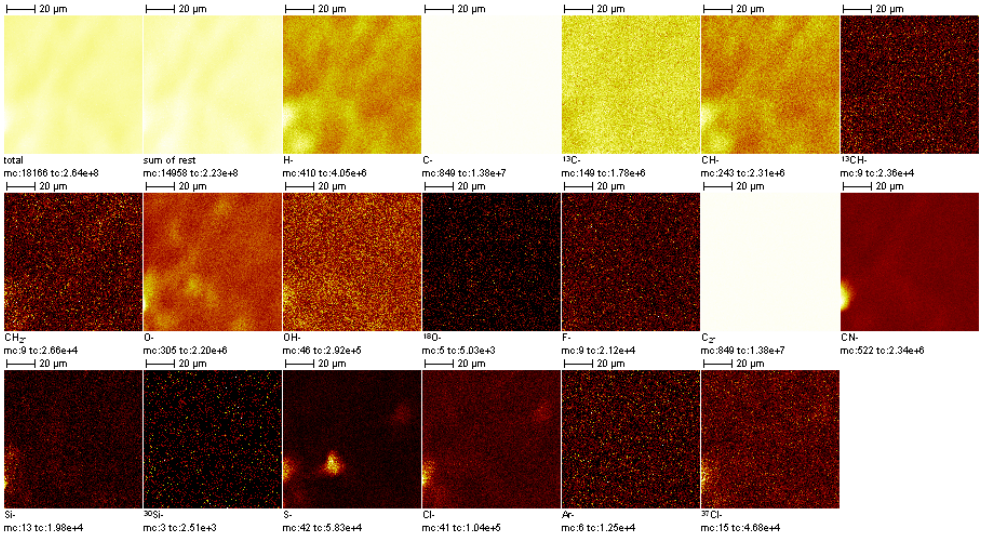

Fig. 59: Spatial distribution of negatively charged ions (sample: irradiated Saint-Laurent A2 graphite from the position 5120).

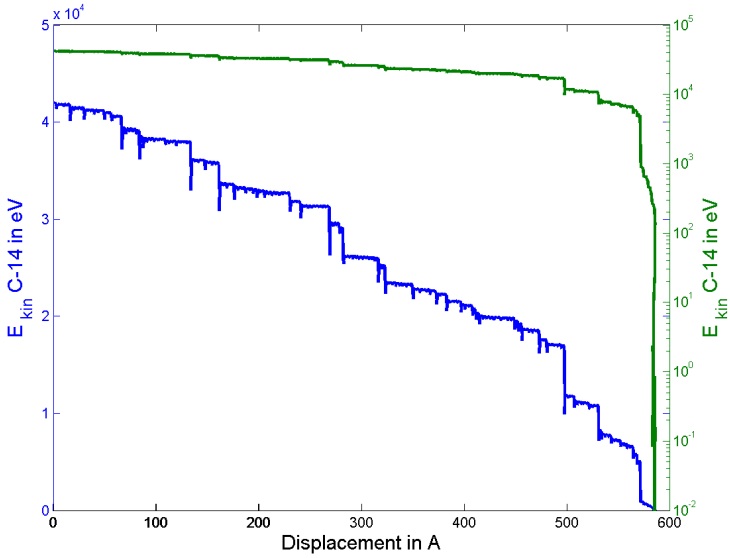

Fig. 60: Displacement and energy loss of a ^{14}C atom in a perfect graphite lattice structure [5].

Acknowledgements

The authors would like to thank U. Breuer for SIMS measurements and M. Klinkenberg for scanning electron microscopy. We particularly thank U. Scherer and M. Baier (Aachen University of Applied Sciences) for digital autoradiography. This study is part of the European project CARBOWASTE (Grant No. FP7-211333). The financial support is gratefully acknowledged.

References

[25] Nightingale, R.E. (1962): Nuclear graphite, Academic Press, New York.

[26] Dovesi, R. et al. (1978): Chemisorption of periodic over-layers of atomic nitrogen on graphite, Surface Sci. 77, 409–415.

[27] Fromherz, T. et al. (1993): Chemisorption of atomic H, C, N and O on a cluster-model graphite surface, Mon. Not. R. Astron. Soc. 263, 851–860.

[28] Telling, R.H. et al. (2007): Radiation defects in graphite, Phil. Mag. 87, 4797–4846.

[29] Nabbi, R. et al. (2012): Molecular dynamic simulation of the transport behavior of C-14 in irradiated nuclear graphite, Irradiation damage and ^{14}C formation in nuclear graphite, Joint meeting in conjunction with the FP7 CARBOWASTE program, Manchester.

4.14. Assessment of proliferation risks based on mathematical models

C. Listner, I. Niemeyer, M. J. Canty*, A. Rezniczek#, G. Stein§

Corresponding author: c.listner@fz-juelich.de

* IBG-3, Forschungszentrum Jülich GmbH
# UBA Unternehmensberatung GmbH, Herzogenrath
§ Consultant, Bonn

Introduction

Due to the experiences made in the past, the IAEA has developed a vision of a new verification model – the State-level concept (SLC). While the former approach has focused on declared nuclear material and facilities, the new concept concentrates on facts about a State. In order to increase effectiveness and efficiency, the IAEA wishes to migrate from a mechanistic verification procedure to a risk-based prioritization of its activities.
While differentiating between States due to different risk levels seems reasonable, one has to assure that no single State will be discriminated. Therefore, the State-level concept is to be objective, transparent, reproducible, standardized and documented (for details see [1]). Furthermore, the State-level concept should be applicable to all States with commitments regarding nuclear non-proliferation, i.e. item- or facility-specific Safeguards agreements (INFCIRC/66), comprehensive Safeguards agreements (CSA) with and without Additional Protocol as well as voluntary offer agreements (VOA) in nuclear weapon states (NWS).
According to [2], the State-level concept comprises three steps leading to a specific State-level Safeguards approach:

1. Identification of plausible acquisition paths.
2. Specification and prioritization of State-specific technical objectives.
3. Identification of safeguards measures to address the technical objectives.

In the present paper, we will concentrate on the first step of the process, the acquisition path analysis (APA), as this is still a major difficulty when elaborating a State-level approach.
According to [3], an acquisition path (AP) is defined as a sequence of activities which a State could consider in order to acquire weapons usable material. The acquisition path analysis (APA) analyzes all plausible APs, aiming to determine whether a proposed set of safeguards measures will be effective.
Up until now, the IAEA has implemented APA mainly based on expert judgment. This has led to a procedure that, although standardized, cannot fulfill the requirements mentioned above. Therefore, the IAEA is looking for a methodology and software tool that helps structuring the process of APA. The tool should visualize the acquisition paths in order to help the analyst maintain an overview of the situation in a State. It should automate the process in order to be independent of subjective reasoning and thus guarantee reproducibility. Finally, a software tool assisting the analyst should integrate into existing systems and models at the IAEA.
In the following sections, we describe a new formalized procedure using network analysis techniques and game theory in order to assess proliferation risks and help distributing allocate the inspectorate's resources in a reasonable way.

Materials and Methods

As mentioned in the previous section, the IAEA's physical model serves as a basis for APA. It comprises an overview of all known relevant processes for converting nuclear source material to weapon usable material (see definition in [3]). In Fig. 61, a generic version is depicted. The yellow boxes represent material forms which are transformed to other material forms by using specific processes symbolized by arrows in the model. In the figure, the acronym "DU" stands for direct use, "IU" for indirect use and "NU" for natural uranium.
Within the physical model, an AP always starts at the "Origin" box followed by the diversion or undeclared import of the first material form. From there, consecutive process steps consisting either of misuse of declared facilities or of processing in undeclared facilities are needed in order to finally reach for weapons usable material, i.e. any material in the physical model with the prefix "DU".

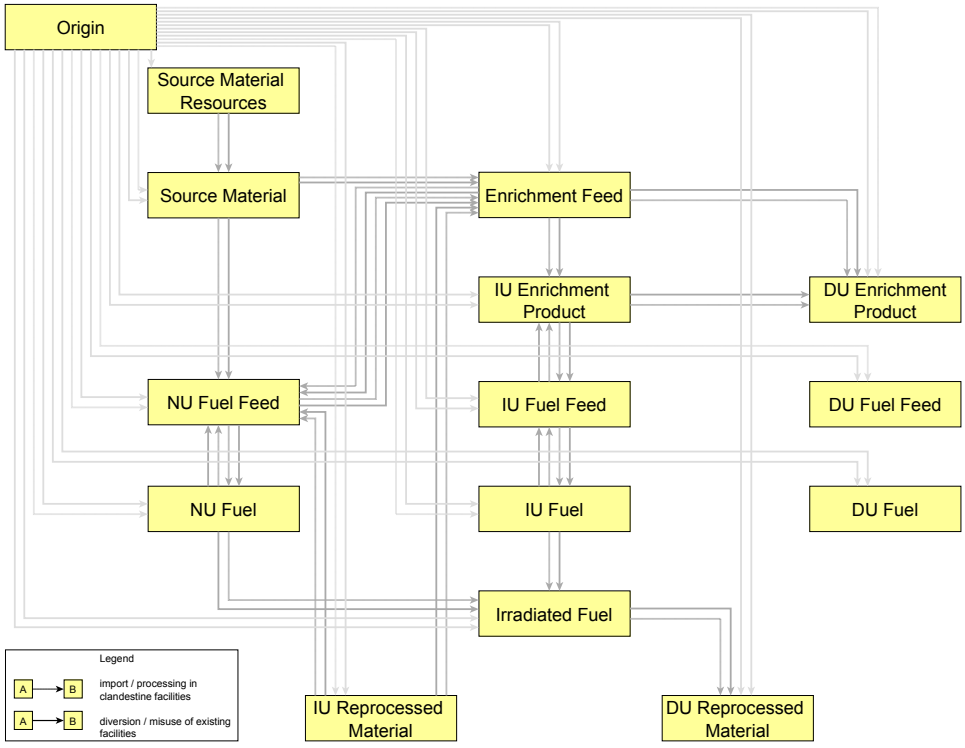

Fig. 61: Generic physical model.

From a mathematical point of view, the physical model can be considered as a directed graph. Therefore, it is possible to apply graph theory to the APA problem in order to find all technically plausible paths.
In a directed graph, nodes can be connected by edges. To each edge a scalar number can be associated to measure the edge's length. Sequences of edges are called paths whose lengths are calculated by the sum of the edge weights. The concept of graph theory applied to acquisition path analysis implies a node being a material form in the physical model, an

edge representing a process and a path standing for the acquisition path itself. Edge weights can be used to reflect the attractiveness of a process.
Using the model of a mathematical graph, acquisition paths can be found using several algorithms. The shortest path between two nodes can be found using e.g. the Dijkstra algorithm (see [4]). However, for a comprehensive analysis of a State's nuclear options, all paths from "Origin" to any of the "DU" material forms have to be assessed. This can be easily accomplished using enumeration techniques that prevent cycles contributing to an acquisition path.
Besides finding acquisition paths, APA ought to assess paths with respect to their suitability for a nuclear weapons program. As this comprises a strategic aspect, game theory is the appropriate tool to accomplish this task.
Game theory is a mathematical approach with the ability to model strategic situations between opposing players. By strategic situation, a choice between different decision alternatives is meant where decision making does not only depend on the protagonists' own courses of action but also on those of their opponents. Applied to APA, the inspectorate and the state are the opposing players. The strategies of the State are the acquisition paths themselves, as well as the strategy of compliant behavior. For the inspectorate, the different safeguards approaches, i.e. the inspection of a subset of all processes, can be considered as strategies. Each combination of the players' strategies may be associated with the players' utilities, thus leading to a bi-matrix representation of the game (for details see [5]).
Using this problem formulation, game theory provides a solution using the concept of Nash equilibrium. A Nash equilibrium in a two-person game is defined as a strategy combination for which neither of the players can deviate unilaterally in order to increase his or her utility. Thus, a relative scale is defined upon which different acquisition path configurations can be evaluated and compared. The effectiveness of a given inspection regime can be measured on the basis of the inspectorate's payoff. The most efficient strategy for the IAEA is the minimum effort strategy being part of a Nash equilibrium in which the State behaves legally.
Using both graph theory and game theory, a new 3-step approach to acquisition path analysis was established. This approach is depicted in Fig. 62.
The first step, network modeling, parameterizes the model. With respect to the edge weights, GIF PR/PP (see [6]) proposes six measures for evaluating proliferation resistance which can also be used to model attractiveness in the case of APA. For this paper, three of these measures, technical difficulty (TD), proliferation time (PT) and proliferation cost (PC), are taken into account. Using these dimensions, the analyst is given the opportunity to rate each process based on a scale from 0 (very attractive), to 3 (very unattractive).
In the second stage of the process, the network analysis, all paths with their respective lengths are enumerated and sorted in decreasing order of attractiveness. Additionally, the paths are visualized using the GraphML format (see [7]) and yEd Editor (freely available at www.yworks.com). This step is carried out in a fully automatic way using a Python script including the NetworkX toolbox (see [8]).

Fig. 62: 3-step approach to acquisition path analysis.

Finally, in the third stage of the process, the strategic assessment, the strategic options of both the IAEA and the State are evaluated using the game theoretic approach described above. To accomplish this, actions of the inspectorate are associated with costs and presumed detection probabilities. Based on a cost threshold *W*, it is possible to compute the Nash equilibria sequentially and thus to obtain the inspectorate's minimum effort strategy for inducing compliant behavior on behalf of the State.

An Example Case Study

Using the method described in the previous section, it was possible to carry out a case study based on the example of Germany and its commitments with the IAEA. On the one hand, Germany possesses a complex nuclear fuel cycle with a great deal of nuclear experience and know-how. On the other hand, the IAEA may be assumed to have a high detection probability for clandestine activities due to the Additional Protocol being in force.

At first, the generic physical model is adopted to the situation in Germany leading to the removal of several edges, e.g. the edge representing the misuse of declared reprocessing facilities. This customization is necessary in order to reflect the declared processes properly.

Additionally, the Safeguards Implementation Report from 2011 served as a basis for estimating the inspectorate costs and the detection probabilities. Expert judgment was applied to assess the attractiveness of each edge in the physical model. After these steps, the adjacency matrix was available for further analysis. To accomplish the modeling, Microsoft Excel was used, allowing for a CSV-export of the relevant data.

Based on the outcome of the first step, all paths between the "Origin" node and any "DU" node were enumerated, visualized and sorted according to their attractiveness in the second step, making use of the Python script described in the previous section. Thus, a list of 1041 paths was generated. Moreover, for each path a separate chart was generated visualizing the respective acquisition path and its attractiveness (see an example in Fig. 63).

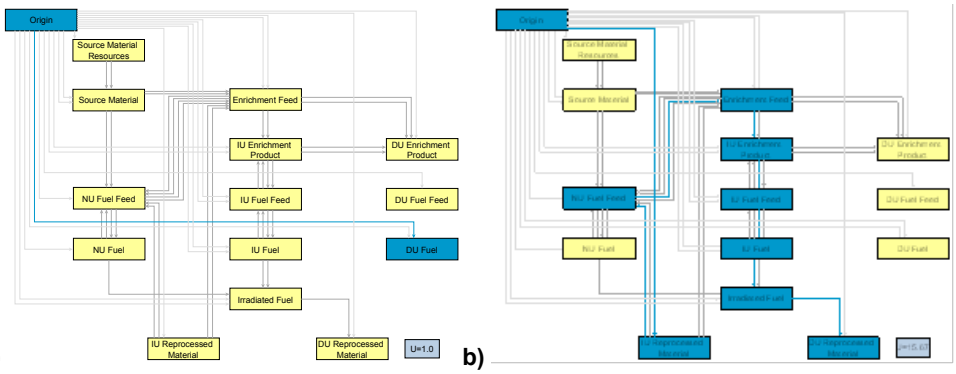

Fig. 63: The most (a) and least (b) attractive path for the example case study of Germany.

In the third step, the 1041 acquisition paths together with compliant behavior were considered as the State's strategies. For the IAEA, any combination out of 16 distinct activities was assumed to be a strategy. The costs for each combination of inspectorate activities were calculated based on the input from the first stage of the process. By setting a limit on the inspectorate's costs, a set of strategies for the IAEA was determined. Then, the Nash equilibrium was calculated. If it did not comprise compliant behavior on behalf of the State, the threshold was increased. This approach led to the results in Tab. 11.

Tab. 11: Results of the game theoretic analysis for the example case study of Germany.

W [EUR]	Number of Inspectorate Strategies	State's behavior	Effectiveness [%]
100,000	1	Non-compliant	0
200,000	5	Non-compliant	0
300,000	9	Non-compliant	0
400,000	23	Non-compliant	0
500,000	41	Non-compliant	0
600,000	77	Non-compliant	0
700,000	118	Non-compliant	0
800,000	168	Compliant	100

According to the model, a budget of 800,000 EUR is sufficient to induce legal behavior. Further increasing *W* does not change this behavior. When comparing this to the 2011 budget of 5,700,000 EUR spent in Germany, one can see that a significant increase in efficiency without losing effectiveness is possible. It should be noted that, in general, effectiveness values between 0 and 100% can arise when the State's Nash equilibrium strategy is illegal behavior but there is a finite chance of detection. This situation does not arise in the German fuel cycle example, however.

Conclusions and Outlook

Within this paper, a new 3-step methodology for acquisition path analysis was presented. The approach is modular and accounts for automation. However, it should only be seen as a

tool assisting but not replacing the analyst. A first example of the methodology's usage was presented showing plausible results.
Future work will, inter alia, comprise the enhancement of the cost model, the additional visualization of the game theory results and the integration into existing systems at the IAEA.

Acknowledgements

This work was financed by the German Safeguards Support Programme to the International Atomic Energy Agency under task JNT C 01871.

References

[1] C. Listner et al; Proceedings of the 53rd INMM Annual Meeting. 2012.
[2] J.N. Cooley; Seventh INMM/ESARDA Joint Workshop Future Directions for Nuclear Safeguards and Verification. 2011.
[3] IAEA. "IAEA Safeguards Glossary". In: International Nuclear Verification Series No.3 (2001).
[4] E.W. Dijkstra; Numerische Mathematik 1.1 (1959), pp. 269-271.
[5] M.J. Canty. Resolving conflicts with Mathematica: algorithms for two-person games. AP, 2003.
[6] GEN IV International Forum. Evaluation Methodology for Proliferation Resistance and Physical Protection of Generation IV Nuclear Energy Systems. 2006.
[7] U. Brandes, M. Eiglsperger, and J. Lerner. "GraphML primer". Online available at http://graphml.graphdrawing.org/primer/graphml-primer.html (accessed April 02, 2013). 2011.
[8] A. Hagberg, D. Schult, and P. Swart. "NetworkX Library". Code available at http://networkx.github.com/ (accessed April 02, 2013). 2004.

4.15. The Cooperation between Forschungszentrum Jülich and the IAEA Safeguards Analytical Service

M. Dürr, A. Knott, I. Niemeyer, B. Heuel-Fabianek*, S. Küppers**, D. Bosbach

Corresponding author: ma.duerr@fz-juelich.de

* S: Department for Safety and Radiation Protection
** ZEA-3: Central Institute of Engineering, Electronics and Analytics

Abstract

The International Atomic Energy Agency (IAEA) plays a central part in verifying the compliance of States with their commitment to the exclusively peaceful use of nuclear energy. The application of safeguards by the IAEA involves analytical measurements of samples taken during inspections. The development and advancement of analytical techniques with support from the Member States contributes to strengthened and more efficient verification of compliance with non-proliferation obligations. Forschungszentrum Jülich and the IAEA's Safeguards Analytical Service initiated a cooperation, in which the laboratories in Jülich support the IAEA. First steps have been undertaken within the cooperation through development of a setup for production of particles needed for quality control and validation of particle analysis techniques for environmental swipe samples. Furthermore, Forschungszentrum is seeking to be qualified as a member in the IAEA's Network of Analytical Laboratories (NWAL) for Nuclear Material Analysis to perform analytical tasks in support of the IAEA safeguards mission.

Introduction

Pursuant to the "Treaty on the Non-Proliferation of Nuclear Weapons" [1], the IAEA controls the use of nuclear energy for exclusively peaceful purposes in the signatory non-nuclear weapon States. To this end, the IAEA is mandated to apply so-called safeguards in those States according to a model agreement, the comprehensive safeguards agreements [2]. The backbone of comprehensive safeguards is the control and accountancy of the entire nuclear material inventories and flows of the state, which are verified by the IAEA through inspections at nuclear facilities. Since the 90's these agreements are supplemented by the Additional Protocol [3] and the introduction of additional strengthening measures which are intended to verify that the declaration on the peaceful use of nuclear energy is in fact complete. The combination of comprehensive safeguards with the Additional Protocol is considered as the standard for verifying the peaceful use of nuclear energy.

For bulk handling fuel-cycle facilities, the IAEA takes material samples to detect a possible diversion of material for non-peaceful purposes. The samples typically covering species like uranium-oxide powders, uranium hexaflouride, fuel pellets, spent fuel input solutions in reprocessing, are collected by IAEA inspectors and shipped to the analytical laboratory for analysis. The samples are analyzed using destructive analysis (DA) to verify the correctness of the material accountancy. DA brings the advantage of offering a controlled environment which delivers precise and accurate measurement results. Low uncertainties in determination of the isotope content alleviate detection of diversion and contribute to more efficient and effective verification. Guidelines for typical target measurement uncertainties for assay of

nuclear material samples are described in the International Target Values [4], and reach 0.1 % relative uncertainty for destructive analysis.
Since the introduction of strengthening measures in the 90's, analytical measurements support the IAEA in drawing conclusion on the absence of undeclared activities within a state. To this end environmental sampling, i.e. taking swipe samples within nuclear facilities and during so-called "Complementary Access Inspections", provides a tool to the IAEA to draw conclusions on the existence or non-existence of undeclared nuclear material or activities. Swipe sampling employs highly sensitive analytical techniques capable of detecting trace amounts of nuclear isotopes collected on the swipe, and therefore enables the IAEA to trace signatures resulting from handling with nuclear materials.
The significance of analytical measurements has been recognized by the IAEA and the Member States and currently effort is undertaken to strengthen the IAEA's capabilities in this area in the dedicated project "ECAS" (Enhancing Capabilities of the Safeguards Analytical Services). ECAS mainly involves the construction of new laboratories and has an assigned budget of 65.9 Mio € for the period of 2009-2014, including contributions provided by Member States and their Support Programs to the IAEA. [5]
The IAEA performs the analysis 'in-house' via the Safeguards Analytical Service (SGAS) but also relies on the Network of Analytical Laboratories (NWAL), i.e. laboratories that have been certified to conduct analysis tasks for the Agency. The German Support Programme to the IAEA, which is coordinated by the Federal Ministry of Economics assisted by IEK-6, contributes to the development and advancement of safeguards and has become increasingly engaged in providing support in the area of analytical measurements. A joint initiative of the three units of Forschungszentrum Jülich IEK-6 (Institute for Nuclear Waste Management and Reactor Safety), S (Department for Safety and Radiation Protection), ZEA-3 (Central Institute of Analytics), presented their analytical capabilities in two visits of IAEA representatives to Jülich in September 2011 and November 2011. In September 2012, representatives from Forschungszentrum Jülich were invited to visit the IAEA analytical laboratories located in Seibersdorf, Austria, and various areas of collaboration could be identified.
Among the potential areas, Forschungszentrum Jülich contributes in two topics of immediate interest to the IAEA Safeguards Analytical Services. Two "tasks" were implemented in mutual agreement between the German Support Programme and the IAEA. One task deals with the production of particles for quality control, the other with the qualification of Forschungszentrum Jülich as a member in the NWAL for support in nuclear material analysis.

NWAL Qualification of Forschungszentrum Jülich

As result of the consultations between IAEA's SGAS and Forschungszentrum Jülich, the IAEA sent a request to the German Support Programme for support of the candidacy of Jülich for membership in the NWAL. The German Federal Ministry of Economics and Technology nominated Forschungszentrum Jülich as a candidate laboratory for analysis of nuclear material samples. The qualification process serves to establish the organizational and contractual relationship between SGAS and the NWAL candidate. The quality management system and the proficiency will be evaluated by the coordination section within SGAS. The scope of the analysis to be performed in Jülich will cover the analysis of uranium based materials and matrices and special analyses. The joint offering of the three institutes at Forschungszentrum Jülich IEK-6, S, ZEA-3 provides the possibility to cover a variety of

analysis tasks (Fig. 64). For analysis of routine samples taken to verify the nuclear material accountancy, nuclear material samples will be handled and prepared in the controlled area of IEK-6 which has a license for such amounts of material (grams of enriched fuel). It is planned to perform uranium assay using isotope dilution mass spectrometry, where sample dissolution, spike addition and dilution are performed at the IEK-6. The diluted solution is then handed over to the Department for Safety and Radiation Protection for isotopic analysis with a multi-collector inductively coupled plasma mass spectrometer.

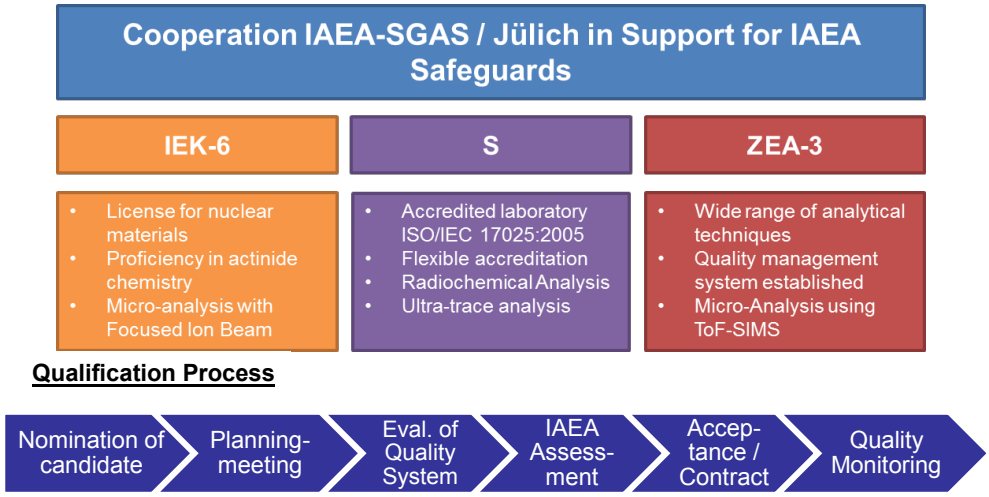

Fig. 64: Top: Overview over the laboratory capabilities at the Forschungszentrum Jülich Bottom: Scheme of the qualification process of a candidate laboratory for membership in the IAEA Network of Analytical Laboratories for Nuclear Material Analysis.

ZEA-3 is not licensed to handle materials with radioactivity above the exemption limit, but offers a wide variety of analytical techniques. Most notably, ZEA-3 owns a Time-of-Flight Secondary Mass Spectrometer (ToF-SIMS), which provides interesting capabilities in particle analysis. An advantage of the ToF-SIMS is the high sensitivity over the full mass-range thus complementing the sector-field mass analyzers of the mass spectrometers that are customarily used by safeguards laboratories for isotopic measurements in particle analysis. The high proficiency and experience level at ZEA-3 with ToF-SIMS will provide a tool for supplementing systematic studies of particulate materials, e.g. in identifying background contributions which interfere in particle analysis. This has become of even more importance since the introduction of Large-Geometry SIMS in SGAS, which allows highly sensitive and accurate isotopic analysis of major and minor isotopes in submicron sized particles containing uranium.
Concerning quality management the consortium of the three units IEK-6, S and ZEA-3 have agreed to work towards a harmonized procedure regulation for providing the joint services to the IAEA-SGAS. The unit “S” has a flexible accreditation according to ISO/EC 17025:2005 and will have a leading role in supervising the quality management system of IEK-6 and ZEA-3. The qualification process involves several steps and has a projected time-frame of two years.

Production of Particles for Quality Control

Reference materials are required for the proper calibration of analytical instruments such as mass spectrometers, the development and improvement of measurement techniques, and as quality control materials. Besides the NWAL for nuclear material analysis, the IAEA also operates a network of analytical laboratories for the analysis of environmental samples. Particle analysis methods are an important part of the services provided by this network. To assure the quality of results submitted by the NWAL, the IAEA must distribute quality control materials containing known amounts of the isotopes of interest.

For bulk analytical techniques certified reference materials have been produced, e.g. by the European Commission's Institute for Reference Materials and Measurements and the U.S. Department of Energy's New Brunswick Laboratory, but for the analysis of micrometer sized particles reference materials are very limited. Therefore the IAEA needs to acquire standard materials in particulate form that will be used to prepare quality control samples for the NWAL, and method and measurement development by the NWAL including the IAEA's Environmental Sample Laboratory (ESL).

Within a joint PhD project performed collaboratively at SGAS and IEK-6, a setup for production of particles for quality assurance and quality control will be developed to assist the IAEA in acquiring the urgently needed particle reference materials in a timely manner (Fig. 65). In order to fit the purpose, the particles should be uniform in size and elementary content, in particular for uranium/plutonium, isotopic content and morphology. Uniformity is reached by generating mono-disperse particles using a Vibrating Orifice Aerosol Generator (VOAG) using a well-defined and characterized feed solution prepared from certified reference material. The droplets generated with the aerosol generators are post processed via in-situ heat treatment of the particles while they are transported in an air-stream [6]. The heat treatment calcinates the particles in order to obtain stable oxidic particles as a product of the process.

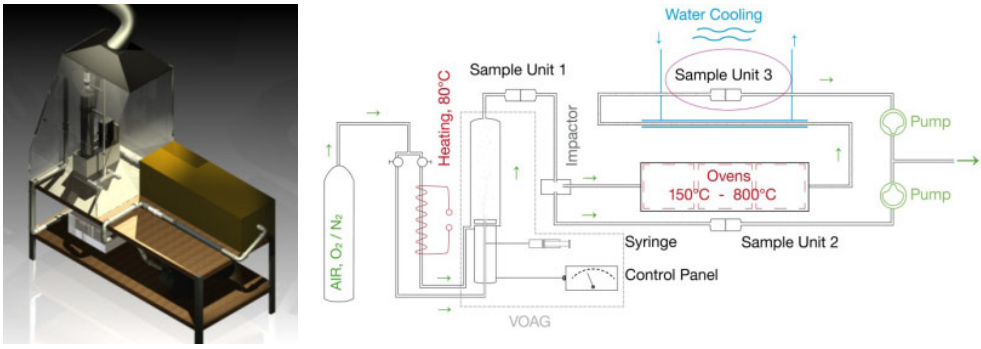

Fig. 65: Left: CAD model of the setup for production of mono-disperse particles for quality control of particle analysis methods and procedures. The total size is approximately 1 meter x 2 meters. Right: Schematic view of the setup.

Particles are collected with a filter from the air-stream from which they be transferred onto suitable substrates. The properties of the product particles need to be determined by analyzing a deterministic aliquot of the whole batch of particles, which requires substantial effort for particles with a target diameter of 1 µm. The size and morphology can be studied by scanning electron-microscopy (SEM) and focused ion beam methods, such like

energy/wavelength dispersive X-ray spectroscopy (EDX/WDX) to assess the internal elemental composition of the particles. The uranium/plutonium- nd the isotopic content of a single particle can be verified by mass spectrometry like Thermal Ionization Mass Spectrometry (TIMS) or Secondary Ioniziation Mass Spectrometry (SIMS). For TIMS particle-analysis a single µm-sized particle is transferred onto a rhenium-filament with micro-manipulators. Additionally, isotope dilution mass spectrometry (IDMS) can be performed to verify the isotopic content [7]. It is planned to verify the particle properties in collaboration with the Joint Research Centre - Institute for Reference Materials and Measurements (JRC-IRMM) in Geel, Belgium.

Conclusion and Outlook

In conclusion, the collaboration between IAEA SGAS and Forschungszentrum Jülich was established and has materialized in two projects, the production of particles for quality control and the qualification of the joint laboratories of IEK-6, S and ZEA-3 for membership in NWAL. The production of particles will be optimized in order to verify that the particles are produced (i) with the properties that make them usable for quality control and (ii) the uniformity across the produced batch of particles. Ideally, the particle synthesis process is understood in full detail. With this regard it would be interesting to exploit analytical techniques and expertise in extracting information on chemical and physical structure. Here micro-analytical techniques like Raman-spectroscopy and Electron-Back-Scatter Diffraction (EBSD) available in the IEK-6 could be explored and tested for suitability as particle analysis techniques in safeguards.
For the qualification as a member of the NWAL, expertise in the IEK-6 in performing quantitative element analysis with ICP-MS could provide an asset in extraction of additional information from uranium based materials and matrices, e.g. uranium ores. The analysis of rare earth elements yields information for geo-location of samples thus providing additional information for IAEA safeguards. The participation in interlaboratory comparisons would be an interesting exercise to benchmark the existing analysis routines.

Acknowledgements

The collaboration is support by the German Support Programme (Task C.43 / A1960 and C.45 /1961) and by the IAEA Special Service Agreement for the PhD project of Mr. A. Knott.

References

[1] “Treaty on the Non-Proliferation of Nuclear Weapons”, INFCIRC/140, 22.April 1970
[2] “The Structure and Content of Agreements Between the Agency and States Required in Connection with the Treaty on the Non-Proliferation of Nuclear Weapons (NPT)” - INFCIRC/153(Corrected), June 1972
[3] “Model Protocol Additional to the Agreement(s) Between State(s) and the Agency for the Application of Safeguards”, INFCIRC/540(Corrected)
[4] “International Target Values 2010 for Measurement Uncertainties in Safeguards Nuclear Materials”, IAEA STR-368, Vienna, November 2010
[5] “Statement at Ground-breaking for IAEA Nuclear Material Laboratory” by IAEA Director General Yukiya Amano, Sept. 7, 2011, http://www.iaea.org/newscenter/statements/2011/amsp2011n018.html
[6] Ranebo et al., Anal. Chem, 82 (2010), 4055
[7] M. Kraiem et al., Anal. Chim. Acta 748 (2012), 37

4.16. 2011-2012 annual report of PKS-WAA

Y. Aksyutina, I. Fast, E. Harren, F. Kreutz, C. Lawniczak, St. Schneider, H. Tietze-Jaensch, M. Weidenfeld

Corresponding author: h.tietze@fz-juelich.de

The PKS-WAA team thoroughly evaluates the scientific and technical means of the radioactive waste conditioning and residue production processes and methods (so-called production process approval). The vitrification and waste conditioning plants are inspected at least twice a year to assure their performance to comply with the approved process specifications.

At the Sellafield site, UK, the process approval comprises the vitrification plant and, by now, the residue export facility for uploading CASTOR flasks for their transport to Germany. In La Hague, France, the Vitrification campaign of the high-level waste (HLW) and its transport back to Germany has been completed. In addition complementary waste streams are subject of on-going process approval and proof tool development, e.g. the nuclear measurement station P2 of the metallic waste compaction plant (ACC) or the CSD-B waste stream of vitrified medium level effluents. PKS assess and evaluates the productions processes and reports its recommendations directly to BfS who is to decide and eventually grant their production approval. The production of CSD-B MAW glass containers has commenced.

The Karlsruhe vitrification plant VEK has become fully operational in Oct. 2009. The whole VEK campaign lasted until late 2010 and has produced the total of 140 high-level vitrified waste containers loaded into five CASTOR flasks that had been transported to the interim storage facility ZLN near Greifswald in February 2011. PKS had inspected and evaluated the whole production campaign, had audited the responsible institutions and persons for production and quality assurance. Hitherto, PKS had evaluated all quality relevant production modifications and findings that were compiled in an experience report of WAK supplementary the handbook of process qualification.

High-level waste nuclear inventory declarations of waste compounds from all the facilities conditioning German HLW have been checked and verified prior to loading and transport. All the accompanying product quality documentation has been checked and certified to comply with the acceptable product properties and process specifications to be viable for the German repository relevant regulatory requirements.

Dedicated R&D is conducted on numerical Monte Carlo methods and simulation programmes to help correctly interpreting the gamma- and neutron emission from highly compacted metallic waste residues. For instance, the effect of a varying concentration / activity and geometrical position of key nuclides in a heterogeneous material embedding are being addressed. The goal is to develop easy-to-use proof tools for examination and evaluation of disposal relevant nuclear properties of heterogeneous radioactive metallic waste compounds. This tool development has undergone a successful benchmarking with real Areva NC compacted metallic compound and their measurement station geometry. These PKS proof tools for CSD-C checking are almost ready for use.

Moreover, the PKS proof tools for high-level was vitrified containers from Sellafield have been amended and adapted, ready for their application. The assessment and quality evaluation for the qualified processing of MAW glass CSD-B from Areva NC has commenced.

Individual experts of PKS-WAA participate in national and international advisory councils and consulting expert groups.

4.17. Disposal of Radioactive Graphite

T. Petersmann, M. Rasulbaev, K. Aymanns

Corresponding author: t.petersmann@fz-juelich.de

Abstract

To minimize the occurrence of radiocarbon in the biosphere high requirements on the retention of this isotope are mandatory. For the repository KONRAD both the total activity for the disposal of ^{14}C-containing waste as well as the annual emplaceable activity of this radionuclide are comparatively low. For the waste disposal KONRAD it is important to clarify the physical and chemical phenomena as well as a complementary characterization of the ^{14}C-containing wastes. In particular, the release mechanisms under repository conditions need to be identified and proposals for specific waste conditioning and packaging must be developed.

Introduction

Gas-cooled, graphite-moderated reactors and water-cooled, graphite-moderated Pressure Tube Reactors were built and operated in the United States, Russia, the U.K., France, Germany and other countries. Some of them are still in use, but most are currently being decommissioned and "greenfield" dismantled. Worldwide there are about 250,000 tons of activated reactor graphite, the largest share (about 70 %) is assigned to the U.K., Russia, France and the USA. Irradiated reactor graphite has high amounts of radiocarbon ^{14}C, resulting from neutron activation of nitrogen, carbon and oxygen.
The disposal of graphite waste is only accomplishable with knowledge of the possibilities of release of radionuclides to the atmosphere. The main focus is on ^{14}C, since this radionuclide comprises the largest quantity in reactor graphite. With a half-life of 5730 years its activity over longer periods remains unchanged. Therefore, the strategy for the disposal of the irradiated graphite is mainly determined by the chemical and physical properties of ^{14}C.

The Situation in Germany

There is about 1000 tons of graphite waste in Germany, which are mainly reflectors and thermal columns of research reactors, and parts of fuel and other structures from the AVR (Arbeitsgemeinschaft Versuchsreaktor Jülich) experimental reactor and the NPP THTR-300 (Thorium-High-Temperature-Reactor) (Tab. 12).

It is planned to dispose graphite waste as low-level and intermediate-level radioactive waste in the nuclear waste disposal KONRAD. All requirements for the radioactive waste, conditioning, packaging and inventory activity are defined in the Waste Acceptance Requirements by the Federal Office for Radiation Protection (BfS: Bundesamt für Strahlenschutz) [2-4]. Below the guaranteed values relevant for waste graphite are summarized and evaluated.

Tab. 12: German reactors (shut down) with graphite inventory [1].

Name	Location	Type	Use	Operation period		Thermal power [MW]
				von	bis	
THTR-300	Hamm-Uentrop	Th-High-Temperature-Reactor	Power production	1983	1989	760
AVR	FZ Jülich	High-Temperature-Reactor	Pilot plant	1969	1988	46
FRJ-2 DIDO	FZ-Jülich	Deuterium moderated reactor	Research reactor Neutron source	1962	2006	23
FRJ-1 MERLIN	FZ-Jülich	Medium Energy Research Light water moderated Industrial Nuclear reactor	Research reactor Neutron source	1962	1985	10
FRH	Medizinische Hochschule Hannover	TRIGA Mark I	Research reactor Neutron source	1973	1997	0.25
FRF-1	Universität Frankfurt	Boiling-water reactor	Research reactor Neutron source	1958	1968	0.5
RFR	Dresden-Rossendorf	Light-Water-Reactor WWR-SM	Research reactor	1957	1991	10
FRM	TU München	Pool-type reactor	Research reactor Neutron source	1957	2000	4
BER-1	Helmholtz-Zentrum Berlin	Boiling-water reactor	Research reactor Neutron source	1958	1972	10

^{14}C guaranteed values

The guaranteed values result of the safety analysis for the proper operation of the waste repository. These are derived values for activity limits of radionuclides and radionuclide groups per waste package [5]. They ensure that the results from emplaced waste discharges do not exceed the approved limits. For KONRAD the activity limits for the following nuclides and nuclide groups are derived: ^{3}H, ^{14}C, ^{129}I, ^{222}Rn, unspecified α-emitters and β/γ-emitters. Following boundary conditions for the derivation of activity limits are given:

- **Geological boundary conditions** defining temperatures limits for the filled emplacement compartments and convergence rates of the overburden.

- **The structural design of the repository** including properties of the final compartment structure, dimensions and number of the emplacement compartments.

- **Operation conditions of the repository** like an estimated upcast ventilation of 34 m³/s and a maximum number of emplaceable waste packages per year of 10,000.

- **The mechanisms of release from the emplacement compartments** are divided in mechanisms for open and closed emplacement compartments. For an open compartment the released activity is defined as entirely air borne. For a closed compartment gas formation and diffusion are set as key parameter.

- **Values for the release of radioactive substances with the upcast air:**

^{3}H	1.5×10^{13}	Bq/a
^{14}C	3.7×10^{11}	Bq/a
^{85}Kr	4.7×10^{7}	Bq/a
^{129}I	7.4×10^{6}	Bq/a
^{222}Rn	1.9×10^{12}	Bq/a
α-aerosol	7.4×10^{7}	Bq/a
β/γ-aerosol	3.7×10^{6}	Bq/a

For the derivation of the guaranteed values a model scenario based on the boundary conditions has been developed. For KONRAD this model scenario estimates an operation period of 40 years. Waste packages will be disposed of in 52 chambers (20.00 m³ volume per compartment) with a maximum of four open emplacement chambers at once. The emplacement compartments will be closed by a closing-off structure. Due to changes in air pressure, an air exchange of 200 % per year is estimated.
The mathematical derivation of the guaranteed values is the result of the model scenario.

$$A_G = \frac{G}{n \times (f_0 \times w_0 + f_a \times w_a)}$$

n max. number of stored waste packages per year = 10^4
A_G guaranteed values per waste package
f_0 release rate from the waste in open storage compartments
f_a release rate from the waste in closed storage compartments
w_0 Weighting factors to characterize the contributions to the release of open storage compartments normalized to the release from the waste in the first year
w_a Weighting factors to characterize the contributions to the release of closed storage compartments normalized to the release from the waste in the first year
G Values for the release of radioactive substances with the upcast air

The results of this calculation lead to the ^{14}C guaranteed values given in the waste acceptance requirements for the waste disposal KONRAD (Tab. 13).

Tab. 13: ^{14}C guaranteed values in Bq/waste-container.

^{14}C	packaging without specified tightness		packaging specified tightness					
			annual permeability factor					
			≤ 0.01		≤ 0.001		≤ 0.0001	
	metallic solids	other waste product groups	metallic solids	other waste product groups	metallic solids	other waste product groups	metallic solids	other waste product groups
unspecified	$8.4x10^{12}$	$1.8x10^{8}$	$9.2x10^{12}$	$2.0x10^{8}$	$9.2x10^{12}$	$2.0x10^{8}$	$9.2x10^{12}$	$2.0x10^{8}$
volatile content 1% < x ≤ 10%		$1.8x10^{9}$		$2.0x10^{9}$		$2.0x10^{9}$		$2.0x10^{9}$
volatile content ≤ 1%		$1.8x10^{10}$		$2.0x10^{10}$		$2.0x10^{10}$		$2.0x10^{10}$

The KONRAD Repository

The amount of reactor graphite and the guaranteed values arising from the safety analysis for the waste disposal KONRAD leads to a major problem. The total capacity of KONRAD is 303.00 m^3, the total permitted ^{14}C activity is $4x10^{14}$ Bq; this leads to an average activity of $1.32x10^{9}$ Bq/m^3. At the end of the operational phase of the repository KONRAD the maximum storable activity of ^{14}C adds up to $4.0x10^{14}$ Bq. A disposal of graphite waste would exhaust up to 80% of the storable ^{14}C activities (Tab. 14). Furthermore it should be noted that a direct disposal without prior conditioning, will exceed the guaranteed values for the normal operation and is not in accordance with the waste acceptance requirements.

Tab. 14: Container and utilized capacity.

^{14}C	guaranteed value [Bq/container]	hypothetical amount of waste containers for $4x10^{14}$ Bq (average volume 10m³/container)	KONRAD capacity
non specified	$1.8x10^{8}$	2.222.222	73 KONRAD
volatile 1% < x ≤ 10%	$1.8x10^{9}$	222.222	7.3 KONRAD
volatile ≤ 1%	$1.8x10^{10}$	22.222	0.73 KONRAD

For disposal of waste containing ^{14}C the KONRAD facility can only be used effectively, if ^{14}C four waste forms meet the requirement of “low volatile fraction ≤ 1%”.

Conditioning method for graphite-containing waste

One standard container for the repository KONRAD is the container type V, which is loaded with waste drums. Depending on the barrel type and design a container can be loaded with up to 26 barrels with a maximum total weight of 20 tons. This container can then be cemented in order to meet the requirements of the Waste Product Group 05 (APG: Abfallproduktgruppe) and the accident-proof packaging of ABK I or II by achieving a compressive strength of min. 10 N/mm² [2-4]. To ensure compliance with the mentioned points, a type of cement is necessary, which is light and flowing and when solidified, reached the required compressive strength.

Irradiated graphite waste can be crushed and then used as an aggregate for geopolymers. In fixative geopolymers it would be distributed over the conditioned barrels in the KONRAD container. Within the given boundary conditions graphite could be disposed cost-neutral with other radioactive waste.

Geopolymers form a stable matrix against fire and corrosion. As encapsulant in the KONRAD containers geopolymer serves not only for fixing the drums or other waste but also allows the conditioning of activated graphite waste into the container. The amount of graphite that can be packaged in a container depends on the ^{14}C activity. Efficiently only weakly activated ^{14}C waste can be used. Graphite / PyC of fuel has too high activity to be used efficiently [6-8].

It could be shown that the density of the generated geopolymer is equal to that of cement and at the same time higher compression strength could be reached. This is crucial, because a lower density helps to stay within the weight limit of 20 tons per container. The amount or activity of graphite must be adapted to the remaining container inventory in compliance to the KONRAD waste acceptance requirements.

References

[1] BfS, (2012)**:** Auflistung kerntechnischer Anlagen in der Bundesrepublik Deutschland - In Stilllegung http://www.bfs.de/de/kerntechnik/Kerntechnische_Anlagen_in_Deutschland.

[2] Brennecke, P. (2010): Anforderungen an endzulagernde radioaktive Abfälle: Endlagerungsbedingungen Endlager KONRAD, SE-IB-31/08-REV-1.

[3] Steyer, S., (2010): Produktkontrolle radioaktiver Abfälle, radiologische Aspekte – Endlager KONRAD, SE-IB-31/08-REV-1.

[4] Steyer, S., (2010): Produktkontrolle radioaktiver Abfälle, stoffliche Aspekte – Endlager KONRAD, SE-IB-31/08-REV-1.

[5] Müller, W., (1989): Systemanalyse KONRAD Teil 3: Grundlagen der Ableitung von Aktivitätsbegrenzungen für den bestimmungsgemäßen Betrieb der Schachtanlage KONRAD, GRS-A-1522.

[6] B.P.S. Engineering GmbH (2010): Machbarkeitsuntersuchungen zum Einbinden von Grafit in ein hydraulisches Bindemittel vom Typ "Geopolymer",

[7] Kong, D.L.Y., (2007): Comparative performence of geopolymers made with metakaolin and fly ash after exposure to elevated temperatures, Cem. Concr. Res., 1583-1589.

[8] Davidovits, J., (1993): Geopolymer Cement to Minimize Carbon-dioxide Greenhouse-warming, Ceramic Transactions, 165-182.

4.18. Evaluation and Parameter Analysis of Burn up Calculations for the Assessment of Radioactive Waste

I. Fast, Y. Aksyutina, H. Tietze-Jaensch

Corresponding author: i.fast@fz-juelich.de

Ivan Fast has been awarded a 2013 scholarship [1], [2], [3] associated with a considerable donation from the Roy G Post foundation that is associated with and supporting the annual International Waste Management Conference Series WM in Phoenix, AZ, USA. The co-authors and affiliated institute congratulates Ivan Fast to his remarkable achievement and success.

Abstract

Burn up calculations facilitate a determination of the composition and nuclear inventory of spent nuclear fuel, if operational history is known. In case this information is not available, the total nuclear inventory can be determined by means of destructive or, even on industrial scale, non-destructive measurement methods. For non-destructive measurements, however, only a few easy-to-measure, so-called key nuclides are determined due to their characteristic gamma lines or neutron emission. From these measured activities the fuel burn up and cooling time are derived to facilitate the numerical inventory determination of spent fuel elements.

Most regulatory bodies require an independent assessment of nuclear waste properties and their documentation. Prominent part of this assessment is a consistency check of inventory declaration. The waste packages often contain residues from different types of spent fuels of different history and information about the secondary reactor parameters may not be available. In this case the so-called characteristic fuel burn up and cooling time are determined. These values are obtained from a correlations involving key-nuclides with a certain bandwidth, thus with upper and lower limits. The bandwidth is strongly dependent on secondary reactor parameter such as initial enrichment, temperature and density of the fuel and moderator, hence the reactor type, fuel element geometry and plant operation history.

The purpose of our investigation is to look into the scaling and correlation limitations, to define and verify the range of validity and to scrutinize the dependencies and propagation of uncertainties that affect the waste inventory declarations and their independent verification. This is accomplished by numerical assessment and simulation of waste production using well accepted codes SCALE 6.0 and 6.1 to simulate the cooling time and burn up of a spent fuel element. The simulations are benchmarked against spent fuel from the real reactor Obrigheim in Germany for which sufficiently precise experimental reference data are available.

Introduction

The quality control of radioactive waste compounds has always been an integral part of the German safety and quality assurance concept for the disposal of radio-toxic waste. Until 1995 reprocessing of nuclear waste had been legally obligatory, then voluntary. Specific and dedicated waste conditioning methods and technologies have engaged at the reprocessing sites in France, Germany and the UK. In 2005 the German atomic act has been revised for the treatment and conditioning of high-level waste (HLW) and transport of spent fuel and reprocessing abroad has been banned. Currently, all spent fuel is temporarily stored at the

nuclear power plant (NPP) sites until further decisions are made on how to proceed and dispose of the accumulating amount of used nuclear fuel (UNF) and HLW.
The German Federal government is in charge of defining societal targets, safety standards and final disposal of German radio-toxic waste from nuclear facilities, namely the nuclear power stations, research and medical institutions and other facilities that legally deal with radioactive or fissile material. In addition, there is a vast program for the decommissioning of nuclear installations. All accumulated nuclear waste of the past has to be disposed of in a professional and safe manner. Therefore, a low-level waste (LLW) and intermediate-level waste (ILW) repository for radio-toxic waste with negligible heat generation is under construction, while an operational repository for German HLW is ways ahead from now. As spent fuel from German has been reprocessed abroad, its repatriation into dedicated national interim storage facilities has not yet been completed. Non-the-less, spent fuel from the more recent past and current operation of German NPPs is piling up in local on-site interim storages waiting for its further processing or final direct disposal.
The product quality control and quality assurance for reprocessed nuclear waste treatment, conditioning and packaging has never been controversial and QA-methods have gradually been developed and implemented at a very high standard. Since 2005, spent fuel is currently accumulating at the interim storage facilities in decay pools and dry transport-storages casks. Only little thought has been devoted on how to check independently the actual nuclear inventory of disposable spent fuel. Mainly burn up and cooling time calculations have been employed. However, the current German acceptance criteria for a virtual HLW repository require an independent verification of the crucial nuclide inventory and therefore, the waste stream properties and time dependent waste product characteristics need be established and checked [4].
Here, we shall present results from numerical simulations of nuclear inventory parameters and their time-dependent propagation which are affected and influenced by secondary reactor parameters. The role and amount of many declarable nuclides are usually determined from correlation laws that allow associating these declarable nuclides with easy-to-measure key nuclides. Again, the individual fuel element history and secondary reactor parameters affect the bandwidth, parameter uncertainties and the validity of the applied correlation laws. This is what we have investigated in more detail, and as a reference case, a nuclear fuel element of the German nuclear power plant Obrigheim has been scrutinized. The engaged software for the burn up calculation is the worldwide accepted program SCALE version 6.0 and 6.1. All calculations include 2D-simulations of one randomly selected fuel element. The bandwidth for activities of selected nuclides is estimated by the means of parameter variation. The validation of these simulation results is based on our own benchmark analysis.

Results

Correlations between easy-to-measure key nuclides and other declarable nuclides are not as solid and universal as one would wish. They must be justified and verified for each individual waste stream, and their uncertainties are subject of specific considerations. Here, we have scrutinized commonly used correlations to assess the cooling time and burn up of spent reactor fuel and have found the range of their validity being limited and the parameter uncertainties being influenced by a number of secondary reactor parameters. This is not so surprising per se, but these limitations of the commonly used correlations should be implemented into the proof tools to check and verify waste inventory declarations. And

uncertainty propagation must be considered for the sake of waste property quality assessment.
The influence of the fuel and moderator properties on the nuclide composition is investigated for burn ups of up to 60 GWd/MTU. The properties of a fuel element, such as geometry, composition of the fuel and moderator parameters correspond to the properties of a fuel element of the Obrigheim reactor. The operation history comprises three cycles and covers the period of four years in total.
The Fig. 66 presents the results of the parameter analysis for ^{154}Eu. The bandwidth for ^{154}Eu shows, that its build up is very sensitive to the parameter change in a section with lower burn up. For low and intermediate burn ups up to approximately 35 GWd/MTU the bandwidth is dominated by the uncertainty of the initial enrichment, while at higher burn ups the influence of the moderator density is the dominant factor. The influence of other parameters is weaker.
It is obvious from Fig. 66 that the activity of ^{154}Eu is not a linear function of the burn up. As ^{154}Eu is not a direct fission product and as it is screened by stable ^{154}Sm its build-up is therefore somewhat delayed. Thus, ^{154}Eu is bred mainly by means of the neutron capture by ^{153}Eu. The maximum production rate of ^{154}Eu is achieved at a burn up of ~50 GWd/MTU, thereafter it is somewhat reduced. The reason is neutron capture by ^{154}Eu, with a cross section of 1500 barn [5]. This behavior can explain the large bandwidth at the beginning and the gradient of the bandwidth after the minimum; this interpretation is supported by the parameter variation of a number of models.

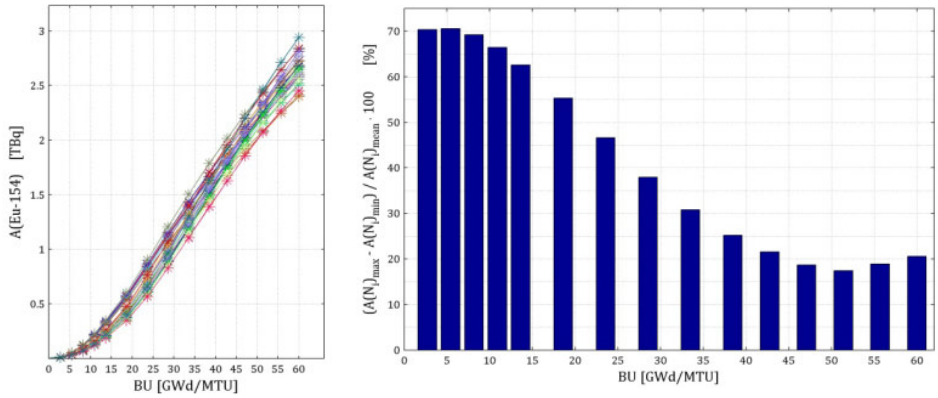

Fig. 66: Build-up of ^{154}Eu as a function of burn up (left) and corresponding bandwidth (right).

The build-up curves presented here qualitatively agree with calculations performed for other light water reactors [6].
The parameter analysis and the determination of the bandwidth for the burn up dependent build-up of individual nuclides clearly show a very strong sensitivity to the variation of the secondary reactor parameters. This seems so, in particular, for the studied key nuclides ^{154}Eu, ^{134}Cs. Apparently, the bandwidth is most sensitive to the variation of the initial fuel enrichment and the reactor's moderator density. The build-up of ^{137}Cs is strictly linear with the burn up and insensitive to any other parameter variations.
In common practice different burn up correlations are used. One of the most commonly applied ones is the ^{154}Eu /^{137}Cs ratio [6]. Usually the dependence of the ^{154}Eu activity on burn up is described by a parabolic square function and the dependence of the ^{137}Cs activity by a

linear function. Therefore, the burn up is commonly considered being a linear function of $^{154}Eu/^{137}Cs$ ratio.

The largest contribution at low and intermediate burn ups of up to 35 GWd/MTU is due to the influence of an unknown initial enrichment on ^{154}Eu production. For higher burn ups the production of ^{154}Eu does not strictly follow the quadratic law and the correlation is not very stringent. This leads, in the first place, to an increased bandwidth or uncertainty. In fact, this is quite a large uncertainty and in many cases higher precision is required. Therefore, it is recommended to use information of the initial fuel enrichment, where ever possible.

As in the case of burn up, many different correlations can be used for the cooling time determination. The common approach is to use two easy measurable nuclides with different half-lives. The ratio of their activities is usually independent of burn up and changes only with the cooling time. Possible candidates are: $^{144}Pr/^{137}Cs$, $^{106}Rh/^{137}Cs$, $^{106}Rh/^{144}Pr$ and $^{154}Eu/^{137}Cs$ [7]. Each one of them has some advantages and disadvantages and the most appropriate one has to be selected upon the application considerations. In our case the important quality is a validity range, which is limited by nuclide half-lives. Here the validity range of correlations involving ^{144}Pr or ^{106}Rh is about 10 years, whereas the one with ^{134}Cs may by applied for approximately 20 years. Therefore it has been selected for our analysis.

The analysis of the burn up and cooling time correlations serves as a very useful tool to estimate the nuclide vector composition and its uncertainties. However, these two commonly used correlations are applicable only in a limited range, because of the specifics of the ^{154}Eu build-up for the burn up correlation and the short-lived nuclide ^{137}Cs for the cooling time correlation.

The knowledge of the secondary reactor parameters, especially initial enrichment and moderator density, is advisable for the optimization of the bandwidth and uncertainties. In order to make a method more general it is necessary to extend and complement it with calculations for other reactor types.

References

[1] I. Fast, Evaluierung und Parameteranalyse von Abbrandrechnungen für die Begutachtung radioaktiver Abfälle, Diplomarbeit, RWTH-Aachen, Forschungszetrum Jülich GmbH, 2012

[2] I. Fast, Y. Aksyutina, H. Tietze-Jaensch, Evaluation and Parameter Analysis of Burn up Calculations for the Assessment of Radioactive Waste – 13187, WM2013 Conference, Phoenix, 2013

[3] Roy G. Post Foundation, http://www.roygpost.org/scholarshippoc/scholarship-winners.html, Online 2013

[4] S. Schneider, H. Tietze-Jaensch, Y. Aksyutina, D. Bosbach, Principles of Product Quality Control of German Radioactive Waste Forms from the Reprocessing of Spent Fuel: Vitrification, Compaction & Numerical Simulation – 12529, WM2012 Conference, Phoenix, 2012

[5] J. Magill, G. Pfennig, J. Galy, Karlsruher Nuklidkarte, European Commission Joint Research Centre Institute for Transuranium Elements, 7. Auflage, 2006

[6] D. D. Cobb et.al., Nondestructive Verification and Assay Systems for Spent Fuels, Los Alamos National Laboratory, 1982, (LA-9041), report, Vol. I, II

[7] IAEA, Application of Nondestructive Gamma-Ray and Neutron Techniques for the Safeguarding of Irradiated Fuel Materials, 1980

[8] OECD, NEA, http://www.oecd-nea.org/sfcompo/Ver.2/Eng/Obrigheim/index.html, SFCOMPO-Datenbank, Online 2012

[9] P. Parbero et.al., Post Irradiation Analysis of The Obrigheim PWR Spent Fuel, Commission of the European Communities, Joint Research Centre Ispra Establishment, Chemistry Division, ESSOR Division, Transuranium Institute (Karlsruhe), Physics Division, Materials Division. 1980, report

[10] Jahrbuch der Atomwirtschaft, 1970, 1972, 1973, 1974, 1975, 1976

[11] IAEA, Determination and Use of Scaling Factors for Waste Characterization in Nuclear Power Plants, 2009

4.19. Non-nuclear applications

Non-Nuclear Applications of Prompt and Delayed Gamma Neutron Activation Analysis

Prompt and Delayed Gamma Neutron Activation Analysis (P&DGNAA) based on neutron generator or isotopic neutron sources is a versatile and powerful non-destructive analytical technique which may found applications in relevant fields such as safeguards (specific detection of nuclear materials), home-land security (detection of dangerous substances like chemicals or explosive), primary natural resources prospection (in situ borehole-logging, analysis of drilling core) and secondary natural resources assay (analysis of baring material, urban-mining, sludge, characterization of Waste Electrical and Electronic Equipment (WEEE) for recycling). Furthermore P&DGNAA may be implemented in industrial processes for parameter optimization and for quality control of products and also to determine the toxicity level of residues.

Know-how gained in R&D of P&DGNAA for the identification and quantification of toxic and reactive elements or substances in 200-l radioactive waste drums is applied: (1) for the detection of deep buried unexploded ordnance (UXO) by means of borehole logging in the framework of homeland security [1, 2]. This is still a highly relevant issue due to legacies of World War II in many areas of Germany. The percentage of UXO is estimated to range between 5 an 15 % to the total of dropped bombs corresponding to 100.000 -300.000 tons of bombs; (2) for the characterization of large volumes of WEEE with respect to rare and precious metal and to toxic elements content to improve recycling process. The MEDINA technology developed for the characterization of radioactive waste has attracted quite some interest in recycling industry. The suitability of P&DGNAA for the determination of elemental content of electronics products was demonstrated by analyzing of mobile phone at the MEDINA facility. The elements Al, O, Fe, Si, Cu, Ni, Cr, S, Co, Sc, Cl, V and B were identified and quantified.

References

[1] J. Kettler, E. Mauerhofer, M. Steinbusch, Detection of unexploded ordnance by PGNAA based borehole-logging, J Radioanal Nucl Chem (2013) 295:2071-2075

[2] Patent DE102008063735B4; Forschungszentrum Jülich GmbH, E. Mauerhofer, J. Kettler, M. Steinbusch

Rare earth element separation by solvent extraction

During the last decades the demand for rare earth elements (REE) increases as a result of rising technology applications (e.g. hybrid cars, wind turbines, industrial catalyst, etc.). China has, beside Australia and the United States, the largest rare earth deposits and has a global monopoly on rare earths mining [1]. Since last years, caused by a Chinese export restriction, a significant increase in rare earth prices was observed. Expecting a rising demand for rare earth metals a shortage of rare earths is upcoming. The separation of rare earth elements, the last step of rare earth mineral beneficiation, is the most value creating procedure. The most challenging separation is the separation of two directly neighboring rare earth elements [2]. There have been major developments in the technology for the separation of high purity rare earths. One advantageous technique for rare earth purification involves hydrometallurgical processes, such as those developed at IEK-6 for actinide(III) partitioning [3]. Both families of f-elements have very similar physical and chemical properties. Many extraction systems with relatively low rare earth separation factors were described in the literature. Neighboring rare earth, being chemically similar, show in Satos report separation

factors from 1.03-2.58 [4]. Satos data were reproduced and for heavier rare earth elements (e.g. Er, Yb) a higher extraction at lower concentrations can be observed. In collaboration with an industrial partner, the IEK-6 will use its expertise to develop more efficient extraction systems for the mutual lanthanide separation.

References

[1] Kynicky, J., Smith, M. P., Xu, C., Elements 2012, 8, 361-367.
[2] Gupta, C. K., Krishnamurthy, N., Extractive metallurgy of rare earths, CRC Press, Boca Raton, Florida, 2005.
[3] Modolo, G., Odoj, R., J. Alloy. Compd. 1998, 271-273, 248-251.
[4] Sato, T., Hydrometallurgy 1989, 22, 121-140.

Application of safeguards methods and techniques in the context of arms control verification regimes

IEK-6 started a discussion with the Bundeswehr Verification Centre (Zentrum für Verifikationsaufgaben der Bundeswehr, ZVBw) located in Geilenkirchen on verification technologies and methodologies. ZVBw, under the guidelines of the Federal Foreign Office and the leadership of the Federal Ministry of Defence, ensures the implementation of the international agreements of Germany with regard to regional and global arms control (as to conventional, nuclear, biological and chemical weapons), confidence building, and non-proliferation. IEK-6 and ZVBw have agreed to investigate whether methods and techniques that were originally developed for verifying safeguards agreements in the context of the Nuclear Non-proliferation Treaty (NPT) could also be used for other verification regimes. Verification measures to be addressed in more detail will be remote sensing and satellite imagery processing as well as mathematical models.

5 Education and training activities

Education in nuclear safety research in particular with RWTH Aachen University is supported by IEK-6. Prof. Dirk Bosbach holds the chair for the disposal of nuclear waste and Prof. Bruno Thomauske the chair for nuclear fuel cycle. Further, a new accredited Master Curriculum "Nuclear Safety Engineering" was established at RWTH Aachen University in 2010. 13 students started this two years programme. A new practical course on nuclear measuring techniques in the radiochemistry laboratories of IEK-6 as well as the lecture "Introduction to Nuclear Chemistry" was launched in 2010 and has attracted almost 50 students from nuclear safety engineering, chemistry, computational engineering science and nuclear technology at RWTH Aachen University. Lectures are also given at the Aachen University of Applied Science by IEK-6 staff.
In the framework of the JARA cooperation Dr. Evgeny Alekseev, leader of the HGF Young Investiator Group, became as Junior professor according to the Jülich model at RWTH Aachen University linked to the Institute of Crystallography. PD Dr. Hartmut Schlenz is teaching at the Faculty of Mathematics and Natural Sciences at the University of Bonn. Dr. Giuseppe Modolo and Dr. Irmgard Niemeyer will habilitate within the next 12 months at RWTH Aachen University and Bergakademie Freiberg.

The IEK-6 also participates in the new graduate school Energy and Climate HITEC, which was founded in 2011 in Jülich. The IEK-6 supports HITEC Theme Days “Nuclear waste disposal and reactor safety” held at RWTH Aachen University, HITEC Methods Days “Application of X-ray diffraction methods in energy research” as well as HITEC Labs “Synthesis methods for immobilizing radioactive elements in ceramic host phases” and “Structural characterization of ceramics by spectroscopic and diffraction methods”, which are hands-on practical training lasting two to three days for small groups of PhD students from various HITEC fields. Furthermore, biannual Orientation Days (in March and October) are organized for new HITEC participates. Second-year PhD students organize a three-day retreat; where they present their projects and the scientific methods employed and discuss them with their fellow PhD students.

5.1. Courses taught at universities by IEK-6 staff

Prof. Dr. D. Bosbach

RWTH Aachen University
Faculty of Georesources and Materials Engineering
Topic: Grundlagen der Kernchemie, Hours: 2 SWS, since WS 2010
Topic: Physikalisch-chemische Grundlagen für die Langzeitsicherheitsanalysen der Nuklearen Endlagerung, Hours: 2 SWS, WS 2009/2010
Topic: Kerntechnisches Messpraktikum, 1 week, since WS 2010

Prof. Dr. B. Thomauske

RWTH Aachen University
Faculty of Georesources and Materials Engineering
Topic: Endlagerung radioaktiver Abfälle und Sicherheitsanalysen, Hours: 2 SWS, WS 2011/2012
Topic: Nuklearer Brennstoffkreislauf I, Hours: 2 SWS, WS 2012
Topic: Produkte und Märkte der Rohstoffindustrie, Hours: 2 SWS, WS 2012
Topic: Rohstoffe und Energieversorgung, Hours: 2 SWS, WS 2012

Prof. Dr. E. Alekseev

RWTH Aachen University
Faculty of Georesources and Materials Engineering
Topic: Grundzüge der Kristallographie, Hours:4, Since WS 2012

PD Dr. H. Schlenz

University of Bonn
Faculty of Mathematics and Natural Sciences
Topics: Crystallography and Applied Mineralogy, Hours: 2 SWS

Dr. G. Modolo

Aachen University of Applied Science, Fachbereich Chemie und Biotechnologie
European Master of Science in Nuclear Applications
Topic: Nuclear Fuel Cycle, Hours: 2 SWS since 2010

RWTH Aachen University
Faculty of Georesources and Materials Engineering
Topic: Brennstoffe, Wiederaufbereitung und Konditionierung, Hours: 2 SWS, since 2011
Topic: Sicherheit in der Wiederaufberbeitung, Hours: 3 SWS, since 2011

Dr. I. Niemeyer

RWTH Aachen University
Faculty of Georesources and Materials Engineering
Topic: Nuclear Safeguards and Non-Proliferation, Hours: 2 SWS, SS 2012

Dr. H. Tietze-Jaensch

University of Poznan
Faculty of Physics, SS 2012
Topic: Neutron Sources, 8 h lecture
Topic: Gamma & Neutron Spectroscopy in Waste Characterization, 2 h lecture

Polytechnical University Warsaw
Faculty of Physics, WS 2012/13
Topic: Nuclear Energy & Safety, 8 h lecture
Topic: Energy Systems, Energy Wende and Sustainable Energy Resources, 6 h lecture

5.2. Graduates

15 PhD students are currently (April 2013) working on research projects related to the safe management of nuclear waste in Jülich. Three PhD candidates had successfully defended their theses during the last two years. Five PhD candidates will finish in 2013. Furthermore, 12 diploma, bachelor, and master theses were finished in 2011/2012. Currently, four students are working on their theses. 17 students passed an internship at IEK-6 during the last two years.

5.2.1 Bachelor, Diploma, Master Thesis

Y. Arinicheva: Struktur- und Stabilitätsuntersuchungen an Monazitkeramiken zur Konditionierung von Minoren Actiniden, Master, RWTH Aachen University, 2012

M. Baier: Autoradiographic investigations of reactor graphite before and after thermal treatment, Master, Fachhochschule Aachen, Campus Jülich, 2012

I. Fast: Evaluierung und Parameteranalyse von Abbrandrechnungen für die Begutachtung radioaktiver Abfälle, Diplom, RWTH Aachen University, 2012

S. Finkeldei: Darstellung und Charakterisierung ZrO2 und ThO2 basierter Keramiken für die nukleare Entsorgung, Diplom, RWTH Aachen University, 2011

C. Fischer: Gewichtsverlust von nichtradioaktivem Graphit bei divergenter thermischer Behandlung sowie Auslegung einer TGA für Messungen mit aktiviertem Graphit, Diplom, Fachhochschule Köln, 2012

C. Göbbels: Studie zum Einsatz von $LaBr_3$-Szintilationsdetektoren im Rahmen der zerstörungsfreien Charakterisierung radioaktiver Abfallfässer, Bachelor, Fachhochschule Aachen, Campus Jülich, 2012

S. Gülland: Process development studies towards a grouped actinide separation from spent nuclear fuel solutions, Bachelor, ZUYD Hogeschool, Heerlen, NL, 2011

J. Heuser: Synthese und Charakterisierung von Samarium-Cer-Monazit für die nukleare Entsorgung von Actinoiden, Diplom, University Bonn, 2011

F. Mildenberger: Identifizierung von Cadmium in homogenen und heterogenen großvolumigen Proben mittels Prompt-Verzögert-Gamma-Neutronen-Aktivierungs-Analyse, Bachelor, Fachhochschule Aachen, Campus Jülich, 2011

C. Rizzato: Investigations on high temperature thermal treatments of virgin AVR graphite, Master, University of Bologna, 2012

T. Schuppik: Synthesis and chemical stability of La, Eu-monazites for conditioning of nuclear waste, Bachelor, ZUYD Hogeschool, Heerlen, NL, 2012

T. Spermann: Identifizierung von Quecksilber in homogenen und heterogenen großvolumigen Proben mittels Prompt-Verzögert-Gamma-Neutronen-Aktivierungs-Analyse, Bachelor, Fachhochschule Aachen, Campus Jülich, 2011

5.2.2 Doctoral Thesis

C. Babelot: Conditioning of Minor actinides in La-Monazite-type Ceramics, RWTH Aachen University, 2012

H. Daniels: Herstellung von uranbasierten Keramiken mittels interner Gelierung zur Konversion von trivalenten Actinoiden, RWTH Aachen University, 2012, Schriften des Forschungszentrums Jülich Energy & Environment, Volume 142, 154 pages, ISBN 978-3-89336-794-8

A. Neumann: Bildung von sekundären Phasen bei tiefengeologischer Endlagerung von Forschungsreaktor-Brennelementen - Struktur- und Phasenanalyse, RWTH Aachen University, 2012, Schriften des Forschungszentrums Jülich Energy & Environment, Volume 153, 329 pages, ISBN 978-3-89336-822-8

5.3. Vocational training

Forschungszentrum Jülich offers different vocational training programs. The three years lasting education is supported by IEK-6 in nuclear / radiochemistry. In 2011/2012 three laboratory assistants were trained in the laboratories of IEK-6. Two of them finished their education successfully in 2012 and received a certificate of apprenticeship.

5.4. Further education and information events

IEK-6 is committed to support the education of young people including schoolchildren in nuclear safety research. Forschungszentrum Jülich participates in the nationwide **"Girls Day".** Girls from 5^{th} to 13^{th} class have the opportunity to become familiar with different professions such as chemist, physicist, or firewoman as well as the working conditions at laboratories, garages and offices. At IEK-6, the topic "No fear of radioactive materials" was presented. Basics about radioactivity in the environment and radioactive decay as well as different measuring techniques were explained. Measurements of different samples were carried out by the girls themselves to get a feeling for radioactivity (Fig. 67) and attract children's interest in science.

Fig. 67: Girls Day 2011 at IEK-6.

In terms of recruiting PhD students in the field of nuclear safety research, IEK-6 is represented at the colloquium “Kernenergie hat Zukunft” which is organized by the Deutsche Atomforum e.V.. The event is addressed to students of technical and scientific disciplines. The PhD students have the opportunity to get information at first hand from energy providers, research institutes, and technical inspection authorities on the manifold job-related perspectives in the field of nuclear energy. IEK-6 had an information desk at the job exchange in Cologne, 2011 to introduce the research activities of the institute and to provide information about master, diploma, and PhD opportunities. In 2011 the participants visited the Forschungszentrum Jülich and the laboratories of IEK-6.

On request by the EC Directorate General (DG) Energy/Nuclear Safeguards (Euratom) and the International Atomic Energy Agency (IAEA), IEK-6 hosted **two Euratom/IAEA training courses** for each 12 inspectors in May 2011 and 2012. The 3-day courses were aimed at improving team work and communication among the joint Euratom/IAEA inspection teams in the European Union. The course contained both theoretical introductions and practical exercises on group formation and group interaction during inspections. Thanks to the support from the Nuclear Services (N) and the Safety and Radiation Protection (S), Jülich made three material balance areas available to perform inspection exercises (physical verification of inventory) under real conditions.
Moreover, IEK-6 held a **Euratom safeguards seminar** for German stakeholders in December 2011. DG Energy offers annual seminars for the EU Member States on the Euratom Treaty and the implementation of Euratom safeguards in the EU at the headquarters in Luxembourg, however, this 2.5-day seminar was intended to lecture in German language and consider important safeguards issues in Germany, such as decommissioning. 40 participants from the nuclear industry, state authorities and safeguards R&D attended the seminar.

5.5. Institute Seminar

The IEK-6 organizes an institute seminar with internal talks and invited speakers, to present the recent research activities. Further information on www.fz-juelich.de/iek/iek-6.

5.5.1 Internal talks 2011

09.03.2011 **N. Qian:** Development of Gamma-Scanning method and system for characterization of radioactive waste drums
T. Krings: Reconstruction of the activity of point sources for the accurate characterization of nuclear waste drums by segmented gamma scanning

23.03.2011 **L. Tian:** Electrochemical method to disintegrate graphite matrix from high temperature gas-cooled reactor (HTGR) fuel elements

30.03.2011 **S. Schneider:** Cluster Computing

04.05.2011 **C. Babelot:** Conditioning of Minor Actinides in Monazite-type Ceramics

11.05.2011 **A. Neumann:** Röntgenographische Charakterisierung endlagerrelevanter sekundärer Phasen

18.05.2011 **A. Wilden:** New results on the partitioning of minor actinides from nuclear waste solutions

23.05.2011 **H. Curtius, G. Modolo, H. Schlenz, I. Niemeyer, H.J. Steinmetz, H. Tietze-Jaensch, E. Mauerhofer, D. Vulpius, M. Rossbach:** Vorträge der Gruppenleiter, Ergebnisse aus 2010 und Ausblick 2011

08.06.2011 **C. Listner:** Objekt basierte Änderungsdetektion für die Analyse digitaler Fernerkundungsdaten
M. Klinkenberg: Elektronenmikroskopie REM/FIB

15.06.2011 **V. Vinograd:** Atomistic Simulation of barium, strontium, sulfate
S. Finkeldei: Darstellung und Charakterisierung Zirkoniumdioxid und Thoriumdioxid basierter Keramiken für die nukleare Entsorgung

22.06.2011 **J. Heuser:** Synthese und Charakterisierung von Sm-Ce-Monazit für die nukleare Entsorgung von Actinoiden
M. Dürr: Status and Trends of Measurement Techniques in Nuclear Safeguards

29.06.2011 **S. Labs:** $ThSiO_4$ zum $USiO_4$ - hydrothermale Synthese von Thorit und Uran-Thoriumsilikat Mischkristallen

06.07.2011 **H. Daniels:** Synthesis of Uranium-based Microsperes via Internal Gelation

13.07.2011 **K. Rozov:** Synthesis, characterization and stabilities of Cl-bearing layered double hydroxides (LDH´s)

C. Fischer: Simulation von Strömungsbildern bei der thermischen Behandlung von Graphit

S. Gülland und T. Schuppik: Vorstellung der Projektarbeiten im Rahmen der Kooperation mit der Hogeschool Zuyd Heerlen

20.07.2011 **M. Weidenfeld:** Glaschemie

F. Brandt: Chemical stability of nuclear waste glass

18.08.2011 **F. Mildenberger:** Identifizierung von Cadmium in homogenen und heterogenen großvolumigen Proben mittels Prompt-Verzögert-Gamma-Neutronen-Aktivierungs-Analyse

T. Spermann: Identifizierung von Quecksilber in homogenen und heterogenen großvolumigen Proben mittels Prompt-Verzögert-Gamma-Neutronen-Aktivierungs-Analyse

5.5.2 Internal talks 2012

25.01.2012 **S. Gülland:** Process Development Studies towards a Grouped Actinide Separation from Spent Nuclear Fuel Solutions

25.01.2012 **A. Wilden:** Der Einsatz von ionischen Flüssigkeiten beim Partitioning. Erste Ergebnisse aus einem Forschungsaufenthalt in Straßburg

15.02.2012 **T. Krings:** Aktivitätsrekonstuktion von Punktquellen in radioaktiven Abfallgebinden mittels Gamma-Scanning

15.02.2012 **C. Genreith:** Prompt-Gamma-Strahlung von Np-237

08.02.2012 **A. Barth:** Management safeguards-relevanter Informationen aus Fernerkundungsdaten mit Hilfe von GI-Technologien

29.02.2012 **M. Weidenfeld:** Störfallverhalten von Siedewasserreaktoren am Beispiel vom KKK

K. Baginski: Dekontamination von Nukleargraphit durch thermische Behandlung

07.03.2012 **C. Listner:** Acquisition Path Analysis in International Safeguards

07.03.2012 **M. Dürr:** Präparation und Analyse von uranhaltigen Partikeln im Rahmen der internationalen Kernmaterialüberwachung

14.03.2012 **A. Havenith:** MEDINA – Multi Element Detektion basierend auf Instrumenteller Neutronenaktivierungsanalyse zur stofflichen Produktkontrolle radioaktiver Abfälle

21.03.2012 **A. Neumann:** Bildung von sekundären Phasen bei tiefengeologischer Endlagerung von Foschungsreaktoren-Brennelementen - Struktur- und Phasenanalyse

25.04.2011 **H. Curtius, G. Modolo, H. Schlenz, H. Tietze-Jaensch M. Dürr, E. Mauerhofer, M. Rossbach, D. Vulpius, H. Krumbach:** Vorträge der Gruppenleiter; Ergebnisse aus 2011 und Ausblick 2012

09.05.2012 **I. Fast:** Evaluierung und Parameteranalyse von Abbrandrechnungen für die Begutachtung von hochradioktiven Abfällen

29.11.2012 **S. Kasselmann:** A new Approach for the Simulation of Nuclide Transmutation Processes

5.5.3 Invited talks 2011

02.03.2011 **Dipl.-Ing. Thomas Horn:** Rückführung radioaktiver Abfälle aus der Wiederaufarbeitung deutscher Brennelemente in Frankreich und England
GNS (Gesellschaft für Nuklear-Service mbH)

19.05.2011 **Dr. Zsolt Revay:** Investigation of nuclear materials in cold neutron beams - prompt gamma activation analysis and neutron imaging techniques at Budapest and at Garching
Technische Universität München FRM-II on leave from Institute of Isotopes Budapest, Hungary

12.07.2011 **Prof. Dr. Serge Stefanovsky:** Glass and ceramic waste forms
Radon, Moskau

21.07.2011 **Dr. Maria Ophelia Jarligo:** Ceramic materials for thermal barrier coating applications
IEK-1, Forschungszentrum Jülich

12.10.2011 **Dr. Gilles Leturq:** Ceramics for the backend of the nuclear fuel cycle: synthesis and properties
CEA Marcoule, France

09.11.2011 **Dr. Klaus Lützenkirchen:** Nuclear Safeguards and Forensics at ITU
European Commission Joint Research Center, Institute for Transuranium Elements (ITU), Karlsruhe

14.11.2011 **Donald Reed:** Actinide Speciation and Oxidation-State Distribution in the Wipp
Los Alamos National Laboratory, USA

24.11.2011 **Dr. Andreas Loida:** Untersuchungen zum Korrosionsverhalten von hoch abgebranntem UO_2 Kernbrennstoff in endlagerrelevanten Wässern
Institut für Nukleare Entsorgung, KIT

5.5.4 Invited talks 2012

11.01.2012 **Priv.-Doz. Dr. Florian Kraus:** Chemie mit Actinoiden in flüssigem Ammoniak
Technische Universität München, Lehrstuhl für Anorganische Chemie mit dem Schwerpunkt Neue Materialien, Arbeitsgruppe Fluorchemie

12.01.2012 **Nan Qian:** Analytical calculation of the collimated detector response for the characterization of nuclear waste drums by segmented gamma scanning
Nuclear Power Tech. & Equip. Engineering Research Center, School of Nuclear Science and Engineering, Shanghai Jiao Tong University

09.02.2012 **Wolfgang Filbert:** Vorläufige Sicherheitsanalyse Gorleben: Stand der Arbeiten zum Endlagerkonzept
DBE TECHNOLOGY GmbH, Forschung und Entwicklung

09.02.2012 **PD Dr. Jürgen Altmann:** Akustische und seismische Messungen zur Entdeckung nicht deklarierter Nuklearaktivitäten: Aufbau, Ziele und Ergebnisse der Messungen im Erkundungsbergwerk Gorleben
Technische Universität Dortmund, Experimentelle Physik III

28.03.2012 **Dr. Lawrence Johnson:** Spent Fuel Studies - Research Needs in Support of Safety Assessment of Spent Fuel Disposal
Coordinator of Research, Development and Demonstration (RD&D), Nagra, Switzerland

03.04.2012 **Prof. Nicolas Dacheux:** Why phosphates appear as promising long-term radwaste matrices? Consequence of structural flexibility and high chemical durability
Université Montpellier 2

03.04.2012 **Dr. Nicolas Clavier:** Closer to the interface: original approaches and tools to monitor sintering and dissolution processes of actinide based oxides.
Chargé de Recherches, Centre national de la recherche scientifique (CNRS)

24.04.2012 **Prof. Bertrand Fritz:** Hydro-geochemical modelling of fluid-rock interaction systems: the reactive transport modelling code KIRMAT. Possible applications to natural or engineered systemsss and Ceramic Waste Forms
Laboratoire d'Hydrologie et de Géochimie de Strasbourg, Université de Strasbourg

27.04.2012 **Prof. Dr. Sergey V. Krivovichev:** Murataite-Pyrochlore Titanate Ceramics for Nuclear Waste Immobilization: Structure, Microstructure and Crystallization
Department of Crystallography, Saint Petersburg State University, Russia

08.05.2012 **Emma Aneheim:** Process Development Studies towards A Grouped Actinide Separation Process at Chalmers

Chalmers University of Technology, Department of Chemical and Biological Engineering, Nuclear Chemistry, Gotheburg, Sweden

31.05.2012 **Prof. Joan de Pablo:** Effect of Burn-up and High Burn-up Structure on UO_2 Spent Fuel Dissolution
Institute for Sustainability Science & Technology, UPC Barcelona Tech, Spain

18.10.2012 **Univ.-Prof. Tobias Reich:** Interaction of neptunium and plutonium with natural clay
Johannes Gutenberg-Universität Mainz (JGU), Institut für Kernchemie

22.10.2012 **Dr. Terry Todd:** Nuclear energy policy and status in the US
Director, Fuel Cycle Science and Technology Division Idaho National Laboratory, USA

05.11.2012 **Dr. Shijun Wu:** Uranium chemistry in complex barates and silicate systems at normal and extreme conditions
Institute of Geosciences, University of Kiel

08.11.2012 **Dr. Lara Duro:** Modelling of the redox evolution in a cementitious repository of LILNW
AMPHOS21, Spain

15.11.2012 **Dr. Klaus-Jürgen Brammer:** Gorleben, Endlagersuchgesetz - Und was kommt dann?
Gesellschaft für Nuklear-Service GmbH, GNS

22.11.2012 **Dr. Y. Aregbe:** EC-JRC-IRMM Support to Nuclear Safeguards, Nuclear Security, Nuclear Safety
European Commission – Joint Research Centre, Institute for Reference Materials and Measurements (IRMM), Geel, Belgium

28.11.2012 **Prof. Dr. Clemens Walther:** Das Institut für Radioökologie und Strahlenschutz der Universität Hannover, derzeitige Arbeiten und Perspektiven
Institut für Radioökologie und Strahlenschutz, Leibniz Universität Hannover

14.12.2012 **Prof. Dr. Neil Hyatt:** Understanding the structure of radiation damaged ceramics for actinide disposition using X-ray Absorption Spectroscopy
University of Sheffield, Royal Academy of Engineering and NDA Chair in Radioactive Waste Management

5.6. Visiting Scientists / Research Visits

Visiting Scientists

Qian Nan 2010/2011 (1 year)

School of Nuclear Science Engineering; Shanghai Jiao Tong University

Lifang Tian 07.02.2011 – 02.04.2011

Tsinghua University, Beijing, China

Marcin Brykała 04.10.2011 - 31.12.2011

Sol-Gel Laboratory, Department of Nuclear Methods of Material Engineering, Institute of Nuclear Chemistry and Technology, Warszaw, Poland

Emma Aneheim 04.2012 - 10.05.2012

Chalmers University of Technology, Department of Chemical and Biological Engineering Nuclear Chemistry, Gotheburg, Sweden

Rosa Maria Rodrigues Galan 10.09.2012 – 05.10.2012

University of Oviedo, Department of Geology, Oviedo, Spain

Research visits of IEK-6 staff

Henrik Daniels 13.01.2011 - 15.04.2011

DRCP/SCPS/Laboratoire Chimie et Conversion des Actinides, CEA, Marcoule France

Andreas Wilden 19.10.2011 - 18.11.2011

IPHC (Institut Pluridisciplinaire Hubert Curien), CNRS (Centre nationale de la recherche scientifique) Strasbourg, France

Thomas Krings 01.04.2012 – 30.06.2012

Nuclear Power Technique and Equipment Engineering Research Centre (NPTE); Shanghai-JIAO Tong University, China

Sarah Finkeldei 26.03.2012 – 08.06.2012

NRG (Nuclear Research and consultancy Group), Petten, Netherlands

Sabrina Labs 03.2012 – 07.2012

Lujan Neutron Scattering Center at Los Alamos Neutron Science Center, Los Alamos, USA

6 Awards

Dr. J. Kettler was awarded with the **"Jülicher Exzellenz-Preis"** for young scientists and the **"RWE Zukunftspreis 2011"** for his doctoral theses "Prompt-Gamma–Neutronen-Aktivierungsanalyse von radioaktivem Abfall".

Fig. 68: Prof. Dr. Achim Bachem, Dr. John Kettler, Prof. Dr. Dirk Bosbach

Dr. A. Bukaemskiy was awarded with the 2nd poster award at the EMRS Conference 2011 in Nice, France within the symposium "Nuclear Materials" for his poster "Physical properties and leaching behaviour of spent fuel BISO coated particles".

J. Assenmacher was awarded with the 2nd poster award at the "Wissenschaftsforum Chemie" 2011 of the GDCh, "Nuklearchemie" in Bremen for her poster "Der Lösungsmitteleinfluss bei der selektiven Actiniden(III)/Lanthaniden(III) Trennung mittels aromatischer Dithiophosphinsäuren".

A. Havenith was awarded with the 1st poster award at NUTECH 2011 Conference in Krakow, Poland, within the symposium "Development and Applications of Nuclear

Technologies“ for his poster "Prompt and Delayed Gamma Neutron Activation Analysis for the Assay of Toxic Elements in Radioactive Waste Packages".

C. Babelot was awarded with the 2nd poster award at 494. WE-Heraeus-Sminars "Innovative Nuclear Power in a Closed Fuel Cycle Scenario" in Bad Honnef for her poster "Conditioning of Minor Actinides in La-Monazite-type Ceramics".

J. Heuser was awarded with the 2nd poster award at the E-MRS 2012 Spring Meeting in Strasbourg, France, within the symposium “Actinide compounds and properties” for her poster “Characterization of Sm- & Tb-Orthophosphates used for Nuclear Waste Management”.

7 Selected R&D projects

7.1. EU projects

ACSEPT - Actinide reCycling by SEParation and Transmutation, 03/2008 - 02/2012; Work package leader: Dr. G. Modolo, FZJ

ASGARD - Advanced fuelS for Generation IV reActors: Reprocessing and Dissolution, 10/2011 – 10/2015, Work package leader: Dr. G. Modolo, FZJ

CARBOWASTE – Treatment and Disposal of Irradiated Graphite and Other Carbonaceous Waste, 04/2008 - 03/2012, Coordination: FZJ

G-MOSAIC - GMES services for Management of Operations, Situation Awareness and Intelligence for regional Crises; 01/2009 - 12/2011

SKIN - Slow Processes in Close-to-Equilibrium Conditions for Radionuclides in Water/Solid Systems of Relevance to Nuclear Waste Management, 01/2011 – 12/2013; Work package leader: Prof. D. Bosbach, FZJ

FIRST-Nuclides - Determination of the first radionuclide release fraction, 01/2012 – 12/2014

7.2. More projects

ImmoRad - Grundlegende Untersuchungen zur Immobilisierung langlebiger Radionuklide durch die Wechselwirkung mit endlagerrelevanten Sekundärphasen; 02/2012 – 01/2015, Bundesministerium für Bildung und Forschung (BMBF)

VESPA - Verhalten langlebiger Spalt- und Aktivierungsprodukte im Nahfeld eines Endlagers und Möglichkeiten ihrer Rückhaltung (07/2010 – 06/2013)
Bundesministerium für Wirtschaft und Technologie (BMWi)

Radiographie mittels schneller Neutronen zur Charakterisierung radioaktiver Abfälle (**Neutronen Imaging**); 05/2012 - 04/2015
Bundesministerium für Bildung und Forschung (BMBF)

Untersuchungen zum grundlegenden Verständnis der selektiven Komplexierung von f-Elementen (**f-KOM**); 07/2012 - 06/2015
Bundesministerium für Bildung und Forschung (BMBF)

Conditioning - Grundlegende Untersuchungen zur Immobilisierung langlebiger Radionuklide mittels Einbau in endlagerrelevante Keramiken; 10/2012-09/2015
Bundesministerium für Bildung und Forschung (BMBF)
Coordination: FZJ

Bestimmung und Validierung nuklearer Daten von Actiniden zur Zerstörungsfreien Spaltstoffanalyse in Abfallproben durch prompt Gamma Neutronenaktivierungsanalyse (**PGAA-Actinide**); 08/2012 – 07/2015
Bundesministerium für Bildung und Forschung (BMBF)

Synthese und Charakterisierung keramischer Samarium-Phosphat- und Samarium-Phosphosilicat-Phasen zur Immobilisierung von Actinoiden; 04/2012 – 04/2015
Deutsche Forschungsgemeinschaft DFG

8 Committee work

Prof. Dr. Dirk Bosbach:

- Designated speaker of the Helmholtz research program „Nuclear Waste Management and Safety as well as Radiation Research“
- Member of the German Alliance for Competence in Nuclear Technology
- Director of JARA section Energy (2010 – 2011)
- Member of the advisory board of Nuclear chemistry division of the German Chemical Society (GDCh)
- Member of the scientific advisory boards of the TALISMAN network
- Member of the scientific advisory board of the ENTRIA Research Platform
- Member of the NEA TDB Iron II expert group

Dr. Martin Dürr

- Institute of Nuclear Materials Management (INMM): International Safeguards Division (ISD)
- European Safeguards Research and Development Association (ESARDA): WG Containment & Surveillance (C&S)
- European Safeguards Research and Development Association (ESARDA): WG Techniques and Standards for Destructive Analysis (DA)
- AG Kernmaterial-Überwachung (AKÜ)

Clemens Listner

- European Safeguards Research and Development Association (ESARDA): WG Verification Technologies and Methodologies (VTM)

Dr. Giuseppe Modolo:

- Technical Programm Committee of the international Solvent extraction Conference: ISEC 2011 and 2014
- International ATALANTE 2012 conference, Technical Conference Committee
- International Global 2013 conference, Technical Conference Committee
- E-MRS 2013, Symposium E: Scientific basis of the nuclear fuel cycle, Scientific Comittee
- Editorial Board of the Journal Solvent Extraction and Ion Exchange
- Distinguished reviewers board of the Journal of Radioanalytical and Nuclear Chemisty

Dr. Irmgard Niemeyer:

- Institute of Nuclear Materials Management (INMM): International Safeguards Division (ISD), Vice-Chair WG Open-source and Geospatial Information
- European Safeguards Research and Development Association (ESARDA): Steering Committee, Symposium Committee, Chair WG Verification Technologies and Methodologies (VTM), WG Knowledge Training and Management (KTM)
- AG Kernmaterial-Überwachung (AKÜ)
- International Society for Photogrammetry and Remote Sensing (ISPRS): International Policy Advi sory Committee (IPAC)
- IEEE Geophysics and Remote Sensing Society (IEEE): Reviewer

Dr. Bernd Richter

- Institute of Nuclear Materials Management (INMM): International Safeguards Division (ISD), Associate Editor
- European Safeguards Research and Development Association (ESARDA): Editorial Committee, WG Containment/Surveillance (C/S)
- AG Kernmaterial-Überwachung (AKÜ)

Dr. Matthias Rossbach:

- International Committee on Activation Analysis
- International Scientific Advisory Committee for the Budapest Neutron Centre, Hungarian Academy of Sciences
- Review Panel Imaging, Analysis, Nuclear and Particle Physics for Beam-time at all Instruments hosted at FRM II Research Reactor, Garching
- Scientific Committee of the 14th International Conference on Modern Trends in Activation Analysis, MTAA14
- Scientific Committee of the 4th Int. Nuclear Chemistry Congress

Priv.-Doz. Dr. Hartmut Schlenz:

- Scientific Committee of the 14th International Conference on Experimental Mineralogy Petrology Geochemistry, Kiel, Germany (2012)
- Nuclear Energy Agency of the OECD: TDB-Fe2 (2011-2015)

Dr. Holger Tietze-Jaensch:

- AK-HAW: Arbeitskreis HAW-Produkte des BMFT and BMWi
- Labonet: akkreditierter deutscher Vertreter im EU-Netzwerk Labonet

- IAEA: akkreditierter deutscher Vertreter beim IAEA Arbeitskreis zur Characterization of Radioactive Waste
- Entrap-SC: Member of the Steering Committee of the EU-Arbeitskreises ENTRAP (European Network of Testing facilities for the quality checking of Radioactive waste Packages)
- Pol.Reg.EnergyComm: akkreditiertes Mitglied in der Kommission für Energieeffizienz der polnischen Regierung, Berater insbeondere für nukleare Energie
- iPAC-WM: Member of the International Advisory Committee of Waste Management, Phoenix, AZ, USA

Dr. Steinmetz:

- International Program Advisory Committee (IPAC) oft he Annual Arizona Waste Management Conference
- Session Co-Chair and Lead Organisator "Russian Session WM 15"
- Expert called by the German Office of Radiation Protection (BfS) as well as the Highest Authorities and Ministries of the German Federal States.

K. Aymanns:

- stellvertretende Obfrau im DIN Ausschuss radioaktive Abwasserbehandlung

9 Patents

E. Mauerhofer, J. Kettler: Neutron activation analysis using a standardized sample container for determining the neutron flux. Internationale Veröffentlichungsnummer: WO 2012/010162 A1, Internationales Veröffentlichungsdatum 26.01.2012

D. Vulpius, W. von Lensa, R. Nabbi, E. Mauerhofer: Verfahren zur Dekontamination von Radionukliden aus neutronenbestrahlten Kohlenstoff- und/oder Graphitwerkstoffen, Deutsche Patentanmeldung 10 2011 016 272.0 vom 06.04.2011

D. Vulpius, W. von Lensa: Verfahren zur Herstellung von Kohlenstoff- und Graphitwerkstoffen sowie dadurch hergestellte Kohlenstoff- und Graphitwerkstoffe, Deutsche Patentanmeldung 10 2011 016 273.9 vom 06.04.2011

10 Publications

The scientific and technical results of the work carried out at IEK-6 are published in relevant journals and presented to interested specialist audience at national and international conferences on the subject.

Tab. 15: Publications 2011/2012

Year		2011	2012
Publications	Peer-reviewed journals	29	42
	Books and journals	1	0
	Proceedings	15	10
Conferences	Presentations	33	43
	Poster	25	27

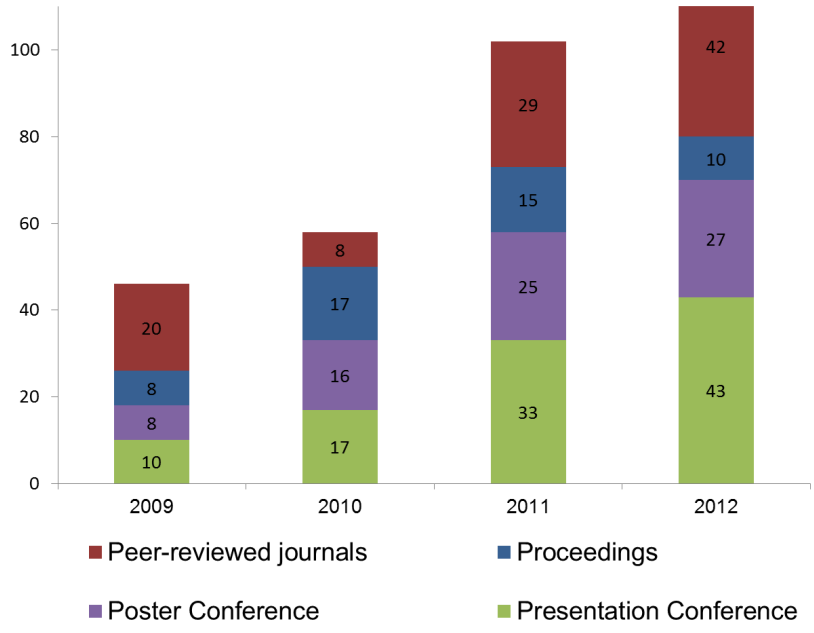

Fig. 69: Publications 2009 – 2012.

10.1. Publications 2011

10.1.1 Journal papers

Peer-reviewed Journals

Alekseev, E.V.; Krivovichev, S.V.; Depmeier, W.: Structural complexity of barium uranyl arsenates: Synthesis, structure, and topology of $Ba_4[(UO_2)_2(As_2O_7)_3]$,$Ba_3[UO_2)_2(AsO_4)_2(As_2O_7)]$, and $Ba_5Ca[(UO_2)_8(AsO_4)_4O_8]$, Crystal Growth and Design, 11 (2011) 7, 3293 – 3300

Alsobrook, A.N.; **Alekseev, E.V.**; Depmeier, W.; Albrecht-Schmitt, T.E.: Incorporation of Mn(II) and Fe(II) into Uranyl Carboxyphosphonates, Crystal Growth and Design, 11 (2011) 6, 2358 - 2367

Alsobrook, A.N.; **Alekseev, E.V.**; Depmeier, W.; Albrecht-Schmitt, T.E.: Uranyl carboxyphosponates that Incorporate Cd(II), Journal of Solid State Chemistry, 184 (2011) 5, 1195 - 1200

Alsobrook, A.N.; Hauser, B.G.; Hupp, J.T.; **Alekseev, E.V.**; Depmeier, W.; Albrecht-Schmitt, T.E.: From Layered Structures to Cubic Frameworks: Expanding the Structural Diversity of Uranyl Carboxyphosphonates via the Incorporation of Cobalt, Crystal Growth and Design, 11 (2011) 4, 1385 – 1393

Bourg, S.; Hill, C.; Caravaca, C.; Rhodes, C.; Ekberg, C.; Taylor, R.; Geist, A.; **Modolo, G.**; Cassayre, L.; Malmbeck, R.; Harrison, M.; de Angelis, G.; Espartero, A.; Bouvet, S.; Ouvrier, N.: ACSEPT - Partitioning technologies and actinide science: Towards pilot facilities in Europe, Nuclear Engineering and Design, 241 (2011) 9, 3427 - 3435

Curtius, H.; Kaiser, G.; Müller, E.; Bosbach, D.: Radionuclide Release from Research Reactor spent fuel, Journal of Nuclear Materials, 416 (2011) 1/2, 211 – 215

Gao, Y.; Marpu, P.M.; **Niemeyer, I.**; Runfola, D.M.; Giner, N.M.; Hamill, T.; Pontius Jr., R.G.: Object-based classification with features extracted by a semi-automatic feature extraction algorithm –SeaTH, Geocarto International, 26 (2011) 3, 211 - 226

Geiger, C.A.; **Alekseev, E.V.**; Lazic, B.; Fisch, M.; Armbruster, T.; Langner, R.; Fechtelkord, M.; Kim, N.; Pettke, T.; Weppner, W.: Crystal Chemistry and Stability of "Li7La3ZrO_{12}" Garnet: A Fast Lithium-Ion Conductor, Inorganic Chemistry, 50 (2011) 3, 1089 - 1097

Hashemi-Nezhad, S. R.; Westmeier, W.; Zamani-Valasiadou, M.; **Thomauske, B.**; Brandt, R.: Optimal ion beam, target type and size for accelerator driven systems: Implications to the associated accelerator power, Annals of Nuclear Energy, 38 (2011) 5, 1144 – 1155

Haussühl, E.; **Vinograd, V.L.**; Krenzel, T.F.; Schreuer, J.; Wilson, D.J.; Ottinger, J.: High temperature elastic properties of Mg-cordierite: experimental studies and atomistic simulations, Zeitschrift für Kristallographie, 226 (2011) 3, 236 - 253

Heberling, F.; Scheinost, A.C.; **Bosbach, D.**: Formation of a ternary neptunyl(V) biscarbonato inner-sphere sorption complex inhibits calcite growth rate, Journal of Contaminant Hydrology, 124 (2011) 1-4, 50 - 56

Heberling, F.; Trainor, T.P.; Lützenkirchen, J.; Eng, P.; Denecke, M.A.; **Bosbach, D.**: Structure and reactivity of the calcite-water interface, Journal of Colloid and Interface Science, 354 (2011) 2, 843 – 857

Hittner, D; Angulo, C.; Basini, V.; Bogusch, E.; Breuil, E.; Buckthorpe, D.; Chauvet, V.; Futterer ,M.A.; van Heek, A.; **von Lensa, W.**; Verrier, D.; Yvon, P.: HTR-TN Achievements and Prospects for Future Developments, Journal of Engineering for Gas Turbines and Power, 133 (2011) 6, 06400

Iqbal, M.; Huskens, J.; **Sypula, M.; Modolo, G.**; Verboom, W.: Synthesis and evaluation of novel water-soluble ligands for the complexation of metals during the partitioning of actinides, New Journal of Chemistry, 35 (2011) 11, 2591 - 2600

Krings, T.; Mauerhofer, E.: Reconstruction of the activity of point sources for the accurate characterization of nuclear waste drums by segmented gamma scanning, Applied Radiation and Isotopes, 69 (2011) 6, 880 - 889

Lewis, F.W.; Harwood, L.M.; Hudson, M.J.; Drew, M.G.B.; Desreux, J.F.; Vidick, G.; Bouslimani, N.; **Modolo, G.; Wilden, A.; Sypula, M.**; Vu, T.-H.; Simonin, J.-P.: Highly Efficient Separation of Actinides from Lanthanides by a Phenantrholine-Derived Bis-Triazine Ligand, Journal of the American Chemical Society, 33 (2011) 33, 13093 - 13102

Listner, C.; Niemeyer, I.: Object-based Change Detection, Photogrammetrie, Fernerkundung, Geoinformation, 4 (2011), 233 – 245

Minet, C., Eineder, M. Rezniczek, A., **I. Niemeyer**: High Resolution Radar Satellite Imagery Analysis for Safeguards Applications. In: ESARDA Bulletin 46 (2011), 57-64

Polinski, M.J.; Wang, S.; **Alekseev, E.V.**; Depmeier, W.; Albrecht-Schmitt, T.E.: Bonding changes in plutonium(III) and americium(III) borates, Angewandte Chemie-International Edition, 50 (2011) 38, 8891 - 8894

Safonov, O.G.; Bindi, L.; **Vinograd, V.L.**: Potassium-bearing clinopyroxene: a review of experimental, crystal chemical and thermodynamic data with petrological applications, Mineralogical Magazine, 75 (2011) 4, 2764 - 2784

von Lensa, W.; Vulpius, D.; Steinmetz, H.-J.; Girke, N.; Bosbach, D.; Thomauske, B.; Banford, A.W.; Bradbury, D.; Grave, M.J.; Jones, A.N.; Grambow, B.; Petit, L.; Pina, G.: Treatment and disposal of irradiated graphite and other carbonaceous waste, ATW - International Journal of Nuclear Power, 56 (2011) , 263 - 269

Villa, E.M.; Wang, S.; **Alekseev, E.V.**; Depmeier, W.; Albrecht-Schmitt, T.E.: Facile routes to Th(IV), U(IV), and Np(IV) phosphites and phosphates, European Journal of Inorganic Chemistry, (2011) 25, 3749 – 3754

Wang, S.; **Alekseev, E.V.**; Depmeier, W.; Albrecht-Schmitt, T.E.: Recent progress in actinide borate chemistry, Chemical Communications, 47 (2011) 39, 10874 - 10885

Wang, S.; **Alekseev, E.V.**; Depmeier, W.; Albrecht-Schmitt, T.E.: $K(NpO_2)_3(H_2O)Cl_4$: A Channel Structure Assembled by Two- and Three-Center Cation-Cation Interactions of Neptunyl Cations, Inorganic Chemistry, 50 (2011) 11, 4692 - 4694

Wang, S.; **Alekseev, E.V.**; Depmeier, W.; Albrecht-Schmitt, T.E.: Surprising Coordination for Plutonium in the First Plutonium(III) Borate, Inorganic Chemistry, 50 (2011) 6, 2079 - 2081

Wang, S.; **Alekseev, E.V.**; Diwu, J.; Miller, H.M.; Oliver, A.G.; Liu, G.; Depmeier, W.; Albrecht-Schmitt, T.E.: Functionalization of Borate Networks by the Incorporation of Fluoride: Syntheses, Crystal Structures,and Nonlinear Optical Properties of Novel Actinide Fluoroborates, Chemistry of Materials, 23 (2011) 11, 2931 - 2939

Wang, S.; Villa, E.M.; Diwu, J.; **Alekseev, E.V.**; Depmeier, W.; Albrecht-Schmitt, T.E.: Role of Anions and Reaction Conditions in the Preparation of Uranium, Neptunium, and Plutonium Borates, Inorganic Chemistry, 50 (2011) 6, 2527 - 2533

Wilden, A.; Schreinemachers, C.; Sypula, M.; Modolo, G.: Direct Selective Extraction of Actinides (III) from PUREX Raffinate using a Mixture of $CyMe_4BTBP$ and TODGA as 1-cycle SANEX Solvent, Solvent Extraction and Ion Exchange, 29 (2011) 2, 190 - 212

Yu, Y.G.; Wentzcovitch, R.M.; **Vinograd, V.L.**; Angel, R.J.: Thermodynamic properties of MgSi(3) majorite and phase transitions near 660 km depth in $MgSiO_3$ and Mg_2SiO_4: A first principles study, Journal of Geophysical Research-Solid Earth, 116 (2011), B02208

10.1.2 Proceedings/Books

Proceedings

Brutscher, J.; Birnbaum, A.; Keubler, J.; Jung, S.; Koestlbauer, M.; **Dürr, M.; Richter, B.**; Schwalbach, P.; v. Zweidorf, A.; Berndt, R.: Design and Performance of the Digital Upgrade of the Mini Multi-Channel Analyser(DMCA), Proceedings of the 33rd ESARDA Annual Meeting, Budapest, Hungary: 16-20 May 2011

Brutscher, J.; Birnbaum, A.; Keubler, J.; Jung, S.; **Richter, B.**; Schwalbach, P.; von Zweidorf, A.; Koestlbauer, M.: Concept and Development Status of the Digital Upgrad of the Mini Multi-channel Analyser (DMCA), JOPAG/03.11-PRG-381

Fricke-Begemann, C.; Noll, R.; Monteith, A.; Maddison, A.; **Dürr, M.**: Feasibility-Study on Laser-Induced Breakdown Spectroscopy for Pre-Screening of Environmental Samples, Proceedings of the 33rd ESARDA Annual Meeting, Budapest, Hungary: 16-20 May 2011

Geist, A.; Müllich, U.; **Modolo, G.; Wilden, A.**: Actinide(III)/lanthanide(III)separation via selective aqueous complexation of actinides(III) in nitric acid, ISEC2011, 19th International Solvent Extraction Conference, Santiago de Chile, Chile: 3-7 October 2011

Geist, A.; Müllich, U.; **Wilden, A.; Gülland, St.; Modolo ,G.**: C5-BPP-a new highly selective extratant for the separation of trivalent actinides from lanthanides, ISEC2011, 19th International Solvent Extraction Conference, Santiago de Chile, Chile: 3-7 October, 2011

Listner, C.; Niemeyer, I.: Object-based change detection using very high-resolution satellite data, Proceedings of the 33rd ESARDA Annual Meeting, Budapest, Hungary: 16-20 May 2011

Listner, C.; Niemeyer, I.: Recent developments in the field of object-based change detection, Publikationen der Deutschen Gesellschaft für Photogrammetrie, Fernerkundung und Geoinformation e.V. Band 20, 2011. - S. 231 - 242

Minet, C.; Eineder, M.; **Niemeyer, I.**: High Resolution Radar Satellite Imagery Analysis for Safeguards Applications, Proceedings of the 33rd ESARDA Annual Meeting, Budapest, Hungary: 16-20 May 2011

Niemeyer, I.; Listner, C.: Object-based Satellite Imagery for Safegjuards Applications, Proceedings of the 52nd INMM Annual Meeting, Palm Desert, USA: 17-21 July 2011

Niemeyer, I.; Listner, C.: Recent Advances Object-based Change Detection, Proceedings of the 2011 IGARSS, Vancouver, Canada: 24-29 July 2011

Niemeyer, I.; Stein, G.; Rezniczek, A.; **Dürr, M.**; Remagen, H.H.: Some Thoughts on State Level Safeguards, Proceedings of the 33rd ESARDA Annual Meeting, Budapest, Hungary: 16-20 May 2011

Stein, G.; Rezniczek, A.; **Niemeyer, I.; Dürr, M.; Richter, B.**: The Role of "Soft" Factors in State Level Safeguards, Proceedings of the 52nd INMM Annual Meeting, Palm Desert, USA, 17-21 July 2011

Sypula, M.; Wilden, A.; Modolo, G.; Geist, A.: Innovative SANEX process for actinide(III)separation from PUREX raffinate using TODGA-based solvents, ISEC2011, 19th International Solvent Extraction Conference, Santiago de Chile, Chile: 3-7 October 2011

Thomauske, B.; Nabbi, R.; Bourauel, P.; Biß, K.; Shetty, N.; Kettler, J.; Backus, S.; Heuters, M.; Hünefeld, M.; Rossbach, M.; Modolo, G.; Mauerhofer, E.; Bongardt, K.; Maier, R.; Esser, F.; Wolters, J.; Hamzic, S.; Kolev, N.; Wank, A.; Koopman, H.; Mertkaya, B.; Ionova, S.; Meister, M.; Cura, H.; Zimmer, A.; Nies, R.; Heidowitzsch, B.; Mishutin, I.; Pshernikov, I.; Greiner, W.: Konzept einer gasgekühlten beschleunigergetriebenen Transmutationsanlage, Synthese Report, Aachen, März 2011, Aachen Nuclear Safety Reports (ANSR) Volume 1, ISBN 978-3-941277-11-3

Wilden, A.; Sypula, M.; Modolo, G.; Geist, A.: Direct actinide(III) separation from PUREX raffinate using a BTBP/TODGA solvent, ISEC2011, 19th International Solvent Extraction Conference, Santiago de Chile, Chile: 3-7 October 2011

Books

Neumeier, S.; Deissmann, G.; **Klinkenberg, M.; Bukaemsky, A.; Modolo, G.; Schlenz, H.; Bosbach, D.**: Radionuklidfixierung in keramischen Materialien, 2011, Technische Keramische Werkstoffe Jochen Kriegsmann (Hrsg.) Bd. 8, Kap. 8.4.1.0

10.1.3 Internal reports

Aksytina, Y.; Weidenfeld, M.; Tietze-Jaensch, H.: Audit und Inspection of Lloyd's Register and Sellafield SLC-WVP at Sellafield by the Produktkontrollstelle PKS from 14.09.10 to 16.09.10 - Results, AZ: PKSINS/AR-ENG/2010, Rev.: 1.2 of 05.01.2011

Aksyutina, Y.; Tietze-Jaensch, H.; Bosbach, D.: Auditierung von LR und Inspektion der Verglasungsanlage WVP Sellafield von Sellafield Ltd. durch die Produktkontrollstelle PKS am 23. und 24.09.2009, Inspektion, PKSINS-ENG II/2009 - Rev.: 1.1 vom 04.08.2011

Aksyutina, Y.; Weidenfeld, M.; Tietze-Jaensch, H.: Audit und Inspection of Lloyd's Register and Sellafield SLC-WVP at Sellafield by the Produktkontrollstelle PKS from 23.03.11 to 24.03.11 - Results, AZ: PKSINS/AR-ENG/2010, Rev.: 1.3 of 04.08.2011

Aksyutina, Y.; Weidenfeld, M.; Tietze-Jaensch, H.: Audit und Inspection of Lloyd's Register and Sellafield SLC-WVP at Sellafield by the Produktkontrollstelle PKS from 27.09.11 to 29.09.11 - Results, AZ: PKSINS/AR-ENG/II 2011, Rev.: 1.3 of 18.11.2011

Assenmacher, J.; Daniels, H.; Gülland, S.; Modolo, G.; Neumeier, S.; Sadowski, F.; Schreinemacher, C.; Sypula, M.; Wilden, A.: EU-Projekt ACSEPT (Contract Number: FP7-CP-2007-211 267), HYBAR No. 7-Half Yearly Beneficiary Activity Report, Reporting Period 01.03.2011 – 31.08.2011

Assenmacher, J.; Daniels, H.; Modolo, G.; Neumeier, S.; Sadowski, F.; Schreinemachers, C.; Sypula, M.; Wilden, A.: EU-Projekt ACSEPT (Contract Number: FP7-CP-2007-211 267) HYBAR n°6-Half Yearly Beneficiary Activity Report, Reporting Period: 01.09.2010-28.02.2011

Banford, A.; Bradbury, D.; Cardinal, G.; Grambow, B.; Jones, A.; Grave, M.; Pina, G.; **Vulpius, D.; v.Lensa, W.**: 3rd Periodic Report European Commission, 7th Framework Programme, Project Carbowaste, Grant Agreement No. FP7-211333, Progress Report P-03.6; 31.05.2011

Bell, K.; Brown, J.; Carrott, M.; Fox, D.; Gregson, C.; Maher, C.; Mason, C.; McLachlan, F.; Müllich, U.; **Assenmacher ,J.; Gülland, S.; Kluxen, P.; Modolo, G.; Sadowski, F.; Schreinemachers, C.; Sypula, M.; Wilden, A.**; Aneheim ,E.; Ekberg, C.; Foreman, M.R.S.; Littley, A.; Löfström-Engdahl, E.; Mabile, N.; Grüner ,B.; Hajkova, Z.; Kvicalova, M.: EU-Projekt ACSEPT (Contract Number: FP7-CP-2007-211 267), Deliverable D1.3.6, "Optimisation of the Formulation of a set of GANEX Extraction Systems: An Group Recovery", 10.10.2011

Button, P.; **Niemeyer, I.**; Okko, O.; Paquette, J.-P.; Parsons, G.; Tadono, T.: Use of SAR Satellite Imagery for Geological Repositories Monitoring, JOPAG/03.11-PRG-385

Deissmann, G.; **Neumeier, S.; Brandt, F.; Modolo, G.; Bosbach, D.**: Elicitation of dissolution rate data for potential waste form types for plutonium, Confidential Report, 2011

Deissmann, G.; **Neumeier, S.; Modolo, G.; Bosbach, D.**: Review of the durability of potential plutonium waste forms under conditions relevant to geological disposal, Bibliography NDA, TN 17644, 2011

Geist, A.; Baron, P.; Casnati, A.; Giola, M.; Hérès, X.; Macerata, E.; Mariani, M.; Miguirditchian, M.; **Modolo, G.**; Mossini, E.; Müllich, U.; Ongari, N.; Panak, P.J.; Rostaing, C.; Ruff, C.; Scaravaggi, S.; **Sypula, M.; Wilden, A.**: EU-Projekt ACSEPT (Contract Number: FP7-CP-2007-211 267), Deliverable D1.3.4, "Optimisation of the Formulation of a set of innovative SANEX System: An(III) Selective Stripping", 29.11.2011

Harren, E.; Kreutz, F.; Tietze-Jaensch, H.: Bericht über Audit und Inspektion der VEK bei der WAK Entsorgungs-GmbH, Karlsruhe, durch die Produktkontrollstelle des Bundesamtes für Strahlenschutz vom 22.-23.06.2010, PKSINS/BER/WAK 2010/06, Rev. 20110125, Berichtszeitraum 12.04. - 21.06.2010

Harren, E.; Kreutz, F.; Tietze-Jaensch, H.: Bericht über die Prüfung der Daten und Unterlagen zu den WAK-VEK HAW-Glaskokillen der Beladung für den Transport CG-057, PKS-WAA-CG-057/2009 - Rev. 20110202, 2011

Harren, E.; Kreutz, F.; Tietze-Jaensch, H.: Bericht über die Prüfung der Daten und Unterlagen zu den WAK-VEK-HAW-Glaskokillen der Beladung für den Transport CG-059, PKS-WAA-CG-059/2010-Rev. 20100908, Prüfberichte Beladung WAK/VEK

Kreutz, F.; Tietze-Jaensch, H.; Bosbach, D.: Bericht über die Prüfung der Daten und Unterlagen zu den COGEMA HAW/-Glaskokillen der Beladung für den Transport VG106, PKS-WAA-VG 106/2011, Version: 1.0 vom 04.02.2011

Kreutz, F.; Tietze-Jaensch, H.; Bosbach, D.: Bericht über die Prüfung der Daten und Unterlagen zu den COGEMA HAW/-Glaskokillen der Beladung für den Transport VG107, PKS-WAA-VG 107/2011, Version: 1.0 vom 21.03.2011

Kreutz, F.; Tietze-Jaensch, H.; Bosbach, D.: Bericht über die Prüfung der Daten und Unterlagen zu den COGEMA HAW/-Glaskokillen der Beladung für den Transport VG108, PKS-WAA-VG 108/2011, Version: 1.0 vom 29.06.2011

Modolo, G.: EU-Project ACSEPT (Contract-Number: FP7-CP-2007-211 267), WPASR No.6, Work-Package Activity Summary Report, WP1.4 - Conversion, Reporting Period: 31/08/2010-01/03/2011

Modolo, G.: EU-Projekt ACSEPT (Contract No.: FP7-CP-2007-211 267), WPASR No.7, Work-Package Activity Summary Report, WP1.4 - Conversion, Reporting Period: 01/03/2011 - 31/08/2011

Moeslinger, M.; Liguori, C.; Neumann, G.; Lange, S.; Stein, M.; Pepper, S.; **Richter, B.**; Schoop, K.: The IAEA's Next Generation Surveillance System, JOPAG/03.11-PRG-387

Produzhina, T.; **Baginski, K.; Vulpius, D.; v. Lensa, W.**: Preliminary report on ^{14}C reduction in graphite and spent fuel matrix, (Bench scale) European Commission, 7th Framework Programme, Project Carbowaste, Grant Agreement No. FP7-211333, Technical Report T-4.4.1; 22.06.2011

Steinhardt, T.; Tietze-Jaensch, H.; Bosbach, D.: Bericht über die Auditierung von Bureau Veritas und Inspektion der Verglasungsanlage AREVA NC La Hague durch die Produktkontrollstelle PKS am 09.05. bis 11.05.2006, PKSINS-FRA I/2006 - Rev.: 1.3 vom 22.02.2011

Vulpius, D.; v. Lensa, W.; Jones, A.; Guy, C.; Comte, J.; Dodaro, A.; Duskesas, G.; Iordache, M.: First radionuclide inventory data on untreated graphite European Commission, 7th Framework Programme, Project Carbowaste, Grant Agreement No. FP7-211333, Deliverable D-3.3.1; 22.06.2011

Weidenfeld, M.; Aksyutina, Y.; Tietze-Jaensch, H.: Audit and Inspection of Bureau Veritas and AREVA NC/La Hague by the Produktkontrollstelle PKS from 10.05. to 13.05.2011, Results - Reference: PKSINS/AR-FRA II/2011, Rev.: 1.1 of 26.07.2011

Weidenfeld, M.; Aksyutina, Y.; Tietze-Jaensch, H.: Audit and Inspection of Bureau Veritas and AREVA NC/La Hague by the Produktkontrollstelle PKS from 23.11. to 25.11.2010, Results - Reference: PKSINS/AR-FRA II/2010, Rev.: 1.2 of 10.03.2011

Wilden, A.; Modolo, G.: BMBF-Projekt "Verbundprojekt: Grundlegende Untersuchungen zur Entwicklung und Optimierung von Prozessen zur Abtrennung langlebiger Radionuklide (Partitioning) - Stabilitätsuntersuchungen und Entwicklung von kontinuierlichen Prozessen“, (Förderkennzeichen: 02NUK012E), 3. Halbjahresbericht, 28.01.2011, Berichtszeitraum: 01.07.2010-31.12.2010

Wilden, A.; Modolo, G.: BMBF-Projekt "Verbundprojekt: Grundlegende Untersuchungen zur Entwicklung und Optimierung von Prozessen zur Abtrennung langlebiger Radionuklide (Partitioning) - Stabilitätsuntersuchungen und Entwicklung von kontinuierlichen Prozessen", 2011, (Förderkennzeichen: 02NUK012E), 4. Halbjahresbericht, 28.07.2011, Berichtszeitraum: 01.01.2011-31.07.2011

10.1.4 Poster

Assenmacher, J.; Schreinemachers, C.; Wilden, A.; Modolo, G.; Bosbach, D.: Der Lösungsmitteleinfluss bei der selektiven Actiniden(III)/Lanthaniden(III) Trennung mittels aromatischer Dithiphosphinsäuren, GDCh-Wissenschaftsforum Chemie 2011, Bremen, Germany: 04-07 July 2011

Babelot, C.; Bukaemskiy, A.; Neumeier, S.; Modolo, G.; Bosbach, D.; Holliday, K.; Stumpf, T.: Conditioning of Minor actinides in La-Monazite-type Ceramics, 494. WE-Heraeus-Seminar, Bad Honnef, Germany: 05-08 December 2011

Bukaemskiy, A.; Fachinger, J.; **Bosbach, D.**: Physical properties and leaching behaviour of spent fuel BISO coated particles, E-MRS Meeting 2011, Nice, France: 09-13 may 2011

Finkeldei, S.; Neumeier, S.; Bukaemskiy, A.; Schlenz, H.; Modolo, G.; Bosbach, D.: Darstellung und Charakterisierung ZrO_2 basierter Keramiken für die nukleare Entsorgung, GDCh-Tagung 2011, Bremen: 04.07.2011 - 07.07.2011

Finkeldei, S.; Neumeier, S.; Bukaemskiy, A.; Schlenz, H.; Modolo, G.; Bosbach, D.; Holliday, K.; Stumpf, T.: Synthesis and characterization of ZrO_2 based ceramics for nuclear waste management, 494. WE-Heraeus-Seminar, Bad Honnef: 05.12.2011 - 08.12.2011

Havenith, A.; Kettler, J.; Mauerhofer, E.: Prompt and Delayed Gamma Neutron Activation Analysis forthe Assay of Toxic Elements in Radioactive Waste Packages, NUTECH 2011, Krakow, Poland: 11-14 September 2011

Heuser, J.; Schlenz, H.; Bosbach, D.: Characterization of monazite-type ceramics used for nuclear waste, International School of Crystallography: The Power of Powder diffraction, Erice, Italy: 02-12 June 2011

Heuser, J.; Schlenz, H.; Bosbach, D.: Characterization of synthetic $Sm_{1-x}Ce_xPO_4$ Ceramics used for Nuclear Waste Management, IUCR 2011, Madrid, Spain: 22-30 August 2011

Heuser, J.; Schlenz, H.; Bosbach, D.: Characterization of synthetic $Sm_{1-x}Ce_xPO_4$ Ceramics used for Nuclear Waste Management, Joint Meeting of German Crystallographic Society, German Mineralogical Society and Austrian Mineralogical Society, Salzburg, Austria: 20-24 September 2011

Heuser, J.; Schlenz, H.; Modolo, G.; Bosbach, D.: Characterization of synthetic Orthophosphate Ceramics used for Nuclear Waste Management, 494. WE-Heraeus-Seminar, Bad Honnef, Germany: 05-08 December 2011

Kettler, J.; Biß, K.; Bongardt, K.; Bourauel, P.; Esser, P.; Greiner, W.; Hamzic, S.; Maier, R.; Mishustin, I.; **Modolo, G.; Nabbi, R.**; Pshenichnov, I.; **Rossbach, M.; Shetty, N.**; **Thomauske, B.; Wolters, J.**: Advanced Gas-cooled Accelerator-driven Transmutation Experiment AGATE, 494. WE-Heraeus-Seminar, Bad Honnef, Germany: 05-08 December 2011

Krings, T.; Mauerhofer, E.: Accurate and reliable reconstruction of isotope specific activity contents of standardized nuclear waste drums by segmented gamma scanning, NUTECH 2011, Krakow, Poland: 11-14 September 2011

Labs, S.; Curtius, H.; Bosbach, D.: Synthesis of lentil shaped $ThSiO_4$ nanoparticles by a hydrothermal route, Goldschmidt Conference, Prague, Czech Republic: 15-19 August 2011

Listner, C.; Niemeyer, I.: Object-based change detection using very high-resolution satellite data, 33rd ESARADA Annual Meeting, Budapest, Hungary: 16-20 May 2011

Magnusson, D.; Geist, A.; **Wilden, A.; Modolo, G.**; Malmbeck, R.: Computer Code Development for Flow-Sheet Design and Modeling with Verification Towards a Novel Partitioning Process, GLOBAL 2011, Nagoya, Japan

Neumann, A.; Klinkenberg, M.; Curtius, H.; Bosbach, D.: XRD analysis of the corrosion products of research reactor fuel elements, Joint Meeting der DGK, DMG and ÖMG 2011, Salzburg, Austria: 20-24 September 2011

Neumann, A.; Klinkenberg, M.; Curtius, H.; Bosbach, D.: XRD analysis of the corrosion products of research reactor fuel elements, XXII IUCR Congress and General Assembly Madrid, 2011 - International Union of Crystallography, Madrid, Spain: 22-30 August 2011

Rozov, K.; Curtius, H.; Bosbach, D.: Synthesis, Characterization and Stability of Mg-Fe-(II)-Al-Cl containing Layered Double Hydroxides (LHDs), 31st International Confernce on the Chemistry and Migration Behaviour of Actinides and Fission Products in the Geosphere MIGRATION'11, Beijing, China: 18-23 September 2011

Schlenz, H.; Heuser, H.; Schmitz, S.; Babelot, C.: Raman spectra of Synthetic Orthophospates used for Nuclear Waste Management, IUCR 2011, Madrid, Spain: 22-30 August 2011

Schlenz, H.; Heuser, J.; Schmitz, S.; Babelot, C.: Raman spectra of Synthetic Orthophosphates used for Nuclear Waste Management, Joint Meeting of German Crystallographic Society, German Mineralogical Society and Austrian Mineralogical Society, Salzburg, Austria: 20-24 September 2011

Schmitz, S.; Schlenz, H.; Bosbach, D.: Structural research on phosphate and phosphosilicate ceramics, which are used for nuclear waste management, International School of Crystallography: The Power of Powder diffraction, Erice, Italy: 02-12 June 2011

Schmitz, S.; Schlenz, H.; Bosbach, D.: Structure analysis of monazite-type ceramics used for nuclear waste management, IUCR 2011, Madrid, Spain: 22-30 August 2011

Schmitz, S.; Schlenz, H.; Bosbach, D.: Structure analysis of monazite-type ceramics used for nuclear waste management, Joint Meeting of German Crystallographic Society, German Mineralogical Society and Austrian Mineralogical Society, Salzburg, Austria: 20-24 September 2011

Schmitz, S.; Schlenz, H.; Modolo, G.; Bosbach, D.: Structure analysis of monazite-type ceramics used for nuclear waste management, 494. WE-Heraeus-Seminar, Bad Honnef, Germany: 05-08 December 2011

Sypula, M.; Wilden, A.; Modolo, G.; Geist, A.: Innovative SANEX process for actinide(III) separation from PUREX raffinate using TODGA-based solvents, 19th International Solvent Extraction Conference, Santiago de Chile, Chile: 17-21 October 2011

10.1.5 Presentations

Conferences:

Alekseev, E.V.; Villa, E.M.; Depmeier, W.; Albrecht-Schmitt, T.E.: Multi-valence states and multi-coordinates in complex actinide borates, Joint Meeting of German Crystallographic Society, German Mineralogic Society and Austrian Mineralogical Society, Salzburg, Austria: 20-24 September 2011

Alekseev, E.V.; Wang, S.; Albrecht-Schmitt, T.E.; Depmeier, W.: From thorium to curium - a structural diversity of actinide borates, Joint Meeting of German Crystallographic Society, German Mineralogic Society and Austrian Mineralogical Society, Salzburg, Austria: 20-24 September 2011

Alekseev, E.V.; Wang, S.; Depmeier, W.; Albrecht-Schmitt, T.E.: Complex topologies as a result of simple relationships between 2D and 3D actinide borates, IUCR 2011, Madrid, Spain: 22-30 August 2011

Alekseev, E.V.; Wang, S.; Depmeier, W.; Albrecht-Schmitt, T.E.: Some aspects of the solid state chemistry of actinide borates, GDCh 2011, Bremen, Germany: 05-08 September 2011

Babelot, C.; Neumeier, S.; Bukaemskiy, A.; Modolo, G.; Schlenz, H.; Bosbach, D.: Conditioning of Minor Actinides in La-Monazite-type Ceramics, E-MRS Spring Meeting 2011, Nice, France: 09-13 May 2011

Daniels, H.; Neumeier, S.; Bukaemskiy, A.; Leturcq, G.; Grandjean, S.; **Modolo, G.; Bosbach, D.**: Fabrication of Uranium-Neodymium Microspheres through Internal-Gelation, E-MRS Spring Meeting 2011, Nice, France: 09-13 May 2011

Fricke-Begemann, C.; Noll, R.; Montheith, A.; Maddison, A.; **Dürr, M.**: Feasibility-Study on Laser-Induced Breakdown Spectroscopy for Pre-Screening of Environmental Samples, 33rd ESARDA Annual Meeting, Budapest, Hungary: 16-20 May 2011

Geist, A.; Müllich, U.; **Modolo, G.; Wilden, A.**: Actinide(III)/Lanthanide(III)Separation via Selective Aqueous Complexation of Actinides(III) in Nitric Acid, 19th International Solvent Extraction Conference, Santiago de Chile, Chile: 17-21 October 2011

Geist, A.; Müllich, U.; **Wilden, A.; Gülland, S.; Modolo, G.**: C5-BPP-a new highly selective extractant for the separation of trivalent actinides from lanthanides, 19th International Solvent Extraction Conference, Santiago de Chile, Chile: 17-21 October 2011

Genreith, C.; Rossbach, M.; Mauerhofer, E. Támas Belgya: Prompt Gamma Characterization of Actinides (237NP), NUTECH 2011, Krakow, Poland: 11-14 September 2011

Girke, N.: Prüftool zur Bewertung der Endlagerfähigkeit von Abfallchargen mit großen Fasskontingenten, KONTEC 2011, Dresden, Germany: 06-08 April 2011

Goryaeva, A.M.; **Vinograd, V.L.**; Winkler, B.; Eremin, N.N.; Urusov, V.S.: An ab initio study of ZrO_2-HfO_2 solid solution with cotunnite structure, IUCR 2001, Madrid, Spain: 22-30 August 2011

Klinkenberg, M.; Curtius, H.; Neumann, A.; Bosbach, D.: Corrosion of Research Reactor Fuel Elements in Mont Terri Clay Pore Water, European Clay Conference – EUROCLAY, Antalya, Turkey: 26 June – 01 July 2011

Krumbach, H.: Anforderungen an die Endlagerdokumentation für schwach- und mittelradioktive Abfälle, KONTEC 2011, Dresden, Germany: 06-08 April 2011

Listner, C.; Niemeyer, I.: Methoden der Fernerkundung zur Unterstützung der Kernmaterialüberwachung, Energie und Rohstoffe 2011, Freiberg, Germany: 07-10 September 2011

Listner, C.; Niemeyer, I.: Recent developments in the field of object-based change detection, Jahrestagung der Deutschen Gesellschaft für Photogrammetrie, Fernerkundung und Geoinformation e.V., Mainz, Germany: 13-15 April 2011

Niemeyer, I.: Satellitenbildauswertung zur Stärkung von Rüstungskontroll- und Abrüstungsvereinbarungen, 5. Symposium "Nukleare und radiologische Bedrohungen", Euskirchen, Germany: 20-22 September 2011

Niemeyer, I.; Listner, C.: Object-based Satellite Imagery for Safeguards Applications, 52nd INMM Annual Meeting, Palm Desert, USA: 17-21 July 2011

Niemeyer, I.; Stein, G.; Rezniczek, A.; **Dürr, M.**; Remagen, H.H.: Some Thoughts on State Level Safeguards, 33rd ESARDA Annual Meeting, Budapest, Hungary: 16-20 May 2011

Rossbach, M.; Mauerhofer, E.; Revay, Z.; Belgya, T.: Prompt Gamma Investigation of Selected Actinides, MTAA 13, College Station, TX, USA: 14-18 March 2011

Schneider, St.: Numerical Evaluation of Super-Compacted Radioactive Waste, High Level Radioactive Waste Management Conference 2011, Albuquerque, USA: 13 April 2011

Stein, G.; Rezniczek, A.; **Niemeyer, I.; Dürr, M.; Richter, B.**: The Role of "Soft" Factors in State Level Safeguards, 52nd INMM Annual Meeting, Palm Desert, USA: 17-21 July 2011

Steinmetz, H.-J.: Carbon-14 and Tritium Content in Contaminated Reactor Graphite after Long-Term-Storage, WM2011 Waste Management Symposia, Phoenix AZ, USA: 27 March – 03 April 2011

Vinograd, V.; Winkler, B.; **Bosbach, D.**: Thermodynamics of mixing in barite-celestite solid solution from quantum-mechanical calculations, Joint Meeting of German Crystallographic Society, German Mineralogic Society and Austrian Mineralogical Society, Salzburg, Austria: 20-24 September 2011

von Lensa, W.; Vulpius, D.; Bradbury, D.; Pina, G.; Grave, M.J.; Banford, A.W.; Grambow, B.: Objectives & progress of the CARBOWASTE project - Treatment and disposal of irradiated graphite and other carbonaceous waste, EPRI 10th International Decommissioning and Radioactive Waste Management Workshop, Lund, Sweden: 19-22 September 2011

Vulpius, D.: Carbowaste Work Package 4 - Treatment & purification of irradiated graphite - Observations and interpretations, EPRI 10th International Decommissioning and Radioactive Waste Management Workshop, Lund, Sweden: 19-22 September 2011

Wilden, A.; Modolo, G.; Bosbach, D.: Abtrennung von Minoren Actiniden aus hochradioaktiven Spaltproduktlösungen, GDCh-Wissenschaftsforum Chemie 2011, Bremen, Germany: 04-07 September 2011

Wilden, A.; Sypula, M.; Modolo, G.: Direct actinide(III) separation from purex raffinate using a BTBP/TODGA solvent, 19th International Solvent Extraction Conference, Santiago de Chile, Chile: 17-21 October 2011

Invited Talks

Niemeyer, I.: Object-based image analysis in remote sensing applications, 3rd Indo-German Frontiers of Engineering Symposium (INDOGFOE), Khandala, India: 16-19 June 2011

Niemeyer, I.: Satellite imagery in safeguards: Progress and prospects, 7th ESARDA/INMM Workshop "Future Directions for Nuclear Safeguards and Verification", Aix-en-Provence, France: 17-20 October 2011

Niemeyer, I.; Dürr, M.; Richter, B.: Nuclear Safeguards R&D Structure in Germany: Coordinating the German Support Programme to the IAEA, Frühjahrstagung der Deutschen Physikalischen Gesellschaft, Dresden, Germany: 13-18 March 2011

Niemeyer, I.; Listner, C.: Recent Advances in Object-based Change Detection, 2011 IGARSS, Vancouver, Canada: 24-29 July 2011

Modolo, G.: Abtrennung von Minoren Actiniden aus Prozesslösungen der Wiederaufarbeitung, Stand der Forschung und Jülicher Beitrag, Kerntechnisches Kolloquium, LRST, RWTH Aachen, Aachen, Germany: 25 October 2011

Modolo, G.: Hydrochemistry for innovative fuels, 494. WE-Heraeus-Seminar, Bad Honnef, Germany: 05-08 December 2011

Neumann, A.: XRD-Charakterisierung der unter Endlagerbedingungen gebildeten Korrosionsprodukte von Forschungsreaktor-Brennelementen, Bruker-AXS XRD-Anwendertreffen, Karlsruhe, Germany: 03-05 May 2011

von Lensa, W.; Vulpius, D.; Bradbury, D.; Pina, G.; Grave, M.J.; Banford, A.W.; Grambow, B.: Treatment and disposal of irradiated graphite and other carbonaceous waste, 4th International Conference on Carbons for Energy Storage/Conversion and Environment Protection, Vichy, France: 25-29 September 2011

Additional/Internal Talks

Aksyutina, Y.: Studies of light nuclei beyond the drip line at the ALADIN-LAND setup, NUSTAR Annual Meeting 2011 at GSI, Darmstadt, Germany: 02-04 March 2011

Brandt, F.; Klinkenberg, M.; Rozov, K.; Bosbach, D.: Recrystallization of Barite in the presence of Radium, 1st Annual Workshop of the SKIN-Project, Barcelona, Spain: 17-18 November 2011

Curtius, H.: Verhalten langlebiger Spalt- und Aktivierungsprodukte im Nahfeld eines Endlagers und Möglichkeiten ihrer Rückhaltung (VESPA), Verbundprojekt VESPA, Jülich, Germany: 20 July 2011

Daniels, H.; Schreinemachers, C.; Leturcq, G.; Grandjean, S.; **Neumeier, S.; Modolo, .**: Progress within WP4 of Domain 1, ACSEPT 3rd Annual Meeting, Manchester, UK: 04–06 April 2011

Deissmann, G.; **Neumeier, S.; Modolo, G.; Bosbach, D.**: Durability of potential plutonium wasteforms under repository conditions, Geological Disposal of Radioactive Waste Conference, Loughborough, UK: 18 October 2011

Dürr, M.: Nuclear Safeguards R&D Structure in Germany: Coordinating the German Support Programme to the IAEA, Meeting of the ESARDA Working Group on Containment and Surveillance, Budapest, Hungary: 15 May 2011

Dürr, M.: Status und Perspektiven messtechnischer Methoden in der Kernmaterialüberwachung, Institutsseminar Nukleare Entsorgung des IEK-6 Forschungszentrum Jülich GmbH, Jülich, Germany: 22 June 2011

Finkeldei, S.: Darstellung und Charakterisierung ZrO_2 and ThO_2 basierter Keramiken für die nukleare Entsorgung, Mitarbeiterseminar Institut für Anorganische Chemie, RWTH Aachen University, Aachen, Germany: 08 September 2011

Listner, C.: Acquisition Path Analysis - An overview of existing methodologies and tools, IAEA-Workshop on Acquisition Path Analysis, Vienna, Austria: 13-17 June 2011

Niemeyer, I.: Safeguards in Germany: Update 2010/11, Safeguards in Germany: Update 2010/11, Palm Desert, USA: 17 June 2011

Schlenz, H.: The Institute for Energy and Climate Research IEK-6 of the Research Center Juelich, HITEC Graduate School, Research Center Jülich, Jülich, Germany: 14 October 2011

Schlenz, H.; Bosbach, D.: Fe solid solutions, NEA meeting of the TDB IV review team on iron (Part 2), OECD, Paris, France: 15 July 2011

Vulpius, D.: The Carbowaste Project: Work Package 3 - Progress Report, EU Project Carbowaste, 3rd Work Package 3 & 4 Meeting, Jülich: 03-04 February 2011

Vulpius, D.: Work Package 4 - Treatment & purification of irradiated graphite - Status report, EU Project Carbowaste, 4th Steering Committee Meeting, Rome, Italy: 13-14 April 2011

Vulpius, D.: Work Package 4 - Treatment & purification of irradiated graphite - Status report, EU Project Carbowaste, 1st Advisory Council Meeting, Paris, France: 09 June 2011

Wilden, A.: FZJ progress report for the 3rd semester 01.07.2010 - 31.12.2010, BMBF Verbundprojekt, 3. Halbjährliches Treffen, Jülich, Germany: 17-18 February 2011

Wilden, A.: FZJ progress report for the 4th semester 01.01.2011-31.07.2011, BMBF Verbundprojekt, Halbjährliches Teffen, Universität Heidelberg und Karlsruher Institut für Technologie, Karlsruhe, Germany: 26 July 2011

Wilden, A.; Sypula, M.; Schreinemachers, C.; Assenmacher, J.; Modolo, G.: Progress report within Domain 1 WP 2 + 3, ACSEPT, Third Annual Meeting, Manchester, UK: 04-07 April 2011

10.2. Publications 2012

10.2.1 Journal papers

Peer-reviewed Journals

Bell, K.; Geist, A.; McLachlan, F.; **Modolo**, **G.;** Taylor, R.; **Wilden, A.:** Nitric Acid Extraction into TODGA, Procedia Chemistry, 2012, *7*, 152-159

Bell, K.; Carpentier, C.; Carrott, M.; Geist, A.; Gregson, C.; Hérès, X.; Magnusson, D.; Malmbeck, R.; McLachlan, F.; **Modolo**, **G.;** Müllich, U.; **Sypula**, **M.;** Taylor, R.; **Wilden, A.**: Progress Towards the Development of a New GANEX Process, Procedia Chemistry, 2012, *7*, 392-397

Brandt, F.; Schäfer, T.; Claret, F.; **Bosbach, D.**: Heterogeneous formation of ferric oxide nanoparticles on chlorite surfaces studied by x-ray absorption spectromicroscopy (STXM), Chemical Geology 2012, *329*, 42–52

Bourg, S., Hill, C., Harrison, M., de Angelis, G., Espartero, A., Bouvet, S., Ouvrier, N., Caravaca, C., Rhodes, C., Ekberg, C., Taylor, R., Geist, A., **Modolo, G.,** Cassayre, L., Malmbeck, R., ACSEPT - Partitioning technologies and actinide science: Towards pilot facilities in Europe. Nuclear engineering and design, 2012, *241*, 3427 - 3435

Brown, J., McLachlan, F.; Sarsfield, M.J.; Taylor, R.J.; **Modolo**, **G.; Wilden, A.**: Plutonium loading of prospective grouped actinide extraction (GANEX) solvent systems based on diglycolamide extractants, Solvent Extraction and Ion Exchange, 2012, *30(2)*, 127-141

Bukaemskiy, A.; Fachinger, J.; **Bosbach, D.**: Physical properties and leaching behaviour of spent fuel BISO coated particles, Progress in Nuclear Energy, 2012, 57, 161-164

Daniels, H.; Neumeier, S.; Bukaemskiy, A.A.; Modolo, G.; Bosbach, D.: Fabrication of oxidic uranium-neodymium microspheres by internal gelation, Progr. Nucl. Energ., 2012, 57, 106-110

Deissmann, G.; Neumeier, S.; Modolo, G.; Bosbach, D.: Durability of potential plutonium wasteforms under repository conditions, Mineralogical Magazine 2012, *76(8)*, 2911-2918

Finck, N.; Dardenne, K.; **Bosbach**, **D.;** Geckeis, H.: Selenide Retention by Mackinawite, 10.1021/es301878y, Environmental Science & Technology. 2012, *46*, 10004−10011

Geist, A.; Müllich, U.; Magnusson, D.; Kaden, P.; **Modolo**, **G.; Wilden**, **A.**; Zevaco, T.: Actinide(III)/lanthanide(III) separation via selective aqueous complexation of actinides(III) using hydrophilic 2,6-bis(1,2,4-triazin-3-yl)-pyridine or 6,6'-bis(1,2,4-triazin-3-yl)-2,2'-bipyridine in nitric acid, Solvent Extraction and Ion Exchange, 2012, *30(5)*, 433-444

Genreith, C.; Rossbach, M.; Mauerhofer, **E.;** Belgya, T.; Caspary, G.: First results of the prompt gamma characterization of ^{237}Np. NUKLEONIKA 2012, *57(4),* 443-446

Holliday, K.S.; **Babelot**, **C.;** Walther, C.; **Neumeier, S.; Bosbach**, **D.;** Stumpf, Th.: Site-selective time resolved laser fluorescence spectroscopy of Eu and Cm doped $LaPO_4$, Radiochimica Acta, 2012, *100(3)*, 189-195

Holliday, K.; **Finkeldei, S.; Neumeier**, **S.;** Walther, C.; **Bosbach**, **D.;** Stumpf, T.: TRLFS of Eu^{3+} and Cm^{3+} doped $La_2Zr_2O_7$: A comparison of defect fluorite to pyrochlore structures, Journal of Nuclear Materials, 2012, *433(1-3)*, 479–485

Iqbal, M.; Struijk, R.G.; Huskens, J.; **Sypula, M.; Wilden, A.; Modolo G.**; Verboom, W.: Synthesis and Evaluation of Ligands with Mixed Amide and Phosphonate, Phosphinoxide, and Phosphonothioate Sites for An(III)/Ln(III) Extraction, New Journal of Chemistry, 2012, *36(10)*, 2048–2059

Krings, T.; Mauerhofer, E.: Reconstruction of the isotope activity content of heterogeneous nuclear waste drums, Applied Radiation and Isotopes 2012, *70*, 1100–1103.

Kowalski, P.M.; Wunder, B.; Jahn, S.: Ab initio prediction of equilibrium boron isotope fractionation between minerals and aqueous fluids at high P and T, Geochimica et Cosmochimica Acta, 2013, *101*, 285-301

Lewis, F.W., Harwood, L.M.; Hudson, M.J.; Drew**,** M.G.B.; **Wilden, A., Sypula, M.; Modolo**, **G.;** Vu, T.-H.; Simonin, J.-P.; Vidick, G.; Bouslimani, N.; Desreux, J.F.: From BTBPs to BTPhens: The Effect of Ligand Pre-Organization on the Extraction Properties of Quadridentate Bis-Triazine Ligands, Procedia Chemistry, 2012, *7*, 231-238

Lewis, F.W.; Harwood, L.M.; Hudson, M.J.; Drew, M.G.B.; **Sypula, M.; Modolo**, **G.;** Videva, V.; Hubscher-Bruderc, V.; Arnaud-Neuc, F.: Complexation of some lanthanides(III), actinides and transition metal ions with a 6-(1,2,4-triazin-3-yl)-2,2':6',2''-terpyridine ligand: implications for actinide(III)/lanthanide(III) partitioning, Dalton Transactions, 2012, *41(30)*, 9209-9219

Ma, J.-L.; Carasco, C.; Perot, B.; **Mauerhofer, E.; Kettler, J.; Havenith, A.**: Prompt gamma neutron activation analysis of toxic elements in radioactive waste packages, Applied Radiation and Isotopes, 2012, *70*, 1261–1263

Magnusson, D.; Geist, A.; Malmbeck, R.; **Modolo, G.; Wilden, A.**: Flow-Sheet Design for an Innovative SANEX Process Using TODGA and SO_3-Ph-BTP, Procedia Chemistry, 2012, *7,* 245-250

Modolo, G.; Wilden, **A.;** Geist, A.; Magnusson, D.; Malmbeck, R.: A review on the demonstration of innovative solvent extraction processes for the recovery of trivalent minor actinides from PUREX raffinate, Radiochim. Acta, 2012, *100*, 715-725

Nelson, A.-G.; **Alekseev, E.V**.; Ewing, R.; Albrecht-Schmitt, T.E.: Barium Uranyl Diphosphonates, J. Solid State Chem. 2012, *192*, 153-160

Niemeyer, I.; Listner, C.; Nussbaum, S.: Object-based Image Analysis Using Very High-resolution Satellite Data, Journal of Nuclear Materials Management (JNMM), 2012, *40(4), Special Issue: Science for Verification,* 100-109

Nikishkin, N.I.; Huskens, J.; **Assenmacher, J.; Wilden, A.; Modolo**, **G.;** Verboom, W.: Palladium–Catalyzed Cross-Coupling of Various Phosphorous Pronucleophiles with Chloropyrazines - Synthesis of Novel An(III)-selective Extractants, Org. Biomol. Chem. 2012, *10(28)*, 5443-5451

Polinski M. J.; Grant, D.J.; Wang, S.; **Alekseev, E.V.**; Cross, J.N.; Villa, E.M.; Depmeier W.; Gagliardi, L.; Albrecht-Schmitt, T.E: Differentiating Between Trivalent Lanthanides and Actinides, JACS, 2012,*134*, 10682-10692

Polinski, M.J.; Wang, S.; **Alekseev, E.V.;** Depmeier, W.; Liu, G.; Haire, R.G.; Albrecht-Schmitt, T.E.: Curium(III) Borate Shows Coordination Environments of Both Plutonium(III) and Americium(III) Borates. Angew. Chem. Int. Ed., 2012, *51*, 1869-1872

Polinski, M.J.; Wang, S.; **Alekseev**, **E.V.;** Cross, J.N.; Depmeier, W.; Albrecht-Schmitt, T.E.: Effect of pH and Reaction Time on the Structures of Early Lanthanide(III) Borate Perchlorates. Inorg. Chem., 2012, *51*, 11541 – 11548

Polinski, M.J.; Wang, S.; Cross, J.N.; **Alekseev**, **E.V.;** Depmeier, W.; Albrecht-Schmitt, T.E.: Effects of Large Halides on the Structures of Lanthanide(III) and Plutonium(III) Borates. Inorg. Chem., 2012, *51*, 7859-7866

Qian, N.; **Krings, T.; Mauerhofer**, **E.;** Wang, D.; Bai, Y.: Analytical calculation of the collimated detector response for the characterization of nuclear waste drums by segmented gamma scanning, J. Radioanal. Nucl. Chem., 2012, *292*, 1325 – 1328

Reilly, S.D.; Gaunt, A.J.; Scott, B.L.; **Modolo, G.;** Iqbal, M.; Verboom, W.; Sarsfield, M.J.: Plutonium(VI) complexation by diglycolamide ligands – coordination chemistry insight into TODGA-based actinide separations, Chem. Commun., 2012, *48*, 9732-9734

Seliverstov, A.N.; Suleimanov, E.V.; Chuprunov, E.V.; Somov, N.V.; Zhuchkova, E.M.; Lelet, M.I.; Rozov, K.B.; Depmeier, W.; Krivovichev, S.V.; **Alekseev E.V.:** Polytypism and oxo-tungstate polyhedra polymerization in novel complex uranyl tungstates. Dalton trans. (Cambridge, England), 2012, *41*, 8512-8514

Suleimanov, E.V.; Somov, N.V.; Chuprunov, E.V.; Mayatskikh, E.F.; Depmeier, W.; **Alekseev, E.V.**: A Detailed Study of the Dehydration Process in Synthetic Strelkinite, $Na[(UO_2)(VO_4)]\cdot nH_2O$ (n = 0, 1, 2). Z. Kristallographie 2012, *227*, 522-529

Sypula, M.; Wilden, A.; Schreinemachers, **C.;** Malmbeck, R.; Geist, A.; Taylor, R.; **Modolo, G.**: Use of polyaminocarboxylic acids as hydrophilic masking agents for fission products in actinide partitioning processes, Solvent Extr. Ion Exch., 2012, *30(7)*, 748-764

Villa, E.M.; **Alekseev, E.V.**; Depmeier, W.; Albrecht-Schmitt, T.E.: Systematic Evolution from Uranyl(VI) Phosphites to Uranium(IV) Phosphates, Inorg. Chem., 2012, *51*, 6548 - 6558

Wang, S.; **Alekseev, E.V.;** Depmeier, W.; Albrecht-Schmitt, T.E.: New Neptunium(V) Borates That Exhibit the Alexandrite Effect, Inorg. Chem., 2012, *51*, 7-9

Wang, S.; Diwu, J.; Jouffret, L.J.; **Alekseev, E.V.**; Depmeier, W.; Albrecht-Schmitt, T.E: Cation-Cation Interactions Between Neptunyl(VI) Unites, Inorg. Chem., 2012, *51*, 7016-7018

Wang, S.; Parker, T.G.; Diwu, J.; Depmeier, W.; **Alekseev, E.V.**; Albrecht-Schmitt, T.E.: Elucidation of Tetraboric Acid with a New Borate Fundamental Building Block in a Chiral Uranyl Fluoroborate, Inorg. Chem., 2012, *51*, 11211 – 11213

Wang, S.; Purse, P.; Wu, P.; Casey, W.H.; **Alekseev, E.V.;** Depmeier, W.; Albrecht-Schmitt, T.E.: Selectivity, Kinetics, and Efficiency of Reversible Anion Exchange with TcO_4^- in a Supertetrahedral Cationic Framework. Adv. Functional Materials, 2012, *22*, 2241-2250 (Selected for Cover Art, Featured on Science Daily)

Wilden, A.; Modolo, G.; Sypula, **M.;** Geist, A.; Magnusson, D.: The Recovery of An(III) in an Innovative-Sanex Process using a Todga-based Solvent and Selective Stripping with a Hydrophilic BTP, Procedia Chemistry, 2012, *7*, 418-424

Wu, S.; Beermann, O.; Wang, S.; Holzheid, A.; Depmeier, W.; Malchereck, T.; **Modolo, G.; Alekseev, E.V.;** Albrecht-Schmitt, T.E.: Synthesis of Uranium Materials under Extreme Conditions: $UO_2[B_3Al_4O_{11}(OH)]$, a Complex 3D Aluminoborate, Chem. Eur. J., 2012, *18*, 4166 – 4169

Wu, S.; Kegler, P.; Wang, S.; Holzheid, A.; Depmeier, W.; Malchereck, T.; **Alekseev, E.V.;** Albrecht-Schmitt T.E.: Rich coordination of Nd^{3+} in $Mg_2Nd_{13}(BO_3)_8(SiO_4)_4(OH)_3$, derived from high-pressure/high-temperature conditions. Inorg. Chem., 2012, *51*, 3941−3943.

Wu, S.; Wang, S.; Diwu, J.; Depmeier, W.; Malchereck, T.; **Alekseev, E.V.;** Albrecht-Schmitt, T.E.: Complex Clover Cross-Sectioned Nanotubules Exist in the Structure of First Uranium Borate Phosphate. Chem.Comm., 2012, *48*, 3479–3481 (Selected for Cover Art Feature)

10.2.2 Proceedings/Books

Proceedings

Bell, K.; Carpentier, C.; Carrott, M.; Geist, A.; Gregson, C.; Hérès, X.; Magnusson, D.; Malmbeck, R.; **Modolo, G.**; Müllich, U.; Taylor, R.; **Wilden, A.**: Towards a new GANEX 2nd cycle process for the co-separation of TRU, Proceedings of the Nuclear Fuel Cycle Conference, Manchester, UK: 23-25 April 2012

Denecke, M.A.; Borchert, M.; Denning, R.G.; de Nolf, W.; Falkenberg, G.; Hönig, S.; **Klinkenberg**, **M.;** Kvashnina, K.; **Neumeier**, **S.;** Patommel, J.; Petersmann, T.; Pruessmann, T.; Ritter, S.; Schroer, C.G.; Stephan, S.; Villanova, J.; Vitova, T.; Wellenreuther, G. (2012): Highly resolved synchrotron-based investigations related to nuclear waste disposal. MRS Online Proceedings Library, 1444, mrss12-1444-y01-05 doi:10.1557/opl.2012.1159

Fricke-Begemann, C.; Noll, R.; Monteith, A.; Maddison, A.; **Dürr, M.**: Assessment of Laser-Induced Breakdown Spectroscopy as a Method to Pre-Screen Environmental Swipe Samples, Proc. Institute of Nuclear Materials Management 53rd Annual Meeting, Orlando, USA: 15-19 July 2012

Listner, **C.;** Canty, M.J.; Rezniczek, A.; **Niemeyer**, **I.;** Stein, G.: A Concept for Handling Acquisition Path Analysis in the Framework of IAEA's State-level Approach, Proc. Institute of Nuclear Materials Management 53rd Annual Meeting, Orlando, USA: 15-19 July 2012

Niemeyer, **I.;** Button, P.; Okko, O.; Paquette, J.-P.; Parsons, G.; Tadono, T.: Safeguarding Geological Repositories, Proc. 13. Geokinematischer Tag, Freiberg, Germany: 10-11 May 2012

Niemeyer, I.; Listner, **C.;** Nussbaum, S.: Object-based Image Analysis Using Very High-resolution Satellite Data, Proc. Institute of Nuclear Materials Management 53rd Annual Meeting, Orlando, USA: 15-19 July 2012

Nussbaum, S.; **Niemeyer, I.**: Geographic Information Systems (GIS) – from Visualization to Analysis, Proc. Institute of Nuclear Materials Management 53rd Annual Meeting, Orlando, USA: 15-19 July 2012

Tietze-Jaensch, H.: Neutron Sources, 16th Int. Seminar on Neutron Scattering Investigations in Condensed Matter, Faculty of Physics, Adam Mickiewicz University, Poznan, Poland: 12 May 2012

Wilden, A.; Schreinemachers, C.; Sadowski, F.; Gülland, S.; Sypula, M.; Modolo, **G.;** Magnusson, D.; Geist, A.; Lewis, F.W.; Harwood, L.M.; Hudson M.J.: Demonstration of a 1-cycle SANEX Process for the Selective Recovery of Trivalent Actinides from PUREX Raffinate Using a CyMe4BTBP/TODGA Solvent, Proceedings of the Nuclear Fuel Cycle Conference, Manchester, UK: 23-25 April 2012

Wilden, A.; Sypula, M.; Modolo, G.; Geist, A: "One-cycle SANEX process development studies and lab-scale demonstrations" Proceedings of 11th Information Exchange Meeting on Actinide and Fission Product Partitioning & Transmutation (IEMPT11) 2010, San Francisco, USA: 01-05 November 2010, published 2012, pp. 247-256.

10.2.3 Internal reports

Aksyutina, Y.; Weidenfeld, M.; Tietze-Jaensch, H.: Audit and Inspection of Lloyd's Register and Sellafield SLC-WVP at Sellafield by the Produktkontrollstelle PKS from 14.03.12 to 15.03.12 – Results - Aktenzeichen: PKSINS/AR- ENG I / 2012, Rev.: 1.3 of 09.07.2012

Aksyutina, Y.; Weidenfeld, M.; Tietze-Jaensch, H.: Audit and Inspection of Lloyd's Register and Sellafield SLC-WVP at Sellafield by the Produktkontrollstelle PKS from 11.09.12 to 13.09.12 – Results - Aktenzeichen: PKSINS/AR- ENG II / 2012, Rev.: 1.3 of 19.11.2012

Aksyutina, Y.; Weidenfeld, M.; Tietze-Jaensch, H.: Auditierung von LR und Inspektion der Verglasungsanlage WVP Sellafield von Sellafield Ltd. durch die Produktkontrollstelle PKS am 23. und 24.09.2009, Aktenzeichen: PKSINS – ENG II/2009, Rev.: 1.3 vom 25.05.2012

Harren, E.; Kreutz, F.; Tietze-Jaensch, H.: Gutachten über den Ergänzungsbericht zum Handbuch zur Verfahrensqualifikation der WAK Entsorgungs GmbH, Karlsruhe durch die Produktkontrollstelle des Bundesamts für Strahlenschutz vom 30.11.2012 PKS BER – WAK 2012-09 – Rev.: 20121130

Harren, E.; Kreutz, F.; Tietze-Jaensch, H.: Bericht über Audit und Inspektion der VEK bei der WAK Entsorgungs GmbH, Karlsruhe durch die Produktkontrollstelle des Bundesamts für Strahlenschutz 26.-27.01.2011, PKSINS / BER – WAK 2011-01, Berichtszeitraum 22.06.2010 bis 25.01.2011, Rev.: 20120713

Bosbach, D.; Brandt, F.; Duro, L.; Grambow, B.; Kulik, D.; Suzuki-Muresan, T.: SKIN PROJECT, 1st Annual Workshop Proceedings, EURATOM, EC 7th Framework Program Collaborative Project, "Slow processes in close-to-equilibrium conditions for radionuclides in water/solid systems of relevance to nuclear waste management", 2012

Neumann, A.: Technical Report T-3.3.5 Characterisation of Graphite by Application of Powder X-ray Diffraction, Forschungszentrum Jülich, Document Number: CARBOWASTE-1207-T-3.3.5, Date of issue of this report: 31.07.2012

Weidenfeld, M.; Aksyutina, Y.; Tietze-Jaensch, H.: Audit and Inspection of Bureau Veritas and AREVA NC I La Hague by the Produktkontrollstelle PKS from 09.05. to 11.05.2012 – Results - Reference: PKSINS/AR - FRA I Rev.: 1.3 of 20.09.12

Wilden, A.; Assenmacher, J.; Modolo, G.: Fachlicher Schlussbericht des BMBF Forschungsvorhabens "Verbundprojekt: Grundlegende Untersuchungen zur Entwicklung und Optimierung von Prozessen zur Abtrennung langlebiger Radionuklide (Partitioning) - Stabilitätsuntersuchungen und Entwicklung von kontinuierlichen Prozessen“ Förderzeichen 02NUK012E.

10.2.4 Poster

Aksyutina, Y.; Schneider, S.; Tietze-Jaensch, H.; Weidenfeld, M.: The German Product Quality control of the compacted nuclear waste. 2nd European Energy Conference, Maastricht, NL: 17-20 April 2012

Dürr, **M.;** Fricke-Begemann, C.; **Mauerhofer, E.; Niemeyer, I.; Rossbach, M.**: Detection of Radioactive and Nuclear Materials: A Link from Non-Proliferation and Nuclear Safety to Security. Future Security 2012, Bonn, Germany: 4-6 September 2012

Fricke-Begemann, C.; Noll, R. Monteith, A.; Maddison, A.; **Dürr, M.**: Assessment of Laser-Induced Breakdown Spectroscopy as a Method to Pre-Screen Environmental Swipe Samples, Institute of Nuclear Materials Materials Management 53rd Annual Meeting, Orlando, USA: 15-19 July 2012

Finkeldei, **S.;** Holliday, K.; **Neumeier, S.**; Walther, C.; **Bosbach, D.**; Stumpf, T.: Time-resolved laser fluorescence of Cm^{3+} and Eu^{3+} doped $La_2Zr_2O_7$, International Workshop on ATAS, Dresden-Rossendorf, Germany: 05-07 November 2012

Gale, J.D.; Demichelis, R.; Raiteri, P.; Quigley, D.; Gebauer, D.; Stack, A.G.; Dovesi, R.; **Vinograd**, **V. L.;** Winkler, B.: Computing the thermodynamics and reactivity of carbonates from solid state to speciation, Goldschmidt Conference 2012, Montreal, Canada: 24-29 June 2012

Heuser, J.; Schlenz, H.; Bosbach, D.: Monazite-type ceramics used for nuclear waste management. EMPG 2012 Conference, Kiel, Germany: 04-07 March 2012

Heuser, J.; Schlenz, H.; Bosbach, D.: Characterization of Sm- and Tb-Orthophosphates used for Nuclear Waste Management, E-MRS Spring Meeting, Strasbourg, France: 14-18 May 2012

Heuser, J.; Schlenz, H.; Bosbach, D.: Characterization of (Sm,Ce)-Orthophosphates used for Nuclear Waste Conditioning, ATALANTE 2012- Nuclear Chemistry for Sustainable Fuel Cycles, Montpellier, France: 02-07 September 2012

Kettler, **J.;** Biß, K.; Bongardt, K.; Bourauel, P.; Esser, F.; Greiner, W.; Hamzic, S.; Maier, R.; Mishustin, I.; **Modolo**, **G.;** Nabbi, R.; Pshenichnov, I.; **Rossbach**, **M.;** Shetty, N.; **Thomauske**, **B.;** Wolters, J.: Advanced Gas-cooled Accelerator-driven Transmutation Experiment – AGATE. 2nd European Energy Conference, Maastricht, NL: 17-20 April 2012

Klinkenberg, M.; Brandt, F.; Rozov, K.; Modolo, G.; Bosbach D.: Recrystallization of Barite in the presence of Ra at elevated temperatures up to 90°C, Goldschmidt Conference 2012, Montreal, Canada: 24-29 June 2012

Klinkenberg, M.; Brandt, **F.;** Breuer, U.; Modolo, G.; Bosbach D.: Recrystallization of Barite in the presence of Radium. EMC^2 2012 European Mineralogical Conference, Frankfurt/Main, Germany: 2-6 September 2012

Labs, S.; Hartl, M.; Daemen, L.; **Curtius, H.; Bosbach D.**: Investigation of the dehydration process of uraniumperoxide, 16. Vortragstagung der GdCh Fachgruppe Festkörperchemie und Materialforschung "Materialchemie für Energie- und Ressourcennutzung", Darmstadt, Germany: 17–19 September 2012. Abstract: Zeitschrift für Anorganische und Allgemeine Chemie, 2012, *638(10)*, 1606

Lewis, F.W.L.M.H.; Hudson, M.J.; Drew, M.G.B.; Desreux, J.F.; Vidick, G.; Bouslimani, N.; **Modolo, G.; Wilden, A.; Sypula M.**; Vu, T.-H.; Simonin, J.-P.: From BTBPs to BTPhens: Improving the properties of actinide-selective solvent extraction reagents by ligant pre-organization, Nuclear Fuel Cycle Conference, Manchester, UK: 23-25, April 2012

Listner, C.; Niemeyer, I.: Advanced Object-based Change Detection Using Very High-Resolution Remote Sensing Imagery. IEEE Geoscience and Remote Sensing Society, Munich, Germany: 22-27 July 2012

Magnusson, D.; Geist, A.; **Wilden, A.; Modolo**, **G.;** Malmbeck, R.: "Flow-sheet design for an innovative SANEX process using TODGA and SO3-Ph-BTP", ATALANTE 2012 – Nuclear Chemistry For Sustainable Fuel Cycles, Montpellier, France: 02-07 September 2012

Mauerhofer, E.; Havenith, **A.;** Carasco, C.; Payan, E.; Kettler, J.; Ma, J.-L.; Perot, B.: Quantitative comparison between PGNAA measurements and MCNP calculations in view of the characterization of radioactive wastes in Germany and France. CARRI, 22nd International Conference on the Application of Accelerators in Research and Industry, Fort Worth, Texas, USA: 5-10 August 2012

Modolo, G.; Wilden, A.; Bosbach, D.; Geist, A.; Malmbeck, R.: The development of innovative partitioning processes for the recovery of minor actinides from PUREX type solutions, 2nd European Energy Conference, Maastricht, NL: 17-20 April 2012

Niemeyer, I.; Listner, C.: Enhancing object-based change detection, XXII Congress of the International Society for Photogrammetry and Remote Sensing, Melbourne, Australia: 25 August - 01 September 2012

Rozov, K.; Curtius, H.; Bosbach, D.: Synthesis, characterization and stabilities of Mg-Zr(IV)-Al-Cl containing layered double hydroxides (LDHs), Goldschmidt conference 2012, Montreal, Canada, 24-29 June 2012

Rozov, K.; Curtius, H.; Bosbach, D.: Preparation, structure and stability of Fe(II)-, Co(II)-, Ni(II)- and Zr(IV)-containing layered double hydroxides (LDHs), 5th International meeting: Clays in Natural and Engineered Barriers for Radioactive Waste Confinement, Montpellier, France: 22-25 October 2012

Rossbach, M.; Genreith, C.; Mauerhofer, **E.;** Firestone, R.B.; Révay, Z.; Kudejova, P.; Belgya, T.: Research Alliance for Validation of PGAA Actinide Nuclear Data. NRC-8, Como, Italia: 17-21 September 2012

Schlenz, H.; Heuser, J.: X-ray diffraction and Raman study of monoclinic TbPO4, ATALANTE 2012- Nuclear Chemistry for Sustainable Fuel Cycles, Montpellier, France: 02-07 September 2012

Schlenz, H.; Heuser, J.; Schmitz, S.: Monazite as a suitable host matrix for the safe disposal of actinides. EMPG 2012 Conference, Kiel, Germany: 04-07 March 2012

Schlenz, H.; Neumeier, S.; Bosbach, D.: Fundamental Research on Ceramic Nuclear Waste Forms at Forschungszentrum Jülich (Germany): Conditioning and Structure Research. 2nd European Energy Conference, Maastricht, NL: 17-20 April 2012

Schmitz, S.; Schlenz, H.; Bosbach, D.: Structural and thermal analysis of Nd-Monazite-type ceramics used for Nuclear Waste Management, E-MRS Spring Meeting, Strasbourg, France: 14-18 May 2012

Weidenfeld, M.; Schneider, S.; Tietze-Jaensch, **H.;** Gauthier, R.: Quality Proof and Numerical Property Simulation of VEK High-Level Vitrified Waste. 2nd European Energy Conference, Maastricht, NL: 17-20 April 2012

Yu, Y.G.; **Vinograd**, **V.L.;** Winkler, B.: Olivine-wadsleyite-ringwoodite phase equilibria in $(Mg,Fe)_2SiO_4$ from first-principles calculations. EMPG 2012 Conference, Kiel, Germany: 04-07 March 2012

10.2.5 Presentations

Conferences:

Aksyutina, Y.; Schneider, S.; Tietze-Jaensch, H.: The German Product Quality Control of the Compacted Metallic Nuclear Waste, Jahrestagung Kerntechnik 2012, Stuttgart, Germany: 22-24 May 2012

Alekseev, E.V.; Villa, E.M.; **Rozov**, **K.B.;** Depmeier, W.; Albrecht-Schmitt, T.E.: Complex behavior of U, Th and Np in phosphite (P^{3+}) systems, E-MRS Spring Meeting, Strasbourg, France, 14-18 May 2012

Alekseev, E.V.; Wu, S.; Depmeier, W.: Structural variability in complex uranyl phosphates and uranyl arsenates of divalent elements. DGK-2012, Munich, Germany: 12-15 March 2012

Brandt, F.; Babelot, C.; Schuppik, T.; Neumeier, S.; Bukaemskiy, A.; Modolo, G.; Bosbach, D.: Conditioning of Minor Actinides in La-Monazite Ceramics, ATALANTE 2012-Nuclear Chemistry for Sustainable Fuel Cycles, Montpellier, France: 02-07 September 2012

Brandt, F.; Klinkenberg, M.; Rozov, K.; Modolo, G.; Bosbach, D.: Replacement of Barite by Radiobarite at close to equilibrium conditions and room temperature, Goldschmidt Conference 2012, Montreal, Canada: 24-29 June 2012

Bukaemskiy, **A.;** Titov, M.; Fachinger, J.; **Bosbach, D.**: Evolution of physico-mechanical properties of thoria-based fuel kernels during leaching, E-MRS Spring Meeting, Strasbourg, France: 14-18 May 2012

Butchins, L.; **Bosbach**, **D.;** Brendebach, B.; Burton, N.; Charnock, J.; Dardenne, K.; Denecke, M.; Doudou, S.; Marquardt, C.; Römer, J.; Schild, D.; Vaughan, D.; Wincott P. and Livens, F.R.: Interactions of Actinide Ions with the Calcite Surface, E-MRS Spring Meeting, Strasbourg, France: 14-18 May 2012

Curtius, H.; Bosbach, D.; Labs, S.: Disposal of Spent Fuel-Radionuclide Release and Secondary Phases, 2nd European Energy Conference, Maastricht, NL: 17-20 April 2012

Curtius, H.; Müller, E.; Klinkenberg, M.; Bosbach, D.: HTR Spent Fuel-Effects of irradiation to the microstructure, Spent Fuel Workshop, Avignon, France: 18-19 April 2012

Denecke, M.A.; Petersmann, T.; de Nolf, W.; **Klinkenberg, M.; Neumeier**, **S.;** Villanova, J.; Prüßmann, T.: Characterization of UO_2/Mo(Pd) thin films as models for ε-particles inspent nuclear fuel using XANES, XRF and tomographic techniques, XAFS-XV: 15th International Conference on X-Ray Absorption Fine Structure, Beijing, China: 22-28 July 2012

Finkeldei, S.; Brandt, **F.;** Holliday, K.; **Bukaemskiy, A.; Arinicheva, Y.; Neumeier, S.; Modolo, G.; Bosbach, D.**: Conditioning of Minor Actinides in Zirconate based Pyrochlore-type Ceramics, ATALANTE 2012- Nuclear Chemistry for Sustainable Fuel Cycles, Montpellier, France: 02-07 September 2012

Finkeldei, S.; Bukaemskiy, A.; Neumeier, S.; Brandt, F.; Schlenz, H.; Modolo, G.; Bosbach, D.: Conditioning of Minor Actinides in zirconate based Pyrochlore. EMPG 2012 Conference, Kiel, Germany: 04-07 March 2012

Fricke-Begemann, C.; Noll, R.; Monteith, A.; Maddison, A.; **Dürr, M.**: Assessment of Laser-Induced Breakdown Spectroscopy as a Method to Pre-Screen Environmental Swipe Samples, Institute of Nuclear Materials Management 53rd Annual Meeting, Orlando, USA: 15-19 July 2012

Genreith, C.; Rossbach, M.; Mauerhofer, **E.;** Belgya, T.; Caspary, G.: Measurement of thermal neutron capture cross sections of ^{237}Np and ^{242}Pu using prompt gamma neutron activation, Ninth International Conference on METHODS AND APPLICATIONS OF RADIOANALYTICAL CHEMISTRY, MARC9, Kailua-Kona, Hawaii, USA: 25-30 March 2012

Heuser, J.; Schlenz, H.; Babelot, C.; Schmitz, S.; Schuppik, T.; Bosbach, D.: Short-range order investigations of $LnPO_4$ using Raman spectroscopy, ATAS-Workshop, Dresden, Germany: 05-07 November 2012

Listner, **C.;** Canty, M.J.; Rezniczek, A.; **Niemeyer**, **I.;** Stein, G.: A Concept for Handling Acquisition Path Analysis in the Framework of IAEA's State-level Approach, Institute of Nuclear Materials Management 53rd Annual Meeting, Orlando, USA: 15-19 July 2012

Mauerhofer, E.; Havenith, **A.;** Carasco, C.; Payan, E.; Kettler, J.; Ma, J.L.; Perot, B.: Quantitative comparison between PGNAA measurements and MCNP calculations in view of the characterization of radioactive wastes in Germany and France, CAARI 2012, Fort Worth, Texas, USA: 05-10 August 2012

Neumann, A.; Curtius, H.; Klinkenberg, M.; Bosbach, D.: Identification and quantification of the corrosion products of research reactor fuel elements, EMPG 2012 Conference, Kiel, Germany: 04-07 March 2012

Neumann, A.; Klinkenberg, M.; Kaiser, G.; Curtius, H.; Bosbach, D.: Secondary Phase Characterization of the Corrosion Products of U_3Si_2-Al Fuel Elements, E-MRS Spring Meeting, Strasbourg, France: 14-18 May 2012

Neumann, A.; Klinkenberg, M.; Kaiser, G.; Curtius, H.; Bosbach, D.: Secondary phase formation during the corrosion of non-radiated UAl_x-Al fuel elements in salt and clay pore solution, ATALANTE 2012- Nuclear Chemistry for Sustainable Fuel Cycles, Montpellier, France: 02-07 September 2012

Neumeier, S.; Babelot, C.; Finkeldei, S.; Schuppik, T.; Bukaemskiy, A.A.; Brandt, F.; Schlenz, H.; Modolo, G.; Bosbach, D.: Conditioning of Minor Actinides in Monazite- and Pyrochlore-type Ceramics, E-MRS Spring Meeting, Strasbourg, France: 14-18 May 2012

Neumeier, S.; Bukaemskiy, A.A.; Brandt, F.; Schlenz, H.; Bosbach, D.: Ceramic Waste Forms for Conditioning of Minor Actinides, EMC^2 2012 European Mineralogical Conference, Frankfurt/Main, Germany: 02-06 September 2012

Neumeier, S.; Daniels, H.; Schreinemachers, C.; Modolo, G.; Bosbach, **D.;** Leturcq, G.; Grandjean, S.: The co-conversion of minor actinides in uranium based fuel by internal gelation, ATALANTE 2012- Nuclear Chemistry for Sustainable Fuel Cycles,. Montpellier, France: 02–07 September 2012

Niemeyer, I.; Dürr, M.; Richter, B.: Internationale Kernmaterialüberwachung ("Safeguards") bei der Endlagerung wärmeentwickelnder radioaktiver Abfälle, 72 Annual Meeting of the German Geophysical Society, Hamburg, Germany: 05-08 March 2012

Niemeyer, I.; Dürr, M.; Richter, B.: Internationale Kernmaterialüberwachung ("Safeguards") bei der Endlagerung wärmeentwickelnder radioaktiver Abfälle, 13. Geokinematischer Tag, Freiberg, Germany: 10-11 May 2012

Niemeyer, I.; Listner, C.: Advances in the use of remote sensing and geoinformation technologies in nuclear non-proliferation and arms control verification regimes, XXII Congress of the International Society for Photogrammetry and Remote Sensing, Melbourne, Australia: 25 August – 01 September 2012

Niemeyer, I.; Listner, **C.;** Nussbaum, S.: Object-based Image Analysis Using Very High-resolution Satellite Data, Institute of Nuclear Materials Management 53rd Annual Meeting, Orlando, USA: 15-19 July 2012

Nussbaum, S.; **Niemeyer, I.**: Geographic Information Systems (GIS) – from Visualization to Analysis, Institute of Nuclear Materials Management 53rd Annual Meeting, Orlando, USA, 15-19 July 2012

Schlenz, H.; Heuser, J.; Schmitz, S.: Monazite as a suitable host matrix for the safe disposal of actinides, E-MRS Spring Meeting, Strasbourg, France: 14-18 May 2012

Schmidt, M., **Bosbach, D.**, Stumpf, T., Walther, C.: Guest ion speciation in a homogeneous solid solution by polarisation-dependent TRLFS, EMC^2 2012 European Mineralogical Conference, Frankfurt/Main, Germany: 02-06 September 2012

Schmitz, S.; Schlenz, H.; Bosbach, D.: Structural and thermal analysis of Nd-Monazite-type ceramics used for Nuclear Waste Management. EMPG 2012 Conference, Kiel: 04-07 March 2012

Schmitz, S.; Schlenz, H.; Bosbach, D.: Structural and thermal analysis of Nd-Monazite-type ceramics used for Nuclear Waste Management, ATALANTE 2012- Nuclear Chemistry for Sustainable Fuel Cycles, Montpellier, France: 02-07 September 2012

Vinograd, V.L.; Brandt, F.; Rozov, K.; Klinkenberg, **M.;** Winkler, B.; **Bosbach, D.**: Solid-aqueous equilibrium in the $BaSO_4$-$RaSO_4$-H_2O system: first-principles calculations and a thermodynamic assessment. EMC^2 2012 European Mineralogical Conference, Frankfurt/Main, Germany: 02-06 September 2012,

Weidenfeld, M.; Tietze-Jaensch, H.; Bosbach, **D.;** Steyer, S.: Product quality control of intermediate level vitrified nuclear waste from radioactive rinsing solutions from the reprocessing of spent nuclear fuel. 7th International Youth Nuclear Congress IYNC2012, Charlotte/North Carolina, USA: 05-11 August 2012

Wilden, A.; Schreinemachers, C.; Sadowski, F.; Gülland, S.; Sypula, M.; Modolo, **G.;** Magnusson, D.; Geist, A.; Lewis, F.W.; Harwood, L.M.; Hudson, M.J.: Demonstration of a 1-cycle SANEX Process for the Selective Recovery of Trivalent Actinides from PUREX Raffinate Using a $CyMe_4$BTBP/TODGA Solvent, Nuclear Fuel Cycle Conference, Manchester, UK: 23-25 April 2012

Wilden, A.; Modolo, G.; Sypula, **M.;** Geist, A.; Magnusson, D.: "The Recovery of An(III) in an innovative-SANEX process using a TODGA-based solvent and selective stripping with a hydrophilic BTP", ATALANTE 2012 – Nuclear Chemistry For Sustainable Fuel Cycles, Montpellier, France: 02-07 September 2012

Wu, S.; Wang, S.; Diwu, J.; Beermann, O.; Depmeier, W.; Holzeid, A.; Malcherek, T.; **Alekseev**, **E.V.;** Albrecht-Schmitt, T.E.: Uranium containing aluminoborate, borophosphates and borate phosphate. EMPG 2012 Conference, Kiel, Germany: 04-07 March 2012

Wu, S.; Wang, S.; Diwu, J.; Beermann, O.; Depmeier, W.; Holzeid, A.; Malcherek, T.; **Alekseev**, **E.V.;** Albrecht-Schmitt, T.E.: Synthesis and structure of first uranyl borophosphates, borate phosphate and aluminoborate, E-MRS Spring Meeting, Strasbourg, France: 14-18 May 2012,

Rizzato, C.; Baginski, K.; Vulpius, D.; von Lensa, W.: Investigations on high temperature thermal treatments of virgin AVR graphite, 8th Workshop on European Collaboration for Higher Education and Research in Nuclear Engineering and Radiological Protection, Athens, Greece: 28-30 May 2012

Rizzato, C.; Baginski, K.; Vulpius, D.; von Lensa, W.: Investigations on high temperature thermal treatments of virgin AVR graphite, EPRI 11th International Decommissioning and Radioactive Waste Management Workshop, Rome, Italy: 22-25 October 2012

von Lensa, W.: Introduction to the CARBOWASTE Project 'Treatment and Disposal of Irradiated Graphite and other Carbonaceous Waste', EPRI 11th International Decommissioning and Radioactive Waste Management Workshop, Rome, Italy: 22-25 October 2012

Invited Talks

Bosbach, D.; Neumeier, S.; Bukaemskiy, A.; Brandt, F.; Schlenz, H.; Modolo, G.: Ceramic waste forms for actinides: Present status and perspectives. E-MRS Spring Meeting, Strasbourg, France: 14-18 May 2012

Bosbach, D.: Die wissenschaftliche Basis für den Langzeitsicherheits-nachweis der Endlagerung hochradioaktiver Abfälle. Salem International College Youth Conference, Salem International College, Spetzgart, Germany: 23 November 2012

Bosbach, D.; Brandt, F.; Klinkenberg, M.; Vinograd, V.; Rozov, K.: Radionuclide solubility control in solid solution – aqueous solution systems, ATALANTE 2012 – Nuclear Chemistry for Sustainable Fuel Cycles, Montpellier, France: 02-07 September 2012

Bosbach, D.; Curtius, H.; Müller, E.; Kaiser, G.; Klinkenberg, M.; Rozov, K.; Neumann, A.: Spent Fuel Corrosion, PSI, Villingen, Switzerland: 30 August 2012

Bosbach, D.: Die wissenschaftliche Basis für den Langzeitsicherheitsnachweis der Endlagerung hochradioaktiver Abfälle. Kerntechnisches Symposium beim 44. Kraftwerks-technischen Kolloquium, Dresden, Germany: 24 October 2012

Bosbach, D.: Transmutation – Eine Alternative zur Endlagerung. AiNT Endlagerworkshop, Bonn, Germany: 26 September 2012

Bosbach, D.: Die wissenschaftliche Basis für den Langzeitsicherheits-Nachweis der Endlagerung hochradioaktiver Abfälle. Kerntechnisches Kollquium, RWTH Aachen University, Aachen, Germany: 22 May 2012

Dürr, M.: Messtechnik für Internationale Überwachungsmaßnahmen der IAEO, Kolloquium Physik TU Dortmund, Dortmund, Germany: 17 January 2012

Eineder, M.; Minet, C.; **Niemeyer, I.**: High resolution SAR-Signatures and 3D Analysis for Safeguards Verification Activities, IAEA Workshop on the Use of Satellite Imageryin Support of Safeguards Verification Activities, Tsukuba, Japan: 14-18 May 2012

Modolo, G.: Recovery of long-lived actinides from High Active Waste solutions using innovative solvent extraction processes, Twente University, Enschede, NL: 18 October 2012

Neumeier, S.; Modolo, G.; Bosbach, D.: The Institute of Energy and Climate Research – IEK-6: Nuclear waste management and reactor safety. German-French research for nuclear safety: Chemistry of the f-elements, Strasbourg, France: 22-23 February 2012

Neumeier, S.; Modolo, G.; Bosbach, D.: The Institute of Energy and Climate Research - IEK-6: Nuclear Waste Management and Reactor Safety. HITEC Graduate School, Research Center Jülich, Jülich, Germany: 19 September 2012

Neumeier, S.; Bosbach, D.: Die wissenschaftliche Basis für den Langzeitsicherheits-nachweis der Endlagerung hochradioaktiver Abfälle. 7th Master Class Course Conference (7. MCCC) "Renewable Energies“, Berlin, Germany: 05 December 2012,

Neumeier, S.: Ceramic Waste Forms for the Conditioning of Minor Actinides. HITEC Theme Day, Energy technology IV – Nuclear waste disposal and reactor safety, RWTH Aachen University, Aachen, Germany: 13 December 2012

Niemeyer, **I.;** Button, P.; Tadono, T.: Lessons learned from a monitoring SAR case study -- geological repositories, IAEA Workshop on the Use of Satellite Imagery in Support of Safeguards Verification Activities, Tsukuba, Japan: 14-18 May 2012

Niemeyer, I.; Dürr, M.; Richter, B.; Listner, C.; Knott, **A.;** Martens, S.; **Niedrée, D.**: Safeguards research and development in support of the International Atomic Energy Agency. HITEC Graduate School, Research Center Jülich, Aachen, Germany: 13 December 2012

Niemeyer, I.; Listner, C.: Satellite Imagery Analysis for Strengthening Non-Proliferation and Arms Control Treaties, 76th Annual Meeting of the German Physical Society (DPG) and DPG Spring Meeting, Berlin, Germany: 25-30 March 2012

Tietze-Jaensch, H.: FZ-Jülich R&D on Advanced Nuclear Waste Management & Safety, IAEA LABONET Technical Meeting on Radioactive Waste Characterization - Practices and Trends, Brussels, Belgium: 21-23 November 2012

Tietze-Jaensch, H.: Nuclear Waste Management and Quality Control, Seminar at the Polish Institute of Nuclear Chemistry & Technology, ICHTJ, Warsaw, Poland: 30 August 2012

Tietze-Jaensch, H.: Energy Research at the Forschungszentrum Jülich, Seminar at the Polish Institute of Nuclear Chemistry & Technology, ICHTJ, Warsaw, Poland: 30 August 2012

Tietze-Jaensch, H.: German Energy-Wende: key dispute of facts vs values, safety & performance prospects of NE vs GE, Energy Cooperation Forum, Warsaw, Poland: 19 December 2012

Tietze-Jaensch, H.: Neutron Sources, 16th Int. Seminar on Neutron Scattering Investigations in Condensed Matter, Faculty of Physics, Adam Mickiewicz University, Poznan, Poland: 12 May 2012

Tietze-Jaensch, H.; Mauerhofer, E.: Reprocessed HLW Inventory Verification and Tasks for HLW / UNF Direct Disposal, IAEA LABONET Technical Meeting on Radioactive Waste Characterization - Practices and Trends, Brussels, Belgium: 21-23 November 2012

Wilden, A.: First results of a collaboration between CNRS Strasbourg and Forschungszentrum Jülich. German-French research for nuclear safety: Chemistry of the f-elements, Strasbourg, France: 22-23 February 2012

von Lensa, W., Steinmetz, H.-J.: CarboDISP: Disposal of Irradiated Graphite - A German BMBF Project; OECD-NEA Radioactive Waste Management Committee, Paris, France: 20 March 2012

von Lensa, W.; Vulpius, D. et al.: Treatment and Disposal of Irradiated Graphite and other Carbonaceous Waste, OECD-NEA Radioactive Waste Management Committee, Paris, France: 20 March 2012,

von Lensa, W.; Vulpius, D. et al.: Treatment and Disposal of Irradiated Graphite and other Carbonaceous Waste; EURADISS, Montpellier, France: 26 October 2012

Petersmann, T.; Steinmetz, H.-J.; von Lensa, W.: Disposal of Radioactive Graphite in Germany, 2nd IAEA RCM on Treatment of Irradiated Graphite to Meet Acceptance Criteria for Waste Disposal, Vienna, Austria: 3-5 December 2012

Additional Talks

Brandt, F.; Curtius, H.; Klinkenberg, M.; Rozov, K.; Vinograd, V.; Alekseev, E.V.; Labs, S.: Kick-off presentation of working plan for ImmoRad - Grundlegende Untersuchungen zur Immobilisierung langlebiger Radionuklide durch die Wechselwirkung mit endlagerrelevanten Sekundärphasen, Teilprojekt C, Bad Herrenalb, Germany: 02-03 April 2012

Brandt, F.; Klinkenberg, M.; Rozov, K.; Bosbach, D.: Recrystallization of Barite in the presence of Radium, 2nd Annual Workshop of the SKIN Project, PSI, Villigen, Switzerland: 21-22 November 2012

Curtius, H.: Verhalten Langlebiger Spalt- und Aktivierungsprodukte im Nahfeld eines Endlagers und Möglichkeiten ihrer Rückhaltung, VESPA Projekttreffen, Dresden-Rossendorf, Germany: 7- 8 May 2012

Curtius, H.: HTR Spent Fuel - Microstructure and Radionuclide Inventory, First Nuclides, First annual Workshop, First Nuclides, Budapest, Hungary: 09-11 October 2012

Curtius, H.: HTR Spent Fuel - Selected Material for First Nuclides, First annual Workshop, First Nuclides, Budapest, Hungary: 09-11 October 2012

Curtius, H.: Retention capability of Fe(II), Co(II) and Ni(II) bearing LDHs for selenite, VESPA –Verbundprojekt-Treffen, Karlsruhe, Germany: 14-15 November 2012

Ebert, E.; Modolo, G.; Neumeier, S.; Schreinemachers, C.; Wilden, A.: Progress report of Beneficiary No 2: Jülich, Domain 2: WP 2.1 Inert Matrix Fuels, ASGARD Meeting, Jáchymov, Czech Republic: 11-14 June 2012

Finkeldei, S.: Conditioning of Minor Actinides in ZrO_2 based ceramics with the pyrochlore crystal structure, Bilateral Meeting NRG/FZJ, Petten, NL: 14 February 2012

Finkeldei, S.: Synthesis of Pu doped Nd-zirconates with the pyrochlore crystal structure, Team Meeting NRG: Irradiation & Development, Petten, NL: 06 June 2012

Fricke-Begemann, C.; Noll, R.; Monteith, A.; Maddison, A.; **Dürr, M.**: Laser-Induced Breakdown Spectroscopy (LIBS) for Safeguards, 34th ESARDA Annual Meeting, Luxembourg, Luxembourg: 22-24 May 2012

Listner, C.: Acquisition Path Analysis, 34th ESARDA Annual Meeting, Luxembourg, Luxembourg, 22-24 May 2012

Modolo, G.; Neumeier, S.: Work plan of beneficiary No. 2: Jülich – WP 2.3: Inert Matrix Fuels, ASGARD, Kick-off meeting, Uddevalla, Sweden: 10-13 January 2012

Modolo, G.: Presentation of the IEK-6: Nuclear Waste Management and Reactor Safety, Institut de Chimie separative de Marcoule, Marcoule, France: 29 October 2012

Modolo, G.: Partitioning, die Abtrennung von Minoren Actiniden aus hochaktiven Spaltproduktslösungen, Kick-Off Meeting zum BASF-FZJ Forschungsprojekt, BASF Ludwigshafen, Germany: 26 November 2012

Omanovic, S.; Modolo, G.: Untersuchung zur Lanthanidentrennung mittels Flüssig-Flüssig Extraktion, Kick-Off Meeting zum BASF-FZJ Forschungsprojekt, BASF Ludwigshafen, Germany: 26 November 2012

Neumeier, S.; Daniels, H.; Schreinemachers, C.; Modolo, G.; Bosbach, **D.;** Leturcq, G.; Grandjean, S.: Synthesis of U, U/Nd, U/Pu and U/Am Microspheres via Internal Gelation, Summary report within Domain 1 WP 4, ACSEPT, 4th Annual Meeting, Karlsruhe, Germany: 20-23 March 2012

Neumeier, S.; Benay, G.; Bukaemskiy, A.; Daniels, H.; Sadowski, F.; Schreinemachers, C.; Weidenfeld, M.; Modolo, G.: FZJ Achievements within Domain 1; WP1.4: Actinide Co-Conversion, ACSEPT – Final Meeting, Montpellier, France: 06-08 September 2012

Neumeier, S.; Klinkenberg, M.: Electronmicroscopy SEM, FIB, (TEM) at IEK-6, Institut de Chimie separative de Marcoule, Marcoule, France: 29 October 2012

Neumeier, S.; Modolo, G.: Work plan of beneficiary No. 2: Jülich – WP 2.1: Conversion from solution to oxide precursors, ASGARD, Kick-off meeting, Uddevalla, Sweden: 10-13 January 2012

Niemeyer, I.; Richter, B.; Dürr, **M.;** Robertson, P.: Possible applications of "NavShoe/FootSLAM" for Indoor Navigation in Safeguards, 34th ESARDA Annual Meeting, Luxembourg, Luxembourg: 22-24 May 2012

Niemeyer, I.; Listner, C.; Barth A.: Satellite imagery in support of nuclear non-proliferation treaties, 34th ESARDA Annual Meeting, Luxembourg, Luxembourg: 22-24 May 2012

Rossbach, M.; Genreith, C.: Nuclear Data of Actinides and Fission Products, TANDEM kick-off meeting, München Garching, Germany: 11-12 September 2012

Schlenz, H.: Presentation of the IEK-6: Nuclear Waste Management and Reactor Safety, HITEC graduate school, Jülich, Germany: March 2012

Schlenz, H.; Bosbach, D.: Fe Solid Solutions, First Draft, OECD Nuclear Agency, Paris, France: May 2012

Schneider, S.; Tietze-Jaensch, H.: Numerical Waste Assessment Tools and PQC, Entrap-SC 33, NES at AIT, Vienna, Austria: 11 April 2012,

Schneider, S.; Tietze-Jaensch, H.: Numerical Waste Assessment Tools and PQC, AK-HAW 85, INE at KIT, Karlsruhe, Germany: 29-30 March 2012

Schreinemachers, C.; Neumeier, S.; Modolo, G.: Progress within WP 2.3.1 of Domain 2, ASGARD Meeting, Jáchymov, Czech Republic: 11-14 June 2012

Vulpius, D.: The CARBOWASTE Project: Work Package 3 – Task 3 "Localisation of impurities and isotopes before & after treatment", EU Project CARBOWASTE, 5th Working Group 3&4 Meeting, Pitesti, Romania: 8-10 February 2012

Vulpius, D.: The CARBOWASTE Project: Work Package 4 "Treatment & purification of irradiated graphite", EU Project CARBOWASTE, 5th Working Group 3&4 Meeting, Romania: 8-10 February 2012

Vulpius, D.: The CARBOWASTE Project: Work Package 4 "Treatment & purification of irradiated graphite" – Status Report, EU Project CARBOWASTE, 5th Steering Committee Meeting, Manchester, UK: 13-15 March 2012

Wilden, A.; Sypula, M.; Schreinemachers, C.; Assenmacher, J.; Sadowksi, F.; Gülland, S.; Modolo, G.: Progress report within Domain 1 WP 2 + 3, ACSEPT, 4th Annual Meeting, Karlsruhe, Germany: 20-23 March 2012

Wilden, A.; Assenmacher, J.; Kluxen, P.; Lange, S.; Sadowski, F.; Schreinemachers, C.; Sypula, M.; Modolo, G.: FZJ Achievements within Domain 1; WP1.2: Ligand design and assessment; WP1.3 Process development, ACSEPT – Final Meeting, Montpellier, France: 06-08 September 2012

Wilden, A.: Der Einsatz von ionischen Flüssigkeiten beim Partitioning. Erste Ergebnisse aus einem Forschungsaufenthalt in Strasbourg, BMBF2020+, 5. Halbjahrestreffen, Karlsruhe, Germany: 02 Februar 2012

Wilden, A.: „FZJ progress report 01.01.2012-31.07.2012“ BMBF 2020+, 6. Halbjahrestreffen, Karlsruhe, Germany: 09 July 2012

von Lensa, W.: HTR Fuel Back-End, ARCHER-Meeting, Jülich, Germany: 6-7 March 2012

11 How to reach us

By car

Coming from Cologne (Köln) take the A 4 motorway (Cologne – Aachen), leave the motorway at the Düren exit, and then turn right towards Jülich (B 56). After about 10 km, turn off to the right onto the L 253, and follow the signs for "Forschungszentrum".
Coming from Aachen take the A 44 motorway (Aachen – Düsseldorf) and leave the motorway at the Jülich-West exit. At the first roundabout turn left towards Jülich, and at the second roundabout turn right towards Düren (B 56). After about 5 km, turn left onto the L 253 and follow the signs to "Forschungszentrum".
Coming from Düsseldorf Airport take the A 52 motorway (towards Düsseldorf/Mönchengladbach), followed by the A 57 (towards Cologne). Turn off at Neuss-West, and continue on the A 46 until you reach the crossroads "Kreuz Wanlo". Take the A 61 (towards Koblenz/Aachen) until you reach "Dreieck Jackerath" where you should take the A 44 (towards Aachen). Continue as described in "Coming from Düsseldorf".

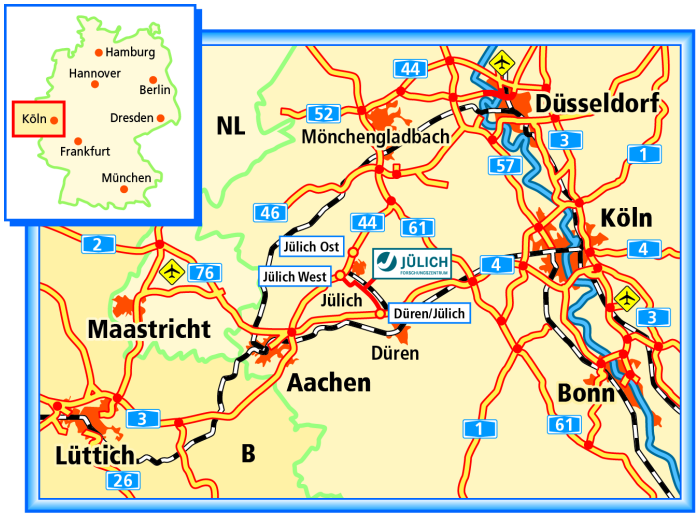

Fig. 70: Euregio Rheinland map.

Coming from Düsseldorf on the A44 motorway (Düsseldorf – Aachen) you have two options:
1. (Shorter route but more traffic) turn right at the Jülich-Ost exit onto the B 55n, which you should follow for approx. 500 m before turning right towards Jülich. After 200 m, before the radio masts, turn left and continue until you reach the "Merscher Höhe" roundabout. Turn left here, drive past the Solar Campus belonging to the University of Applied Sciences and continue straight along Brunnenstrasse. Cross the Römerstrasse junction, continue straight ahead onto Wiesenstrasse and then after the roundabout and the caravan dealers, turn left towards "Forschungszentrum" (signposted).

2. (Longer but quicker route) drive until you reach the "Jülich-West" exit. At the first roundabout turn left towards Jülich, and at the second roundabout turn right towards Düren (B 56). After about 5 km, turn left onto the L 253 and follow the signs to "Forschungszentrum".

Navigation systems

In your navigation system, enter your destination as "Wilhelm-Johnen-Strasse". From there, it is only a few hundred metres to the main entrance – simply follow the signs. The Research Centre itself is not part of the network of public roads and is therefore not recognised by navigation systems.

By train from Cologne Bonn Airport

From the railway station at the airport, take the S13 to Cologne main train station (Hauptbahnhof) and then continue with the regional express to Düren, or go to Köln-Ehrenfeld by regional express and then take the S12 to Düren. Continue from Düren as described in "By train".

By train from Düsseldorf International Airport

From the railway station at the airport, travel to Cologne main train station and then continue on to Düren. Some trains go directly to Düren whereas other connections involve a change at Cologne main train station. Continue from Düren as described in "By train".

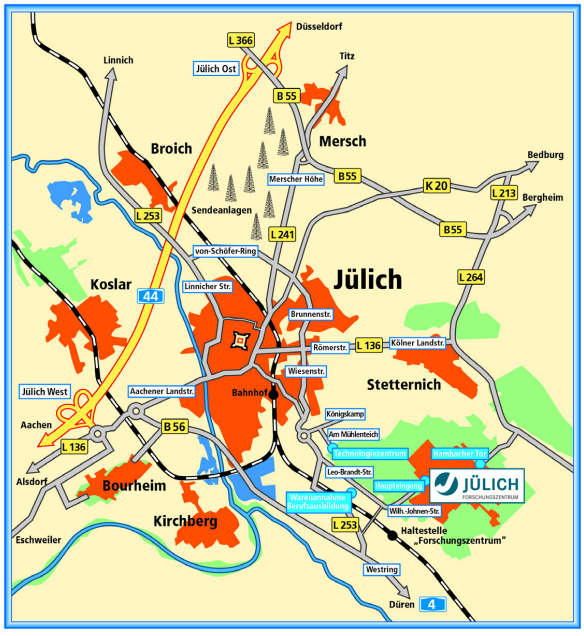

Fig. 71: Forschungszentrum Jülich campus map.

By train:

Take the train from Aachen or Cologne to the train station in Düren. From here, take the local train ("Rurtalbahn" [RTB]) for Jülich and get out at the "Forschungszentrum" stop. To make sure that the train stops at "Forschungszentrum" you should press the request stop button (Haltewunsch) in good time after the "Selgersdorf" stop. Bus number 11 leaves from this stop for the Research Centre (for bus timetables, see "Aachen - Jülich bus connections"). If you walk, it will take you approximately 20 minutes to reach the Research Centre's main entrance.

By bus:

Aachen - Jülich bus connection

The SB11 bus line connects the Research Centre to the local public transport system. Commuters from Aachen travelling to the Research Centre have 19 options every day of reaching their destination and 18 in the other direction to get back to Aachen.

Institute:

Fig. 72: Map showing the Institute, Helmholtz-Ring H18, building no. 05.3.

12 List of figures

13 List of tables

Band / Volume 185
Light Trapping with Plasmonic Back Contacts in Thin-Film Silicon Solar Cells
U. W. Paetzold (2013), X, 175 pp
ISBN: 978-3-89336-895-2

Band / Volume 186
Plant-plant interactions, biodiversity & assembly in grasslands and their relevance to restoration
V. M. Temperton (2013), ca 420 pp
ISBN: 978-3-89336-896-9

Band / Volume 187
Ab initio investigation of ground-states and ionic motion in particular in zirconia-based solid-oxide electrolytes
J. A. Hirschfeld (2013), v, 144 pp
ISBN: 978-3-89336-897-6

Band / Volume 188
Entwicklung protonenleitender Werkstoffe und Membranen auf Basis von Lanthan-Wolframat für die Wasserstoffabtrennung aus Gasgemischen
J. Seeger (2013), V, 130 pp
ISBN: 978-3-89336-903-4

Band / Volume 189
Entwicklung und Herstellung von metallgestützten Festelektrolyt-Brennstoffzellen (MSC-SOFC) mit einem Sol-Gel-Elektrolyten
S. D. Vieweger (2013), xviii, 176 pp
ISBN: 978-3-89336-904-1

Band / Volume 190
Mobile Brenngaserzeugungssysteme mit Mitteldestillaten für Hochtemperatur-PEFC
C. Wiethege (2013), iii, 179 pp
ISBN: 978-3-89336-905-8

Band / Volume 191
Verbundvorhaben Öko-effiziente Flugzeugsysteme für die nächste Generation (EFFESYS) - Teilprojekt Brennstoffzelle, Infrastruktur, Komponenten und System (BRINKS) – Schlussbericht
J. Pasel, R.C. Samsun, H. Janßen, W. Lehnert, R. Peters, D. Stolten (2013), xii, 152 pp
ISBN: 978-3-89336-908-9

Band / Volume 192
Analyse des Betriebsverhaltens von Hochtemperatur-Polymerelektrolyt-Brennstoffzellen
L. Lüke (2013), 156 pp
ISBN: 978-3-89336-909-6

Band / Volume 193
Full-waveform inversion of crosshole GPR data for hydrogeological applications
A. Klotzsche (2013), X, 164 pp
ISBN: 978-3-89336-915-7

Band / Volume 194
Long Term Stability and Permeability of Mixed Ion Conducting Membranes under Oxyfuel Conditions
X. Li (2013), III, 143 pp
ISBN: 978-3-89336-916-4

Band / Volume 195
Innovative Beschichtungs- und Charakterisierungsmethoden für die nasschemische Herstellung von asymmetrischen Gastrennmembranen auf Basis von SiO_2
J. Hoffmann (2013), V, 152 pp
ISBN: 978-3-89336-917-1

Band / Volume 196
Aerosol processes in the Planetary Boundary Layer: High resolution Aerosol Mass Spectrometry on a Zeppelin NT Airship
F. Rubach (2013), iii, 141 pp
ISBN: 978-3-89336-918-8

Band / Volume 197
Institute of Energy and Climate Research IEK-6: Nuclear Waste Management - Report 2011 / 2012 Material Science for Nuclear Waste Management
M. Klinkenberg, S. Neumeier, D. Bosbach (Eds.) (2013), 195 pp
ISBN: 978-3-89336-920-1

Weitere ***Schriften des Verlags im Forschungszentrum Jülich*** unter
http://wwwzb1.fz-juelich.de/verlagextern1/index.asp

Institute of Energy and Climate Research
IEK-6: Nuclear Waste Management

The Nuclear Waste Management section of the Institute of Energy and Climate Research (IEK-6) performs fundamental as well as applied research and development for the safe management of nuclear waste covering issues from the atomic scale to the macroscopic scale of actual waste packages and waste compounds/materials.

After the reactor accident in Fukushima (Japan) in 2011, the German Government decided to shut down immediately eight of 17 nuclear power plants. In the following, the German parliament decided with support of a broad societal consensus to terminate nuclear energy production in Germany, with the last nuclear power plant to be shutdown in 2022. Projections indicate that about a total of 17,200 tons of spent nuclear fuel will be generated by 2022. About 300,000 m3 of low and intermediate level mostly cementitious waste are forecasted to accumulate after shutdown and decommissioning of all German nuclear power plants. The safe management and ultimately the safe disposal of radioactive waste remain grand scientific, political and societal challenges to be met in the next decades. IEK-6 research addresses a number of challenges arising from these new constraints.

IEK-6 research with respect to the **long-term safety of nuclear disposal** includes work on spent nuclear fuel corrosion and the formation of secondary phases – the radio(geo)chemistry of the deep geological repository nearfield, thus contributing to the scientific basis of the safety case. In order to study **innovative waste management strategies** IEK-6 research groups are also focusing on partitioning of actinides and ceramic waste forms. The research programme is supported by a strong **"structure research"** group covering the field of solid state chemistry, crystallography and computational science to model actinide bearing compounds. Application oriented waste management concepts for special categories of radioactive waste are developed by integrating (1) the development of **non-destructive essay techniques**, for which IEK-6 is well known for decades and (2) **waste treatment procedures**. Furthermore, (3) some of this research is guided by the **product quality control group for radioactive waste (PKS)** which is operated by IEK-6 on behalf of the Federal Office of Radiation Protection (BfS) since 1987, to qualify radioactive waste packages in Germany. The IEK-6 **nuclear safeguards group** coordinates on behalf of Federal Ministry of Economics and Technology (BMWi) the German contribution to the **IAEA safeguards support programme**. JÜLICH will become a member of the **IAEA network of analytical laboratories** (qualification process started in 2013) by combining the analytical capabilities of three units (IEK-6, ZEA-3 & S) in JÜLICH. A **scientific collaboration with the IAEA safeguards laboratories** has been established to develop actinide bearing reference materials for particle analysis within the framework of nuclear forensics.

Energie & Umwelt / Energy & Environment
Band / Volume 197
ISBN 978-3-89336-920-1

JÜLICH
FORSCHUNGSZENTRUM